University of California
Santa Barbara

Conformal Perturbation Theory and LLM Geometries

A dissertation submitted in partial satisfaction
of the requirements for the degree

Doctor of Philosophy
in
Physics

by

Alexandra Patrea Mathisen Miller

Committee in charge:

Professor David Berenstein, Chair
Professor Gary Horowitz
Professor Elisabeth Gwinn

September 2018

The Dissertation of Alexandra Patrea Mathisen Miller is approved.

Professor Gary Horowitz

Professor Elisabeth Gwinn

Professor David Berenstein, Committee Chair

June 2018

Conformal Perturbation Theory and LLM Geometries

by

Alexandra Patrea Mathisen Miller

This dissertation is dedicated to the memory of Joe Polchinski.

Acknowledgements

I am grateful for so many people who have helped me during my time at UCSB. My graduate school experience has been filled with many ups and downs and I am certain that I would not have made it to where I am today without the support of so many wonderful people.

First and foremost, I must thank my advisor, David Berenstein. He went above and beyond in his duties by not only advising me in my research, but also by serving as a mentor more generally. During all of my times of self doubt, he was always there to support and encourage me. Thank you, David, for all you have taught me!

To my defense, advancement, and supervisory committee members: Gary Horowitz, Joe Polchinski, Beth Gwinn, and Mark Srednicki. Thank you for your words of wisdom over the years.

To my undergraduate research advisor, Zhigang Chen, and my postdoc mentor, Peng Zhang. Their mentoring and teachings were crucial in both helping me to get into graduate school and to be successful during my time here. Though I ended up completely switching research fields, my experience in the Chen lab has always helped me to be a more well rounded physicist. It's always a plus when a theorist has some idea of what actually goes on in a lab!

To the many professors and teachers throughout my academic career, from my elementary school math and science teachers (Mr. Adamick and Mrs. Mariano), to my high school teachers (Ms. Centeno, Mr. Green, Mr. Kenyon, Ms. Shields, Mr. Souza, and Ms. Zwicker), the wonderful professors at SFSU (Joe Barranco, Roger Bland, Adrienne Cool, Jeff Greensite, Susan Lea, Weining Man, and Barbara Neuhauser), and finally the UCSB faculty (David Berenstein, Nathaniel Craig, Matthew Fisher, Steve Giddings, Gary Horowitz, Don Marolf, Joe Polchinski, and Mark Srednicki). Thank you for all you

have taught me, both in and out of the classroom, and for inspiring me to love to learn!

To my teaching mentors: Tengiz Bibilashvili, Lisa Berry, and Mindy Collin. Being a teacher takes a lot of work. Thank you for giving me the tools necessary to one day achieve my goal of being a great physics teacher!

To Jennifer Farrar, who is the glue that holds the UCSB physics department together and has helped me in so many ways throughout my graduate school career.

To all the wonderful friends I've had throughout my life who are most certainly too numerous to name individually, but categorically can be listed as: UCSB Physics Grads, HEP JC, Broida 6234, Physics Force Soccer, Sting Soccer, Track Tuesday, Pali and other Funk zone homies, UCSB Geologists, SFSU PAC, SFSU Pizza and Milkshake Enthusiasts, and Vanden Drama Club. You know who you are! And special shout outs to my partner, Alex Schrader. To Netta Englehardt, my hero. And to Sebastian Fischetti and Kurt Fujiwara, two of the best friends I could ever ask for!!!

To all of the doctors, nurses, and staff at the UCSB Health Center, the Ridley Tree Cancer Center, Sansum Clinic, SB Fertility Center, Cottage Health, and UCSB CAPS. Especially thanks to Dr. Newman, Dr. Hughes, Dr. Bagalio, and Dr. Lantrip!

Finally, to my wonderful family who have helped shape me into the person I am today. I am eternally grateful for the love and support throughout my whole life. Thank you, Mom and Dad, for encouraging me to be whoever I wanted to be. I love you to the moon and back!

This dissertation was supported by the National Science Foundation Graduate Research Fellowship Program, the Broida-Hirschfelder Fellowship, the Graduate Division Dissertation year Fellowship, funds by the University of California, and the Department of Energy (grants DE-FG02-91ER40618 and DE-SC 0011702).

Curriculum Vitæ

Alexandra Patrea Mathisen Miller

Education

2018	Ph.D. in Physics (Expected), University of California, Santa Barbara.
2015	M.A. in Physics, University of California, Santa Barbara.
2011	B.S. in Physics, San Francisco State University

Publications

1. D. Berenstein and A. Miller, "Code Subspaces for LLM Geometries," accepted for publication in Class. Quant. Grav. [arXiv:1708.00035 [hep-th]].
2. D. Berenstein and A. Miller, "Superposition Induced Topology Changes in Quantum Gravity," JHEP **1711**, 121 (2017) [arXiv:1702.03011 [hep-th]].
3. D. Berenstein and A. Miller, "Logarithmic Enhancements in Conformal Perturbation Theory and Their Real Time Interpretation," [arXiv:1607.01922 [hep-th]].
4. D. Berenstein and A. Miller, "Can Topology and Geometry be Measured by an Operator Measurement in Quantum Gravity?," Phys. Rev. Lett. **118**, 261601 (2017) [arXiv:1605.06166 [hep-th]].
5. D. Berenstein and A. Miller, "Reconstructing Spacetime from the Hologram, Even in the Classical Limit, Requires Physics Beyond the Planck Scale," Int. J. Mod. Phys. D **25**, 1644012 (2016) [arXiv:1605.05288 [hep-th]]. Received honorable mention in 2016 Gravity Research Foundation essay contest.
6. D. Berenstein and A. Miller, "Conformal Perturbation Theory, Dimensional Regularization, and AdS/CFT," Phys. Rev. D **90**, 086011 (2014) [arXiv:1406.4142 [hep-th]].
7. J. Yang, D. Gallardo, A. Miller, and Z. Chen, "Elimination of Transverse Instability in Stripe Solitions by One-Dimensional Lattices," Opt. Lett. **37**, 1571-1573 (2012) [arXiv:1205.0767 [physics]].
8. J. Wang, N.K. Efremidis, A. Miller, C. Lu, P. Zhang, and Z. Chen, "Nonlinear Beam Deflection in Photonic Lattices with Negative Defects" Phys. Rev. A **83**, 033836 (2011).
9. P. Zang, N.K. Efremidis, A. Miller, P. Ni, and Z. Chen, "Reconfigurable 3D Photonic Lattices by Optical Induction for Optical Control of Beam Propagation" Appl. Phys. B **104**, 553 (2011).
10. P. Zang, N.K. Efremidis, A. Miller, Y. Hu, and Z. Chen, "Observation of Coherent Destruction of Tunneling and Unusual Beam Dynamics due to Negative Coupling in Three-Dimensional Photonic Lattices" Opt. Lett. **35**, 3252 (2010).

Abstract

Conformal Perturbation Theory and LLM Geometries

by

Alexandra Patrea Mathisen Miller

This dissertation will focus on various aspects of the AdS/CFT correspondence. Each new result can be thought of as doing at least one of three things: 1) providing support of the duality, 2) using the duality to learn about quantum gravity, and 3) helping to further develop our understanding of the duality. The dissertation is divided into two parts, each dealing with a different physical system.

In the first part, we derive universal results for near conformal systems, which we have perturbed. In order to do this, we start by looking at the conformal correlation functions and compute the corrections that arise when he hit the system with a new operator. We were able to analyze what happens to the dual gravitational system under such circumstances and see that our answers agree, providing support for the AdS/CFT conjecture. These universal results also provided a previously lacking interpretation of the universality of energy found in a quenching your system between the perturbed and unperturbed set-ups. In order to perform these computations, we put our CFT on a cylinder, which happens to be the boundary of global AdS. This provided an IR regulator and we found that the remaining divergences were of the same form as one expects in dimensional regularization. Following along these same lines, we further analyzed the divergence structure of correlators in conformal perturbation theory. We found that on the plane, the logarithmic divergences that show up can be understood in terms of resonant behavior in time dependent perturbation theory, for a transition between states

that is induced by an oscillatory perturbation on the cylinder.

In part two, we restrict to the set of LLM geometries, which are the set of 1/2 BPS solutions to IIB supergravity. In our first work, we analyzed limitations of the duality, showing that boundary expectation values are not enough to determine the classical bulk geometry. Next, we used this system in order to learn about quantum gravity. We first were able to show that a quantum superposition of states with a well defined spacetime topology leads to a new state with a different topology. From this, we were able to prove that for this set of states there cannot exist a quantum topology measuring operator, bringing to doubt whether such an operator can exist in quantum gravity more generally. Finally, we were able to advance our understanding of the dictionary itself by reinterpreting these results in terms of the language of quantum error correction, showing that questions about topology perhaps only make sense within a particular (code) subspace of states.

Contents

Chapter 0

Introduction

0.1 Scales in Physical Theories and the Road to Quantum Gravity

One of the biggest open questions in physics today is: What is the correct theory of quantum gravity? Two of the most fundamental and well tested theories in physics are quantum mechanics and general relativity. In most cases, the effects of these two are seen in very different settings. This is due to the fact they become important at very different scales. In order to define and motivate the need for quantum gravity, I will start by discussing this importance of considering the scale of your system when developing a scientific theory.

Any physical theory has constants associated with it and these provide a scale where the effects of the theory become important. The same physical system is often described by multiple theories and which theory you use depends on the scale at which you probe the theory. For instance, the proper equations needed to analyze the flow of water depend on how closely you look at it. If you care about the dynamics of a river, you would use

the equations of fluid dynamics. But, if you want to zoom in on a droplet of water, you will start to care about the fact that the water is actually made up of individual H_2O molecules and so will need to introduce more fundamental equations describing the motion of the molecules. The size of H_2O molecules is a constant that will help determine which theory you will need to use. On length scales much longer than the size of the molecules, you can take the continuum limit and use the equations of fluid dynamics, but if you zoom in to length scales that are near the size of the molecule, you will need to use a new set of equations.

Students first studying physics will generally start by learning Newton's laws of classical mechanics, which work on every day human scales. But, if we want to understand the many deep mysteries of the universe, we need to consider the physics of systems at all scales. Furthermore, in the case of water, we considered zooming in to shorter lengths, but this is not the only scale you might consider. Indeed, you can consider limiting cases of any physical quantity you might discuss. Historically, there were three particularly interesting limits that ended up leading to paradigm shifts in the way we understand the world around us. The first was from considering objects moving very fast, near the speed of light. In 1905, this led Einstein to propose the theory of special relativity [1], which alters Newton's laws for objects moving at these very high speeds and leads to very unexpected phenomena, such as time dilation, length contraction, and recognizing the speed of light as the universal speed limit. Ten years later, in 1915, Einstein took things a step further and considered very massive objects. He again found that in this limit, Newton's laws simply don't do the trick and a new theory is needed. This was his theory of general relativity [2], which teaches us that very massive objects actually curve the fabric of spacetime itself. And it is this curvature that causes, for instance, the planets to orbit the Sun. Finally, around the same time, physicists were considering the behavior of

objects at very small scales, which led to the development of quantum mechanics, which comes with it a large array of surprises, such as the uncertainty principle, wave-particle duality, and quantum entanglement.

In each of these cases, we learned that Newton's Laws are not fundamental, but instead are approximations that only work at everyday scales. It turned out that special relativity, general relativity, and quantum mechanics are the more accurate descriptions of the universe. A question you might ask is, how do you know when you need to use these new theories and when can you use the classical approximations? With each theory there is an associated constant of nature: special relativity uses the speed of light c, general relativity has Newton's gravitational constant G, and quantum mechanics has Plank's constant $\hbar$. And these constants set the scale at which the theory becomes important. For instance, special relativity only becomes important when objects approach the speed of light. At every day speeds, its effects are too small to notice.

We therefore found that by considering these limits, we were able to discover a more accurate description of the universe. One might next wonder what happens if we consider combinations of these limits. How do very fast large objects behave? Do we again need a new theory in that case? Happily, this particular combination has already been solved. When Einstein developed general relativity, he included special relativity in it. (That's why it is called special: it is the special case of relativity where we are in the limit of flat spacetime). We might also want to consider systems with very fast objects probed at very short distances, combining quantum mechanics with special relativity. This led to the discovery of quantum field theory, which is used in describing the standard model of particle physics, which predicts the phenomena seen at particle accelerators, such as the LHC (Large Hadron Collider). Finally, one might want to consider the very massive objects at very small distance scales. This is the regime of quantum gravity, where

general relativity and quantum mechanics both become important.

One might wonder, usually massive objects are also large, while small objects have a small mass. So, what are the physical systems quantum gravity will actually help us describe? The answer is very dense objects. This leads us to black holes, which are the densest objects in the universe. It is in these extreme places where general relativity alone fails. And, again, it appears that there must be a more fundamental theory, a quantum mechanical theory of gravity. As of today, we still do not know what the correct theory of quantum gravity is. The work in this thesis was all done with the aim of trying to help fill in pieces of the puzzle answering the question: What is the correct theoretical description of the world where quantum mechanics and general relativity collide?

0.2 The Search for a Theory of Quantum Gravity

When classifying the forces of nature, there are four types we consider: electromagnetic, weak, strong, and gravity. The first three of these are all well understood within the framework of Quantum Field Theory (QFT). They are represented by force carrying particles and so are well incorporated into the Standard Model. One might hope then that quantum gravity is described by a graviton (the particle carrying the force of gravity) and can also be understood using QFT. This, unfortunately does not work. Infinities appear and prevent you from extracting physically meaningful predictions. These infinities are commonplace in QFT. However, there are usually only a finite number of them and so they can be systematically removed. This process is referred to as renormalization. In describing the graviton, we find that there are an infinite number of infinites that arise and so renormalization is no longer sufficient. For this reason, it was discovered that we need something new in order to describe quantum gravity.

These infinities (divergences) generally have two physical origins: from either the very short or the very long length scale. The infinites from short distances are referred to as Ultraviolet (UV) divergences and come from the fact that we are including contributions from infinite energy interactions, whereas those from the large scale are referred to as Infrared (IR) and come from the fact that we integrate over infinite space.

String theory is a framework that treats fundamental particles as tiny vibrating strings instead of as points in space. The finite size of particles softens the UV divergences and so is a much better behaved theory. The fundamental constant of string theory is the string scale and only near this scale will you be able to notice the stringy nature of the particles. If you look at them at larger distances, then they will simply appear to be points in space, reducing to our standard picture of a point particle. Originally, string theory was written down in the late 1960's in order to describe the strong force, which governs the interactions of hadrons. But, it was eventually discarded in favor of quantum chromodynamics. Today, it is believed that string theory may instead be the correct framework for describing quantum gravity. This is in part because not only does string theory allow for the existence of graviton, but its existence is required for consistency. That is, all particles of the standard model have a spin associated with them. This is simply one of their basic properties, just like their electric charge. For instance, electrons have spin 1/2, whereas photons have spin 1. In 1965, Weinberg showed that any massless spin 2 particle must be a graviton and such a particle arises naturally in string theory, suggesting that it is a good candidate framework for quantum gravity. Furthermore, there are two main requirements that we have for any possible theory of quantum gravity: 1) that it is consistent with the postulates of quantum mechanics; and 2) that it agrees with the results of General Relativity in the classical limit. String theory does both of these things.

There is still a lot that we do not know about string theory, but much progress has been made. And in 1997 [3], Juan Maldacena had a novel idea that completely changed the way we look at the theory. He conjectured that type IIB superstring theory in $AdS_5 \times S^5$ is dual to $\mathcal{N} = 4$ Super-Yang-Mills, which lives in four spacetime dimensions. In other words, he hypothesized that a particular supersymmetric form of string theory (a theory of quantum gravity) is deeply mathematically related to a different theory that does not contain gravity. This is an incredibly surprising, philosophically interesting, and practically useful result. It says that any physical observable you can compute on one side of the duality can be mapped to a result on the other side. To date, physicists have worked on both sides of the duality to learn lessons about the other side. While the conjecture has not yet been proven, there is a great deal of evidence for it and the body of evidence seems to grow every day. All of the work in this thesis has approached quantum gravity using AdS/CFT as a tool. As such, I will use the following section to introduce some basic background of the duality.

0.3 AdS/CFT

Dualities are both remarkable and incredibly useful tools for science. A duality states that one physical system can be described in two or more ways that often look incredibly different, consisting of different interactions and degrees of freedom. This allows one to look at the same physical system through very different lenses, providing new insights and intuitions. These can be especially useful in the case of strong-weak dualities, where one side is strongly coupled, while the other is weakly coupled. This is because we have many more methods at our disposal for approaching weakly coupled theories. For two theories to be truly dual, everything you can compute on one side must correspond to

something on the other side, every degree of freedom must have a partner.

Gauge/Gravity dualities [3, 4, 5] are remarkable and useful for all the same reasons listed above, and more. There are various motivations one might have for studying them. Many prefer to work in the limit where one can learn about strongly couple field theories. There the mapping is incredibly useful because the gravitational theory reduces to classical gravity, which we know how to deal with, while the field theory side is strongly coupled and this is therefore generally much more challenging. I, on the other hand, prefer to use the duality in the other direction and the work of this thesis reflects that. I prefer to use the duality in order to learn about quantum gravity, which we are still far from completely understanding. We can compute observables in field theory, which we have good intuition for and map them to the other side in order to learn about quantum gravity.

The first example of a gauge/gravity duality was conjectured by Juan Maldacena and said that type IIB string theory on $AdS_5 \times S^5$ is dual to $\mathcal{N}$=4 Super-Yang-Mills in $D = 4$ [3]. It might seem surprising that a gravitational theory could be dual to one without gravity and even more surprising that the two theories live in a different number of spacetime dimensions. But, this amazingly is the case. This latter property is a result of the holographic principle [6, 7, 8], which is due to the fact that the gravitational theory is highly redundant and therefore should be able to be described by degrees of freedom living in fewer dimensions.

Since this original example, many more examples of gauge/gravity dualities have been studied, some with more success than others. There are an array of other examples of AdS/CFT, as well as examples where the gravitational theory has other asymptotic boundary conditions and correspondingly the field theory has other symmetries. For instance, there are higher spin versions of AdS/CFT [9, 10, 11, 12]. And, with the goal

in mind of developing a duality that describes our universe, there have been many efforts to develop a dS/CFT duality [13, 14, 15, 16, 17, 18]. One of the primary differences (and challenges) this duality has is that whereas in AdS/CFT the radial direction emerges holographically, in dS/CFT the time direction is emergent, which is challenging to reconcile with unitary time evolution. Others have considered flat space holography [19, 20], which rather than being dual to a conformal theory, has as its dual a BMS invariant field theory. It is still an open question which CFTs (or more general gauge theories) have a gravitational dual.

All of of the work in this thesis deals with quantum gravity on a spacetime with asymptotically AdS boundary conditions and is dual to a conformal field theory. To give you a feel for this, in the following sections, I will give brief introductions to the two sides of the duality, as well as describe some of the pieces of the dictionary, and discuss some of the recent advances of our understanding. For more thorough reviews of the correspondence, see [21, 22, 23, 24, 25].

0.3.1 Classical Ads

One of the primary reasons why studying quantum gravity in Anti-de Sitter (AdS) space is nice is because it acts like a finite sized box in that, though it is infinite in size, if we send a signal to the boundary, it will return in finite proper time. For this reason, it is a nice space in which to perform controlled experiments. This also means that boundary conditions must be imposted in order to get a well-defined solution. That is, we do not have a well-posed initial value problem in terms of information specified on a spacelike slice (we will see later that these boundary conditions will be directly related to our dual conformal theory). In order to get a better feel for AdS, let's review the basic facts about it. For a more thorough look, see any of the standard general relativity texts, for instance

[26, 27, 28, 29]. Alternatively, most of the AdS/CFT reviews mentioned above give an overview.

Anti-de Sitter (AdS) space is one of the three maximally symmetric solutions to Einstein's equations. The other two being Minkowski and de Sitter space. AdS is the solution with a negative cosmological constant, whereas de Sitter has a positive constant and Minkowski space has vanishing cosmological constant. It is invariant under $SO(d+1,1)$. If we embed $d+1$ dimensional Euclidean AdS space into $\mathbb{R}^{d+1,1}$, it is given by a hyperboloid:

$$-(X^0)^2 + (X^1)^2 + \cdots + (X^{d+1})^2 = -R^2, \quad X^0 > 0 \tag{0.1}$$

We can define Poincare coordinates of AdS by taking

$$X^0 = R\frac{1+x^2+z^2}{2z} \tag{0.2}$$

$$X^\mu = R\frac{x^\mu}{z} \tag{0.3}$$

$$X^{d+1} = R\frac{1-x^2-z^2}{2z} \tag{0.4}$$

where $x^\mu \in \mathbb{R}^d$ and $z > 0$. The metric in these coordinates is given by

$$ds^2 = R^2\frac{dz^2 + \delta_{\mu\nu}dx^\mu dx^\nu}{z^2} \tag{0.5}$$

In these coordinates, we see that the $z = 0$ boundary is just $\mathbb{R}^d$. And, if we move into the bulk, each fixed z is simply another copy of $\mathbb{R}^d$, which is scaled down as z increases. For this reason, one can interpret moving into the bulk as an RG (renormalization group) flow. These coordinates are often referred to as the Poincare Patch because they do not actually cover the full AdS space. A second useful coordinate system (which will cover

the full space) is given by

$$X^0 = R\cosh\tau\cosh\rho \tag{0.6}$$

$$X^\mu = R\Omega^\mu\sinh\rho \tag{0.7}$$

$$X^{d+1} = -R\sinh\tau\cosh\rho \tag{0.8}$$

where Ω^μ parameterizes a unit $(d-1)$ dimensional sphere. The metric is given by

$$ds^2 = R^2\left[\cosh^2\rho d\tau^2 + d\rho^2 + \sinh^2\rho d\Omega_{d-1}^2\right] \tag{0.9}$$

This metric is often referred to as Global AdS because, unlike the Poincare Patch, it covers the full space. It is conformal to a solid cylinder and therefore the AdS/CFT correspondence is often drawn as a cylinder with the conformal theory living on the boundary. Both this and the Poincare metric representations are fairly common in the AdS/CFT literature, and which is more useful is generally decided on a case by case basis.

0.3.2 Conformal Field Theory

A Conformal Field Theory (CFT) is a Quantum Field Theory (QFT) that is invariant under local changes of scale:

$$g'_{\mu\nu}(x') = \Omega(x)g_{\mu\nu}(x) \tag{0.10}$$

An example of such a transformation is a constant scale transformation, where $\Omega(x) = \lambda$ is constant across all spacetime.

$$g'_{\mu\nu}(x') = \lambda g_{\mu\nu}(x) \tag{0.11}$$

This simply zooms in or out of your entire system (increasing or decreasing everything uniformly). More generally $\Omega(x)$ can be a local scale transformation, which might zoom in on some areas, but out in others. One can alternatively think of the set of conformal transformations as being the set of angle preserving transformations. This a more liberal constraint that that which leads to Poincare transformations, which only preserve the norm of vectors. Notice the Poincare group a subset of the Conformal group, restricted to the special case where $\Omega(x) = 1$. The set of allowed transformations is therefore enlarged and includes the usual translations, boosts, and rotations, as well as dilatations and special conformal transformations (which can be though of as an inversion, followed by a translation, and then another inversion). We see that the symmetry group of a d-dimensional CFT is enhanced from that of a normal QFT to $SO(d+1,1)$. Notice that this matches with the isometry group of AdS in $(d+1)$-dimensions. When considering the space of all allowed QFTs, the CFTs lie at critical points of the RG flow, where the beta-functions vanish.

These are only the most basic defining properties of a CFT. Part I of this thesis contains all of my work on conformal perturbation theory. So, I will begin that part with a chapter, giving a more thorough introduction to some of the special properties of conformal field theory.

0.3.3 A few words about Strings and $\mathcal{N} = 4$

The original example of and AdS/CFT duality said that type IIB string theory on $AdS_5 \times S^5$ was dual to $\mathcal{N}$=4 Super-Yang-Mills in $d = 4$ spacetime dimensions. For a full description of both sides of this duality, please see any of the aforementioned gauge/gravity duality reviews or the original work itself. Here, I will only provide a few words about what the two sides are.

First, the gravity side. There are five consistent superstring theories: type I, type IIA, type IIB, Heterotic $E_8 \times E_8$, and Heterotic $SO(32)$. These all can only live in ten spacetime dimensions can be related to each other via dualities (for instance, type IIA and IIB can be related via T-duality). Both type II theories have maximal supersymmetry (32 supercharges) and are theories of closed strings. They differ in that IIB is chiral, while IIA is non-chiral. Both can also have D-branes as excited states and open strings can be attached to them. The massless fields of IIB are: $G_{\mu\nu}$, $GB_{\mu\nu}$, Φ, C, $C_{\mu\nu}$, $C_{\mu\nu\lambda\rho}$, and two gravitini and two dilatini. In the low energy limit,

You might wonder why we are studying a supersymmetric theory when evidence of supersymmetry in our Universe is yet to be found. One can certinaly study bosonic string theory, but it contains a tachyon (a field with mass$^2 < 0$), which causes a serious instability. Moving to one of the supersymmetric theories removes this problem. Furthermore, we know that fermions exist in our universe and so we need a theory that contains fermionic degrees of freedom anyway. For a more thorough introduction to string theory more generally, some standard references are [30, 31, 32, 33, 34].

On the other side, we have $\mathcal{N}$=4 super-Yang-Mills theory in $d = 4$ spacetime dimensions with gauge group $SU(N)$ and Yang Mills coupling $g_{\rm YM}$. This, matching the gravity side, is a maximally supersymmetric theory. It is, of course, also conformal (thus, the C in AdS/CFT). We already saw that the matching of the symmetries when we looked

at AdS and CFT individually, in this example, both bosonic symmetries are extended to the superconformal version. Part of why this original example is nice is because it has so many symmetries. We now know many examples of gauge/gravity duals with much less symmetry.

0.4 Conformal Perturbation Theory

In this section, I will provide an introduction to some of the basic aspects of Conformal Field Theory (CFT) in $d > 2$ spacetime dimensions that will be important in understanding chapters one and two of this thesis. Perhaps the most important thing you will need to know is that the one-, two, and three- point correlation functions of any CFT are completely determined up to a set of constants. One can derive them by simply enforcing the transformation properties of the operators in the correlator. By doing this, for scalar primary fields, one finds

$$\langle \phi(x) \rangle = 0 \tag{0.12}$$

$$\langle \phi_1(x_1)\, \phi_2(x_2) \rangle = \frac{\delta_{\Delta_1,\Delta_2}}{|x_1 - x_2|^{2\Delta_1}} \tag{0.13}$$

$$\langle \phi_1(x_1)\, \phi_2(x_2)\, \phi_3(x_3) \rangle = \frac{C_{123}}{|x_{12}|^{2a}\, |x_{13}|^{2b}\, |x_{23}|^{2c}} \tag{0.14}$$

where

$$\begin{aligned} 2a &= \Delta_1 + \Delta_2 - \Delta_3 \\ 2b &= \Delta_1 + \Delta_3 - \Delta_2 \\ 2c &= \Delta_3 + \Delta_2 - \Delta_1 \end{aligned} \tag{0.15}$$

the Δ_i are the operator dimensions, and the C_{123} are the structure constants (also known as OPE coefficients). One can find similar expressions for descendants by simply taking the derivatives, as well as for operators with spin. For higher point functions, you being to have conformal invariants, so enforcing covariance of the operators is no longer enough. That is, for four points, you can write the expressions

$$u = \frac{|x_{12}|\,|x_{34}|}{|x_{13}|\,|x_{24}|} \quad v = \frac{|x_{12}|\,|x_{34}|}{|x_{14}|\,|x_{23}|} \tag{0.16}$$

which alone are invariant under any conformal transformation and so an arbitrary function of these two can be included in the correlator without changing its transformation properties. For instance, the four-point function can be expressed as

$$\langle \phi_1(x_1)\,\phi_2(x_2)\,\phi_3(x_3)\,\phi_4(x_4)\rangle = f(u,v)\prod_{i<j}^{4}|x_{ij}|^{\gamma_{ij}} \tag{0.17}$$

where $\sum_{j\neq i}\gamma_{ij} = -2\Delta_i$. Higher point functions have even more conformal invariants that you can write down.

In chapters one and two, we start with a conformal theory in an arbitrary number of spacetime dimensions and perturb it with an operator $\mathcal{O}$ of dimension Δ. That is, if call the action of our conformal theory S_{CFT}, then the perturbed theory will have an action $S = S_{\text{CFT}} + \alpha\int d^dx\mathcal{O}(x)$. The partition function is given by

$$Z = \int \mathcal{D}\phi e^{-S} = \int \mathcal{D}\phi e^{-S_{\text{CFT}}-\alpha\int d^dx\mathcal{O}(x)} \tag{0.18}$$

We can compute an n-point partition function in the perturbed theory by

$$\langle \phi_1\phi_2\ldots\phi_n\rangle = \int \mathcal{D}\phi\,\phi_1\phi_2\ldots\phi_n e^{-S_{\text{CFT}}-\alpha\int d^dx\mathcal{O}(x)} \tag{0.19}$$

We can Taylor expand the latter part of the exponential as

$$e^{-\alpha \int d^d x \mathcal{O}(x)} = \sum_{n=0}^{\infty} \left(-\alpha \int d^d x \mathcal{O}(x) \right)^n \tag{0.20}$$

Our correlator can therefore be re-expressed as

$$\langle \phi_1 \phi_2 \dots \phi_n \rangle = \int \mathcal{D}\phi \, \phi_1 \phi_2 \dots \phi_n e^{-S_{\text{CFT}}} \sum_{n=0}^{\infty} \left(-\alpha \int d^d x \mathcal{O}(x) \right)^n \tag{0.21}$$

$$= \langle \phi_1 \phi_2 \dots \phi_n \rangle_{\text{CFT}} - \alpha \int d^d x \, \langle \phi_1 \phi_2 \dots \phi_n \mathcal{O}(x) \rangle_{\text{CFT}} + \mathrm{O}(\alpha^2) \tag{0.22}$$

We see, therefore, that the correlator in the perturbed theory can be written as a sum over integrals of correlators in the unperturbed theory. And, because the unperturbed theory is conformal, we know the form of the correlators, at least up to three-points. Therefore, the work in computing the corrections is reduced to computing integrals.

0.5 LLM Geometries

The LLM Geometries are the set of 1/2 BPS solutions of type IIB supergravity. They were first classified by Lin, Lunin, and Maldacena in 2004 [63]. Because of their high degree of symmetry, we can make a lot of progress on both sides of the duality and therefore they are an incredibly useful example of AdS/CFT. The supergravity solutions can all be described by the metric

$$ds^2 = -\frac{y}{\sqrt{\frac{1}{4} - z^2}} (dt + V_i dx^i)^2 + \frac{\sqrt{\frac{1}{4} - z^2}}{y} (dy^2 + dx^i dx^i) + y \left(\sqrt{\frac{\frac{1}{2} - z}{\frac{1}{2} + z}} \right) d\Omega_3^2 + y \left(\sqrt{\frac{\frac{1}{2} + z}{\frac{1}{2} - z}} \right) d\tilde{\Omega}_3^2 \tag{0.23}$$

where $i = 1, 2$. Each solution is completely characterized by $z(y, x_i)$ (the vector V satisfies a differential equation that ties it to z). The function z obeys a linear elliptic sourceless PDE:

$$\partial_i \partial_i z + y \partial_y \left(\frac{\partial_y z}{y} \right) = 0 \tag{0.24}$$

which requires a boundary condition at $y = 0$, which is often referred to as the LLM plane. Non-singularity of the ten dimensional metric requires $z = \pm\frac{1}{2}$ at this locus (this forces only one of the two spheres to shrink to zero size, while the other stays finite). From here, one can compute

$$z(x_1, x_2, y) = \frac{y^2}{\pi} \int \frac{z(w_1, w_2, 0)\, dw_1\, dw_2}{[(x_1 - w_1)^2 + (x_2 - w_2)^2 + y^2]^2} \tag{0.25}$$

Notice that the integral is always convergent if $z(w_1, w_2, 0)$ is bounded. Each non-singular solution can be represented by a black and white coloring of the plane, where the two colors are representing the two possible boundary conditions for the function $z(x_1, x_2, 0)$.

The other side of the duality corresponds to the 1/2 BPS solutions of $\mathcal{N}$=4 Super Yang Mills. In this infinite N limit, this can be described by a free chiral boson on a circle. In a Fock space representation, we can build all allowed states by an infinite set of raising and lowering operators. We can alternatively work in a basis, where each state is represented by an allowed Young Tableaux. The details of these two bases are given in chapter four, section three.

0.6 Thesis Outline

All of the work contained in this thesis deals with doing at least one of three things: providing support of the AdS/CFT correspondence, utilizes it as a tool for understanding

quantum gravity, and/or advances our understanding of the duality. It is separated into two parts, each dealing with a particular system. Part I includes my study of Conformal Perturbation Theory, while Part II consists of my analysis of the LLM Geometries. Here, I will discuss the system studied in each part and briefly review our primary findings presented in each chapter.

There are two chapters in part I and both of them provide results within the framework of conformal perturbation theory in an arbitrary number of spacetime dimensions d. The results of each chapter are universal in that the initial conformal theory is not specified; we only use the fact that it is conformal.

In chapter one, we consider perturbing the theory by a scalar operator of dimension Δ (allowing it initially to be marginal, relevant, or irrelevant) and compute the first order correction to the one-point function in such a set-up. We found that in trying to compute this naively, one runs into both UV and IR divergences. By transforming our system from the plane to the cylinder, we were able to tame the IR divergences, leaving only those in the UV. We found that the divergence structure exactly matched what one would find in a standard dimensional regularization scheme in QFT.

Exciting a scalar operator on the CFT is dual to exciting a scalar field in the bulk. We computed the first order asymptotic behavior of such a field and, following the rules of the AdS/CFT dictionary, were able to show that it agreed with the CFT result. In this chapter, we also computed the energy in quenching between the perturbed and unperturbed systems. What we found provided a deeper understanding of previous results of [41, 42, 43, 44] in that in our set-up it was clear why the energy in such a quench should be universal.

In chapter two, we again work within the framework of conformal perturbation theory and analyze the divergence structure of corrections to various correlation functions one

might encounter. Here we consider higher point functions and allow the deformation to have a spacetime dependent scaling profile. In the special case of marginal deformations, we related our our computations to time dependent perturbation theory on the cylinder and noted that singularities could be reinterpreted as resonances that arise in time dependent perturbation theory. The logarithmic enhancements in the plane computations reflect the secular behavior for resonant perturbations in the cylinder.

Part II of this thesis utilizes the LLM Geometries. These are the set of half BPS states of type IIB supergravity. Because of their high degree of symmetry, we are able to perform computations on both sides of the duality and so this provides an incredibly useful playground for both learning about the duality and using it to learning about quantum gravity.

In chapter three, we delve into how much information is needed from the hologram in order to learn about the bulk theory. We use the LLM Geometries as an example and show that, in that case, the expectation values of the boundary theory do no provide enough information to reconstruct the classical bulk solution. Indeed, multiple bulk geometries can be associated with the same boundary expectation values. Furthermore, these bulk geometries are not just a little different, but can be topologically distinct.

In chapter four, we use the fact that the example of the LLM Geometries is one where we understand both sides of the duality well in order to learn about quantum gravity. One of our primary findings was that one can superpose states with topologically distinct spacetime geometries that will give rise to new states with a classical spacetime dual, which has a completely different topology than any of the original spacetimes. Specifically, we show that coherent states on the field theory side have topologically trivial gravitational duals. But, one can superpose these coherent states and form new states whose dual is again a classical geometry, but now has a non-trivial topology. From

this, we were able to prove that there cannot exist a topology measuring operator for this set of states, which suggests that one should not assume that such an operator exists in quantum gravity more generally. We end the chapter by discussing alternative ways to extract the topological information, including using entanglement entropy and uncertainty. In order to show these things rigorously, chapter four has several sections building up the technology for preforming computations. Along the way, we show that the Murnaghan-Nakayama rule (which is a rule for determining characters in the theory of finite groups) encodes the fermi statistics of our Hilbert space.

Finally, chapter five contains a re-examining of the findings of chapter four. We show that questions about the topology of the gravitational dual to a field theory state only have non-ambiguous answers within a particular (code) subspace of states. We discuss how the language of code subspaces is natural for understanding the AdS/CFT dictionary in this case, which supports many of the recent ideas by the community regarding holographic code subspaces, such as in [122]. In order to do this, we went beyond the infinite N limit of chapter four.

Note that Appendix D contains the short companion paper to the work included in chapter four.

0.7 Permissions and Attributions

1. The content of Chapter 1 is the result of work in collaboration with David Berenstein, and have previously appeared in Physical Review D (Phys. Rev. D) [35]. It is reproduced here with the permission of the permission of the American Physical Society (APS), College Park, MD, USA. `http://publish.aps.org/info/terms.html`.

2. The contents of Chapter 2 and Appendix A are the result of work in collaboration with David Berenstein [36].

3. The content of Chapter 3 is the result of work in collaboration with David Berenstein, and has previously appeared in The International Journal of Modern Physics D [37]. It is reproduced here with the permission of the permission of World Scientific. `https://www.worldscientific.com/page/authors/author-rights`.

4. The contents of Chapter 4, Appendix B, and Appendix C are the result of work in collaboration with David Berenstein, and have previously appeared in The Journal of High Energy Physics [38]. It is reproduced here with the permission of the permission of the International School of Advanced Studies (SISSA). `http://jhep.sissa.it/jhep/help/JHEP/CR_OA.pdf`.

5. The contents of Chapter 5 and Appendix E are the result of work in collaboration with David Berenstein, and previously appeared in the Journal Classical and Quantum Gravity [39]. It is reproduced here with the permission of the permission of the Institute of Physics (IOP). `http://authors.iop.org/atom/help.nsf/LookupJournalSpecific/WebPermissionsFAQ~**`.

6. The content of Appendix D is the result of work in collaboration with David Berenstein, and previously appeared in Physical Review Letters [40]. It is reproduced here with the permission of the permission of the American Physical Society (APS). `http://journals.aps.org/copyrightFAQ.html`.

Part I

Conformal Perturbation Theory

Chapter 1

Conformal perturbation theory, dimensional regularization, and AdS/CFT

1.1 Introduction

Consider a conformal field theory in d dimensions perturbed by a relevant (scalar) operator $\mathcal{O}$ of dimension $\Delta < d$. We are interested in evaluating the correlators of $\mathcal{O}$ in the presence of the perturbation. The partition function is

$$Z = \langle \exp(-\alpha \int d^d x \mathcal{O}(x)) \rangle = \left\langle \sum_{n=0}^{\infty} \frac{1}{n!} \left(-\alpha \int d^d x \mathcal{O}(x) \right)^n \right\rangle \tag{1.1}$$

and the formal evaluation of correlators with the infinite sum in the equation above is what is known as conformal perturbation theory. To begin with such a program, one can

compute the one point function of $\mathcal{O}(x)$ as follows

$$\langle \mathcal{O}(x) \rangle = \left\langle -\alpha \int d^d y \mathcal{O}(y)\mathcal{O}(x) + \dots \right\rangle = -\alpha \int d^d y \frac{1}{|x-y|^{2\Delta}} + \dots \tag{1.2}$$

The right hand side is infinite regardless of Δ. The divergence comes either from the small distance UV regime, or from the long distance IR regime. This is because we have to perform an integral of a scaling function. The problem seems ill defined until one resums the full perturbation expansion. This is a very important conceptual point in the AdS/CFT correspondence [3] where standard 'experiments' insert time dependent or time independent sources for various fields on the boundary of AdS [5, 4] and these in turn can be associated with sources for an operator such as $\mathcal{O}(x)$. Some of these results have been argued to be universal in [41, 42, 43, 44], independent of the AdS origin of such a calculation. We want to understand such type of results under a more controlled setting, where we can use the philosophy of conformal perturbation theory to get finite answers *ab initio* without a resummation.

A natural way to solve the problem above is to introduce a meaningful infrared regulator, so that the only divergences that survive arise from the UV of the theory and can then be handled via the usual procedure of renormalization. Such a natural regulator is provided by the conformal field theory on the cylinder $S^{d-1} \times \mathbb{R}$, which also happens to be the conformal boundary of global AdS spacetime, rather than just the Poincaré patch. The cylinder also is conformally equivalent to flat space and provides both the radial quantization and the operator state correspondence. In this sense, we are not modifying the AdS space in a meaningful way. However, a constant source for $\mathcal{O}(x)$ in such a geometry is different than a constant source on the Poincaré patch.

In the rest of the paper we discuss the details of such a computation for two uni-

versal quantities. These are the one point function of $\mathcal{O}(x)$, and the energy stored in a configuration where we quench from $\alpha \neq 0$ to $\alpha = 0$. We also explain how to deal with general time dependent sources in the conformal field theory side for more general AdS motivated experiments. Because we work with arbitrary d, Δ, our results can naturally be cast as a real space dimensional regularization formalism.

We find that the AdS answer, which is generally finite for the one point function, matches this notion of dimensional regularization. The only singularities that arise are those that one associates with logarithmic divergences. We are also able to match this result to the CFT calculation exactly, where the calculation is more involved. We also argue how to calculate the energy of the configuration and that having solved for the one point function naturally produces the result for this other computation.

1.2 One point functions on the sphere

What we want to do is set up the equivalent calculation to (1.1) and (1.2), but where we substitute the space $\mathbb{R} \times S^{d-1}$ in the integral. That is, we want to compute

$$\langle \mathcal{O}(\tau, \theta) \rangle \simeq \left\langle -\alpha \int d^{d-1}\Omega' d\tau' \mathcal{O}(\tau', \theta') \mathcal{O}(\tau, \theta) + \dots \right\rangle = -\alpha C_\Delta \tag{1.3}$$

for τ a time coordinate on $\mathbb{R}$ and θ an angular position on the sphere. Because the operator $\mathcal{O}$ is not marginal, α has units and we need to choose a specific radius for the sphere. We will choose this radius to be one. Our job is to compute the number C_Δ. Because the sphere times time as a space is both spherically invariant and time independent, properties that are also shared by the perturbation, we find that the result of equation (1.3) should be independent of both θ and τ. As such, we can choose to

perform the angular integral by setting the point θ at the north pole of the sphere, so that we only need to do an integral over the polar angle in θ'. We want to do this calculation both in the AdS spacetime and in conformal field theory. We will first do the AdS calculation and then we will do the conformal field theory calculation.

The AdS calculation

As described in the introduction, we need to compute the answer in global AdS spacetime. We first describe the global AdS geometry as follows

$$ds^2 = -(1+r^2)dt^2 + \frac{dr^2}{(1+r^2)} + r^2 d\Omega_{d-1}^2 \tag{1.4}$$

We need to find solutions for a perturbatively small scalar field ϕ with mass m and time independent boundary conditions at infinity. Such a perturbation is a solution to the free equations of motion of the field ϕ in global AdS. Such boundary conditions allow separation of variables in time, angular coordinates and r. A solution which is time independent and independent of the angles can be found. We only need to solve the radial equation of motion. Using $|g| \propto r^{2(d-1)}$ we find that we need to solve

$$\frac{1}{r^{d-1}}\frac{\partial}{\partial r}\left(r^{(d-1)}(1+r^2)\frac{\partial}{\partial r}\right) - m^2\phi(r) = 0 \tag{1.5}$$

The nonsingular solution at the origin is provided by

$$\phi(r) = A\,{}_2F_1\left(\frac{d}{4} - \frac{1}{4}\sqrt{d^2+4m^2}, \frac{d}{4} + \frac{1}{4}\sqrt{d^2+4m^2}; \frac{d}{2}; -r^2\right) \tag{1.6}$$

where A indicates the amplitude of the solution. We now switch to a coordinate $y = 1/r$ to study the asymptotic form of the field by expanding near $y \simeq 0$. In this coordinate

system we have that

$$ds^2 = -\frac{dt^2}{y^2} - dt^2 + \frac{dy^2}{y^2(1+y^2)} + \frac{d\Omega^2}{y^2} \simeq -\frac{dt^2}{y^2} + \frac{dy^2}{y^2} + \frac{d\Omega^2}{y^2} \tag{1.7}$$

So zooming into any small region of the sphere on the boundary $y = 0$ we have an asymptotic form of the metric that matches the usual Poincare slicing of AdS. In such a coordinate system the asymptotic growth or decay of $\phi(y)$ in the y coordinate is polynomial, proportional to $y^{\Delta_\pm}$ and can be matched to the usual dictionary for a flat slicing, where $\Delta_\pm = \frac{d}{2} \pm \frac{1}{2}\sqrt{d^2 + 4m^2}$. We have made the match $\Delta_+ = \Delta$, the operator dimension for irrelevant perturbations. For relevant perturbations we get a choice.

Reading the coefficients of this expansion has the same interpretation as in flat space: one is a source and the other one is the response. Writing this as

$$\phi(y) \simeq A(f_+ y^{\Delta_+} + f_- y^{\Delta_-}) \tag{1.8}$$

we find that $f_+ = \Gamma(d/2)\Gamma(d/2 - \Delta_+)/\Gamma(1/2(\Delta_-))^2$, and f_- is the same expression with Δ_+ replaced by Δ_-. We now use

$$\Delta = \Delta_+ \tag{1.9}$$

in what follows to distinguish between vev and source, although we will find the answer is symmetric in this choice.

The relation between source and vacuum expectation value is then

$$f_+ = \frac{\Gamma(\frac{d}{2} - \Delta)\Gamma(\frac{1}{2}\Delta)^2}{\Gamma(\Delta - \frac{d}{2})\Gamma(\frac{d}{2} - \frac{\Delta}{2})^2} f_- \tag{1.10}$$

We have artificially chosen $\Delta = \Delta_+$ over Δ_- to indicate the vacuum expectation value

versus the source as one would do for irrelevant perturbations, but since the expressions for f_+ and f_- are symmetric in the exchange of Δ_+ and Δ_-, we can eliminate the distinction in equation (1.10). Notice that this relation seems to be completely independent of the normalization of the field ϕ. We will explain how to get the correct normalization later.

The conformal field theory computation

The basic question for the conformal field theory computation is how does one compute the two point function on the cylinder. Since the cylinder results from a Weyl rescaling of the plane, the two point functions are related to each other in a standard way. The Weyl rescaling is as follows

$$ds^2 = d\vec{x}^2 = r^2\left(\frac{dr^2}{r^2} + d\Omega_{d-1}^2\right) \to d\tau^2 + d\Omega_{d-1}^2 \tag{1.11}$$

which uses a Weyl factor of r^2 (the rescaling of units is by a factor of $r = \exp(\tau)$). As a primary field of conformal dimension Δ, $\mathcal{O}(x)$ will need to be rescaled by $\mathcal{O}(\theta, r) \simeq r^{\Delta}\mathcal{O}(x)$ to translate to the new rescaled metric. For the two point functions this means that

$$\langle \mathcal{O}(\tau_1, \theta_1)\mathcal{O}(\tau_2, \theta_2)\rangle_{cyl} = \frac{\exp(\Delta\tau_1)\exp(\Delta\tau_2)}{|x_1 - x_2|^{2\Delta}} = \frac{1}{(\exp[(\tau_1 - \tau_2)] + \exp[(\tau_2 - \tau_1)] - 2\cos(\theta_{rel}))^{\Delta}} \tag{1.12}$$

where θ_{rel} is the angle computed between the unit vectors $\hat{x}_1, \hat{x}_2$ in standard cartesian coordinates. If we choose $\hat{x}_1$ to be fixed, and at the north pole, the angle θ_{rel} is the polar angle of the insertion of $\mathcal{O}$ over which we will integrate. Since the answer only depends on the the difference of the times, $\tau_2 - \tau_1$, the end result is time translation invariant.

Notice that we have used throughout conformal primaries that are unit normalized in the Zamolodchikov metric.

Now we need to integrate over the angles and the relative time τ. Our expression for C_Δ reduces to the following definite double integral

$$C_\Delta = \int_{-\infty}^{\infty} d\tau \int_0^\pi d\theta \sin^{d-2}\theta Vol(S_{d-2}) \frac{1}{2^\Delta(\cosh\tau - \cos\theta)^\Delta} \tag{1.13}$$

$$= 2^{1-\Delta} Vol(S_{d-2}) \int_1^\infty du \frac{1}{\sqrt{u^2-1}} \int_{-1}^1 dv (1-v^2)^{\frac{d-3}{2}} [u-v]^{-\Delta} \tag{1.14}$$

where we have changed variables to $u = \cosh\tau$ and $v = \cos\theta$. For the integral to converge absolutely, we need that $0 < 2\Delta < d$, but once we find an analytic formula for arbitrary $0 < 2\Delta < d$ we can analytically continue it for all values of Δ, d. The volume of spheres can be computed in arbitrary dimensions as is done in dimensional regularization, so we also get an analytic answer for the variable d itself. Any answer we get can therefore be interpreted as one would in a real space dimensional regularization formalism, where we keep the operator dimension fixed but arbitrary, but where we allow the dimension of space to vary. The final answer we get is

$$C_\Delta = \pi^{\frac{(d+1)}{2}} 2^{1-\Delta} \left[\frac{\Gamma(\frac{d}{2}-\Delta)\Gamma(\frac{\Delta}{2})}{\Gamma(\frac{d}{2}-\frac{\Delta}{2})^2 \Gamma(\frac{1}{2}+\frac{\Delta}{2})} \right] \tag{1.15}$$

Divergences

On comparing the answers for the AdS and CFT calculation, equations (1.10) and (1.15) seem to be completely different. But here we need to be careful about normalizations of the operator $\mathcal{O}$ in the conformal field theory and the corresponding fields in the gravity formulation. We should compare the Green's function of the field ϕ in gravity and take it to the boundary to match the two point function one expects in the CFT

dual. The correct normalization factor that does so can be found in equation (A.10) in [45]. Naively, it seems that we just need to multiply the result from equation (1.15) by $\frac{\Gamma(\Delta)}{2\pi^{\frac{d}{2}}\Gamma(\Delta-\frac{d}{2}+1)}$ and then we might expect

$$\frac{f_+}{f_-} \simeq \frac{\Gamma(\Delta)}{2\pi^{\frac{d}{2}}\Gamma(\Delta-\frac{d}{2}+1)} C_\Delta. \tag{1.16}$$

However, if we compare the ratio of the left hand side to the right hand side we get that the ratio of the two is given by

$$\frac{f_+}{f_-}\left(\frac{\Gamma(\Delta)}{2\pi^{\frac{d}{2}}\Gamma(\Delta-\frac{d}{2}+1)} C_\Delta\right)^{-1} = 2\Delta - d = \Delta_+ - \Delta_- \tag{1.17}$$

Happily, this extra factor is exactly what is predicted from the work [46] (in particular, eq. 4.24). See also [47, 48]. This is because one needs to add a counter-term to the action of the scalar field when one uses a geometric regulator in order to have a well defined boundary condition in gravity.

We see then that the gravity answer and the field theory answer match each other exactly, for arbitrary d, Δ once the known normalization issues are dealt with carefully. Now we want to interpret the end result C_Δ itself.

The expression we found has singularities at specific values of Δ. These arise from poles in the Γ function, which occur when $(d/2 - \Delta)$ is a negative integer. However, these poles are cancelled when $(d - \Delta)/2$ is a negative integer, because we then have a double pole in the denominator. For both of these conditions to be true simultaneously, we need both d and Δ to be even, and furthermore $\Delta \geq d$. The origin of such poles is from the UV structure of the integral (1.2). The singular integral (evaluated at $x = 0$)

is of the form

$$A_{sing} = \int_0^\epsilon d^d y\, y^{-2\Delta} \propto \int_0^\epsilon dy\, y^{d-1-2\Delta} \simeq \int_{1/\epsilon}^\infty dp\, p^{d-1}(p^2+m^2)^{-g} \tag{1.18}$$

where $g = d - \Delta$ and in the last step we introduced a momentum like variable $p = 1/y$ and a mass m infrared regulator to render it into a familiar form for dimensional regularization integrals that would arise from Feynman diagrams. Singularities on the right hand side arise in dimensional regularization in the UV whenever there are logarithmic subdivergences. This can be seen by factorizing $p^2 + m^2 = p^2(1 + m^2/p^2)$ and expanding in power series in m^2. Only when $d - 1 - 2g - 2k = -1$ for some non-negative integer k do we expect a logarithmic singularity. In our case, with $-g = \Delta - d$, the condition for such a logarithmic singularity is that $-g = \Delta - d = -\frac{d}{2} + k$, which is exactly the same condition as we found for there to exist poles in the numerator of equation (1.15). The first such singularity arises when $\Delta = d/2$. Beyond that, the integral in equation (1.14) is not convergent, but is rendered finite in the dimensional regularization spirit. Notice that this was never really an issue in the gravitational computation, since the final answer depended only the asymptotic expansion of hypergeometric functions and we never had to do an integral. The presence of singularities in gravity has to do with the fact that when $\Delta_+ - \Delta_-$ is twice an integer, then the two linearly independent solutions to the hypergeometric equation near $y = 0$ have power series expansions where the exponents of y match between the two. Such singularities are resolved by taking a limit which produces an additional logarithm between the two solutions. We should take this match to mean that the AdS gravity computation already *knows* about dimensional regularization.

Another interesting value for Δ is when we take $\Delta \to d$. The denominator will have a

double pole that will always render the number $C_{\Delta=d} = 0$. This is exactly as expected for a marginal operator in a conformal field theory: it should move us to a near conformal point where all one point functions of non-trivial local operators vanish.

1.3 The energy of a quench

After concluding that the AdS and CFT calculation really did give the same answer for a constant perturbation we want to understand the energy stored in such a solution. This needs to be done carefully, because as we have seen divergences can appear. Under such circumstances, we should compare the new state to the vacuum state in the absence of a perturbation and ask if we get a finite answer for the energy. That is, we need to take the state and quench the dynamics to the unperturbed theory. In that setup one can compute the energy unambiguously.

We would also like to have a better understanding of the origin of the divergences in field theory, to understand how one can regulate the UV to create various states we might be interested in. For this task we will now do a Hamiltonian analysis. Although in principle one could use a three point function including the stress tensor and integrate, performing a Hamiltonian analysis will both be simpler and more illuminating as to what is the physics of these situations. Also, it is more easily adaptable to a real time situation.

A Hamiltonian approach

The perturbation we have discussed in the action takes the Euclidean action $S \to S + \alpha \int \mathcal{O}$. When thinking in terms of the Hamiltonian on a sphere, we need to take

$$H \to H + \alpha \int d\Omega' \mathcal{O}(\theta') \tag{1.19}$$

and we think of it as a new time independent Hamiltonian. When we think of using α as a perturbation expansion parameter, we need to know the action of $\int d\Omega' \mathcal{O}(\theta')$ on the ground state of the Hamiltonian $\mathcal{O}(\theta')\,|0\rangle$. This is actually encoded in the two point function we computed. Consider the time ordered two point function with $\tau_1 > \tau_2$

$$\begin{aligned}
\langle \mathcal{O}(\tau_1,\theta_1)\mathcal{O}(\tau_2,\theta_2)\rangle_{cyl} &= \frac{1}{(\exp[(\tau_1-\tau_2)]+\exp[(\tau_2-\tau_1)]-2\cos(\theta_{rel}))^{\Delta}} && (1.20)\\
&= \sum_s \langle 0|\mathcal{O}(\theta_1)\exp(-H\tau_1)\,|s\rangle\,\langle s|\exp(H\tau_2)\mathcal{O}(\theta_2)|0\rangle && (1.21)\\
&= \sum_s \exp(-E_s(\tau_1-\tau_2))\,\langle 0|\,\mathcal{O}(\theta_2)\,|s\rangle\,\langle s|\,\mathcal{O}(\theta_1)\,|0\rangle && (1.22)
\end{aligned}$$

where s is a complete basis that diagonalizes the Hamiltonian H and we have written the operators $\mathcal{O}(\tau) \simeq \exp(H\tau)\mathcal{O}(0)\exp(-H\tau)$ as corresponds to the Schrodinger picture. The states $|s\rangle$ that can contribute are those that are related to $\mathcal{O}$ by the operator-state correspondence: the primary state of $\mathcal{O}$ and it's descendants. When we integrate over the sphere, only the descendants that are spherically invariant can survive. For a primary $\mathcal{O}(0)$, these are the descendants given by $(\partial_\mu\partial^\mu)^k\mathcal{O}(0)$. The normalized states corresponding to these descendants will have energy (dimension) $\Delta+2k$, and are unique for each k. We will label them by $\Delta+2k$. We are interested in computing the amplitudes

$$A_{\Delta+2k} = \langle \Delta+2k| \int d\Omega' \mathcal{O}(\theta')\,|0\rangle \qquad (1.23)$$

These amplitudes can be read from equation (1.21) by integration over θ_1, θ_2. Indeed, we find that

$$\int d^{d-1}\Omega \langle \mathcal{O}(\tau_1,\theta_1)\mathcal{O}(\tau_2,\theta_2)\rangle_{cyl} = 2^{-\Delta} Vol(S_{d-2}) \int_{-1}^{1} dv (1-v^2)^{\frac{d-3}{2}} [\cosh(\tau) - v]^{-\Delta} \quad (1.24)$$

$$= \pi^{\frac{d}{2}} 2^{1-\Delta} \cosh[\tau]^{-\Delta}\ {}_2\tilde{F}_1[\frac{\Delta}{2}, \frac{1+\Delta}{2}; \frac{d}{2}; \cosh^{-2}(\tau)] \quad (1.25)$$

$$= M \sum |A_{\Delta+2k}|^2 \exp[(-\Delta-2k)\tau] \quad (1.26)$$

where $\tau = \tau_1 - \tau_2$ and ${}_2\tilde{F}_1$ is the regularized hypergeometric function. From this expression further integration over Ω_1 is trivial: it gives the volume of the sphere $Vol(S^{d-1})$. We want to expand this in powers of $\exp(-\tau)$. To do this we use the expression $\cosh(\tau) = \exp(\tau)(1+\exp(-2\tau))/2$, and therefore

$$\cosh^{-a}(\tau) = \exp(-a\tau)2^a[1+\exp(-2\tau)]^{-a} = \sum_{n=0}^{\infty} 2^a \exp(-a\tau - 2n\tau)(-1)^n \frac{\Gamma[a+n]}{n!\Gamma[a]} \quad (1.27)$$

Inserting this expression into the power series of the hypergeometric function appearing in (1.25) gives us our desired expansion. Apart from common factors to all the amplitudes $A_{\Delta+2k}$ (which are trivially computed for $k=0$) we are in the end only interested in the k dependence of the amplitude itself. After a bit of algebra one finds that

$$|A_{\Delta+2k}|^2 \propto \frac{\Gamma[k+\Delta]\Gamma[\Delta - \frac{d}{2} + k + 1]}{\Gamma[1+\Delta-\frac{d}{2}]^2 \Gamma[k+\frac{d}{2}]k!} \quad (1.28)$$

and to normalize we have that

$$|A_{\Delta}|^2 = [Vol(S^{d-1})]^2 \quad (1.29)$$

For these amplitudes to make sense quantum mechanically, their squares have to be positive numbers. This implies that none of the Γ functions in the numerator can be negative. The condition for that to happen is that the argument of the Γ function in the numerator must positive and therefore $\Delta \geq \frac{d}{2} - 1$, which is the usual unitary condition for scalar primary fields. Also, at saturation $\Delta = d/2 - 1$ we have a free field and then the higher amplitudes vanish $A_{k>0}/A_0 = 0$. This is reflected in the fact that $\partial_\mu \partial^\mu \phi = 0$ is the free field equation of motion.

We are interested in comparing our results to the AdS setup. In the CFT side this usually corresponds to a large N field theory. If the primary fields we are considering are single trace operators, they give rise to an approximate Fock space of states of multitraces, whose anomalous dimension is the sum of the individual traces plus corrections of order $1/N^2$ from non-planar diagrams. In the large N limit we can ignore these corrections, so we want to imagine that the operator insertion of $\mathcal{O}$ is a linear combination of raising and lowering operators $\int d\Omega \mathcal{O}(\theta) \simeq \sum A_{\Delta+2k} a^\dagger_{2k+\Delta} + A_{\Delta+2k} a_{2k+\Delta}$ with $[a, a^\dagger] = 1$. In such a situation we can write the perturbed Hamiltonian in terms of the free field representation of the Fock space in the following form

$$H + \delta H = \sum E_s a_s^\dagger a_s + \alpha (\sum A_{\Delta+2k} a^\dagger_{2k+\Delta} + A_{\Delta+2k} a_{2k+\Delta}) + O(1/N^2) a^\dagger a^\dagger a a + \dots \quad (1.30)$$

Indeed, when we work in perturbation theory, if this Fock space exists or not is immaterial, as the expectation value of the energy for a first order perturbation will only depend on the amplitudes we have computed already. It is for states that do not differ infinitesimally from the ground state that we need to be careful about this and this Fock space representation becomes very useful.

When we computed using conformal perturbation theory abstractly, we were consid-

ering the vacuum state of the Hamiltonian in equation (1.30) to first order in α. We write this as

$$|0\rangle_\alpha = |0\rangle + \alpha\,|1\rangle \tag{1.31}$$

and we want to compute the value of the energy for the unperturbed Hamiltonian for this new state. This is what quenching the system to the unperturbed theory does for us. We find that

$$\langle 0_\alpha|\, H\,|0\rangle_\alpha = \alpha^2\,\langle 1|\, H\,|1\rangle \tag{1.32}$$

Now, we can use the expression (1.30) to compute the state $|0\rangle_\alpha$. Indeed, we find that we can do much better than infinitesimal values of α. What we can do is realize that if we ignore the subleading pieces in N then the ground state for $H + \delta H$ is a coherent state for the independent harmonic oscillators $a^\dagger_{2k+\Delta}$. Such a coherent state is of the form

$$|0\rangle_\alpha = \mathcal{N}\exp(\sum \beta_{2k+\Delta} a^\dagger_{2k+\Delta})\,|0\rangle \tag{1.33}$$

For such a state we have that

$$\langle H + \delta H\rangle = \sum (2k+\Delta)|\beta_{2k+\Delta}|^2 + \alpha\beta_{2k+\Delta}A_{2k+\delta} + \alpha\beta^*_{2k+\Delta}A_{2k+\delta} \tag{1.34}$$

and the energy is minimized by

$$\beta_{2k+\Delta} = -\alpha\frac{A_{2k+\Delta}}{2k+\Delta} \tag{1.35}$$

Once we have this information, we can compute the energy of the state in the unperturbed setup and the expectation value of $\mathcal{O}$ (which we integrate over the sphere). We find that

$$\langle H\rangle = \sum (2k+\Delta)|\beta_{2k+\Delta}|^2 = \alpha^2 \sum \frac{|A_{2k+\Delta}|^2}{2k+\Delta} \tag{1.36}$$

$$\langle \mathcal{O}\rangle \simeq \sum 2A_{k+2\Delta}\beta_{2k+\Delta} \simeq -2\alpha \sum \frac{|A_{2k+\Delta}|^2}{2k+\Delta} \tag{1.37}$$

so that in general

$$\langle H\rangle \simeq -\frac{\alpha\langle \mathcal{O}\rangle}{2} \tag{1.38}$$

That is, the integrated one point function of the operator $\mathcal{O}$ over the sphere and the strength of the perturbation is enough to tell us the value of the energy of the state. For both of these to be well defined, we need that the sum appearing in (1.36) is actually finite. Notice that this matches the Ward identity for gravity [41] integrated adiabatically (for a more general treatment in holographic setups see [49]).

This is what we will take on next.

Amplitude Asymptotics, divergences and general quenches

Our purpose now is to understand in more detail the sum appearing in (1.36). What we are interested in is the convergence and asymptotic values for the terms in the series, that is, we want to understand the large k limit. This can be read from equation (1.28) by using Stirlings approximation $\log\Gamma[t+1] \simeq (t)\log(t) - (t)$ in the large t limit. We find that after using this approximation on all terms that depend on k, that

$$\begin{aligned}
\log(A^2_{2k+\Delta}) &\simeq (k+\Delta-1)\log(k+\Delta-1) + (k+\Delta-d/2)\log(k+\Delta-d/2) && (1.39)\\
&\quad -(k+d/2-1)\log(k+d/2-1) - k\log(k) + O(1) && (1.40)\\
&\simeq (\Delta-1+\Delta-\frac{d}{2}-(\frac{d}{2}-1))\log k = (2\Delta-d)\log k && (1.41)
\end{aligned}$$

So that the sum is bounded by a power law in k

$$\sum \frac{|A_{2k+\Delta}|^2}{2k+\Delta} \simeq \sum \frac{1}{k^{d+1-2\Delta}} \tag{1.42}$$

Again, we see that convergence of the sum requires $2\Delta - d < 0$. This is the condition to have a finite vacuum expectation value of both the energy and the operator $\mathcal{O}$. If we consider instead the L^2 norm of the state, the norm is finite so long as $d + 2 - 2\Delta > 1$, that is, so long as $\Delta < (d+1)/2$. The divergence in the window $d/2 \leq \Delta < (d+1)/2$ is associated with the unboundedness of the Hamiltonian, not to the infinite norm of the state.

In general we can use higher order approximations to find subleading terms in the expression (1.41). Such approximations will give that $A_{2k+\Delta}$ will have a polynomial expression with leading term as above, with power corrections in $1/k$. Only a finite number of such corrections lead to divergent sums, so the problem of evaluating $\langle \mathcal{O} \rangle$ can be dealt with using a finite number of substractions of UV divergences. In this sense, we can renormalize the answer with a finite number of counterterms. A particularly useful regulator to make the sum finite is to choose to modify $A_{2k+\Delta} \to A_{2k+\Delta} \exp(-\epsilon(2k+\Delta))$. This is like inserting the operator $\mathcal{O}$ at time $t = 0$ in the Euclidean cylinder and evolving it in Euclidean time for a time ϵ. Because the growth of the coefficients is polynomial in k, any such exponential will render the sum finite. We can trade the divergences in the sums for powers of $1/\epsilon$ and then take the limit $\epsilon \to 0$ of the regulated answer. This is beyond the scope of the present paper.

Notice that we can also analyze more general quenches from studying equation (1.34). All we have to do is make α time dependent. The general problem can then be analyzed in terms of linearly driven harmonic oscillators, one for each $a^\dagger, a$ pair. Since the driving

force is linear in raising and lowering operators, the final state will always be a coherent state as in equation (1.33) for some β which is the linear response to the source. The differential equation, derived from the Schrodinger equation applied to a time dependent coherent state, is the following

$$i\dot{\beta}_{2k+\Delta}(t) = (2k+\Delta)\beta_{2k+\Delta} + \alpha(t)A_{2k+\Delta} \tag{1.43}$$

The solution is given by

$$\beta_{2k+\Delta}(t) = \beta_{2k+\Delta}(0)\exp(-i\omega t) + A_{2k+\Delta}\int_0^\infty dt'\alpha(t')\theta(t-t')\exp(-i\omega(t-t')) \tag{1.44}$$

with $\omega = 2k+\Delta$ the frequency of the oscillator.

Consider the case that α only acts over a finite amount of time between $0, \tau$ and that we start in the vacuum. After the time τ the motion for β will be trivial, and the amplitude will be given by

$$\beta_{2k+\Delta}(\tau) = A_{2k+\Delta}\exp(-i(2k+\Delta)\tau)\int_0^\tau dt'\alpha(t')\exp(i\omega t') \tag{1.45}$$

and all of these numbers can be obtained from the Fourier transform of $\alpha(t)$. Notice that these responses are always correct in the infinitesimal α regime, as can be derived using time dependent perturbation theory. What is interesting is that in the large N limit they are also valid for $\alpha(t)$ that is not infinitesimal, so long as the $O(1/N)$ corrections can still be neglected. One can also compute the energy of such processes. In particular, so long as $\Delta < d/2$, any such experiment with bounded $\alpha(t)$ will give a finite answer.

The simplest such experiment is to take α constant during a small interval $\tau = \delta t <<$

1. For modes with small ω, that is, those such that $\omega\delta t < 1$, we then have that

$$\beta_{2k+\Delta}(\tau) \simeq A_{2k+\Delta}\alpha\delta t \tag{1.46}$$

While for those modes such that $\omega\delta t > 1$, we get that

$$|\beta_{2k+\Delta}(\tau)| \simeq \alpha\frac{A_{2k+\Delta}}{\omega} \tag{1.47}$$

When we compute the energy of such a configuration, we need to divide the sum between high frequency and low frequency modes. The energy goes as

$$E \simeq \sum \omega|\beta_{2k+\Delta}|^2 \simeq \int_0^{1/(2\delta t)} dk\omega|A_{2k+\Delta}\alpha\delta t|^2 + \int_{1/(2\delta t)}^{\infty} dk\frac{|\alpha A_{2k+\Delta}|^2}{\omega} \tag{1.48}$$

now we use the fact that $|A_{2k+\Delta}|^2 \simeq k^{2\Delta-d}$ and that $\omega \propto k$ to find that

$$E \simeq |\alpha|^2(\delta t)^{d-2\Delta} \tag{1.49}$$

which shows an interesting power law for the energy deposited into the system. One can similarly argue that the one point function of $\mathcal{O}(\tau)$ scales as $\alpha(\delta t)^{d-2\Delta}$: for the slow modes, the sum is proportional to $\sum A_{2k+\Delta}^2\alpha\delta t$, while for the fast modes one can argue that they have random phases and don't contribute to $\mathcal{O}(\tau)$.

If we want to study the case $\Delta \geq d/2$, divergences arise, so we need to choose an $\alpha(t)$ that is smooth enough that the high energy modes are not excited in the process because they are adiabatic, but if we scale that into a δt window, the adiabatic modes are going to be those such $\omega\delta t > 10$, let's say. Then for these modes we take $\beta \simeq 0$, and then the estimate is also as above. For $\Delta = d/2$, in an abrupt quench one obtains a logarithmic

singularity rather than power law, coming from the UV modes. This matches the results in [44] and gives a reason for their universality as arising from the universality of 2-point functions in conformal perturbation theory. Essentially, the nature of the singularities that arise is that the amplitudes to generate descendants are larger than amplitudes to generate primaries, so the details of the cutoff matter.

Here is another simple way to understand the scaling for the one point function of the operator $\mathcal{O}(\tau)$. The idea is that we need to do an integral similar to $\int d^d x \mathcal{O}(\tau)\alpha(x)\mathcal{O}(x)$, but which takes into account causality of the perturbation relative to the response. If we only turn on the perturbation by a small amount of time δt, the backwards lightcone volume to the insertion of an operator at $\tau = \delta t$ is of order δt^d, and this finite volume serves as an infrared regulator, while the two point function that is being integrated is of order $\delta t^{-2\Delta}$. When we combine these two pieces of information we get a result proportional to $\delta t^{d-2\Delta}$, which again is finite for $\Delta < d/2$ and otherwise has a singularity in the corresponding integral. Similarly, the energy density would be an integral of the three point function $T\mathcal{O}\mathcal{O} \simeq \delta t^{-2\Delta-d}$ times the volume of the past lightcone squared which is again proportional to δt^{2d}, giving an answer with the scaling we have already found. The additional corrections would involve an extra insertion of $\mathcal{O}$ and the volume of the past lightcone, so they scale as $\delta t^{d-\Delta}$, multiplied by the amplitude of the perturbation. This lets us recover the scalings of the energy [44] in full generality.

A note on renormalization

So far we have described our experiment as doing a time dependent profile for $\alpha(t)$ such that $\alpha(t) = 0$ for $t > \tau$. Under such an experiment, we can control the outcome of the operations we have described and we obtain the scaling relations that we want. If on the other hand we want to measure the operator $\mathcal{O}(\theta)$ for some $t < \tau$, we need to be

more careful. This is where we need a better prescription for subtracting divergences. To linear order in $\alpha(t)$, all UV divergences should be polynomial in the coupling constants and their derivatives. Also, since we are working to linear order in $\alpha(t)$, these can only depend on $\alpha(t)$ and it's time derivatives. Another object that can show up regularly is the curvature of the background metric in which we are doing conformal field theory. That is, we can have expressions of the form $\partial_t^k \alpha(t) R^s$ appearing as counterterms in the effective action. These are particularly important in the case of logarithmic divergences, as these control the renormalization group.

For our purposes, we need to identify when such logarithmic divergences can be present. In particular, we want to do a subtraction of the adiabatic modes (which do contribute divergences) to the one point function of $\mathcal{O}(\theta, t)$ at times $t < \tau$. To undertake such a procedure, we want to solve equation (1.43) recursively. We do this by taking

$$\beta_{2k+\Delta}(t) = -\alpha(t)\frac{A_{2k+\Delta}}{2k+\Delta} + \beta^1_{2k+\Delta}(t) + \beta^2_{2k+\Delta}(t) + \dots \tag{1.50}$$

where we determine the $\beta_i(t)$ recursively for high k by substituting $\beta_{2k+\Delta}(t)$ as above in the differential equation. The solution we have written is correct to zeroth order, and we then write the next term as follows

$$-i\dot{\alpha}(t)\frac{A_{2k+\Delta}}{2k+\Delta} = (2k+\Delta)\beta^1_{2k+\Delta}(t) \tag{1.51}$$

and in general

$$i\dot{\beta}^{n-1}_{2k+\Delta}(t) = (2k+\Delta)\beta^n_{2k+\Delta}(t) \tag{1.52}$$

This will generate a series in $\frac{1}{(2k+\Delta)^n}\partial_t^n \alpha(t)$, which is also proportional to $A_{2k+\Delta}$. We then substitute this solution into the expectation value of $\mathcal{O}(t, \theta)$, where we get an expression

of the form

$$\langle \mathcal{O}(t) \rangle \simeq \sum_{k,\ell} |A_{2k+\delta}|^2 \frac{c_\ell}{(2k+\Delta)^{\ell+1}} \partial_t^\ell \alpha(t) \simeq \int dk \sum_\ell \frac{1}{k^{2\Delta-d}} \frac{c_\ell}{(2k+\Delta)^{\ell+1}} \partial_t^\ell \alpha(t) \quad (1.53)$$

The right hand side has a logarithmic divergence when $2\Delta - d + \ell = 0$. Notice that this divergence arises from the combination $\beta + \beta^*$, so the terms with odd derivatives vanish because of the factors of i in equation (1.52). Thus, such logarithmic divergences will only be present when ℓ is even. We need then that $\Delta = d/2 + k$, where k is an integer. Notice that this is the same condition that we need to obtain a pole in the numerator of the Gamma function in equation (1.14). We see that such logarithmic divergences are exactly captured by dimensional regularization. As a logarithmic divergence, it needs to be of the form $\log(\Lambda_{UV}/\Lambda_{IR}) = \log(\Lambda_{UV}/\mu) + \log(\mu/\Lambda_{IR})$. In our case, the IR limit is formally set by the radius of the sphere, while the UV is determined by how we choose to work precisely with the cutoff. The counterterm is the infinite term $\log(\Lambda_{UV}/\mu)$, but the finite term depends on the intermediate scale μ, which is also usually taken to be a UV scale which is finite. This lets us consider the Lorentzian limit by taking a small region of the sphere and to work with δt as our infrared cutoff: only the adiabatic modes should be treated in the way we described above. Then the logarithmic term scales as $\log((\mu\delta t))\partial_t^{2\Delta-d}\alpha(t)$. These logarithmic terms are exactly as written in [44]. Notice that after the quench, we have that $\alpha(t) = 0$ and all of it's derivatives are zero, so no counterterms are needed at that time. We only need the pulse $\alpha(t)$ to be smooth enough so that the state we produce has finite energy.

1.4 Conclusion

In this paper we have shown how to do conformal perturbation theory on the cylinder rather than in flat space. The main reason to do so was to use a physical infrared regulator in order to understand the process of renormalization of UV divergences in a more controlled setting. We showed moreover that the results that are found using AdS calculations actually match a notion of dimensional regularization where the dimension of the perturbation operator stays fixed. In this sense the AdS geometry knows about dimensional regularization as a regulator. This is an interesting observation that merits closer attention. In particular, it suggests that one can try a real space dimensional regularization approach to study perturbations of conformal field theory.

We then showed that one could treat in detail also a time dependent quench, and not only where we able to find the energy after a quench, but we also were able to understand scalings that have been observed before for fast quenches. Our calculations show in what sense they are universal. They only depend on the two point function of the perturbation. The singularities that arise can be understood in detail in the Hamiltonian formulation we have pursued, and they arise from amplitudes to excite descendants increasing with energy, or just not decaying fast enough. In this way they are sensitive to the UV cutoff associated to a pulse quench: the Fourier transform of the pulse shape needs to decay sufficiently fast at infinity to compensate for the increasing amplitudes to produce descendants. We were also able to explain some logarithmic enhancements for the vacuum expectation values of operators during the process of the quench that can be understood in terms of renormalizing the theory to first order in the perturbation. Understanding how to do this to higher orders in the perturbation is interesting and should depend on the OPE coefficients of a specific theory.

Chapter 2

Log enhancements in conformal perturbation theory and their real time interpretation

2.1 Introduction

Since the advent of the AdS/CFT correspondence [3], the study of conformal field theories [1] has advanced substantially, as one can solve difficult problems in the dual gravity theory instead. Many of the results found this way are not particular to gravitational theories: they are universal in conformal field theory. For example, in the study of quenches, one can find the anomalous scaling of various dynamical expectation values [43, 50]. This behavior can be understood from conformal perturbation theory, as shown in [35]. In particular, in this last work, it was argued that many of the problems can be handled by the use of dimensional regularization on the cylinder, where one leaves the

[1] This includes deformations away from the conformal fixed point.

operator dimensions fixed, but integrates the angular variables in arbitrary number of spacetime dimensions.

In this paper, we study corrections to various correlation functions in conformal perturbation theory, using dimensional regularization techniques. These results will be universal and can be applied to the gravitational theory via the AdS/CFT duality. Specifically, we will analyze the divergence structure of these corrections and provide a novel interpretation of their origin.

The general problem we are studying is that of a theory which has been deformed away from a conformal fixed point by a scalar operator $\lambda \int d^d x f(x) \mathcal{O}_D(x)$ (the subscript D standing for deformation). We consider relevant, marginal, and irrelevant operators with dimension h_D and work in arbitrary number of spacetime dimensions d. Notice, we further allow the deformation to be spacetime dependent, including the function $f(x)$ and taking the constant λ to be our small parameter. Correlation functions in the new theory take the form

$$\langle \mathcal{O}_1(x_1) \dots \mathcal{O}_N(x_N) \rangle_\lambda = \left\langle \mathcal{O}_1(x_1) \dots \mathcal{O}_N(x_N) e^{\lambda \int d^d x f(x) \mathcal{O}_D(x)} \right\rangle_{\text{CFT}} \tag{2.1}$$

where the correlators on the left hand side indicate the path integral in perturbed theory, while those on the right are in the conformal theory. One can expand the right hand side to find

$$\begin{aligned} \langle \mathcal{O}_1(x_1) \dots \mathcal{O}_N(x_N) \rangle_\lambda = & \langle \mathcal{O}_1(x_1) \dots \mathcal{O}_N(x_N) \rangle_{\text{CFT}} \\ & + \lambda \int d^d x f(x) \langle \mathcal{O}_1(x_1) \dots \mathcal{O}_N(x_N) \mathcal{O}_D(x) \rangle_{\text{CFT}} + O(\lambda^2) \end{aligned} \tag{2.2}$$

We assume that the conformal field theory in question has a known set of operator dimensions (a spectrum of conformal representations), and known three point functions.

One then simply includes, for instance, the known form of the three point function

$$\langle \mathcal{O}_1(z)\mathcal{O}_2(w)\mathcal{O}_3(x)\rangle_{\rm CFT} = \frac{f_{123}}{|z-w|^{h_1+h_2-h_3}|x-z|^{h_1+h_3-h_2}|x-w|^{h_2+h_3-h_1}} \tag{2.3}$$

and only needs to integrate to find the desired corrections.

However, these integrals can be tricky and are divergent. Consider, for instance, the correction to the one point function when the theory is perturbed by a constant deformation

$$\langle \mathcal{O}_D(0)\rangle_\lambda = \lambda \int \frac{d^d x}{|x|^{2h_D}} + O(\lambda^2) \tag{2.4}$$

where we have used the known form of the two point function in a CFT. This expression diverges either at the origin (a UV divergence) or at infinity (an IR divergence), or both if $h_D = d/2$. Transforming the theory to the cylinder can provide an infrared regulator (the size of the cylinder). The answer will then be IR finite, but there still might be UV divergences. This is what was studied by the present authors in [35]. In that paper, it was shown how to remove the divergences by using a modified version of dimensional regularization, where d is varied, but the operator dimensions are fixed. This was shown to be very similar to keeping d fixed and varying the dimensions of the operators: the results were expressed in terms of gamma functions of linear combinations of d, h_D. Logarithmic divergences occurred at special values associated with the pole structure of the gamma functions. This was also shown to be equal to the solution of the problem in the gauge/gravity duality.

Let's explicitly see how this IR divergence was tamed. To transform the operators from the plane to the cylinder, one must introduce powers of the Weyl rescaling. That is,

$$\langle \mathcal{O}_1 \dots \mathcal{O}_N\rangle_{\rm cyl} = |x_1|^{\Delta_1} \dots |x_N|^{\Delta_N} \langle \mathcal{O}_1 \dots \mathcal{O}_N\rangle_{\rm plane} \tag{2.5}$$

It was this additional factor that helped with the convergence of the integral. Interestingly, one can alternatively think of this factor of as having come from having made the deformation spacetime dependent, with a source that scales as $f(x) = |x|^{h_D - d}$

$$\langle \mathcal{O}(z) \rangle_\lambda = \lambda \int d^d x f(x) \frac{1}{|x-z|^{2h_D}} + O(\lambda^2) = \lambda \int d^d x \frac{1}{|x|^{d-h_D}} \frac{1}{|x-z|^{2h_D}} + O(\lambda^2) \quad (2.6)$$

In this case, the infrared cutoff is provided by the fact that the profile of $f(x)$ dies sufficiently fast at infinity. (Note the additional factor of $|x|^d$ comes from the change of measure associated to the Weyl rescaling transformation.)

In this work, we will consider various functions that make these integrals more convergent and will discuss the physics of the divergences that remain. In particular, we will see that the correlators have logarithmic enhancements and will show that some of the singularities that appear in the process of evaluating the integrals with dimensional regularization techniques can be understood in terms of secular (resonant) behavior in time dependent perturbation theory on the cylinder.

The paper is organized as follows: We first consider three physically interesting master integrals and analyze the divergences in the resulting expressions. Next, we study the special case of marginal deformations. And finally, we relate our computations to time dependent perturbation theory on the cylinder and see how the singularities can be interpreted as secular resonances that arise in time dependent perturbation theory. The poles and logarithmic enhancements in the plane computations end up reflecting the secular behavior for resonant perturbations in the cylinder.

2.2 Dimensional regularization master integrals

There are three integrals we will consider explicitly in this work. They are all generically of the form

$$I = \int \frac{d^d x\, f(x)}{|x - x_1|^{\alpha_1} \dots |x - x_N|^{\alpha_N}} \tag{2.7}$$

There is a vast array of literature on these Feynman integrals. For a general reference, we suggest [51].

And, in fact, each of our computations have been performed in some form elsewhere. We include the details for completeness and so that one may track the divergence structure throughout the computation. It will be this structure that we are ultimately concerned with.

As is standard practice in evaluating these types of integrals, we will find it to be very useful to introduce Schwinger parameters, given by

$$\frac{1}{|B|^{2a}} = \frac{1}{\Gamma(a)} \int_0^\infty dt t^{a-1} \exp(-t|B|^2) \tag{2.8}$$

2.2.1 Fourier transform of the two point function

The first integral we consider is

$$I_\Delta[\vec{k}; z] = \int d^d x |z - x|^{-2\Delta} \exp(ikx) \tag{2.9}$$

Like in the previous work [35], this gives the first order correction to the one point function in the presence of a deformation. However, rather than regulating by transforming to the cylinder, here we introduce a source that is oscillating in position space $f(x) \simeq \exp(ikx)$. These deformations can be studied in a dual gravitational theory, where they produce

a lattice that breaks translation invariance [2] (see for example [53, 54]). Here, the IR regulator is provided by the scale of the oscillations. The point is that for large distances, the integral is oscillatory and mostly cancels, removing the possible infrared divergence. The small dimensionless parameter is $\lambda|k|^{\Delta-d} << 1$. This has already been computed in other places [48, 55, 56].

We compute with varying d, keeping Δ fixed. One can see that integral is UV divergent if $2\Delta \geq d$, but otherwise should converge. This is because the large radius region is tamed by the oscillatory nature of the integral. In this sense, the momentum scale cuts off the possible infrared singularity.

To perform the integral, we first write it in terms of a Schwinger parametrization

$$I_\Delta[\vec{k};z] = \frac{1}{\Gamma[\Delta]} \int d^d x' \int_0^\infty ds s^{\Delta-1} \exp(-s|x-z|^2) \exp(ikx) \tag{2.10}$$

The net result is that the integral becomes Gaussian in x, and can be done by the usual rules of dimensional regularization. Shifting first the integration variable from x to $x' = x - z$, we get

$$I_\Delta[\vec{k};z] = \frac{1}{\Gamma[\Delta]} \exp(i\vec{k}\vec{z}) \int d^d x' \int_0^\infty ds s^{\Delta-1} \exp(-s|x'|^2) \exp(i\vec{k}\vec{x}') \tag{2.11}$$

and then complete the square to find

$$I_\Delta[\vec{k};z] = \frac{1}{\Gamma[\Delta]} \exp(i\vec{k}\vec{z}) \int d^d x' \int_0^\infty ds s^{\Delta-1} \exp(-s|x'|^2) \exp(-|k|^2/4s) \tag{2.12}$$

[2] One can also do this by adding random disorder [52], which we will not study.

The Gaussian integral is trivially done in d dimensions, giving us

$$I_\Delta[\vec{k};z] = \frac{\sqrt{\pi}^d}{\Gamma[\Delta]} \exp(i\vec{k}\vec{z}) \int_0^\infty ds s^{\Delta-1} s^{-d/2} \exp(-|k|^2/4s) \tag{2.13}$$

Finally, we can change variables to $\tilde{s} = 1/s$, so that

$$I_\Delta[\vec{k};z] = \frac{\sqrt{\pi}^d}{\Gamma[\Delta]} \exp(i\vec{k}\vec{z}) \int_0^\infty d\tilde{s} \tilde{s}^{-\Delta-1} \tilde{s}^{d/2} \exp(-\tilde{s}|k|^2/4) \tag{2.14}$$

which we immediately recognize as a gamma function. The final answer is

$$I_\Delta[\vec{k};z] = \frac{\Gamma[d/2-\Delta]}{\Gamma[\Delta]} \sqrt{\pi}^d \exp(i\vec{k}\vec{z}) \left(|k|^2/4\right)^{\Delta-d/2} \tag{2.15}$$

Generically, the UV divergences for $\Delta > d/2$ have been removed by analytic continuation. The integral is always UV convergent for large enough d, if Δ is kept fixed. This defines a function of d, Δ that can be continued to values where the naive integral has a UV divergence.

Notice that there is a singularity whenever $\Delta - d/2$ is a non-negative integer. These arise as poles in the gamma function. The singularity at $\Delta = d/2$ is exactly a logarithmic divergence. For the other cases, the singularity is a subleading logarithmic divergence. To get a finite answer in those cases, we need to add a counterterm. The counterterm is a polynomial in k^2, multiplied by $1/\epsilon$, where $\epsilon = d - d_0$ is the small parameter that deforms the dimension d away from the dimension d_0 of interest. Because it is polynomial in k^2, it is local. This is a contact term. We write the full expression as follows

$$\langle \mathcal{O}(x)\mathcal{O}(z)\rangle \simeq |z-x|^{-2\Delta} + b_{CT} \Box^{\Delta-d/2} \delta^d(x-z) \tag{2.16}$$

The full final answer needs to be expanded in Taylor series in $d - d_0$. This produces an extra logarithm from

$$(|k|^2)^{d_0/2-d/2} \simeq 1 - \frac{\epsilon}{2}\log(k^2/\mu^2) \tag{2.17}$$

Combined with the pole in the gamma function we get an enhancement of the answer by a logarithm, where we have introduced a renormalization group scale μ^2 for dimensional reasons. The μ^2 lets us shift the finite part of the counterterm to be whatever we wish it to be.

2.2.2 First order correction to the two point function

Another interesting profile is to consider a different scaling function as follows

$$f(x) \simeq 1/|x|^{\alpha} \tag{2.18}$$

where we can choose γ to be real or complex. If we want $f(x)$ to be real, we can also take the real part of the expression. This leads to the same integral that appears when considering a correction to the two point function of two different primary operators $\mathcal{O}_1(z), \mathcal{O}_2(w)$ in conformal perturbation theory. In this case, the infrared regulator is provided by the distance between the operators.

If we consider two such primary operators $\mathcal{O}_1$, $\mathcal{O}_2$ of dimensions h_1, h_2 and a perturbation of the field theory by a scalar operator $\mathcal{O}_D(x)$, then the two point function Green function for the operators is

$$\langle \mathcal{O}_1(z)\mathcal{O}_2(w)\rangle_\lambda = \frac{\delta_{h_1,h_2}}{|z-w|^{h_1+h_2}} + \lambda \int d^d x \langle \mathcal{O}_1(z)\mathcal{O}_2(w)\mathcal{O}_D(x)\rangle_{\text{CFT}} + \dots \tag{2.19}$$

where $\mathcal{O}_D(x)$ is the operator that perturbs away from the conformal fixed point. The

Kronecker delta appearing in the expression can generically depend on spin labels of the operators, and the direction vector between z, w. We will be interested in the simplest setting where both $\mathcal{O}_1, \mathcal{O}_2$ are primary scalar operators (and so is $\mathcal{O}_D$, in order not to break rotational symmetry). If $h_1 \neq h_2$, the first term vanishes, as the two operators then have a vanishing two point function in the conformal field theory. The fact that the right hand side does not generically vanish beyond the leading order in conformal perturbation theory will be referred to as operator mixing.

If we use the known form of the three point function in a CFT, we see that the integral we wish to perform is

$$I[z, w, h_D, d, h_1, h_2] = \int d^d x \frac{1}{|x - z|^{h_1 + h_D - h_2} |x - w|^{h_2 + h_D - h_1}} \tag{2.20}$$

As can be seen, the integral diverges in the infrared if in the asymptotic $|x| \to \infty$ region we have that

$$\int_{x_0}^{\infty} d^d x \frac{1}{|x|^{2h_D}} \tag{2.21}$$

is divergent. The integral is infrared convergent if $2h_D \geq d$.

Similarly, the integral is UV divergent for $x \simeq z$ if $h_1 + h_D - h_2 \geq d$. The same is true near $x \simeq w$ if $h_2 - h_1 + h_D \geq d$, and these follow from keeping the most singular terms near each one of the insertions of the operators.

Adding these two, we find that there is always a UV divergence if $h_D \geq d$. That is, if the operator that performs the deformation $\mathcal{O}_D(x)$ is marginal or irrelevant. The divergences then need to be regulated before getting the correct (renormalized) physical answer.

A standard procedure in the literature is to perform a geometric cutoff: do the integrals until we are within a distance $\delta x < \Lambda^{-1}$ (see for example [57, 58]). This is problem-

atic at higher orders. These integrals can also be handled via dimensional regularization, which is the procedure we will follow. Here we keep h_1, h_2, h_D fixed, and evaluate the integrals for a variable complex d. The integral is defined in the non-convergent region by analytically continuing in d past the singularities.

We will now perform the integral. Again, we start with Schwinger parameterization, which is valid for $a \geq 0$. With this, we find

$$I[z,w,h_D,d,h_1,h_2] = \frac{\int d^dx \int_0^\infty dt_1 \int_0^\infty dt_2 t_1^{\left(\frac{\Delta h+h_D}{2}\right)-1} t_2^{\left(\frac{h_D-\Delta h}{2}\right)-1}}{\Gamma\left(\frac{h_1+h_D-h_2}{2}\right)\Gamma\left(\frac{h_2+h_D-h_1}{2}\right)} \exp(-t_1|x-z|^2 - t_2|x-w|^2) \tag{2.22}$$

where we have introduced $\Delta h = h_1 - h_2$. The Schwinger parametrization is allowed as long as both $h_D \pm \Delta h \geq 0$ and it is defined for other values of these quantities by analytic continuation, contingent on the Γ function being evaluated at a non-singular value (the singularities occur when $2(|\Delta h| - h_D)$ is a non-negative integer). As we see, the net result is that integral over x again becomes Gaussian.

It is convenient to change variables to $t_1 = ty, t_2 = t(1-y)$, so that $dt_1 dt_2 = t dt dy$, so that $t = t_1 + t_2$ as is usually done with Feynman parameters. We get then that

$$\begin{aligned} I[z,w,h_D,d,h_1,h_2] &= \frac{\int d^dx \int_0^\infty t^{h_D-1} dt \int_0^1 dy y^{\left(\frac{\Delta h+h_D}{2}\right)-1}(1-y)^{\left(\frac{h_D-\Delta h}{2}\right)-1}}{\Gamma\left(\frac{h_1+h_D-h_2}{2}\right)\Gamma\left(\frac{h_2+h_D-h_1}{2}\right)} \\ &\quad \times \exp(-ty|x-z|^2 - t(1-y)|x-w|^2) \end{aligned} \tag{2.23}$$

We now complete the square to do the Gaussian integral over x, to get that

$$\begin{aligned} I[z,w,h_D,d,h_1,h_2] &= \frac{\int_0^\infty t^{h_D-1} dt \int_0^1 dy y^{\left(\frac{\Delta h+h_D}{2}\right)-1}(1-y)^{\left(\frac{h_D-\Delta h}{2}\right)-1}}{\Gamma\left(\frac{h_1+h_D-h_2}{2}\right)\Gamma\left(\frac{h_2+h_D-h_1}{2}\right)} \\ &\quad \times \frac{\sqrt{\pi}^d \exp(-ty(1-y)|z-w|^2)}{t^{d/2}} \end{aligned} \tag{2.24}$$

The Gaussian integral has been evaluated in an arbitrary number of (complex) dimensions d by analytic continuation from positive integer dimension, as is standard in dimensional regularization.

What we need to do now is understand the region of t, y plane that picks up the singularities corresponding to $x \simeq z$ or $x \simeq w$ from passing from the equation (2.23) to equation (2.24). Obviously, the Gaussian is convergent as long as $t > 0$, so all the UV singularities are related to the region near $t \simeq 0$. In particular, t_1 small is the UV region of the singularity at z, and t_2 near zero is the UV region near the singularity at w.

Upon integration in t, we get that

$$I[z, w, h_D, d, h_1, h_2] = \frac{\int_0^1 dy y^{\left(\frac{\Delta h + h_D}{2}\right)-1}(1-y)^{\left(\frac{h_D - \Delta h}{2}\right)-1}}{\Gamma\left(\frac{h_1+h_D-h_2}{2}\right)\Gamma\left(\frac{h_2+h_D-h_1}{2}\right)} \times \frac{\sqrt{\pi}^d \Gamma[h_D - d/2]}{[y(1-y)|z-w|^2)]^{(h_D - d/2)}} \tag{2.25}$$

Pulling out the constants that do not need to be integrated further, we find

$$\begin{aligned} I[z, w, h_D, d, h_1, h_2] &= \frac{\sqrt{\pi}^d \Gamma[h_D - d/2]}{\Gamma\left(\frac{h_1+h_D-h_2}{2}\right)\Gamma\left(\frac{h_2+h_D-h_1}{2}\right)|z-w|^{2h_D-d}} \\ &\quad \times \int_0^1 dy y^{\left(\frac{d+\Delta h-h_D}{2}\right)-1}(1-y)^{\left(\frac{d-\Delta h-h_D}{2}\right)-1} \end{aligned} \tag{2.26}$$

The dependence on $|z-w|$ could have been guessed by dimensional analysis. This step also leads to a Gamma function with a singularity at $h_D = d/2$. This is the infrared singularity that appears in the integral for large x.

We now get, upon performing the integral over the last remaining variable, that the full answer is

$$I[z, w, h_D, d, h_1, h_2] = \frac{\sqrt{\pi}^d \Gamma[h_D - d/2]}{|z-w|^{2h_D-d}\Gamma\left(\frac{h_1+h_D-h_2}{2}\right)\Gamma\left(\frac{h_2+h_D-h_1}{2}\right)} \frac{\Gamma\left(\frac{d+\Delta h-h_D}{2}\right)\Gamma\left(\frac{d-\Delta h-h_D}{2}\right)}{\Gamma(d-h_D)} \tag{2.27}$$

This is the correct answer as long as the two gamma functions in the numerator have a positive argument. This in particular requires that $d > h_D$. In other regions, the result is defined by analytic continuation in d, first evaluated at large d, and then we bring down d to the physical dimension of interest.

This final answer is very similar to the answers one gets from regular dimensional regularization of Feynman diagrams in field theory. Indeed, the integrals that have been done are of the same type. Here the improvements in the answer are obtained by taking large d first. This is because we are not allowing the dimension of the operators to change as we change d. Thus, marginal operators become relevant as we take d large and keep the dimension of the deformation h_D fixed.

Singularities in the final answer occur when $h_D \pm \Delta h - d$ is an even non-negative integer. These appear as poles of the gamma function. There is also a pole in the denominator that occurs if $h_D - d$ is a non-negative integer. In all other cases, where there are no singularities, we have obtained a finite answer. This is the dimensionally regularized answer for the correction to the two point function.

In terms of the α, β variables, this integral is given by

$$I[z-w,\alpha,\beta,d] = \frac{\pi^{d/2}\Gamma\left(\frac{d-\alpha}{2}\right)\Gamma\left(\frac{d-\beta}{2}\right)\Gamma\left(\frac{1}{2}(-d+\alpha+\beta)\right)(z-w)^{-\alpha-\beta+d}}{\Gamma\left(\frac{\alpha}{2}\right)\Gamma\left(\frac{\beta}{2}\right)\Gamma\left(d-\frac{\alpha}{2}-\frac{\beta}{2}\right)} \tag{2.28}$$

2.2.3 First order correction to the three point function

To get a correction to a three point function, we usually need to integrate a four point function of the form

$$\langle \mathcal{O}_1(\omega_1)\mathcal{O}_2(\omega_2)\mathcal{O}_3(\omega_3)\rangle_\lambda = \int d^d y \langle \mathcal{O}_1(\omega_1)\mathcal{O}_2(\omega_2)\mathcal{O}_3(\omega_3)\mathcal{O}_D(y)\rangle \tag{2.29}$$

in the vast majority of the cases, such four point functions are not known exactly.

If one does perturbation theory with operators that are polynomials in a scalar field, or in the example of string scattering amplitudes in flat space, the integrals one needs to perform reduce to a finite number of integrals of the type

$$I[\overrightarrow{\omega}, \alpha_1, \alpha_2, \alpha_3, d] = \int d^d x \frac{1}{|x-\omega_1|^{2\alpha_1}|x-\omega_2|^{2\alpha_2}|x-\omega_3|^{2\alpha_3}} \tag{2.30}$$

The precise details of the integral evaluation can be found in the appendix A. The techniques are similar to the ones used before, but in general the answer is not particulalry simple.

It turns out that a similar integral is also obtained if we are working on a correction of a two point function where we have added some position dependence to the deformation. We will study this particular case in detail later on.

2.3 Marginal deformations

It is interesting to analyze the special case of marginal deformations, where $h_D = d$ in equation (2.31). In that case, we find the following: there is always a pole in the denominator at $h_D = d$. This means that unless the numerators are singular, the answer actually vanishes. This is expected from the usual rules of unitary conformal field theories. Two point functions of primary operators of different dimensions should vanish at a conformal fixed point.

For a singularity in the numerator to occur we require that Δh is an even integer. There are two cases of interest. When $\Delta h \neq 0$ and the special case where $\Delta h = 0$. Let us first analyze the case where $\Delta h \neq 0$, but still an even integer. In that case we find

that the answer is equal to

$$I[z,w,h_D,d,h_1,h_2]=\frac{\sqrt{\pi}^d\Gamma[h_D-d/2]}{|z-w|^{2h_D-d}\Gamma\left(\frac{\Delta h+h_D}{2}\right)\Gamma\left(\frac{h_D-\Delta h}{2}\right)}\frac{\Gamma\left(\frac{d+\Delta h-h_D}{2}\right)\Gamma\left(\frac{d-\Delta h-h_D}{2}\right)}{\Gamma(d-h_D)} \tag{2.31}$$

If we keep h_D fixed and analytically continue in d we find that only one of the two numerators can become singular. The answer in the limit is of the form

$$\lim_{\epsilon\to 0}\Gamma[\epsilon/2-m]/\Gamma[\epsilon]\times\text{finite}=\text{finite} \tag{2.32}$$

and this suggests that there could be finite mixing.

However, because in this case we have that $\Delta h = 2m$, the operators $\mathcal{O}_1(x)$ and $\Box^m\mathcal{O}_2(x)$ have the same dimension. It is easy to see that we can modify $\mathcal{O}_1$ with a finite counterterm $\mathcal{O}_1 - c\Box^m\mathcal{O}_2$ that removes the mixing. In this sense, this is no different that $\Delta h \neq 0$ and we see the absence of mixing. Such a term can be interpreted as a contact term in the OPE. It is also in this case, when the dimension h_D is even, that there can also be an extra pole in the denominator that arises from the Schwinger parametrization of the denominators. This can produce a double pole in the denominator and makes the end result vanish.

Now, only the special case where $\Delta h = 0$ and the operator is marginal remains to be studied. The limit looks like

$$\lim_{\epsilon\to 0}\Gamma[\epsilon/2]\Gamma[\epsilon/2]/\Gamma[\epsilon]\simeq 4/\epsilon+\text{finite} \tag{2.33}$$

In this case we produce a universal logarithm. This is a correction to the anomalous

dimension of the operator $\mathcal{O}_1$. It depends only on the OPE coefficient

$$h_D(y)\mathcal{O}_1(x) \simeq f_{11D}|x-y|^{-h_D}\mathcal{O}_1(x) + \dots \tag{2.34}$$

but not on the dimension of the operator h_1. In that sense, the integral we have to perform is always universal.

2.4 Position and time dependent perturbations

As described in the introduction, the second master integral that we evaluated in the previous section can also be interpreted in terms of a position dependent excitation on the cylinder. To see this, we convert the variables from the integral to the natural ones on the cylinder.

To first order, the correction to the one point function on the cylinder in the presence of a deformation with an $f(x) = e^{i\omega\tau}$ factor is given by

$$\langle \mathcal{O}_D(\Omega', \tau')\rangle_{cyl} = \lambda \int_{cyl} d^{d-1}\Omega d\tau \exp^{i\omega\tau} \langle \mathcal{O}_D(\Omega,\tau)\mathcal{O}_D(\Omega,\tau')\rangle_{cyl} \tag{2.35}$$

where τ is the natural euclidean time coordinate on the cylinder and ω is a complex variable. When ω is real we have a bounded and oscillating perturbation of the conformal field theory on the cylinder.

Using the fact that in radial quantization we have $\tau \simeq \log r$, and that to convert to

the punctured plane we need extra factors of $|r|^{-h_D}$ to be inserted, we get that

$$\int_{cyl} d^{d-1}\Omega d\tau \exp^{i\omega\tau}\langle \mathcal{O}(\Omega,\tau)\mathcal{O}(\Omega,\tau')\rangle_{cyl} = \int d^d x|x|^{i\omega+h_D-d}|y|^{h_D}\langle \mathcal{O}(x)\mathcal{O}(y)\rangle \quad (2.36)$$

$$= \int d^d x|x|^{i\omega+h_D-d}|y|^{h_D}\frac{1}{|x-y|^{2h_D}} \quad (2.37)$$

This can be written as

$$\int_{cyl} d^{d-1}\Omega d\tau \exp^{i\omega\tau}\langle \mathcal{O}(\Omega,\tau)\mathcal{O}(\Omega,\tau')\rangle_{cyl} = I(|y|,\alpha,\beta,d)|y|^{h_D} \quad (2.38)$$

provided we identify

$$\alpha = -h_D - i\omega + d, \beta = 2h_D \quad (2.39)$$

in the master integral (2.28). The result is then given by

$$\frac{\pi^{d/2}\Gamma\left(\frac{1}{2}\left(d-2h_D\right)\right)\Gamma\left(\frac{1}{2}\left(h_D-i\omega\right)\right)\Gamma\left(\frac{1}{2}\left(i\omega+h_D\right)\right)z^{h_D+i\omega}}{\Gamma\left(h_D\right)\Gamma\left(\frac{1}{2}\left(d-i\omega-h_D\right)\right)\Gamma\left(\frac{1}{2}\left(d+i\omega-h_D\right)\right)} \quad (2.40)$$

This has the expected Euclidean time dependence. Notice that this has singularities where

$$i\omega = \pm(h_D+2k) \quad (2.41)$$

and k an integer. This is natural, as when we go from Euclidean to Lorentzian signature in a Wick rotation, we should make $\omega = i\tilde{\omega}$ imaginary in order to obtain a real frequency $\tilde{\omega}$. This then corresponds to driving the field theory on the cylinder with a time dependent source at frequency $\tilde{\omega}$. At the values of $\pm\tilde{\omega} = h_D + 2k$ we obtain resonances. These happen exactly at the energies of the spherically invariant excitations of the scalar $\mathcal{O}$ on the cylinder (see [35] for a description of driving the conformal field theory in Hamiltonian mechanics).

The exponent is also given by

$$i\omega - h_D + h_D = i\omega \tag{2.42}$$

as one expects from the translation properties of the integral in the cylinder coordinates. The way we deal with the resonance in this case is to analytically expand in $\tilde{\omega}$ at the required frequency and keep the first subleading term. This gives the usual secular growth of the resonance as $t\exp(i\tilde{\omega}t)$.

This response can also be obtained from the AdS dual following similar steps to those found in [35]. We need to solve the differential equation for the radial coordinate

$$-\frac{1}{r^{d-1}}\partial_r((1+r^2)r^{d-1}\partial_r\phi(r) + m^2 f(r) + \tilde{\omega}^2/(1+r^2)\phi(r) = 0 \tag{2.43}$$

This is in a coordinate system where

$$ds^2 \simeq -dt^2(1+r^2) + dr^2(1+r^2)^{-1} + r^2 d\Omega^2 \tag{2.44}$$

The problem of the asymptotic shape near $r \to \infty$ ends up ends up being controlled by the asymptotic expansion of the hypergeometric function

$$\phi(r) \propto \ {}_2F_1\left(\frac{(d-h_D-\tilde{w})}{2}, \frac{(h_D-\tilde{w})}{2}, \frac{d}{2}, -r^2\right) \tag{2.45}$$

with the usual relation between the mass in AdS and the dimension of the operator $m^2 = \sqrt{h_D^2 - dh_D}$. This produces the correct ratio of the Γ functions. The factors of π etc, are explained in detail in [35].

We can also notice that from this result we can recover the Fourier transform of the

two-point function in equation (2.15). The idea is simple. If we take $\omega \to \infty$ in equation (2.40), we are driving the theory in the cylinder with a Euclidean time dependence that is oscillatory and that has a wavelength that is much smaller than the size of the cylinder. In this limit, we would expect that if we zoom in to the region where we have the operator, the infrared cutoff scale induced by the driving of the field theory is at a higher energy than the infrared cutoff provided by the geometry. This second cutoff should become invisible, up to "finite size" corrections. To take the limit, we use Stirlings approximation for the gamma functions that depend on ω, $\Gamma(\gamma) \simeq \exp(\gamma \log \gamma - \gamma)$.

We find this way that in the limit the answer becomes

$$\langle \mathcal{O}_D(\tau) \rangle = \frac{\pi^{d/2} \Gamma\left(\frac{1}{2}\left(d - 2h_D\right)\right)}{\Gamma\left(h_D\right)} \exp(i\omega\tau) \times F(\omega) \tag{2.46}$$

where

$$F(\omega) = \exp \gamma_1 \log \gamma_1 - \gamma_1 + \gamma_2 \log(\gamma_2) - \gamma_2 - \gamma_3 \log(\gamma_3) + \gamma_3 - \gamma_4 \log(\gamma_4) + \gamma_4) + O(1/\gamma) \tag{2.47}$$

where the γ_i are the various ω dependent variables that appear as arguments in the Gamma functions. A straightforward evaluation shows us that

$$F(\omega) = \exp((d - 2h_D)\log(2) + (2h_D - d)\log(\omega)) = \left(\frac{\omega^2}{4}\right)^{h_D - d/2} \tag{2.48}$$

and this matches the Fourier transform with all the factors of two and normalization factors on the nose.

We can go one step further. We can also consider the case where we compute a correction to a two point function in the presence of a position dependent perturbation

with a radial profile. This is handled by the integral

$$\langle \mathcal{O}_1(x_1)\mathcal{O}_2(x_2)\rangle_\omega \simeq f_{12D}\int d^dx \frac{|x|^{i\omega+h_D-d}}{|x-x_1|^{\Delta h+h_D}|x-x_2|^{-\Delta h+h_D}} \tag{2.49}$$

where we have used the same convention for the profile as in equation (2.37), so that it corresponds to an oscillating driving of the cylinder after the conformal rescaling that places the origin at the infinite past. This gives rise to a more complicated integral. But, in the special case where either $x_1 = 0$ or $x_2 = 0$, it takes the same form as the simpler master integral we have already evaluated.

What is important for us, is that this modifies the exponents in the usual three point function as follows

$$\Delta h + h_D \to \Delta h + h_D - i\omega - h_D + d = \Delta h - i\omega + d \tag{2.50}$$

keeping the other one, $h_D - \Delta h$, fixed.

The ω dependent gamma factors end up being given by

$$\frac{\Gamma\left[\frac{h_D-i\omega}{2}\right]\Gamma\left[\frac{i\omega-\Delta h}{2}\right]}{\Gamma\left[\frac{d+\Delta h-i\omega}{2}\right]\Gamma\left[\frac{d-h_D+i\omega}{2}\right]} \tag{2.51}$$

when we choose x_1 to be at the origin.

One set of poles in the numerator occur when $\tilde{\omega} = -i\omega = 2k - \Delta h$. This again can be interpreted as a resonance. After all, putting the operator $\mathcal{O}_1$ at the origin puts the field theory in the vacuum of the representation of the conformal group associated to $\mathcal{O}_1$ (the lowest weight state), which is spherically invariant. This is an immediate consequence of the conformal rescaling that takes the plane to the cylinder. This has energy h_1 relative to the usual vacuum. Because we are integrating with a spherically invariant perturbation

profile, the states that are generated need to be spherically invariant. We can think of this as an amplitude in the cylinder Hamiltonian theory of the form

$$\int d\tau \exp(i\tilde{\omega}\tau) \sum_k s_k \langle \mathcal{O}_2, 2k, \tau_2 | \mathcal{O}_D(\tau) | \mathcal{O}_1, 0, -\infty \rangle \tag{2.52}$$

where the ground state of the $\mathcal{O}_1$ representation is converted into a sum of states in the $\mathcal{O}_2$ representation by the action of the perturbation. The coefficients s_k appear from how the operator $\mathcal{O}_2$ at a particular radial time excites the individual states. This is explained in [35]. Since $|\mathcal{O}_1, 0, -\infty\rangle$ is an eigenstate of the radial Hamiltonian, we can choose the initial time to be anywhere we want, and we can make that coincide with the lower end of the integration in the variable τ.

Here, spherical symmetry of the initial state and the perturbation guarantees that the operator $\mathcal{O}_2$ can only destroy spherically invariant states. These can only have energies $h_2 + 2k$ with k an integer. In this sense, we can schematically write

$$\mathcal{O}_D \simeq a_D^\dagger + f_{12D} \sum f_k a_{2,k}^\dagger a_{1,0} \tag{2.53}$$

where the f_k are determined by the conformal symmetry (this is related to the conformal block structure of the OPE between the representations $\mathcal{O}_1, \mathcal{O}_2, \mathcal{O}_D$, it basically describes how descendant amplitudes are related to the primary amplitudes). The gamma function pole happens exactly at resonance for a transition between a state with energy h_1 and a state of energy $h_2 + 2k$. The resonance in this case is constructive interference between the perturbations at different times. Again, in time dependent perturbation theory such resonances produce secular behavior (linear growth in time), which becomes a logarithm after passing from the cylinder to the plane.

Let us explain this. The usual formula for time dependent perturbation theory is

$$|f\rangle = P \exp\left(\int i V_{int}(t) dt\right) |i\rangle \tag{2.54}$$

where V is in the interaction picture. This has a natural time dependence of $\exp(i(w_f - w_i)t)$ for a transition between states of energies labeled by their frequencies w_i, w_f. If we add to the problem an external time dependence at frequency ω we get that the driving of the transition oscillates at a shifted frequency $\omega - \Delta w$. This gives us a linearly growing transition in time if $\omega - \Delta w = 0$, this is the secular term in perturbation theory. In our case the frequency of the final state is any of the spherically invariant descendants of $\mathcal{O}_2$

There is a second pole. This one does not depend on Δh. Instead, it corresponds to the topology for a transition of the form

$$\langle \mathcal{O}_D, 2k, \tau | \, \mathcal{O}_2(\tau_2) \, | \mathcal{O}_1, -\infty \rangle \tag{2.55}$$

where the secular behavior is produced because it has a time dependence that exactly cancels the time dependence of $\langle \mathcal{O}_D, 2k, \tau|$ in the Schrödinger picture. This is why ω ends up with the other sign in the pole of the gamma function.

Using the results of appendix A, we can actually solve the full problem without restricting to putting one of the operators at the origin. This way we obtain the full correction to the two point function on the cylinder. We will now show that many of the singularities in the final answer have the same interpretation. The idea is to do an integral of the form

$$I \simeq \int d^d x \frac{1}{|x - w_0|^{2a} |x - w_1|^{2b} |x - w_2|^{2c}} \tag{2.56}$$

with $2a = (d - h_D) - i\omega$, $2b = h_D + \Delta h$, $2c = h_D - \Delta h$. The answer is then given by

$$\mathcal{N} \int_0^\infty dt \left(\sqrt{t}\right)^{d/2-2} \prod_{j=1}^{3} \Omega_j^{-a_t+d/2+a_j} K_{d/2+a_j-a_t}\left(\sqrt{2t}\Omega_j\right) \tag{2.57}$$

where $a_t = a_1 + a_2 + a_3$ and $\mathcal{N}$ is a normalization factor given by

$$\mathcal{N} = \frac{\pi^{d/2} 2^{a_t-d}}{\Gamma\left[a_1\right]\Gamma\left[a_2\right]\Gamma\left[a_3\right]\Gamma\left[d-a_t\right]} \tag{2.58}$$

which is non-singular. The functions K are modified Bessel functions. It is convenient to change variables to $x \propto \sqrt{t}$.

There are two types of singularities that can show up. Some of them result from integration over the variable x, and others result from the normalization of the modified Bessel function, whose expansion is as follows

$$K_\nu(x) \simeq x^\nu 2^{-1-\nu}\Gamma[-\nu](1 + O(x^2)) + 2^{-1+\nu}x^{-\nu}\Gamma[\nu](1 + O(x^2)) \tag{2.59}$$

The singularities all arise from the $x \simeq 0$ region. At large x, $K_\nu(x) \simeq \exp(-x) \times$ power law, so the $x \to \infty$ limit of the integral is convergent.

Singularities in the integral arise when $d/2 - 1 \pm \nu_1 \pm \nu_2 \pm \nu_3$ is a negative integer [59], where the ν are the labels of the Bessel function. But notice that when we compute, we

find that

$$\begin{aligned} a_2 + a_3 &= h_D && (2.60)\\ 2a_t &= (d - h_D) - i\omega + 2h_D && (2.61)\\ &= d + h_D - i\omega && (2.62)\\ d/2 + a_1 - a_t &= d/2 - h_D && (2.63)\\ d/2 + a_2 - a_t &= i\omega/2 + \Delta h/2 && (2.64)\\ d/2 + a_3 - a_t &= i\omega/2 - \Delta h/2 && (2.65) \end{aligned}$$

so only two of the labels of the Bessel functions depend on ω and Δh, and not the third. When we take the combinations $\pm\nu_2 \pm \nu_3$, either the dependence on Δh or the dependence on ω cancels, so the singularities in ω that arise from the integrals do not depend on Δh, which is what we are seeking to find.

Thus, the singularities we want to analyze must arise from the normalization factors of the modified Bessel functions. These are in the Γ factors. Poles will arise whenever $\pm(i\omega/2 \pm \Delta h/2)$ are integers. That is the same as writing

$$i\omega = \pm\Delta h \pm 2k \tag{2.66}$$

Half of these singularities are transitions where a descendants of the first operator (in the initial state) is excited at a resonant frequency with descendants of the second operator. The point is that the first operator not being at the origin produces a linear combination of the lowest energy state in the representation and it's descendants. Any one of which could be the one in resonance. The second set of singularities arises from reversing the order of the operators (thinking of $\mathcal{O}_2$ as generating the initial state, rather than $\mathcal{O}_1$).

Both are generally required because in the Euclidean answer we can interchange the order of the operators without encountering a singularity. Again, spherical symmetry of the perturbation forces the state generated by $\mathcal{O}_1$ to have the same angular quantum numbers as the state annihilated by $\mathcal{O}_2$ (or viceversa). This is what produces a difference that is twice an integer, rather than just an integer. After all, states with the same angular momentum that are descendants of a single state, differ in their energies by twice an integer.

The upshot is that the poles in ω that depend on Δh can always be interpreted in terms of resonant transitions.

Part II

LLM Geometries

Chapter 3

Reconstructing spacetime from the hologram, even in the classical limit, requires physics beyond the Planck scale.

Understanding how quantum mechanics and gravity can be made compatible is one of the thorniest problems in theoretical physics. This is especially true in light of the black hole information paradox [60]. One of the main claims of the AdS/CFT correspondence [3] is that it provides a definition of quantum gravity for spacetimes that are asymptotically of the form $AdS_{d+1} \times X$ in terms of a quantum field theory in d-dimensions that resides on the boundary of the AdS geometry. In this setup, the information paradox is resolved in principle: the quantum field theory of the boundary does not violate quantum mechanics. We do not yet understand how the paradox is resolved in terms of the geometric variables of gravity.

The boundary theory is often referred to as the hologram, while the full higher dimensional geometry is called the bulk. A rather important open problem in the study of this duality is the problem of reconstruction: how to derive the geometric data of the bulk spacetime from the hologram. The hope is that if we understand this procedure sufficiently well, we might finally understand what was the *wrong assumption* in the original calculation by Hawking.

Here, we will discuss how much information is needed from the hologram in order to reconstruct the bulk spacetime, specifically when the spacetime is a classical solution of gravity. This problem is well understood near the vacuum state. Fields in the AdS spacetime are in one to one correspondence with certain families of local operators on the boundary [4]. The expectation values of these operators are related to the behavior of the solutions of the classical fields as they approach the boundary. Very small classical excitations in the bulk imprint themselves on these expectation values of the hologram in a way that makes it possible to reconstruct the bulk solution from the expectation values in a perturbative expansion [61, 62].

Does this work beyond a perturbative argument? In this essay, we will argue that the answer to this question is generically no. The way we will argue for this outcome is with a very concrete counter-example, where we can see the failure explicitly. We will then argue that there is a mechanism in the quantum field theory that provides the additional data necessary to reconstruct the spacetime, but that this data is hidden in modes that lie beyond the Planck scale from the point of view of the vacuum geometry.

The counter-example can be constructed in the maximally supersymmetric theory with excited states that preserve as much supersymmetry as possible. The complete set of these solutions has been classified by Lin, Lunin and, Maldacena [63] and we will refer to them as LLM geometries. What makes this example special is that we also understand

the complete set of such states in the dual field theory [64, 65], so we can understand the problem in detail not only in the geometric space of classical solutions, but also in the Hilbert space of the quantum theory.

The LLM geometries are completely specified by a single function $z(w, \bar{w}, y)$, which must obey a known differential equation. They are regular and horizon free. Geometric regularity forces $z(w, \bar{w}, 0)$ to take one of two possible values, $\pm 1/2$. This can be represented by a two-coloring of the complex $w, \bar{w}$ plane. A single round disk will give rise to the $AdS_5 \times S^5$ spacetime. These patterns have fixed area and are identical to the configuration space of a fixed amount of incompressible liquid in two dimensions.

The coloring can be described by a step function $\rho(w, \bar{w})$ that takes the value one in the region of one color and is zero otherwise. Given $\rho(w, \bar{w})$, the solution for z is

$$z(w, \bar{w}, y) = \frac{1}{2} - \frac{y^2}{\pi} \int \frac{\rho(w', \bar{w}') d^2 w'}{(|w - w'|^2 + y^2)^2} \tag{3.1}$$

The boundary of the LLM geometries is located in the region where $r^2 = (y^2 + w\bar{w}) \to \infty$ and $z \to 1/2 - N(r^2 - w\bar{w})/r^4 + O(1/r^4)$. Indeed, z admits an expansion in powers of $w/r^2, \bar{w}/r^2, 1/r^2$. The expressions that arise are linear in the moments $M_{m,n} = \int \rho(w, \bar{w}) w^n \bar{w}^m d^2 w$ of $\rho(w, \bar{w})$. As shown in the works [66, 67] (see also [68] for how to use some higher moments as conserved charges with which to distinguish quantum states), the problem of computing expectation values of fields on the boundary can be reduced to studying a particular set of these multipole moments. Conversely, in this essay, we will see if it is possible to determine ρ from only a subset of the moments.

To see that this is a reasonable possibility, consider a small deformation of the lowest energy state, which is represented by a circular disk of radius $r_0 = \sqrt{N}$ (as shown in the left figure of 3.1). We want the edge to be slightly deformed, so that in polar coordinates

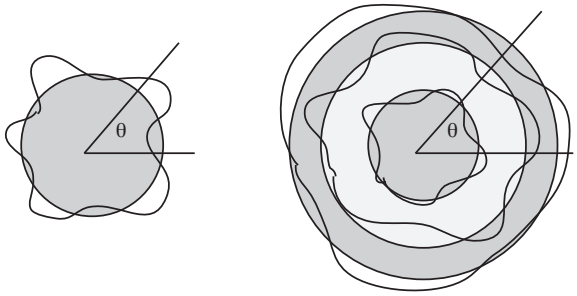

Figure 3.1: An example of a single droplet, versus a multi-droplet geometry, deformed away from a setup of concentric circles. Notice that a ray starting from the origin intersects various deformations of the edges.

the edge of the droplet can be described by a radial function $r(\theta) = r_0 + \delta r(\theta)$. In these coordinates, $w = r\exp(i\theta)$ and because ρ is just a step function, we can integrate along the radial direction to get

$$M_{0,m} = \iint \rho(r,\theta) r^m \exp(-im\theta) r dr d\theta \tag{3.2}$$

$$= N\delta_{m,0} + \int d\theta r_0^{m+1} \delta r(\theta) \exp(-im\theta) d\theta + O(\delta r^2) \tag{3.3}$$

We see that to linear order, the moments $M_{m,0}$ become exactly the Fourier modes of $\delta r(\theta)$. Higher $M_{n,m}$ are also linear in these Fourier modes, so they are redundant. We now see why it is reasonable to think that the subset of moments $M_{0,m}$ might be sufficient to calculate the function z and hence the full geometry: we need only to perform the inverse Fourier transform to build the geometry. This procedure fails in general geometries.

Consider now the coloring illustrated on the right of figure 3.1, which shows a droplet excitation with a deformed disk and annulus that are concentric. We can quantify the deformations by a set of functions, $\delta r_i(\theta)$ for each edge. One can then repeat the calculations that ended up with the Fourier coefficients (3.3). However, in this case one would

immediately see that the $M_{0,m}$ would only capture a particular linear combination of the three δr_i. This problem increases as one considers geometries with more droplets. We find then that it is impossible to reconstruct the geometry from the knowledge of this restricted data.

We can also compute the $M_{n,m}$ for the multi-droplet geometry and find that to linearized order they give a different linear combination of the Fourier modes of δr_i. So, in general, to reconstruct the bulk we would need roughly one of the $M_{n,m}$ for each mode of δr_i. Classically, the state can have an arbitrary number of such circles, so to solve the problem in the general case, we would need all of the $M_{n,m}$. This is the same as knowing the function z (and therefore the full geometry) at the start. To reconstruct spacetime, we need to know it already. We find that reconstruction in the general case is not only hard, but it is ambiguous: many geometries can have the same classical boundary data. This is a counterexample to bulk reconstruction in the sense of [61], because some fluctuations in the bulk are not coupled linearly to the expectation values that are available on the boundary.

Now, we will discuss the implications of this observation for the full quantum problem, rather than just the classical problem. The difficulty in reconstructing the interior is not on first figuring out if the state preserves supersymmetry. The condition we need to satisfy is that the charge of the state under one of the rotations of the sphere is equal to the energy of the state. Both of these are readily measured on the boundary. The problem really lies in that we need more modes than are available on the vacuum to describe the excited state of the multi-edge droplet picture in figure (3.1), one mode for each of the Fourier modes of $\delta r_i(\theta)$. Where do these modes come from?

To better understand the physics of the boundary, we need to use the dictionary [4]. The single-particle states that preserve this amount of symmetry are massless in

ten dimensions. The list of modes can be read off from a table [69, 70]. Because these modes preserve a large amount of supersymmetry, they can be followed from families of operators in the free field theory limit of the boundary theory as we increase the strength of interactions. This physics is determined by the eigenvalues of a single matrix degree of freedom in the quantum field theory [65]. Let us say there are N such eigenvalues. This means that we only need to know up to N invariants of the matrix to compute them. This was argued to be a form of the stringy exclusion principle [71]. These eigenvalues, when properly quantized, actually determine quantum droplets of incompressible fluids in two dimensions. The counting of excitations of the ground state droplet give a single tower of states that stops at mode N. This has fewer degrees of freedom than the classical gravitational theory, where the tower has no end, but notice in the latter case we had assumed that $N \to \infty$ first.

Here is where the physics of the Planck scale enters. A particle with momentum of order the Planck scale is not a mode with momentum $n = N$, but it is at much smaller values, around $n = N^{1/4}$. The vast majority of the modes that are required to describe the field theory data for such a supersymmetric state lie beyond the Planck scale.

To describe the degrees of freedom of the additional edges of the droplets, we need to borrow supersymmetric modes from the UV somehow, as these are the only other modes that preserve the correct amount of supersymmetry. It is now becoming clear why it was not possible to reconstruct the bulk with the classical theory: the physics responsible for the new modes of the geometry is way above the cutoff. In the strict classical limit, where N approaches infinity, this cutoff was sent to infinity first!

A natural question is how something that started its life at short wavelengths (high energies) became effectively a mode that is present in the long wavelength limit of the theory in the excited state. The way this must happen is that the map in equation (3.3)

is non-linear. A non-linear combination of modes adds the frequencies and wavelengths of the linear fields. To get a long wavelength (low frequency), there must be negative contributions as well as positive ones. The negative contributions in frequency indicate that the state is not in the ground state, but in an excited state. Bound states of large positive and large negative energy will have the required characteristics.

That such bound states play an important role implies that the modes are organized in a non-trivial way in the quantum wave function. This requires the right type of entanglement between the different UV modes. This entanglement allows one to change the topology of spacetime creating a droplet configuration with multiple edges. These multi-edge geometries actually have different topologies of the spacetime [63], thus realizing some of the ideas of Van Raamsdonk where topology changes of spacetime are related to entanglement [72]. It is natural to speculate that this is more generally true in gravity and that this paves a way to resolve the paradox of Hawking [60]. Transplanckian modes are doing something important.

Chapter 4

Superposition induced topology changes in quantum gravity

4.1 Introduction

4.1.1 The Question: Can topology be measured by an operator measurement in quantum gravity?

The AdS/CFT correspondence [3] has provided a detailed model of quantum gravity in terms of a dual quantum field theory. This has been an incredibly helpful tool, shedding light on several puzzles of quantum gravity. For instance, it has shown that the black hole information paradox [60] is soluble within a quantum mechanical framework (at least in principle). It is natural to ask what else the AdS/CFT correspondence tells us about quantum gravity. The careful reframing of the Hawking paradox in terms of information theory, resulting in the AMPS paradox [73], suggests that our ideas about quantum gravity might need rather large modifications in the presence of black hole horizons. The

correspondence supplies a method for rigorously analyzing these questions. We can ask if basic assumptions about the nature of gravity are actually valid or not. We will focus in particular on the problem of measuring the topology of a spacetime. Specifically, our question is: In the context of the AdS/CFT correspondence, can we determine the topology of a spacetime via a simple quantum mechanical operator measurement or instead does it require some other procedure?

Classically, spacetimes with different topologies can often be characterized by different topological invariants, which can be computed via, for instance, the Gauss-Bonnet theorem and its generalizations. Our current semiclassical understanding of quantum gravity suggests that some states will be represented by a sum over states whose spacetimes are topologically distinct. This should lead to a picture of spacetime that microscopically has the attributes of a spacetime foam [74]. This semiclassical quantization of gravity suggests that the metric and the topology are observables.

The simplest example of topology change in the AdS/CFT correspondence arises from the Hawking-Page phase transition for black holes in AdS [75]. This can be understood as a confinement/deconfinement phase transition in gauge theory [76]. Here, the transition leads to a new topology of spacetime, certainly in the Euclidean field theory. However, one can argue that this change is hidden behind the horizon if one considers the real time dynamics of a black hole. The Einstein-Rosen bridge of the maximal extension of the AdS black hole geometry connects to another region of spacetime that is completely hidden behind the horizon of the black hole and is not accessible to an observer on the boundary of AdS space in finite time measurements. More precisely, it is expected that the eternal black hole in AdS is equivalent to the field theory double of the thermal state [77], so the other asymptotic boundary of the spacetime corresponds to a copy of the degrees of freedom of the first field theory that is completely independent of the original

theory, except for the fact that the state in the double field theory is entangling the two copies of the field theory. In this sense, the topology change requires the addition of a hidden sector to the original field theory.

On the other hand, a true topology change that is not hidden behind a horizon can be obtained when studying bubbling solutions in AdS [63]. In this case, it is possible to show that various spacetime topologies can be supported by the same boundary field theory. Indeed, it is even possible to argue that the bubbles can be tiny and almost indistinguishable from perturbative excitations of the geometry. The multi-bubbling solutions can sometimes be interpreted as spacetime foam. A natural question to ask is if we can measure the geometry (and even more coarsely, the macroscopic topology) uniquely, for sufficiently smooth configurations and their superpositions, or if the notion of geometry and topology is highly dependent on the state that we are studying. That is, is the topology of spacetime a quantum observable in this minisuperspace model?

As the full theory is a complete quantum mechanical system, we can consider arbitrary superpositions of geometries (with the same or different topology). Under the naive rules of semiclassical quantum mechanics, one could argue that there should be a "topology measuring" operator that distinguishes the different topologies, so that one could in principle divide the Hilbert space into superselection sectors that are eigenstates of the topology operator. However, Van Raamsdonk has suggested that topology and geometry arise from quantum entanglement [72]. In that case, it would be impossible to produce such a topology measuring operator. For example, entanglement of a factorization of the Hilbert space can be obtained from superpositions of states, each of which has no such entanglement. These could all have fixed topology, while the new superposed state could be a state with a different topology. In the case studied by Van Raamsdonk, this was associated with the double field theory interpretation of the black hole geometry [77],

but one might imagine that this could be applicable more generally [78]. This program for understanding geometry goes under the "ER=EPR" banner. One can also ask if the topology changes due to entanglement always require black hole horizons.

The main difficulty in being precise about this idea is that models of holographic quantum field theories where this could be analyzed tend to be too complicated to understand how to evaluate entanglement properties of most states, except perhaps for very special states like the field theory double. This is also beyond the Ryu-Takayanagi setup [79], as that setup assumes a single background geometry: it is not known how to make it compatible with superpositions of (macroscopically distinct) states.

4.1.2 The Set-up: The set of half BPS states in $\mathcal{N} = 4$.

In this paper, we work in a venue that is free from black hole horizons, in a setup where a complete description of the quantum states that contribute to the phenomenon can be understood in excruciating detail: the corresponding states have been completely classified in the dual field theory and a complete basis for the states is known. The field theory in question is the theory of a chiral free boson in two dimensions. Here, it arises as a limit of the minisuperspace of half BPS states in $\mathcal{N} = 4$ SYM, though it can also appear in many other holographic duals in a similar limit fashion. The supergravity dual configurations that correspond to smooth horizonless geometries with various topologies are well known and have been classified completely by Lin, Lunin and Maldacena [63]. They can be classified by black and white colorings of the plane, with some restrictions on the area of the colored regions that enforce the Dirac quantization condition. We will call these the LLM solutions. If one quantizes the solutions around the ground state droplet (a circular disk, which corresponds to the $AdS_5 \times S^5$ spacetime), one gets chiral edge excitations of the droplet [80]. We want to analyze this system in in a limit where

these edge excitations are described by a free field, this is the infinite N limit. In this work, our calculations will all be in this limit.

This free field theory is interpreted as an effective closed string theory that is UV complete from the point of view of quantum mechanics: we do not need any information from outside the free chiral boson system to compute quantum mechanical amplitudes and probabilities. The main reason for requiring the theory to be free is that it provides us with a canonical factorization of the full Hilbert space in terms of a mode decomposition of the free field. This makes it possible to compute the entanglement and uncertainty properties of the different modes, which will ultimately relate to the topology of the associated LLM geometry.

To address various technical issues that are required to make the arguments more forceful and precise, the theory of the chiral boson is constructed in a novel way by considering only the combinatorics of the symmetric group. This is an abstraction of the description of the state dynamics of in the $\mathcal{N} = 4$ SYM dual that is necessary in order to be able to take the free field limit. This construction is independent of the gravity realization, but we can ask to what extent the gravity picture is forced on us and in particular, if the combinatorial construction suggests to us a particular notion of locality.

We start with the idea that there are two natural basis for states. The first basis is what we would call the multi-trace basis in a matrix model. It can be thought of as being built from conjugacy classes and we will often refer to it as the closed string basis. The second is the set of characters of a matrix in representations of the group. As this can be built by irreducible representations, we can also represent these states by Young diagrams. We will often refer to this basis as the D-brane basis. The first one is approximately orthogonal from large N arguments [4]. The second one is exactly orthogonal by direct computation [64] in $\mathcal{N} = 4$ SYM, and also when used in the study

of 2D Yang Mills theory [81]. These can be described entirely in terms of group theory without any reference to matrices. This property allows a limit that can be interpreted as the exact $N = \infty$ limit of a matrix model and we can show directly that it corresponds to a free field theory. This is the limit where we will work in this paper.

4.1.3 The Answer: No, topology cannot be determined via a single operator measurement in this model.

In this paper, we argue that the topology of spacetime in quantum gravity cannot be measured by an operator. The main argument has been presented by us already in [40]. But, here we provide all the computational details. In that work, it was explained how the topology of simple classes of states ends up encoded in the uncertainty and entanglement of various variables, echoing the observation of Van Raamsdonk. These computations are not simple operator measurements. Instead, we showed how one can extract the topological information of a large class of interesting states, including some that are not fully classical, but have an interpretation as a state a few excited quanta on top of a classical background.

The argument for the non-existence of a topology measuring operator follows from considering a particular generating series of states in the D-brane basis and their precise description in the string basis, an effective notion of locality emerges naturally, giving rise to a local field theory on a circle that is the chiral boson quantum field theory. That is, the circle on which the chiral boson theory lives on is deduced from the combinatorics of the symmetric group. It turns out that the simplest such multi-D-brane generating series can be shown to be exactly given by a coherent state of the chiral boson. In this sense, the natural D-brane states are completely classical solutions of the free field theory

and end up being associated with the same topology as the vacuum (that is, the same topology as $AdS_5 \times S^5$, which has trivial topology).

We will then show that there are other *bubbling solution states* that can be interpreted geometrically as states with a topology that is macroscopically very different from each of the coherent states. These states will correspond to Young tableaux states in the field theory. Recall that coherent states are over-complete, so we can get any other state by superposing them. In particular, we can superpose them to form one of these states with a different classical topology. From this, it follows that there cannot be any quantum observable (in the sense of projectors in a Hilbert space) that can distinguish the two collections [40].

What we show instead is that the new bubbling states have an effective dynamics for nearby states whose collective dynamics is given by *multiple chiral bosons*, so that the states correspond to a new classical limit of the field theory. We will call these collective modes the IR (infrared) fields, while the original chiral field will be called the UV (ultraviolet) field theory. A similar statement about multiple chiral bosons is found in the work [82] as a suggestion for the dynamics around special sets of configurations, although one can already intuitively understand this from the original work [63]. Here we explain how this works in detail in a way that lets us go beyond simple Young diagram reference states. The work we do is aimed at being able to do computations. Our work makes it possible to understand how an effective cutoff in these multiple chiral bosons is generated dynamically by the state. We also develop the tools that allow us to explore what happens when we move beyond the cutoff.

The effective dynamics of these collective fields is subject to a stringy exclusion principle, and the UV field modes are in the vacuum well beyond this exclusion regime. The notion of new topology and geometry only makes sense for these states (and coherent

excitations of their collective dynamics) when we study their physical properties at low and intermediate scales. They can be regarded as semiclassical states (superpositions of quantum excitations around a vacuum) for high energy observables. This is similar to the study of multi-throat configurations. We are also able to study in detail the amount of entanglement of the UV theory modes, essentially mode per mode, and to use that to characterize the topology of the new classical limits we need to compute other quantities in the quantum theory that end up being non-linear in the wave-function of the configuration. These are related to measuring how classical the state is (uncertainties), and how entangled the state is from a canonical preferred factorization of the full Hilbert space of states.

Perhaps more important than the statement that topology is not an operator, is the fact that it can still be computed from the wavefunction of the system for states that are sufficiently classical. One can check that effective field theory makes sense in the vicinity of such states, although the cutoff required to make sense of effective theory was out of reach to the techniques used in that paper. This paper provides the technical details that are required to explore these ideas in a controlled setting without making any approximations: we can analyze a complete description of the states that were studied in [40] as well as other states that were not covered there. With this information we can explore the physics of the cutoff directly. This way we will find that the computed value of the topology varies as we vary the cutoff. In this sense, the topology that we will assign to spacetime depends on choices that we make. These choices are physical: a cutoff is usually related to the limits of an experimental setup. In the right double scaling limit, one should see that all cutoffs can be pushed to infinity and that the usual classical picture of gravity is correct.

The main goal of this paper is to desctibe a situation where the topology of spacetime

can be well understood in what turns out to be a *free field theory model of quantum gravity*. That is, we will show that the topology of spacetime can already be argued to change in a regime where physics should be perturbative. An advantage to having a setup in free field theory is that there will be a mode expansion, which will provide us with various ways of factorizing the Hilbert space in a canonical way. This factorization makes it possible to compute entanglement entropies that have a physical meaning.

4.1.4 The Outline

The paper is organized as follows. In section two, we review LLM geometries, which are dual to half BPS states in $\mathcal{N} = 4$ SYM. These are the geometries we will study throughout the paper. In section three, we build up the technology used to perform most of our calculations. This comes from analyzing the Hilbert space formed by considering conjugacy classes and irreducible representations of the symmetric group. This Hilbert space describes the free chiral boson in one dimension, which is also known to be equivalent to the space of half BPS states when $N \to \infty$ (where we will work). In section four, we show how to build D-branes using both the conjugacy class basis and the irreducible representation basis. To go between these basis, one needs the characters of the group. So, in section five, we introduce the Murnaghan-Nakayama rule, which provides a useful way to compute these characters. Further, we explain how our Hilbert space can also be used to describe free fermions and show how the Murnaghan-Nakayama rule encodes the fermi statistics.

In section six, we get to the real meat of the paper. Here, we study various states whose duals form classical geometries. We show that one set of these come from coherent states of the raising and lowering operators in our oscillator bases. However, we show that these are not the only states that give rise to classical geometries and further, the

new states have a different topology than the coherent states. We argue by contradiction that this leads to the fact that there cannot be a topology measuring operator in this set-up. In section seven, we show how uncertainty measurements can provide a method to compute topology in not one, but several measurements. We then discuss states that should not be thought of as having a classical dual. Further, we analyze how to make progress studying more complicated geometries with folds. Finally, in section eight, we discuss a second method for determining topology, this time from entanglement entropy calculations.

4.2 Droplet geometries and the limits of semiclassical reasoning

Half BPS states in $\mathcal{N} = 4$ SYM for $U(N)$ gauge group (at weak coupling) are described exactly by the Hilbert space of N free fermions in a harmonic oscillator potential [64, 65]. The dynamics is fully solvable and all the states can be counted. In the study of the AdS/CFT correspondence, the dual geometries have also been completely classified [63]: they are described in terms of incompressible droplets on a two plane. This is a semiclassical description of the phase space dynamics of the free fermions, which can also be associated with the study of the integer quantum hall effect on a plane [65] (indeed, the description that bosonizes small edge excitations of the droplets has been known previously [83]). One can work backwards from supergravity solutions to argue for the free fermion description [84, 80], but the analysis becomes convoluted when the droplets reach the minimal quantum size of $\hbar$. Indeed, there is more than one path to obtain certain solutions, especially the ones that have different topologies and it is not clear how the system takes care of over-counting in the supergravity regime (see for example

[85]). This is taken care of by the "matrix model" realization of the dynamics. That is, the dual holographic CFT explains how to take care of the overcounting.

What is clear is that the over-counting is in some sense handled by a stringy exclusion principle [86]. This idea was used to argue that BPS states bubble into giant gravitons [71]. In the case of giant gravitons, the stringy exclusion principle is stated by saying that trace modes become dependent for finite size matrices. In a sense, this gives a hard bound on the number of modes that are available to us and turns the effective dynamics of the traces into an interacting theory. This is mainly the statement that there are constraints related to over-counting, so that there is no unconstrained free field theory description of the system. The map of the states between the AdS and the CFT took much longer to sort out, especially since the discovery of the dual giant gravitons [87, 88]. This was sorted out eventually in [89, 64], and the geometric interpretation came out later [65, 63].

There is a set of natural questions that can be asked.

1. What is the set of states that can be accurately described by (semiclassical) droplet geometries?

2. How is the stringy exclusion principle implemented in detail for these different droplet geometries?

3. Are there topology measuring operators?

4. Is there a limit of the system where the full dynamics of all the states is an unconstrained free field theory?

5. Are interactions necessary for understanding the topology changes?

The last question only makes sense if the answer to the fourth question is affirmative. Indeed, all questions become more interesting if the answer to the fourth question is

affirmative. This is because in that case one would have a UV complete free theory in the gravity variables, rather than the N free fermion description. This would mean that there is no intrinsic stringy exclusion principle in the dynamics, and such a stringy exclusion principle would only appear effectively on particular solutions of the theory. Moreover, it is not clear that one can obtain a topology change in such a free theory. One is used to thinking about free theories as having a unique classical limit. A topology change would indicate that there is more than one possible classical limit. The main goal of the paper is to argue that the answer to question 4 is YES, that the answer to questions 3, 5 is NO, and to produce detailed partial answers for questions 1 and 2. In particular, we will construct the multi-droplet dynamics from first principles around a preferred collection of states, in which the details of the stringy exclusion principle can be understood.

4.2.1 Review of LLM geometries

We will start the analysis with a review of the salient features of the LLM solutions in supergravity [63] that we need. The solutions that preserve half the supersymmetries in $\mathcal{N} = 4$ SYM preserve an $SO(4) \times SO(4) \times \mathbb{R}$ bosonic symmetry of $SO(4,2) \times SO(6)$. The extra $\mathbb{R}$ symmetry is split evenly between the $SO(2,4)$ and the $SO(6)$. A geometry with those symmetries has the form

$$ds^2 = -\frac{y}{\sqrt{\frac{1}{4}-z^2}}(dt+V_i dx^i)^2+\frac{\sqrt{\frac{1}{4}-z^2}}{y}(dy^2+dx^i dx^i)+y\left(\sqrt{\frac{\frac{1}{2}-z}{\frac{1}{2}+z}}\right)d\Omega_3^2+y\left(\sqrt{\frac{\frac{1}{2}+z}{\frac{1}{2}-z}}\right)d\tilde{\Omega}_3^2 \tag{4.1}$$

where $i = 1, 2$. The two copies of $d\Omega_3^2$ and $d\tilde{\Omega}_3^2$ are three-spheres that realize the $SO(4) \times SO(4)$ symmetry. The metric is completely characterized by $z(y, x_i)$: the vector

V satisfies a differential equation that ties it to z. The function z obeys a linear elliptic sourceless PDE:

$$\partial_i \partial_i z + y \partial_y \left(\frac{\partial_y z}{y} \right) = 0 \tag{4.2}$$

and requires a boundary condition at $y = 0$. This locus is called the LLM plane. Non-singularity of the ten dimensional metric requires $z = \pm\frac{1}{2}$ at this locus (this forces only one of the two spheres to shrink to zero size, while the other stays finite). From here, one can compute

$$z(x_1, x_2, y) = \frac{y^2}{\pi} \int \frac{z(w_1, w_2, 0)\, dw_1\, dw_2}{[(x_1 - w_1)^2 + (x_2 - w_2)^2 + y^2]^2} \tag{4.3}$$

Notice that the integral is always convergent if $z(w_1, w_2, 0)$ is bounded. This is guaranteed by the non-singularity condition. We can represent the areas of $\pm 1/2$ as a two coloring of the LLM plane. The area of each one of the two colored regions is quantized in fundamental units [63]. The topology of the spacetime that arises from each two-coloring is directly related to the topology of the diagram. The vacuum solution will be $AdS_5 \times S^5$. We will see that this is associated with a solid disk in the LLM plane. We will refer to this as a state with trivial topology. We will see that there are excited states with trivial topology, which are represented by wiggles on the disk and states with non-trivial topology, which can result from rings or additional disks, etc.

This is a complete description of all the LLM solutions. We are interested in taking a limit where the areas of the regions with $z = \pm 1/2$ are both infinite. Moreover, we want the edge between the two areas to be compact. There are two ways to do so. Each of them has their own advantages.

The first way to do so is to consider a half filled plane, with two regions. Naively, this is the plane wave geometry with an infinite edge. To obtain the compact edge we

perform a periodic identification with a translation along the edge. This is done without distorting the geometry above. The disadvantage is that the asymptotic behavior of the geometry is not the one of $AdS_5 \times S^5$ geometry any longer.

The second way to do so is to consider the strict $N \to \infty$ limit of excitations of $AdS_5 \times S^5$ with finite energy. Since the edge of the droplet grows in size like $\sqrt{N}$ in fundamental units of the LLM area quanta, all the features of the solutions get compressed in the radial direction. To see the topological features, we need to rescale the coordinates to keep the coordinates of objects on the edge finite, even if the distance is effectively shrinking. This does not affect the topology of the configuration, but it distorts the geometry. We will study both of these. The reason is that both of them give rise to the same Hilbert space of states, even if they correspond to very different sets of geometries in ten dimensions.

4.2.2 Periodic LLM solutions

First, we will just study the LLM solutions that are periodic, with an infinite black and white area after the periodic identification.

We will be particularly interested in solutions that are independent of one of the LLM plane variables. These are stationary and represent states that do not evolve under Hamiltonian evolution. In the semiclassical limit, these are eigenstates of the Hamiltonian.

In the geometry represented by (4.3), we can choose that variable to be w_2. Then we have that

$$z(x_1, x_2, y) = \frac{y^2}{2} \int \frac{z(w_1, 0, 0) dw_1}{[(x_1 - w_1)^2 + y^2]^{3/2}} \tag{4.4}$$

where $z(w_1, 0, 0)$ will alternate between values of $-1/2, 1/2$ in regions, and we will also

assume that x_2 is a periodic coordinate. The master integral we need is

$$\int_a^b \frac{dw_1}{[(x_1-w_1)^2+y^2]^{3/2}} = \frac{1}{y^2}\left[\frac{(b-x_1)}{\sqrt{(b-x_1)^2+y^2}} - \frac{(a-x_1)}{\sqrt{(a-x_1)^2+y^2}}\right] \tag{4.5}$$

This will give us the contribution for a region a to b where $z=+\frac{1}{2}$ (a $z=-\frac{1}{2}$ region will simply have an overall sign difference). Notice the $1/y^2$ that appears here will cancel the numerator in (4.4). Our vacuum will be the solution with

$$z_0(w_1,w_2,0) = \theta(w_1) - \frac{1}{2} \tag{4.6}$$

for which

$$z(x_1,x_2,y) = \frac{x_1}{2\sqrt{x_1^2+y^2}} \tag{4.7}$$

The excited solutions will be determined by requiring that the domain where

$$\Delta z(w_1,w_2,0) = z_0(w_1,w_2,0) - z(w_1,w_2,0) \neq 0 \tag{4.8}$$

has compact support (remember we have imposed that w_2 is periodic), and that moreover

$$\int [z_0(w_1,w_2,0) - z(w_1,w_2,0)]\, dw_1\, dw_2 = 0 \tag{4.9}$$

We can understand the first condition by realizing that

$$z(x_1,x_2,y) = z_0(x_1,x_2,y) + \sum_{\text{images}} \frac{y^2}{\pi}\int_{\mathcal{D}} \frac{-\Delta z(w_1,w_2,0)\, dw_1\, dw_2}{[(x_1-w_1)^2+(x_2-w_2)^2+y^2]^2} \tag{4.10}$$

where $\mathcal{D}$ is the finite support where the two can differ. To implement the periodicity of w_2, we need to sum over images under discrete translation in x_2 (as indicated in the

sum). The infinite sum goes as $1/x_1^3$ asymptotically at large x_1, rather than the naive $1/x_1^4$. This is due to the sum over images, which is clear for translation invariant solutions in equation (4.4). Let us explain this fact.

The sum can be performed explicitly, by writing the sum over images in detail

$$z(x_1, x_2, y) = z_0(x_1, x_2, y) + \sum_{n=-\infty}^{\infty} \frac{y^2}{\pi} \int_{\mathcal{D}} \frac{-\Delta z(w_1, w_2, 0)\, dw_1\, dw_2}{[(x_1 - w_1)^2 + (x_2 - w_2 - 2\pi n)^2 + y^2]^2} \tag{4.11}$$

and where we have taken the period to be 2π (this is a convenient choice).

$$\begin{aligned} & \sum_{n=-\infty}^{\infty} \frac{y^2}{\pi} \frac{1}{[(x_1 - w_1)^2 + (x_2 - w_2 - 2\pi n)^2 + y^2]^2} \\ = \;& i \frac{y^2 \left[\cot(\varphi) + \cot(-\bar{\varphi})\right]}{4(2\pi)((w_1 - x_1)^2 + y^2)^{3/2}} - \frac{y^2}{16\pi} \frac{\left[\csc^2(\varphi) + \csc^2(\bar{\varphi})\right]}{((x_1 - w_1)^2 + y^2)} \end{aligned} \tag{4.12}$$

where

$$\varphi = \frac{(w_2 - x_2) + i\sqrt{(w_1 - x_1)^2 + y^2}}{2} \tag{4.13}$$

We would like to see how this expression behaves asymptotically, at large x_1. Let's look at the expression one term at a time. The terms of the form $\csc(a + ib)$ will decay exponentially fast, beating out the polynomial in x_1, which multiplies them. So, these terms can be dropped. The cotangent pieces, however, can be re-expressed using

$$\cot(a + ib) = \frac{1 - i \tan a \tanh b}{\tan a + i \tanh b} \tag{4.14}$$

and again, as $b \to \infty$, we find that $\tanh(b) \to 1$ up to exponentially suppressed terms. We then get that

$$z(x_1, x_2, y) \to z_0(x_1, x_2, y) + \int_{\mathcal{D}} \frac{-\Delta z(w_1, w_2, 0) y^2\,(2)}{4(2\pi)((w_1 - x_1)^2 + y^2)^{3/2}} dw_1 dw_2 \tag{4.15}$$

Notice that this matches (4.4) when we make $\Delta z(w_1, w_2, 0)$ independent of the second variable, and integrate over the range (2π).

This implies that $z(x_1, x_2, y)$ and $z_0(x_1, x_2, y)$ have the same asymptotics at finite y and $x_1 \to \pm\infty$ up to order $1/x_1^3$, while the second condition improves the match to a higher order. Expanding the expression asymptotically in powers of x_1^{-1} we find that

$$\Delta z(x_1, x_2, y) = -y^2 \int_{\mathcal{D}} \Delta z(w_1, w_2, 0)\, dw_1\, dw_2 \left(\frac{1}{4\pi x_1^3} + \frac{3w_1}{4\pi x_1^4} + O(x_1^{-5}) \right) \tag{4.16}$$

This shows how the first term vanishes with the condition (4.9). This is a coordinate choice: the coordinate x_1 is only well defined up to translation invariance, as moving the origin of x_1 changes the domain where $\Delta z \neq 0$.

The next term is the first subleading term of the gravity solution and its coefficient can be interpreted as the energy (see also the similar analysis in [90])

$$E \propto \int_{\mathcal{D}} \Delta z(w_1, w_2, 0)\, w_1\, dw_1\, dw_2 \tag{4.17}$$

This is positive, because $\Delta z \geq 0$ for $w_1 > 0$ and $\Delta z \leq 0$ for $w_1 < 0$. We see that compactness of $\mathcal{D}$ gives rise to a finite energy. The area quantization condition forbids us from trying to place smaller droplets very far away without incurring a large energy cost. In principle, it is possible to produce finite energy configurations if we allow a droplet to have a thinning finger whose width decreases as it tries to reach infinity: these will inevitably become smaller than Planck size features in the metric and we should be worried about using those solutions in the semiclassical regime.

This set of solutions is interpreted as a set of droplets for an incompressible fluid on the x_1, x_2 plane (we can choose $z(x_1, x_2, 0) = 1/2$ as the liquid, and the other region as an absence of liquid). The first equation tells us that we have a finite energy solution, and the

second one says that the number of liquid particles is conserved. The semiclassical Dirac quantization condition requires that the areas of the individually connected (compact) regions with $z(w_1, w_2, 0) > 0$ and $z(w_1, w_2, 0) < 0$ both be quantized. Each different droplet topology corresponds to a different spacetime topology. Our set of semi-classical coherent states will be droplet geometries that satisfy all of these properties. In the particle/hole language, we have both an infinite number of particles and vacancies. This tells us that there are no upper bounds on the energy of either a single particle being moved into the vacancy region, or for a vacancy being moved into a particle region. These are "giant gravitons" and "dual-giant gravitons." Saying that there is no upper bound on any of their energies is roughly stating that there is no stringy exclusion principle.

Once we have these semiclassical states, we can build a Hilbert space by taking superpositions of these geometries. Notice that coherent states are usually over-complete, so the set of solutions by itself does not tell us how this completion is supposed to work in practice. This is what the dual gauge theory actually accomplishes. Once we resolve this problem of what the correct theory is, we can reconstruct the geometric states and ask questions about quantum gravity.

As discussed previously, we are also particularly interested in geometries that have an extra translation symmetry. The translation symmetry comes from the lack of dependence on the periodic variable x_2. The black and white pattern is therefore represented by a black and white pattern on a cylinder that is rotationally invariant. The area of a (finite) droplet is then the size of the periodic variable 2π times the height of the region. This is quantized. Therefore any such configuration is described by a set of integers: the ordered heights of the regions. These alternate between the two colors. Since the basic configuration has the bottom half of the cylinder filled and the top half empty, the configurations must be asymptotically colored in the same way. This means that there

are as many finite white regions as there are finite black regions. This can be represented as in the figure 4.1.

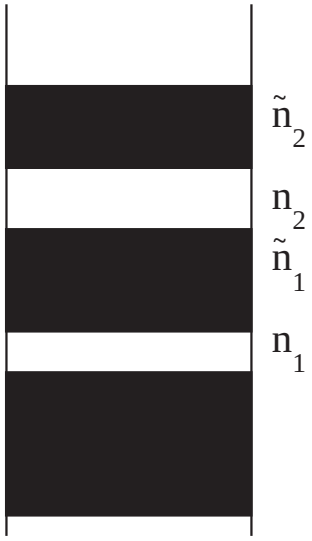

Figure 4.1: Periodic LLM solutions are characterized by strips. The quantities $n_1, \tilde{n}_1, n_2, \tilde{n}_2 \ldots$ are quantized and can be taken to be integers.

It is worth noticing that no additional information than the integers $n_i, \tilde{n}_i$ is required. This is because condition (4.9) gives an equation for the ground state level relative to the strip configuration. This level is obtained by requiring that the area in black above the 'zero level' is equal to the area in white under the 'zero level'. There is only one such level. The important point for us is that the (translationally invariant) geometry is determined by the collection of integers $n_1, \tilde{n}_1, \ldots$. These are all unconstrained integers. In that sense, we should think of the geometry as being free from a 'stringy exclusion principle' that would limit the integers somehow.

4.2.3 Zooming onto the edge

Now, consider the case where we take $N \to \infty$, while keeping the energy fixed, of an LLM geometry that asymptotes to $AdS_5 \times S^5$ (in the dual field theory we are considering a state with finite scaling dimension, but $N \to \infty$). We will also require that the geometry has an extra symmetry, this time of rotations around a center of the geometry in polar coordinates. The corresponding solutions are given by concentric rings in black and white. Since the area of the droplet is N, when we scale $N \to \infty$ the area becomes infinite. It is also important to understand that the energy of the solution is given by [63]

$$E = \frac{1}{2}\int_{\mathcal{D}} z(w,\bar{w},0)\, w\, \bar{w}\, d^2\, w - \frac{1}{2}\int_{\mathcal{D}_0} z_0(w,\bar{w},0)\, w\, \bar{w}\, d^2 w \tag{4.18}$$

where the domain $\mathcal{D}$ is the region of the droplet covered in black. We would like to measure the energy relative to that of the ground state, which is why we subtract off the integral over the ground state black droplets (we label this $\mathcal{D}_0$). We can check that the full integral is over the region where $\Delta z \neq 0$, like in the previous subsection. The region $\mathcal{D}_0$ is a circular droplet centered around the origin with radius $r \simeq \sqrt{N}$ in fundamental units. Because the radius of the droplet scales with N, the values of $w, \bar{w}$ where z differs from z_0 also scale in the same way. We also want to keep the areas of small subdroplets fixed and of order one. To understand these configurations, it becomes convenient to change coordinates to a variation of angular polar coordinates $y = r^2/2 - r_0^2/2, \theta$ that are centered near the edge of the droplet, so that $dy\, d\theta \simeq r\, dr\, d\theta = d^2 w$ is the natural area element. This means that we do the change of coordinates in a way that preserves the area measure. In this way, quantization of the circular area droplets is given immediately by requiring that the black and white rings have quantized y sizes. This change of coordinates was sketched in [40], but with most of the details on scaling of coordinates

ommitted. This is depicted pictorially in the figure 4.2.

Figure 4.2: Pictorial description of the change of coordinates $(w, \bar{w}) \to (y, \theta)$. The change of variables is area preserving.

Because the area of the new region is required to have the same area as the original droplet, one can check readily that $\int_{\mathcal{D}} z(w, \bar{w}, 0)\, r_0^2\, d^2w - \int_{\mathcal{D}_0} z_0(w, \bar{w}, 0)\, r_0^2\, d^2w = 0$.

This way we find that the energy is given also by a simple expression

$$E \propto \int_{\tilde{\mathcal{D}}} \Delta z(y, \theta)\, y\, dy\, d\theta \tag{4.19}$$

This is very similar to equation (4.17) if we identify the two sets variables $w_1 \to y$, $w_2 \to \theta$. The advantage is that now we can take $N \to \infty$, keeping y fixed and the areas fixed. Indeed, we find that the description of the droplets that survive the limit become identical to the pictorial representation in figure 4.1, even though the ten dimensional geometries are very different.

What needs to be understood is that the variable y being of order one implies that $2y \simeq r^2 - r_0^2 = (r_0 + \delta r)^2 - r_0^2 \simeq 1$. This means that $\delta r \simeq 1/\sqrt{N}$. In practice, this means that in order to take the limit we have zoomed onto the edge of the droplet. In the y coordinates taking $N \to \infty$ is trivial, but in the regular polar coordinates r, the shift in the radial coordinate scales as $1/\sqrt{N}$ relative to the edge. From the point of view of the topology of the configurations, it should not matter how we scale the coordinates.

Topology is after all a very coarse feature.

However, from the point of view of geometry (which includes distances), the features that we are trying to zoom in to are typically smaller than the Planck scale. The main reason for taking the limit is that at finite N, the negative y coordinate has a finite depth of order N. When we take $N \to \infty$ we remove this constraint and can work on the cylinder. This means that the numbers $n_i, \tilde{n}_i$ are unconstrained and there is no stringy exclusion principle. What is important for us is that in this limit the corresponding modes of the supergravity theory become free [76]. This is because the energy is of order one rather than N^2.

It is important to understand that taking this limit at the level of geometries for different topologies is suspect. In a free limit of a quantum field theory we would expect that the classical solutions that survive would be related to coherent states of a field. These would be solutions where the edge of the droplet is deformed, but there is no topology change. It is natural to ask if both of these types of solutions can be thought of as allowed classical limits simultaneously in the supergravity theory or not. This is not resolved directly within the supergravity theory.

The claim that topology cannot be measured by an operator in [40] depends on this assumption being true. If both types of "classical limits" survive in the quantum theory with different topology, then the fact that coherent states are complete means that states with the new topology (different than the ground state) can be made by superposing coherent state geometries. The coherent states are expected to all have trivial topology. This means that one can induce a topology change (of different classical limits) by superposition of solutions in one (trivial) topological class. The main goal of the paper is to explain how this works in detail in the Hilbert space of states of the free theory that arises from the $N \to \infty$ limit of half BPS states of the $\mathcal{N} = 4$ SYM theory.

A particularly important claim of the LLM setup [63] is that these concentric ring solutions are a complete basis of states for the Hilbert space of BPS states in $\mathcal{N} = 4$ SYM. That is because these solutions can be put into 1-1 correspondence with Young tableaux. The Young tableaux states are a complete basis of states of the dual $\mathcal{N} = 4$ SYM theory [64]. Such classification of states has been exploited in many setups (see for example [91, 92]). It is important to notice that most of these will have topological features on scales that are much shorter than the AdS planck scale. The typical such solution should not be treated as classical objects in these extreme situations.

4.3 A Hilbert space from group theory

4.3.1 Irreducible representations and conjugacy classes

As is well understood in the theory of orbifolds, twisted sector states for closed strings are assigned conjugacy classes of the group [93, 94]. Similarly, D-brane charges are associated with representations of the group [95]. Here we will use this fact to develop technology that we will use for the remainder of the paper. We will start by first describing how to go back and forth between irreducible representations and conjugacy classes in general. These will ultimately form two bases in our Hilbert space. In section 4.3.2, we specifically discuss the symmetric group, which will allow us to build a Fock space where we can create multi-string states. The Hilbert space we build will be exactly that of the free chiral boson in one dimension (exactly as desired in the infinite N limit). In this limit, the Hilbert space will be factorizable. This will, for instance, later provide a clear way to compute entanglement entropies.

In the study of finite groups, one can use character tables to go from conjugacy classes to projectors on representations [96]. These two sets are in one to one correspondence

with each other, and there is a linear map between the vector spaces that they generate at the group algebra level. This linear map can be promoted into a change of basis in a Hilbert space, so that one furnishes a model where D-branes can be understood as linear combinations of strings. This is a model where a D-brane is thought of as a soliton for a (closed) string theory: the D-brane state can be written directly in terms of string states. In this toy model, we start from nothing but the group, so we might want to think of this procedure as orbifolding the theory of a target space which is a point. Our goal is to eventually apply this procedure to the symmetric group, where additional structures are present and to connect this information with the study of matrix models.

The idea is rather simple. Consider a finite group Γ, with elements σ, and the usual transform in the group algebra

$$P_R = \frac{1}{|\Gamma|} \sum_{\sigma \in \Gamma} \chi_R(\sigma)\, \sigma \tag{4.20}$$

where R labels the irreducible representations of Γ. The object P_R is a projector in the group algebra that projects into the irreducible representation R and $\chi_R(\sigma)$ is the character of σ in the irreducible representation R. Because the characters only depend on the conjugacy class of σ, we can convert this sum into an equation relating the conjugacy classes and the projectors themselves

$$P_R = \frac{1}{|\Gamma|} \sum_{[\sigma] \in \mathrm{Conj}[\Gamma]} \chi_R([\sigma])\, d_\sigma\, [\sigma] \tag{4.21}$$

where d_σ is the degeneracy of the class (number of elements in the class), and this defines $[\sigma]$, which is simply the average over the elements of the class.

Now, we can promote this equation to an equation in a (finite) Hilbert space of states,

where we have two basis: one furnished by strings (conjugacy classes), and another one labeled by irreducible representations R, which we call the D-branes. Again, these are labels that we add to the two basis to reiterate the classification properties of the corresponding objects in orbifold theories. We thus write

$$|[R]\rangle = \frac{1}{|\Gamma|} \sum_{[\sigma]\in \mathrm{Conj}[\Gamma]} \chi_R([\sigma])\, d_\sigma \; |[\sigma]\rangle \tag{4.22}$$

and treat both the $[R]$ and the $[\sigma]$ as non-zero elements in a Hilbert space. One can expect that strings associated with different conjugacy classes are orthogonal to each other (they are different twisted sectors), and that different D-branes are also orthogonal to each other (they have different D-brane charges). Therefore, we require that

$$\langle [\sigma]|[\sigma']\rangle = \delta_{[\sigma],[\sigma']}\, f_{[\sigma]} \tag{4.23}$$

$$\langle [R]|[R']\rangle = \delta_{[R],[R']}\, g_{[R]} \tag{4.24}$$

This is a non-trivial set of orthogonality conditions: it is not guaranteed that they can be made compatible. The inverse transformation, relating the conjugacy classes and the representations is

$$|[\sigma]\rangle = \sum_{[R]} \chi_R([\sigma^{-1}])\, |[R]\rangle \tag{4.25}$$

where we use the characters of the conjugacy class of the inverse elements. Remember that $\chi_R([\sigma^{-1}]) = \chi_R([\sigma])^*$. Using the conjugacy class of the identity (which has the identity as its only element), we find

$$\langle [id]|[R]\rangle = \frac{\chi_R([id])}{|\Gamma|} f_{[id]} \tag{4.26}$$

Now, expressing the vector $|[id]\rangle$ in terms of the inverse function (4.25), we find that

$$\sum_{[R']} \chi_{R'}([id]) \langle [R'] \rangle [R] = \chi_R[id] g_{[R]} \tag{4.27}$$

Comparing the two expressions, we find that

$$g_{[R]} = \frac{1}{|\Gamma|} f_{[id]} \tag{4.28}$$

so the norm of the kets associated with the representations is independent of the representation.

Similarly, we can now apply this information to the trivial representation $\triangle$, which is such that $\chi_\triangle([\sigma]) = 1$ for all $[\sigma]$. We find that

$$\langle \triangle \rangle [\sigma] = \sum_{[R]} \chi_R([\sigma]) \langle \triangle \rangle [R] = \chi_\triangle([\sigma]) \langle \triangle \rangle \triangle = g_\triangle \tag{4.29}$$

Writing $|\triangle\rangle$ in terms of the class vectors, we find

$$\langle \triangle \rangle [\sigma] = \frac{d_\sigma}{|\Gamma|} \chi_\triangle[\sigma]^* f_{[\sigma]} = \frac{d_\sigma}{|\Gamma|} f_{[\sigma]} \tag{4.30}$$

Putting these two together we get that

$$f_{[\sigma]} = g_\triangle \frac{|\Gamma|}{d_\sigma} \tag{4.31}$$

So, we find that the representations are all normalized to the same value (which we can choose to be equal to one) and the class function kets are proportional to the inverse of the degeneracy of the class.

Since we only used the kets $|\triangle\rangle$ and $|id\rangle$ to normalize everything, we need to check consistency. This is straightforward. The orthogonality of representation kets becomes equivalent to the orthogonality of the rows of the character table. The orthogonality of the conjugacy classes ends up being related to the orthogonality of the columns of the character table (see [96], pp 17, exercise 2.21).

4.3.2 Fock space from the symmetric group

At this point, this can be thought of as a curiosity. The reason is that as written, this exercise should be thought of as a first quantized setup. Single string states can be reshuffled via a "Fourier transform" into single D-brane states. We have made no mention of multi-string states.

This all changes when we consider the symmetric group S_n. As argued in [97, 98], the conjugacy classes of the symmetric group should be associated with multi-strings, rather than single strings. Similarly, one can imagine that the representation theory left hand side should be generically associated with multiple D-branes, rather than a single D-brane. In essence, when we consider the symmetric group, the theory should be for all practical purposes second-quantized. This becomes precise when we consider the more general object generated by the symmetric group S_n for all values of n

$$\mathcal{H} = \oplus_{n\geq 0}\mathcal{H}_{S_n} \tag{4.32}$$

with the Hilbert space constructed as above. We can now also add (multi-) strings to a configuration. Consider a conjugacy class in S_n and a group element $g_1 \in S_n$ that represents it. Similarly, consider another conjugacy class and a group element $g_2 \in S_m$ that represents it. There is a natural embedding of the product of symmetric groups into

a larger symmetric group $\mu : S_n \times S_m \to S_{n+m}$. Here the S_{n+m} acts as permutations of a set of $n+m$ elements and the S_n acts only on the first n elements, while the S_m acts only on the last m elements. This gives a natural element of S_{n+m} for the two group elements, namely $\mu(g_1 \times g_2) \simeq \mu(g_1 \times 1) \circ \mu(1 \times g_2)$. Now, it is important to notice that this defines a unique conjugacy class in S_{n+m} which is irrespective of the representatives g_1, g_2 that were chosen. This is done as follows.

A group element of S_n can be written in a cycle presentation of permutations of the set $\{1, \dots n\}$. As is well known, the conjugacy classes are in one to one correspondence with the lengths of the cycle decomposition. A conjugacy class thus gives a partition of $n = \sum_s w_s s$ where we have w_s cycles of length s. We do this for g_1, so that $[g_1] \simeq \prod_s [s]^{w_s}$, where we pick the cycles of length $[s]$ as generators, and similarly for $[g_2] \simeq \prod_s [s]^{w'_s}$. With this we find that

$$[g_1] \otimes [g_2] \simeq \prod_s [s]^{w_s + w'_s} \simeq [g_1 \otimes g_2] \simeq [g_2] \otimes [g_1] \tag{4.33}$$

which shows that the cycle decomposition is irrespective of the elements of the class that we pick. We also find that the product of conjugacy classes is commutative, and the set is generated by the primitive cycles of length $[s]$. We will call $[s] := t_s$ so that the set of states can be thought of as (a particular completion of) the set of polynomials in an infinite set of variables $\{t_s\}$. The decomposition of the Hilbert space into the different $\mathcal{H}_{S_n}$ can be thought of as being graded by n, and the grading is additive on the product we defined. The product operation we defined is just the product of polynomials when extended linearly. The degree of $[s]$ is s. We will call this function for a monomial the energy of the state. A conjugacy class associated to the monomial $t_1^{w_1} \dots t_k^{w_k}$ will be said to have w_1 particles of energy 1, w_2 particles of energy 2, etc.

The most important question for us is to address is how we are going to relate the inner products of the different $\mathcal{H}_{S_n}$ to each other. There are two routes we can take. The first route is to declare that the irreducible representations of all the symmetric groups have norm equal to one. This can be twisted by the energy, so an irreducible of energy n has norm $|T|^n \simeq \exp(E \log(|T|))$. A second route is to assume that the norm of a two particle state, where the two particles have different energy, is the product of the norms of the corresponding single particle states. This is a factorization condition. This will be shown to be equivalent to the first route after a computation.

To do a computation, we need to find both the dimension of the symmetric group $|S_n| = n!$ and also the number of elements in a conjugacy class d_σ (remember we have labeled these as $\prod_s [s]^{w_s} \simeq t_1^{w_1} \dots t_k^{w_k}$ with $\sum_k w_k k = n$). The number of elements of a conjugacy class of the symmetric group is known to be given by

$$d_\sigma = \frac{n!}{\prod_k w_k! k^{w_k}} = \frac{|\Gamma|}{\prod_k w_k! k^{w_k}} \tag{4.34}$$

from equation (4.31), we find that

$$||t_1^{w_1} \dots t_k^{w_k}||^2 = {}_n\langle [\sigma] \rangle [\sigma]_n = {}_n\langle \triangle \rangle \triangle_n \frac{|\Gamma|}{d_\sigma} = {}_n\langle \triangle \rangle \triangle_n \prod_k w_k! k^{w_k} \tag{4.35}$$

So, if we choose ${}_n\langle \triangle \rangle \triangle_n = |T|^n$, the right hand side becomes equivalent to a norm on a bosonic Fock space where to each t_k we assign a raising operator of norm squared $k|T|^k$. That is, we associate a raising and a lowering operator pair $(a_k^\dagger, a_k)$, with commutation relations

$$[a_k, a_k^\dagger] = k|T|^k \tag{4.36}$$

with all others vanishing. Obviously, the simplest choice is to take $|T| = 1$. The raising

operator acts by multiplication by t_k, namely $a_k^\dagger \to t_k$, and the adjoint acts by $k\partial_{t_k}$. The inner product can be computed using

$$\langle g \rangle\, f = \int \prod_k dt_k d\bar{t}_k \exp\left(-\sum_k \frac{t_k \bar{t}_k}{k}\right) \bar{g}(\bar{t}) f(t) \tag{4.37}$$

where the normalization factor of the measure is such that

$$\langle 1 \rangle\, 1 = 1 \tag{4.38}$$

If we take the factorization condition instead, we find that

$$|t_a t_b| = ab\, {}_a\langle \triangle \rangle \triangle_{a\, b} \langle \triangle \rangle \triangle_b = ab\, {}_{a+b}\langle \triangle \rangle \triangle_{a+b} \tag{4.39}$$

for all a, b with $a + b$ constant. This would suggest that

$${}_a\langle \triangle \rangle \triangle_{a\, b} \langle \triangle \rangle \triangle_b = {}_{a+b}\langle \triangle \rangle \triangle_{a+b} \tag{4.40}$$

but this only seems to work if $a \neq b$ and $a, b \neq 0$.

With this, one can show that it works for all a, b. Consider ${}_2\langle \triangle \rangle \triangle_2$. By the naive factorization condition, it is independent of ${}_1\langle \triangle \rangle \triangle_1$. From here, we can form ${}_3\langle \triangle \rangle \triangle_3 = {}_2\langle \triangle \rangle \triangle_{2\,1} \langle \triangle \rangle \triangle_1$ uniquely, and similarly ${}_4\langle \triangle \rangle \triangle_4 = {}_3\langle \triangle \rangle \triangle_{3\,1} \langle \triangle \rangle \triangle_1 = {}_2\langle \triangle \rangle \triangle_{2\,1} \langle \triangle \rangle \triangle_1^2$. When we get to ${}_5\langle \triangle \rangle \triangle_5$, there is a consistency condition

$$\begin{aligned} {}_5\langle \triangle \rangle \triangle_5 &= {}_3\langle \triangle \rangle \triangle_{3\,2} \langle \triangle \rangle \triangle_2 = {}_4\langle \triangle \rangle \triangle_{4\,1} \langle \triangle \rangle \triangle_1 & (4.41) \\ &= {}_2\langle \triangle \rangle \triangle_{2\,1}^2 \langle \triangle \rangle \triangle_1 = {}_2\langle \triangle \rangle \triangle_{2\,1} \langle \triangle \rangle \triangle_1^3 & (4.42) \end{aligned}$$

Clearing out the common terms, we find that ${}_2\langle\triangle\rangle\triangle_2 = {}_1\langle\triangle\rangle\triangle_1^2$, and one can then easily show that we get ${}_n\langle\triangle\rangle\triangle_n = {}_1\langle\triangle\rangle\triangle_1^n$ for all other n.

4.3.3 Physical Interpretations

The Hilbert space we have constructed is the Hilbert space of a chiral boson in one dimension (again, this is theory we get when we consider the infinite N limit, and so is what we wanted). We have a single oscillator of energy k and left moving momentum k for each k. This is natural considering that in the computation of elliptic genera one builds an extra chiral circle [97]. We have the momentum modes of the chiral boson field theory, but we still need to argue that there is preferred notion of a local field that also arises from this construction. This will be taken up in the next section.

One should also remember that there is a straightforward relation between a chiral boson field theory and edge states in a quantum hall droplet [83]. The relation uses the theory of symmetric polynomials in many variables to go from traces to Schur polynomials. The Schur functions are associated with representations of the symmetric group S_k (described by Young tableaux) , and one can directly write these in terms of free fermions. The same combinatorics appears in the study of half BPS states in $\mathcal{N} = 4$ SYM [64] and the representation of the physics in terms of droplets and fermions was explored in detail in [65]. Surprisingly, the description of half BPS geometries in the gravity dual of $\mathcal{N} = 4$ SYM is also in terms of droplets: a droplet configuration with specified shape corresponds to a particular solution of the supergravity equations of motion [63], as we described in the pervious section. It has also been argued recently that similar physics might control a wide class of AdS/CFT dual configurations when one studies elements of the chiral ring that are extremal [99]. It was this particular observation that led us to try to understand the problem using group theory of the symmetric group without any

particular matrix model in mind. The map that realizes this correspondence assigns

$$\mathrm{Tr}(\tilde{Z}^{\ell}) \simeq t_{\ell} \tag{4.43}$$

where $\tilde{Z}$ can be either an elementary matrix valued field (like in $\mathcal{N} = 4$ SYM), or a composite matrix field (this would be common in toric field theories or some simple orbifolds). The main reason that this works is that to any conjugacy class of the symmetric group one naturally associates a multi-trace object constructed from the permutation itself. This was critical in the computations of [64] that show that Schur functions associated with different Young tableaux are orthogonal. Here we have reversed the arguments: assuming orthogonality of Young tableaux and conjugacy class states leads to a unique consistency condition that gives precisely a free chiral boson. Thus, in this setup, we do not have any non-trivial three point functions: we are strictly in the $N = \infty$ limit. The free fermions that realize the correspondence for the free field that we have here are associated with a system of free fermions for a Cuntz oscillator. The Cuntz oscillator algebra is defined by

$$\beta^{\dagger} |n\rangle = |n + 1\rangle \tag{4.44}$$

usually with $\beta |0\rangle = 0$. For us, we have an infinite sea of fermions, so all we require is that the set of $|n\rangle$ is labeled by integers (both positive and negative). We set by convention the Fermi-sea energy at $n = 0$. The Cuntz oscillators appear repeatedly also in the study of open spin chain dual states to open strings in the AdS/CFT correspondence [100] and their coherent states are especially important to describe the ground state energies of the corresponding open spin chains [101, 102]. What we have described here corresponds to the strict $N = \infty$ limit of the corresponding matrix models.

In a certain sense, the picture we have been advocating above is building a bridge

between matrix string theory and an abstract version of a (holomorphic) matrix model, in a vein similar to [103], but with very few states to consider. The picture we have is greatly inspired by the observation that requiring orthogonality of the Young tableaux states and a large N counting for correlators, at leading order in N produced a result where the norm of Young tableaux states is independent of the shape of the tableaux and only depends on the number of boxes [99]. Here we have even removed the large N counting hypothesis and replaced it by the weaker orthogonality of multi-string states. The fact that the harmonic oscillators that are constructed in this fashion have the correct statistics to correctly describe quantum fields in one dimension is derived from the compatibility of the two basis of states and the Fourier transform that relates them to each other.

4.4 D-brane creation operators and constructing local fields

4.4.1 The D-brane

It is instructive now to consider the simplest (trivial) representation of the symmetric group, which we have labeled $[\triangle]_n$ in the previous section. This is associated with a Young tableaux with n boxes and only one row. Using our polynomial formulation, we have that

$$|\triangle\rangle_n = \sum_{\overrightarrow{\omega} \in p(n)} \prod_k \frac{1}{k^{w_k} w_k!} (t_k)^{w_k} \tag{4.45}$$

where $p(n) := \{ \overrightarrow{\omega} \,|\, \sum_k k\omega_k = n\}$ are the partitions of n and we have used the fact that all characters are one for the trivial representation. We also have included the explicit

value of the degeneracy of corresponding conjugacy classes in the sum, extracted from equation (4.34). Notice that this is an equation relating states. In the raising/lowering operator notation, this state would have been created by

$$|\triangle\rangle_n = \sum_{\vec{\omega}\in p(n)} \prod_k \frac{1}{k^{w_k} w_k!} (a_k^\dagger)^{w_k} |0\rangle \tag{4.46}$$

which would be equivalent. From here we find that

$$\Lambda^n |\triangle\rangle_n = \sum_{\vec{\omega}\in p(n)} \prod_k \left(\frac{(\Lambda^k)}{k} t_k\right)^{w_k} \frac{1}{w_k!} \tag{4.47}$$

We notice that apart from the constraint $\sum_k k w_k = n$, the right hand side represents a series expression for an exponential function. It is convenient to sum over n and consider a generating series for these representations, so that we can write

$$|\triangle;\Lambda\rangle = \sum_{n=0}^{\infty} \Lambda^n |\triangle\rangle_n = \sum_{n=0}^{\infty} \sum_{\vec{\omega}\in p(n)} \prod_k \left(\frac{(\Lambda^k)}{k} t_k\right)^{w_k} \frac{1}{w_k!} = \exp\left(\sum_k \Lambda^k \frac{t_k}{k}\right) \tag{4.48}$$

The trivial representations of each S_n correspond to the totally symmetric representations of the group $U(N)$ with n boxes (as shown below), and have an interpretation as a single dual giant graviton [64]. That is, it has an interpretation as a single D-brane in an $AdS_5 \times S^5$ geometry.

$$|\Delta\rangle_n = \boxed{}\boxed{}\cdots\boxed{n} \tag{4.49}$$

Here, we find that when we move away from thinking of Λ as formal parameter, and rather think of it as an actual c-number, the right hand side can be interpreted as a coherent state of the harmonic oscillators represented by t_k. We will now push the

idea that a special generating series of interesting objects should be more than a formal expression and actually have physical meaning. The reason this is a coherent state is that it is an exponential of a linear combination of raising operators. We still need to find the range of Λ that is appropriate for this expression.

We can consider the norm of the state

$$\langle \triangle; \Lambda \rangle \triangle; \Lambda = \sum_n (\bar{\Lambda}\Lambda)^n = \frac{1}{1 - \bar{\Lambda}\Lambda} \tag{4.50}$$

and we see that it is convergent for $|\Lambda| < 1$. This can be similarly obtained from the exponential and the gaussian measure (4.37). The proof is instructive. Consider

$$\begin{aligned} \langle \triangle; \Lambda \rangle \triangle; \Lambda &= \int \prod_k dt_k d\bar{t}_k \exp\left(- \sum_k \frac{t_k \bar{t}_k}{k} \right) \exp\left(\sum_k \bar{\Lambda}^k \frac{\bar{t}_k}{k} \right) \exp\left(\sum_k \Lambda^k \frac{t_k}{k} \right) && (4.51) \\ &= \int \prod_k dt_k d\bar{t}_k \exp\left(- \sum_k \frac{(t_k - \bar{\Lambda}^k)(\bar{t}_k - \Lambda^k)}{k} \right) \exp\left(\sum_k \frac{\Lambda^k \bar{\Lambda}^k}{k} \right) && (4.52) \end{aligned}$$

where to arrive at the second line we completed the square. Shifting the integration variables, we find that

$$\langle \triangle; \Lambda \rangle \triangle; \Lambda = \exp\left(\sum_k \frac{\Lambda^k \bar{\Lambda}^k}{k} \right) = \exp(-\log(1 - \Lambda\bar{\Lambda})) = \frac{1}{1 - \Lambda\bar{\Lambda}} \tag{4.53}$$

where we have recognized the Taylor series for $\log(1-x)$ in the exponential. If we didn't already know that the $|\triangle\rangle_n$ were orthonormal, the coefficients in the Taylor series that appear in (4.50) after expanding in (4.53) would have shown that.

The fact that this generating series produces a coherent state for the oscillators is important in more than one way. First, it shows that the D-brane can be thought of as a "soliton" of the free field theory: a non-dissipating solution of the classical equations of

motion. This is how, in the weak string limit, a D-brane can be thought of as a localized classical source for string fields, where away from the D-brane location one has a solution of the classical equations of motion. This is usually encoded in how different boundary states overlap by considering how closed strings propagate from one boundary state to the other [104]. Another example where D-branes decay into string fields can be found in [105].

Since this D-brane state is a coherent state, it is an eigenstate of the lowering operators represented by $(t_k)^\dagger \simeq k\partial_{t_k}$. We find that for these states

$$\langle a_k\rangle_{\Delta;\Lambda} = \langle (t_k)^\dagger\rangle_{\Delta;\Lambda} = \Lambda^k, \quad \langle a_k^\dagger\rangle_{\Delta;\Lambda} = \langle t_k\rangle_{\Delta;\Lambda} = \bar{\Lambda}^k \tag{4.54}$$

This behavior is expected from the collective coordinate treatment in setups at finite N [106, 99]. In these other approaches, the coherent states in question are described in terms of Slater determinants of coherent states for generalized oscillator algebras.

The states we have found are also of minimal uncertainty for all the oscillators. This will become important when we try to describe other classical limits later in the paper.

The next thing that is interesting to compute is the average energy per oscillator in each one of these states. This is captured by

$$\langle E_k\rangle_{\Delta;\Lambda} = \langle k t_k\partial_{t_k}\rangle_{\Delta;\Lambda} = (\Lambda\bar{\Lambda})^k \tag{4.55}$$

so that the expectation value of the energy is

$$\langle E\rangle_{\Delta;\Lambda} = \sum_{k>0}(\Lambda\bar{\Lambda})^k = \frac{\Lambda\bar{\Lambda}}{1-\Lambda\bar{\Lambda}} \tag{4.56}$$

the energy carried by the state is large in the limit where $|\Lambda| \to 1$, but in this limit the

state becomes non-normalizable. It makes sense to consider states near this limit, where $\Lambda \simeq (1-\epsilon)^{1/2}\exp(i\gamma)$ with ϵ infinitesimally small and acting as a cutoff. In that case, the energy per oscillator degree of freedom goes to one, but this means that each oscillator has on average low occupation number

$$\langle \hat{N}_k \rangle_{\Delta;\Lambda\to\exp(i\gamma)} = \langle E_k \rangle_{\Delta;\Lambda\to\exp(i\gamma)}/k = 1/k. \tag{4.57}$$

The excitations are then still a coherent state for all oscillators, and if we cut off the degrees of freedom in the UV, we find a finite energy lump determined by the cutoff. The failure of the state to be normalizable is due to the infinitude of modes that can be excited, not to any one oscillator mode going bad on its own. Also, the amplitudes for the different modes are phase correlated. This is important. The reason is that we want to build a field out of the oscillators $a_k, a_k^\dagger$. The geometry where the fields live should be on a circle (we have argued that we have the degrees of freedom of a chiral boson in the previous section).

4.4.2 Field of the brane

The finiteness properties and phase correlations we have found suggest that we can think of the field generated by the D-brane state as being a classical profile everywhere except at the position of the brane itself. We will use this intuition to argue that there is a preferred linear combination of the oscillators that gives nice properties for the field profile in the limit we want. We will posit that the field operator take the following hermitian combination as an ansatz

$$\hat{\phi}(\theta) = \sum_{k>0} f_k[a_k \exp(-ik\theta) + a_k^\dagger \exp(ik\theta)] \tag{4.58}$$

where f_k is a set of positive numbers. At this stage, we are simply making an educated guess as to the form of the operator. Later, we will find that it is consistent with all expectations and declare it to have been the correct choice. Although we could have added phases to f_k, the phase correlation of the modes suggest that we set all the phases equal to each other. Scale invariance of the chiral boson suggests that we take $f_k \simeq 1/|k|^\alpha$ for some exponent α which is yet to be determined. Replacing the expectation values from (4.54) and taking the limit, we find that the profile associated with the D-brane is given by

$$\phi(\theta) = \langle\hat{\phi}(\theta)\rangle_{\Delta;\Lambda=\exp(i\gamma)} = \sum_{k>0} f_k[\exp(ik(\gamma-\theta)) + \exp(-ik(\gamma-\theta))] \tag{4.59}$$

The phases give (maximal) constructive interference at $\theta = \gamma$, which we will call the position of the D-brane. This is why it is important to choose all phases as we did: it produces the maximum possible constructive interference of the profile at a point. This is tantamount to saying that we have localized the peak as much as possible. Everywhere else, the phase sums can cancel enough that the result is finite. Taking $f_k = 1/|k|^\alpha$, the result can be written in terms of Polylog functions. We will now argue that if we instead choose $f_k = 1$, the answer becomes extremely simple, and we should therefore choose this value. This choice will have preferable geometric consequences. We find

$$\phi(\theta) = \langle\hat{\phi}(\theta)\rangle_{\Delta;\Lambda=\exp(i\gamma)} = \sum_{k\neq 0} \exp(ik(\gamma-\theta)) = 2\pi\delta(\gamma-\theta) - 1 \tag{4.60}$$

That is, the field away from the position of the brane becomes constant and has an exactly flat shape in the tail of the D-brane. We will promote this property to the reason why we make this choice for the field. This is a geometric condition. Because the field

does not have a mode at $k = 0$, it is required that

$$\int_0^{2\pi} d\theta\, \phi(\theta) = 0 \tag{4.61}$$

which is verified readily. This is actually true for any choice of the f_k, subject to convergence at $|\Lambda| < 1$. For the particular choice we made, we have a quantization condition on the area under the δ-function distribution, which is 2π. The energy can also be written simply in terms of $\phi(\theta)$. More precisely

$$E[\phi] = \left\langle \sum_k a_k^\dagger a_k \right\rangle = \left\langle \frac{1}{2\pi} \int d\theta \left(\frac{1}{2} : \hat{\phi}(\theta)^2 : \right) \right\rangle = \frac{1}{2\pi} \int d\theta \left(\frac{1}{2} \phi(\theta)^2 \right) \tag{4.62}$$

where we use the normalization of the modes in (4.36) with $|T| = 1$. This shows that the choice for the field coefficients in equation (4.58) is also determined by being able to write a local expression for the energy: a single integral of the field and a finite number of its derivatives. The rightmost term in (4.62) is the classical contribution to the energy for a smooth $\phi(\theta)$.

There is a second natural choice for a field. This is the field that is obtained by considering $|\Lambda| = 1$ and looking for the combination of modes that appears in the exponent of (4.48). The idea is that when we declared the generating function (4.48) to be singled out by our representation basis and the convergence properties, the limit defined a preferred combination of modes.

It is convenient to call this field χ and define it to be

$$\hat{\chi}(\theta) = \sum_{k>0} \frac{1}{ik} \exp(ik\theta)\, a_k^\dagger + c.c \tag{4.63}$$

The factor of i in the denominator is a convention we choose, which gives

$$|\triangle; \Lambda \to \exp(i\gamma)\rangle =: \exp(i\chi(\gamma)) : |0\rangle \tag{4.64}$$

One easily finds that the field χ and the field ϕ are related by

$$\partial_\theta \chi(\theta) = \phi(\theta) \tag{4.65}$$

so that locality in the sense of χ (in terms of the smooth variable θ) ends up being equivalent to locality in the sense of ϕ. Indeed, the field χ is what we would usually call the free boson and the field ϕ is the associated current. The local energy is the standard stress tensor for the chiral boson. This matches the derivations in [83] very well.

The field $: \exp(i\chi(\theta)) :$ is usually thought of as a fermionic field written in the bosonized language (see [31], pp 11, eq. 10.3.10).

4.4.3 The anti-brane and its field

The other natural representation of the symmetric group is the alternating representation. This representation is also one dimensional, and the character counts how many transpositions (modulo 2) are in a group element. For a cycle $[s]$, the sign assigned to it is

$$sign[s] = (-1)^{s-1} \tag{4.66}$$

This is multiplicative, meaning that $sign[a \circ b] = sign[a]sign[b]$. When we consider the equivalent of equation (4.67), we get that the sum over characters is

$$|\bigtriangledown\rangle_n = \frac{1}{|\Gamma|}\sum_{[\sigma]\in S_n}\chi_{\bigtriangledown}([\sigma])d_\sigma|[\sigma]\rangle = \left|\sum_{\overrightarrow{\omega}\in p(n)}\prod_k \frac{1}{k^{w_k}w_k!}((-1)^{k-1}t_k)^{w_k}\right\rangle \tag{4.67}$$

where we used the multiplicative rule on the right hand side. We have labeled the states with $\bigtriangledown$ instead of $\bigtriangleup$. In the language of Young diagrams, this representation corresponds to a single column with n boxes.

$$|\bigtriangledown\rangle_n = \begin{array}{|c|}\hline\ \\\hline\ \\\hline\vdots\\\hline\ \\\hline\end{array} \tag{4.68}$$

This also corresponds to a totally antisymmetric representation of $U(N)$ with n indices. These states correspond to giant graviton states [89] in the AdS/CFT correspondence. We now want to do a similar generating function to the one in (4.48) for these states. Consider the following

$$\begin{aligned}
|\bigtriangledown, -\Omega\rangle &= \sum_n \Omega^n |\bigtriangledown\rangle_n && (4.69)\\
&= \sum_n \sum_{\overrightarrow{\omega}\in p(n)} \Omega^n \prod_k \frac{1}{k^{w_k}w_k!}((-1)^{k-1}t_k)^{w_k} && (4.70)\\
&= \sum_n \sum_{\overrightarrow{\omega}\in p(n)} \prod_k \frac{1}{w_k!}\left(\frac{\Omega^k}{k}(-1)^{k-1}t_k\right)^{w_k} && (4.71)\\
&= \sum_n \sum_{\overrightarrow{\omega}\in p(n)} \prod_k \frac{1}{w_k!}\left(-\frac{(-\Omega)^k}{k}t_k\right)^{w_k} && (4.72)\\
&= \exp\left(-\sum_k \frac{(-\Omega)^k}{k}t_k\right) && (4.73)
\end{aligned}$$

where we have made a sign convention choice in how we wrote Ω in the generating series, versus how we wrote it in the previous state. We find that with this convention

$$|\bigtriangledown, \Lambda\rangle = \exp\left(-\sum_k \Lambda^k \frac{t_k}{k}\right) \tag{4.74}$$

so that in the same limit as before we have that

$$|\bigtriangledown; \Lambda \to \exp(i\gamma)\rangle =: \exp(-i\chi(\gamma)) : |0\rangle \tag{4.75}$$

which is the other fermion field. The natural notion of locality derived from the states $|\bigtriangleup; \Lambda\rangle$ and $|\bigtriangledown; \Lambda\rangle$ are the same. It is now trivial to show that for these new solutions

$$\langle\hat{\phi}(\theta)\rangle_{\bigtriangledown;\Lambda=\exp(i\gamma)} = -\sum_{k\neq 0} \exp(ik(\gamma-\theta)) = -2\pi\delta(\gamma-\theta) + 1 \tag{4.76}$$

There is also a symmetry that sends $\bigtriangleup \leftrightarrow \bigtriangledown$. This is 'particle-hole' duality and is implemented by $\chi(\theta) \to -\chi(\theta)$, and $\phi(\theta) \to -\phi(\theta)$. In some finite matrix models built from microscopic fermionic degrees of freedom, this can be implemented exactly [107].

We will call the two families of operators

$$B_{\pm,\Lambda} = \exp\left(\pm\sum_k \Lambda^k \frac{t_k}{k}\right) \tag{4.77}$$

acting on any state the D-brane creation operators. That is, up to including $: \exp(\pm i\chi(\gamma)) :$, which is non-normalizable.

4.4.4 Multiple brane states

Consider acting with a D-brane creation operator on a state that already has one D-brane. At the level of the oscillator representation of states, this is straightforward. We can write

$$B_{+,\Lambda_1} B_{+,\Lambda_2} |0\rangle = \exp\left(\sum_k \left(\Lambda_1^k + \Lambda_2^k\right) \frac{t_k}{k}\right) \tag{4.78}$$

We easily find that this is also a classical state, which results from the superposition of the two profiles of the individual D-branes. The classical field is characterized by

$$\langle (t_k^\dagger) \rangle_{\Delta,\Lambda_1;\Delta,\Lambda_2} = \Lambda_1^k + \Lambda_2^k \quad \langle t_k \rangle_{\Delta,\Lambda_1;\Delta,\Lambda_2} = \bar{\Lambda}_1^k + \bar{\Lambda}_2^k \tag{4.79}$$

and

$$\langle \hat{\phi}(\theta) \rangle_{\Delta,\Lambda_1;\Delta,\Lambda_2} = 2\Re e \left(\frac{\Lambda_1 e^{-i\theta}}{1-\Lambda_1 e^{-i\theta}} + \frac{\Lambda_2 e^{-i\theta}}{1-\Lambda_2 e^{-i\theta}}\right) \tag{4.80}$$

Similarly, we can write

$$B_{+,\Lambda_1} B_{-,\Lambda_2} |0\rangle = \exp\left(\sum_k \left(\Lambda_1^k - \Lambda_2^k\right) \frac{t_k}{k}\right) \tag{4.81}$$

$$\langle \hat{\phi}(\theta) \rangle_{\Delta,\Lambda_1;\bigtriangledown,\Lambda_2} = 2\Re e \left(\frac{\Lambda_1 e^{-i\theta}}{1-\Lambda_1 e^{-i\theta}} - \frac{\Lambda_2 e^{-i\theta}}{1-\Lambda_2 e^{-i\theta}}\right) \tag{4.82}$$

Notice that if we take $\Lambda_1 = \Lambda_2$ in the second profile, the fields cancel. This tells us that the two types of D-brane states annihilate one another into the vacuum [1].

We will now use the D-brane basis (the basis using irreducible representations of S_n), to better understand how these generating functions behave. We will use Young tableaux to compute the multi-brane states. The correct multiplication table is governed by the

[1]The more precise version of this cancellation is that the OPE expansion of the two fermion fields contains the identity

Littlewood-Richardson coefficients [64] (see also the discussion in [99]). Remember that $|\Delta\rangle_n$ is associated with a tableaux with n boxes in a row. These are the objects that appear in $|\triangle, \Lambda\rangle$. We want to compute

$$B_{+,\Lambda_1} B_{+,\Lambda_2} |0\rangle = \sum_{n,m} \Lambda_1^n \Lambda_2^m \underbrace{\square\square\cdots\square}_{n} \times \underbrace{\square\square\cdots\square}_{m} \tag{4.83}$$

The multiplication of two of these objects is similar to addition of angular momentum in $U(2)$, so that

$$\underbrace{\square\square\cdots\square}_{n} \times \underbrace{\square\square\cdots\square}_{m} \tag{4.84}$$

$$= \underbrace{\square\square\cdots\square}_{n+m} + \underbrace{\begin{array}{l}\square\square\cdots\square\\ \square\end{array}}_{n+m-1} + \cdots + \begin{array}{l}\square\square\cdots\cdots\cdots\square\\ \square\square\cdots\square\end{array} \tag{4.85}$$

where we assume $n \geq m$ in the second line, but we can also have the opposite ordering in which case we exchange n, m. We see that all states have only two rows in their Young diagrams. We will group together all diagrams with two rows of lengths r and s with $r \geq s$. To find the coefficient of these, we need to consider the decomposition $r + s = n + m$, such that $|n - m| \leq s$ and to sum over these possibilities. When we perform this sum we obtain

$$\Lambda_1^r \Lambda_2^s + \Lambda_1^{r-1} \Lambda_2^{s+1} + \cdots + \Lambda_1^s \Lambda_2^r = \frac{\Lambda_1^{r+1} \Lambda_2^s - \Lambda_1^s \Lambda_2^{r+1}}{\Lambda_1 - \Lambda_2} \tag{4.86}$$

That is, we can write identically that

$$(\Lambda_1 - \Lambda_2) B_{+,\Lambda_1} B_{+,\Lambda_2} |0\rangle = \sum_{r \geq s} \begin{vmatrix} \Lambda_1^{r+1} & \Lambda_1^s \\ \Lambda_2^{r+1} & \Lambda_2^s \end{vmatrix} \begin{array}{l}\square\square\cdots\cdots\cdots\square\\ \square\square\cdots\square\end{array} \tag{4.87}$$

where the coefficients are very easily written in terms of determinants. This suggests that the full set of states with two classical D-branes acting on the vacuum can be interpreted as a set of fermionic wave functions (Slater determinants), as long as we multiply them on the left by a Vandermonde determinant made from the Λ parameters. The point is that the complexity of the coefficients of the tableaux in equation (4.87) is very small. Notice that even though $r \geq s$, this implies that $r+1 > s$, so the Slater determinants never vanish, unless we have that $\Lambda_1 = \Lambda_2$ (this is trivial in the left hand side, as the full ket is multiplied by $\Lambda_1 - \Lambda_2$). Notice that if both D-brane states are normalizable, so is their product. The same arguments work for the product of various D-brane states, but the combinatorics of multiplying the Young tableaux are more complicated. The simplest way to understand it is through the relation between free fermions and formal matrix models for a generalized oscillator (this is described in [99]).

We can also compute the norm of the state to obtain

$$\begin{aligned}
||(\Lambda_1-\Lambda_2)B_{+,\Lambda_1}B_{+,\Lambda_2}|0\rangle||^2 = & \sum_{r\geq s}\left\|\begin{matrix}\Lambda_1^{r+1} & \Lambda_1^s\\ \Lambda_2^{r+1} & \Lambda_2^s\end{matrix}\right\|^2 = \sum_{r\geq s}||\Lambda_1^{r+1}\Lambda_2^s-\Lambda_1^s\Lambda_2^{r+1}||^2 \\
= & \sum_{r\geq s}||\Lambda_1^{r+1}\Lambda_2^s||^2+\sum_{s\geq r}||\Lambda_1^r\Lambda_2^{s+1}||^2 \\
& -\sum_{r\geq s}\Lambda_1^{r+1}\Lambda_2^s\bar{\Lambda}_1^s\bar{\Lambda}_2^{r+1}-\sum_{s\geq r}\Lambda_1^r\Lambda_2^{s+1}\bar{\Lambda}_1^{s+1}\bar{\Lambda}_2^r \\
= & \sum_{r,s}||\Lambda_1^r\Lambda_2^s||^2-\Lambda_1^r\Lambda_2^s\bar{\Lambda}_1^s\bar{\Lambda}_2^r \\
= & \frac{1}{1-||\Lambda_1||^2}\frac{1}{1-||\Lambda_2||^2}-\frac{1}{1-\Lambda_1\bar{\Lambda}_2}\frac{1}{1-\Lambda_2\bar{\Lambda}_1}
\end{aligned}$$

where we have relabeled r, s in some of the sums in the second line, and next we add and subtract the $r+1=s$ and $s+1=r$ contribution to obtain unrestricted sums that can

be evaluated explicitly on the last line. This expression is equal to

$$||(\Lambda_1 - \Lambda_2)B_{+,\Lambda_1}B_{+,\Lambda_2}\,|0\rangle\,||^2 = ||\,|\Delta,\Lambda_1\rangle\,||^2||\,|\Delta,\Lambda_2\rangle\,||^2 - \langle\Delta,\Lambda_2\rangle\,\Delta,\Lambda_1\,\langle\Delta,\Lambda_1\rangle\,\Delta,\Lambda_2 \tag{4.88}$$

after we recognize the result (4.50) and we think of $\Lambda, \bar{\Lambda}$ as independent variables. This results in the typical norm for two-particle states in fermion systems: the product of the norms minus the exchange contribution.

The multiplication rules for two B_- operators will give a similar result, but with Young tableaux with two columns, rather than two rows. This follows from the $\phi \to -\phi$ symmetry, which flips tableaux along the main diagonal. The other example with two branes is what happens when we multiply B_{+,Λ_1} and B_{-,Λ_2}. This is the most interesting example because one can get a cancellation between the two. It is instructive to see how this comes about from multiplying the corresponding Young tableaux, as follows

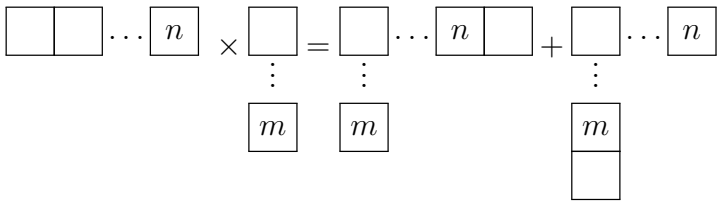

(4.89)

and to each of these we associated the coefficient $\Lambda_{+,1}^n(-\Lambda_{-,2})^m$. Now, we only get two possible tableaux on the right hand side. If we fix the Young diagram to have r boxes on the first row and s boxes on the first column, we get by summing over possibilities $\Lambda_1^r(-\Lambda_2)^{s-1} + \Lambda_1^{r-1}(-\Lambda_2)^s = \Lambda_1^{r-1}(-\Lambda_2)^{s-1}(\Lambda_1 - \Lambda_2)$, except in the case of no boxes,

where we get 1. That is, we find that

$$B_{+,\Lambda_1}B_{-,\Lambda_2}\left|0\right\rangle = 1 + \sum_{r\geq 1, s\geq 1} \Lambda_1^{r-1}(-\Lambda_2)^{s-1}(\Lambda_1-\Lambda_2) \begin{array}{|c|}\hline \quad \\ \hline \end{array} \cdots \boxed{r} \\ \vdots \\ \boxed{s} \tag{4.90}$$

and now the right hand side simplifies if we divide by $(\Lambda_1 - \Lambda_2)$ (rather than when we multiply by it). If we compute the norm of the state (when dividing by $(\Lambda_1 - \Lambda_2)$) we get that

$$\left|\left|\frac{B_{+,\Lambda_1}B_{-,\Lambda_2}\left|0\right\rangle}{\Lambda_1-\Lambda_2}\right|\right|^2 = \frac{1}{||\Lambda_1-\Lambda_2||^2} + |\left|\triangle,\Lambda_1\right\rangle|^2|\left|\bigtriangledown,\Lambda_2\right\rangle|^2 \tag{4.91}$$

and apart from the first term, it shows that the two types of fermionic "particles" are distinguishable. In this setup, when $\Lambda_1 \to \Lambda_2$, the first term develops a pole. That is, the 1 dominates the norm of the state, but this can be subtracted if we are careful, and then we can get a smooth two particle state in the limit.

Formally, when we consider a state $|\psi\rangle$, which results from applying various $B_\pm$ operators, we can identify the expectation values as supertraces of a complex supermatrix

$$\left\langle\psi\right| a_k \left|\psi\right\rangle = \sum \Lambda_{+i}^k - \sum_j \Lambda_{-j}^k = Str \begin{pmatrix} {\mathbf{\Lambda}_+}^k & \vdots & 0 \\ \cdots & \cdots & \cdots \\ 0 & \vdots & {\mathbf{\Lambda}_-}^k \end{pmatrix} = Str[\mathbf{\Lambda}^k] \tag{4.92}$$

where we identify the different values $\Lambda_{+,-}$ with the corresponding eigenvalues. The values of Λ are then interpreted as collective coordinates for the D-brane states. The interesting prefactor of the wave functions where we multiply by

$$\prod_{i<j}(\Lambda_{+,i}-\Lambda_{+,j})\prod_{i<j}(\Lambda_{-,i}-\Lambda_{-,j})\prod(\Lambda_{+,i}-\Lambda_{-,j})^{-1} \tag{4.93}$$

is a super-Vandermonde determinant.

4.5 Free fermions and the Murnaghan-Nakayama rule

We see that it is rather helpful to be able to go from the conjugacy class basis to the representation basis efficiently. Therefore it makes sense to understand how to compute the characters $\chi_R(\sigma)$ more precisely in order to be able to make progress. The main tool to do so is the Murnaghan-Nakayama rule, as described in appendix B. This gives a recursive way to compute the characters of the symmetric group. We will now see that this rule is essentially encoding the fact that the tableaux states correspond to free fermions.

We will prove this fact now. To do so, let us analyze the main result of the appendix, where the Murnaghan-Nakayama rule can be rewritten as an operator equation in the Hilbert space of states

$$s\partial_{t_s} |R\rangle = \sum_{\text{hooks of length } s} (-1)^{f_{\text{hook}}} |\tilde{R}_{\text{hook}}\rangle \tag{4.94}$$

where f_{hook} is the number of rows spanned by the hook, minus one, and $\tilde{R}_{hook}$ is the Young tableaux R with the skew hook corresponding to the hook that has been singled out removed. A skew hook is a set of boxes at the edge of the tableaux whose removal produces an allowed tableaux, and they are in one to one correspondence with regular hooks (see appendix B).

Remember that $s\partial_{t_s} \simeq a_s$ is the lowering operator of the mode s in the Fock space.

This equation above can also be read as follows

$$\langle \tilde{R}| \, a_s \, |R\rangle = (-1)^{f_{\text{hook}}} \tag{4.95}$$

or taking adjoints

$$\langle R| \, a_s^\dagger \, |\tilde{R}\rangle = (-1)^{f_{\text{hook}}} \tag{4.96}$$

where $|\tilde{R}\rangle$ is a particular diagram appearing in the sum with one hook removed. For instance, consider the state corresponding to the representation given by

$$|R\rangle = \tag{4.97}$$
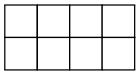

We could apply the lowering operator a_3. Equation 4.94 gives

$$a_3 \tag{4.98}$$
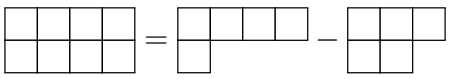

We could then dot this with the state given by

$$|\tilde{R}\rangle = \tag{4.99}$$
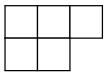

And we find

$$\langle \tilde{R}| \, a_3 \, |R\rangle = -1 = (-1)^1 \tag{4.100}$$

as expected.

We will now show how this arises using free fermion intuition. Proving equation (4.95) is equivalent to proving equation (4.94), which in turn gives a proof of the Murnaghan-Nakayama rule.

We need to think of what $a_s^\dagger$ is doing in terms of the eigenvalue representation (the fermions in Matrix models). The idea is that to each eigenvalue of an infinite matrix we associate a Cuntz oscillator pair $\beta_\ell \beta_\ell^\dagger = 1$ (which commute with each other for different ℓ) and we will treat these eigenvalues as Fermions (see [99] for details on how to build fermionic systems from general oscillators). The operator

$$a_s^\dagger = \sum_{\ell=0}^{\infty} (\beta_\ell^\dagger)^s = Tr((\beta^\dagger)^s) \tag{4.101}$$

is a trace of the powers of the raising operator $\beta^\dagger$ thought of as a matrix. The ground state of the multiple particle system $\bullet$ is defined by the Slater determinant

$$\bullet \simeq \lim_{N\to\infty} |-1/2\rangle\, |-3/2\rangle \ldots |-(2N-1)/2\rangle_{\text{antisymm}} \tag{4.102}$$

where we have set the Fermi sea at energy zero, and all the (infinite tower of) negative energy states are occupied. If all the $|j\rangle$ are orthonormal, the procedure of antisymmetrization gives a normalization factor in front of the state with an $\mathcal{N} = ((N+1)!)^{-1/2}$ to obtain a normalized state. This is common to all states in what follows. Pictorally, we will represent our ground state as

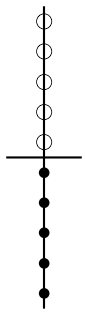

(4.103)

Notice we have chosen to label the energy of each particle at half integers, rather

than filling the Fermi sea to zero and having the particles occupy integer energies. We did this because it makes the particle/hole duality more explicit and symmetric. This is simply a convention and everything would follow in the same way if all particle energies were shifted by 1/2, as it is always energy differences that are measured.

A complete basis of states is given by

$$|\{n\}\rangle \simeq \lim_{N\to\infty} |n_1\rangle\, |n_2\rangle \dots |n_N\rangle_{\text{antisymm}} \tag{4.104}$$

with $n_1 > n_2 > n_3 > \cdots > n_N$, half integers, and for all sufficiently large j we require that $n_j = -\frac{2j-1}{2}$.

We will now show how to go directly from one of these states to a Young tableaux representation, which we will associate with it. Consider the numbers given by $r_j = n_j - n_j^0 = n_j - (\frac{1}{2} - j)$, e.g. $r_1 = n_1 - (-\frac{1}{2})$, $r_2 = n_2 - (-\frac{3}{2})$. These numbers will give the differences between the particles excited positions and their ground state position. We can check easily that $r_i - r_{i+1} = n_i - n_{i+1} - 1 \geq 0$, since the n_i are strictly decreasing integers and moreover that $r_i = 0$ for sufficiently large i. We assign to this set a Young diagram with rows of length $r_1, \dots r_s$ for all the r_k that are different from zero. This is an allowed tableaux because the integers are non-increasing. Details of the pictorial representation of this assignment can be found in appendix C. We can clearly invert this map, because knowing r_i is equivalent to knowing the n_i. Now, instead of $|\{n\}\rangle$ we use the tableaux $|\tilde{R}\rangle$.

Now we act with $a_s^\dagger = Tr((\beta^\dagger)^s)$ on $|\tilde{R}\rangle$ and get that

$$a_s^\dagger\, |\tilde{R}\rangle \propto \lim_{N\to\infty} \sum_{\ell=1}^{N} |n_1\rangle\, |n_2\rangle \dots |n_{\ell-1}\rangle\, |n_\ell + s\rangle\, |n_{\ell+1}\rangle \dots |n_N\rangle_{\text{antisymm}} \tag{4.105}$$

If the state has two of the n_j equal to each other, the antisymmetrization procedure will remove the term from the sum. Now, we need to check if the new state has the n_s in decreasing order or not. If it does not, we need to reshuffle the n_s, by moving the $n_{\ell+s}$ to the left until we get a proper order. We do this by transposition of nearest neighbors, moving $n_\ell + s$ as we go along. Each such transposition is an exchange of two fermions, so it costs a factor of (-1). The sign we get is $(-1)^{\#\text{transpositions}}$.

As an example of how this works, we would have

$$\begin{aligned} a_2^\dagger \Big(&|5/2\rangle\,|3/2\rangle\,|-1/2\rangle\,|-7/2\rangle\,|-9/2\rangle\ldots|n_N\rangle_{\text{antisymm}}\Big) \\ &= |9/2\rangle\,|3/2\rangle\,|-1/2\rangle\,|-7/2\rangle\,|-9/2\rangle\ldots|n_N\rangle_{\text{antisymm}} \\ &- |7/2\rangle\,|5/2\rangle\,|-1/2\rangle\,|-7/2\rangle\,|-9/2\rangle\ldots|n_N\rangle_{\text{antisymm}} \\ &+ |5/2\rangle\,|3/2\rangle\,|-1/2\rangle\,|-3/2\rangle\,|-9/2\rangle\ldots|n_N\rangle_{\text{antisymm}} \\ &- |5/2\rangle\,|3/2\rangle\,|-1/2\rangle\,|-5/2\rangle\,|-7/2\rangle\ldots|n_N\rangle_{\text{antisymm}} \end{aligned} \tag{4.106}$$

Notice the second and fourth terms have negative signs because we had to perform one transposition on each to find a state with the proper ordering. Notice also that we dropped all terms that would have had two n_i's that are equal to each other and so would go away upon antisymmeterization. Now we want to think about how the transpositions affected the Young diagrams these states correspond to.

Because various of the n_i have been moved to the right, we find that for these that have moved we get that $n_{i+1}^{\text{new}} = n_i^{\text{old}}$, so $r_{i+1}^{\text{new}} = n_{-1+i}^{\text{old}} - (-i) = r_i^{\text{old}} + 1$. That is, in the Young diagram we have moved the row i to the $i+1$ row and added one extra box to the right (this is equivalent to moving the corner of the row one to the right and one down). There is still the one that got moved to the left. This one row was moved upward

by #transpositions, and each such transposition makes the corresponding row we are tracking shorter by one (this is the opposite of the +1 to the right that we have found for the others). The net effect is that we have added just s boxes to the Young diagram and gotten a normalized state for each ℓ that is allowed. That is, we get that

$$a_s^\dagger |\tilde{R}\rangle = \sum_{\text{hooks}} (-1)^{\#\text{transpositions}} |R_{\text{allowed}}\rangle \tag{4.107}$$

The motion to the right and down produces a skew hook of length s added to the original tableaux (we just color in the new boxes in a different color than those of $\tilde{R}$). The sign we find is the same sign that is assigned by the Murnaghan-Nakayama rule. The number of transpositions is the number of rows that have changed minus one!

As a simple example consider $a_5^\dagger$ $\square\square\square$.

What does this correspond to in the Fermi sea picture of appendix C? We have 5 units of energy we are adding and there are several options we have for where to put them. The state we are starting with is

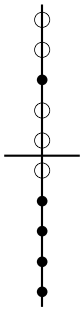

(4.108)

We could imagine giving all the energy to the already excited particle. This gives

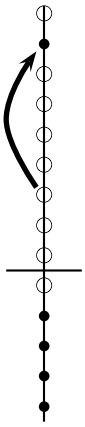

(4.109)

which we know corresponds to a totally symmetric diagram with 8 boxes.

However, we could have made a different choice and excited the top particle out of the fermi sea. This would give

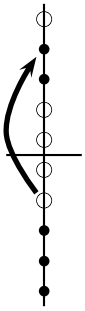

(4.110)

Notice that to get to this position, we had to pass the already excited particle (we had to perform a transposition), and therefore had to pick up a minus sign. We find, then, that the negative sign, which previously was simply a part of the MN rule, actually encodes the exchange statistics of fermions.

Carrying on, we we could imagine exciting the second particle from the fermi sea, but

we know this should not be allowed by the Pauli exclusion principle:

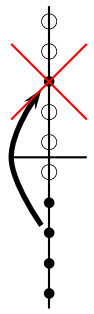

(4.111)

If we think about this in terms of Young tableau, we see that this would have corresponded to a diagram that is not allowed. Specifically, it would have corresponded to something of the form

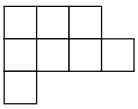

(4.112)

We know that this is not an allowed diagram and that fact encodes the exclusion principle.

The end result is that

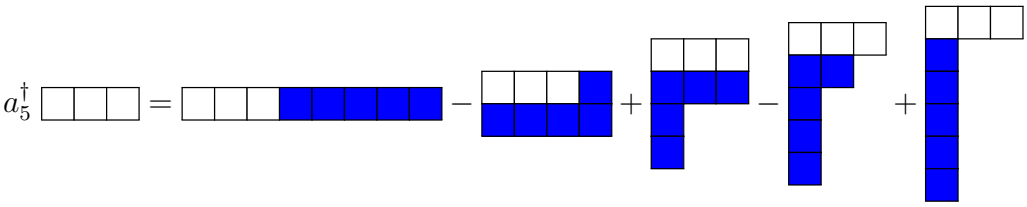

(4.113)

The outcome of this computation is that

$$\langle R|\, a_s^\dagger\, |\tilde{R}\rangle = (-1)^{\#\text{transpositions}} = (-1)^{f_{\text{hook}}} \tag{4.114}$$

as we wanted to prove. Moreover, the sign of the Murnaghan-Nakayama rule is nothing

other than the Fermi statistics. The boxes colored in blue are exactly the skew hooks that can be added to the original tableaux. These are always at the border of the tableaux such that adding them produces an allowed tableaux.

The upshot is that rather than trying to compute the $\chi_R(\sigma)$ directly, we compute the action of the t_s and its adjoints on the basis of Young tableaux (the D-brane basis). This algebraic action is simple and will let us establish a lot of facts in the next sections.

4.6 Multi-edge geometries: new classical limits with different topologies

In this section we will think of the classical field $\phi(\theta)$ as a displacement of the geometric interface between two fluids, made of particles and holes. This is the main viewpoint in treating the system as a set of free fermions as exemplified in the description of the quantum hall effect [83]. This is a geometric interpretation that also appears naturally in studying bubbling solutions [63], where the two fluids in question arise as the two possible values of a function on a plane that give rise to a regular BPS geometry in ten dimensions. Some of the treatment here follows the previous work by the authors [40].

Let us start with a simple identity for the classical energy of a configuration, where we use

$$E[\phi] = \frac{1}{2\pi}\int d\theta\, \frac{1}{2}\,\phi(\theta)^2 = \frac{1}{2\pi}\int d\theta \left[\int_0^{\phi(\theta)\geq 0} h\, dh - \int_0^{-\phi(\theta)>0} (-h)\, dh\right] \tag{4.115}$$

That is, we introduced and auxiliary field h and divided the coordinate θ into the regions $\phi(\theta) \geq 0$ and the regions $\phi(\theta) < 0$. This makes sense in the classical theory for smooth functions, but not quite in the quantum theory. The first region is associated

with moving particles into spaces that had been occupied by holes, and the second one is associated with moving holes where there were particles. Both particles and holes are conserved because $\int \phi(\theta)\, d\theta = 0$. We want to associate a function with this change of occupation, that takes the value $+1$ when particles occupy a hole state, and takes the value -1 when holes occupy previously occupied particle states. The function should otherwise vanish. This function is the relative density of particles with respect to the ground state $\tilde{\rho}(\theta, h) = \rho_+(\theta, h) - \rho_+^0(\theta, h)$. It can also be symmetrically constructed from the hole density with few modifications. The energy can then be expressed as

$$E[\phi] = \frac{1}{2\pi} \iint \tilde{\rho}(\theta, h)\, h\, dh\, d\theta \tag{4.116}$$

Notice that this formula is very similar to (4.17). The main difference is that in (4.17) one is allowed to have arbitrary regions with $\rho \neq 0$, while in (4.116) we have a description not only with fixed topology, but also with a unique height for the boundary between holes and particles for each θ. The field ϕ is given by

$$\phi(\theta) = -\int dh\, h\, \partial_h \tilde{\rho}(\theta, h) \tag{4.117}$$

This uses the fact that ρ can be written as Heaviside step functions whose derivative is a delta function, precisely at the height of the droplet. The contribution at $h = 0$ vanishes. Alternatively, we can integrate by parts to find that

$$\phi(\theta) = \int \tilde{\rho}(\theta, h)\, dh \tag{4.118}$$

and the conservation of particles and holes can be expressed as

$$\iint \tilde{\rho}(\theta, h)\, d\theta\, dh = 0 \tag{4.119}$$

Basically, we are expressing the states as pictures on a two dimensional cylinder. We will use this identity together with previous observations (particularly equation (4.60)) to understand how new classical limits can appear from different quantum states that are not classical in the oscillator representation.

4.6.1 Fixed energy single D-brane state

Let us start with a single D-brane state, but instead of considering the coherent states (4.48), we want to consider a state of the form $|\triangle\rangle_n$ for a fixed n: a single D-brane with fixed energy, and we want to think of it formally as a superposition of non-normalizable states $|\triangle, \exp(i\gamma)\rangle$ by doing a Fourier transform. The state $|\triangle\rangle_n$ is an eigenstate of the momentum operator, so it is translation invariant. Because the state is a superposition of classical states, it is not a classical state with respect to the usual variables $a_k^\dagger, a_k$ any longer. For example, it does not factorize into a product of coherent states because it has a fixed energy and it is not in the vacuum. Indeed, it is possible to show that in this state $\langle a_k \rangle = \langle a_k^\dagger \rangle = 0$, yet the energy is not zero (as one would conclude for coherent states). The naive classical state we would associate with this profile is the ground state. Because in the end the corresponding state is not a coherent state, we will be interested eventually in characterizing to what extent it violates the properties of the coherent state. For example, if a state has minimal uncertainty then it is a coherent state. Conversely, a non-trivial uncertainty serves as a measure of how much the state differs from a coherent state. Similarly, a coherent state is a product state (a pure state mode per mode).

Entanglement between the modes measures to what extent the mode per mode quantum state is not pure. We will take the problem of measuring these later in the paper.

What we want to do is we want to find an *alternative* classical description of this particular state so that when we insert the right value of $\tilde{\rho}(\theta, h)$ in equation (4.116), we get the right energy. We want to declare that this state can be classical as well, even if it is not a coherent state. Our goal is to come up with a prescription for how to do this consistently.

Moreover, we want the relative density to be translation invariant, so $\tilde{\rho}$ is independent of θ. To be classical, it should take the same prescribed nominal values from before $\tilde{\rho} = +1, -1, 0$. In principle, a value in between can be obtained from statistically averaging states (a density matrix state rater than a pure state). Those will not be treated as classical states but as statistical states. Here, we want the state to be pure, so no averaging should be performed.

Now, let us look precisely at (4.60). The idea behind building the new classical solution is that acting with a D-brane state lowers the level of ϕ by a prescribed amount: -1 in our conventions, and the area under the delta function is identified with the amount of area that a single D-brane (particle) occupies. We need to move this occupied area somewhere else, but we want to leave the lowering of the level interface exactly as the -1 demands: this is after all the classical field everywhere else away from the δ function distribution. Because of translation invariance, we should add horizontal strips with $\tilde{\rho} = 1$ to the picture in order to conserve area. Since we are acting with a single D-brane, this horizontal strip should be connected (a single object), and of width one because of area conservation. We are building this picture by hand, but we are inspired by the description of states in [63]. To match the energy of the state, there is only one place where we can put the strip: the topmost edge of the strip should be at height n.

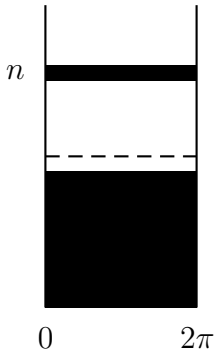

Figure 4.3: The black and white LLM plane drawing corresponding to a D-brane with fixed energy n.

If we use equation (4.118), we find that the field $\phi(\theta)$ vanishes, just as expected from the expectation values of the quantum state. However, when we analyze it from the point of view of (4.117) we realize that the expectation value of the field vanishes by adding three contributions

$$\phi = \int dh\, h\, (\delta(h-n) - \delta(h-n+1) + \delta(h+1)) = n - (n-1) - 1 \tag{4.120}$$

one from each of the edges of the ρ density. That is, we should think of the field $\phi(\theta)$ essentially as becoming a multi-valued function of θ, and the expectation value of the field is obtained by summing over these values with signs. We have gone from one well defined classical edge to three. This should be thought of as a topology transition. Notice that the superposition of states that gave rise to the state we want can be performed for finite values of Λ as well. In this interpretation, superpositions of classical coherent states with one topology can give rise to a topology change.

Notice that this new state is macroscopically different from each of the states that is used to make it, even statistically. For example, all the coherent states have $\tilde{\rho}(\theta, h) \geq 0$ strictly non-increasing as a function of h when $h \geq 0$. So when we take a classical statistical average of these states, this property should still hold. The new $\tilde{\rho}$ does not

have this property.

If for all original classical states we assign the same topology where the edge is a circle, then we find that there is no operator measurement in the Hilbert space that can distinguish the strip from the coherent states [40]. The argument is by contradiction. It proceeds as follows:

Suppose first that all coherent states are associated with a fixed (trivial) topology. Imagine now that such an operator exists. The operator should be such that all states with a trivial topology have the same eigenvalue. We can imagine building one such operator if we simply count the total number of edges to characterize the topology. We then get the same number for all coherent states: 1 (because they are described by a single height function), and so we are describing the identity operator. The strip topology state is a superposition of these, so the operator should evaluate to 1 as well, which clearly fails to count the number of edges appropriately. Therefore, there is no such topology measuring operator.

This means that topological type should be associated with details of a particular classical approximation of a state, and not with measurement of an operator. Notice that at this stage we have made no reference to entanglement as a source for topology changes [72, 78]. We are also stating that the set of classical states is even more overcomplete than regular coherent states. That there might be an overcompleteness that exceeds the standard overcompleteness of coherent states has been hinted at in [108] for situations involving the interior of a black hole. It was also argued there (following [109]) that gravitational physics requires state dependence, which implies that gravitational physics can not be encoded in operators. These works, in some sense, already assume that the $ER = EPR$ conjecture is true [78], so that non-trivial entanglement measures a topology change. As is well known, entanglement is not an operator measurement in Hilbert space,

although it can be computed in simple enough setups.

Back to our main discussion, since the strip state is not a coherent state, one can presume it is a state with larger uncertainty on each oscillator. We can actually compute these uncertainties using the techniques developed in section 4.5. We will see later that the spirit of (4.120) can be made precise for a large number of quantum states in the field theory, and the microscopic quantum field ϕ can be written as a sum with signs of other effective fields that appear as quantizations of small deviations away from a particular multi-strip configuration that should be thought of as a 'ground state' classical configuration with a coherent state excitation of its collective coordinates.

Let us finish analyzing this one configuration at a large but finite energy n. The Young diagram describing the state has n boxes and is completely horizontal.

$$|\Delta\rangle_n = \square\square\ldots\boxed{n} \tag{4.121}$$

We can evaluate the expectation values of the mode number operators $E_s = a_s^\dagger a_s$, $\hat{N}_s = s^{-1} a_s^\dagger a_s$ by the Murnaghan-Nakayama rule (see appendix B) in a straightforward fashion

$$ {}_n\langle\Delta|\, a_s^\dagger a_s\, |\Delta\rangle_n = {}_{n-s}\langle\Delta|\Delta\rangle_{n-s} = \begin{cases} 1 & \text{if } s \leq n \\ 0 & \text{Otherwise} \end{cases} \tag{4.122}$$

so the average energy per mode is constant up to mode n where it cuts off abruptly. The average occupation number per mode s is $1/s$, exactly as in equation (4.57). This shows why the state is a very close approximation to a regularized "fermion field state."

It also makes sense to ask which of the states $|\Delta, \Lambda\rangle$ is the best approximation to

$|\Delta\rangle_n$. The normalized probability amplitude to go from one to the other is

$$ {}_n\langle\Delta|\Delta;\Lambda\rangle = \Lambda^n\sqrt{1-\Lambda\bar{\Lambda}} \tag{4.123} $$

So that

$$ |{}_n\langle\Delta|\Delta;\Lambda\rangle|^2 = (\bar{\Lambda}\Lambda)^n(1-\Lambda\bar{\Lambda}) \tag{4.124} $$

This is maximized for

$$ \Lambda\bar{\Lambda} = \frac{n}{n+1} \tag{4.125} $$

For this value of $\Lambda\bar{\Lambda}$, we would find that the energy of the best coherent state approximation to the state to be exactly n, the energy of the state. For large n, the size of the overlap is of order $(en)^{-1}$ where e is Euler's constant. It is also easy to check the equations $a_s = a_1^s$ for these states, just as expected from the fact that all the coherent states that can be superposed to obtain the state satisfy them.

This means that the state $|\Delta\rangle_n$ should be thought of as an overlap of order n approximately orthogonal coherent states. That is roughly the number of states that would be needed to get the probabilities $\sum_i |{}_n\langle\Delta|\Delta;\Lambda_i\rangle|$ to add up to order one: what we need in order to say that we closely approximate the state $|\Delta\rangle_n$.

One can use this result to state that a superposition of a large number of states in quantum gravity might have very different properties (even different topology) than any of the individual states that make up the system. This is a result that has been argued quite effectively in [110], where the goal was to show that entanglement entropy can be thought of as an operator for a sufficiently small superposition of classical states, but not when we take the limit.

One can do a similar analysis with a single hole state of fixed energy $|\bigtriangledown\rangle_n$ and the

results are very similar.

Now, we can also evaluate the quantities

$$ {}_n\langle\Delta|\, a_s a_s^\dagger\, |\Delta\rangle_n = \langle (a_s - \langle a_s\rangle)(a_s^\dagger - \langle a_s^\dagger\rangle)\rangle = s + \langle a_s^\dagger a_s\rangle = s+1 \tag{4.126} $$

for $s \leq n$. These can be thought of as the net quantum uncertainty of the solution (including the ground state uncertainty, which is s). This shows that the state has low uncertainty (mode per mode) and can therefore be interpreted classically.

4.6.2 More general one stripe geometries

Now we will turn our attention to other states that have a similar interpretation. These are "translation invariant condensates of branes". The idea is to look at states whose Young diagram looks as follows

$$ |\Box_{L,M}\rangle = \tag{4.127} $$

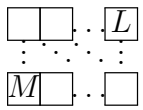

That is, a rectangular Young diagram with L columns and M rows.

We can visualize this state in the fermion picture (assuming $L > M$) as follows

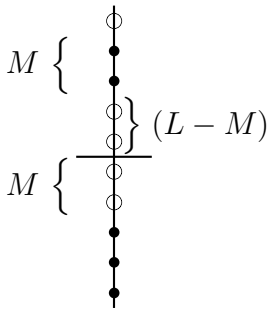

(4.128)

where there is a gap of size L between the filled sea and the excitation, and then the

excitation has width M (this corresponds to M filled states). This is natural from identifications in the figure 8 of [63]. These states are also translation invariant and share many of the properties of the previous state $|\triangle_n\rangle$, which would correspond to $|\square_{n,1}\rangle$. The natural identification with states in the droplet picture is to extend the representation (4.128) to a stripe configuration where the holes and filled states become extended on an interval $(0, 2\pi)$. The gap between the filled regions is of width L, and the filled top region is of width M. The corresponding LLM droplet picture is shown below.

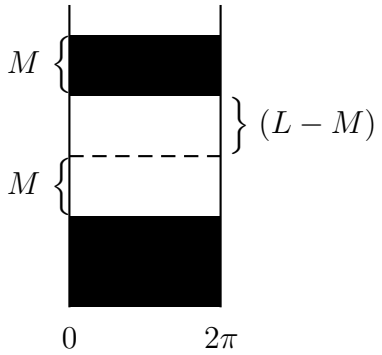

Figure 4.4: The black and white LLM plane drawing corresponding to a rectangular Young tableaux with $L \times M$ boxes.

Since these states are of fixed energy and $a_s^\dagger, a_s$ change the energy, we also have that $\langle a_s \rangle_{LM} = \langle a_s^\dagger \rangle_{LM} = 0$. Again, if this were a classical state in the usual classical limit of regular coherent states we would find that it should correspond to the vacuum. We want to interpret this state also as a classical state, with a black and white pattern as described. The configuration now has three edges: one at the very topmost of the most excited state, one (anti-) edge where the gap ends, and one more edge where the infinitely deep sea ends. We use the labeling edge for an edge where the filled states are below and the empty states above. We will use the label anti-edge for the opposite set, where the empty sites are below and occupied sites are above. The energy of this state is LM.

What we call the field ϕ again becomes multi-valued, with one contribution from each

(anti-) edge. The vanishing of the (zero mode of the) field is governed by adding three contributions

$$\phi = \int dh\, h\, (\delta(h - L) - \delta(h - (L - M)) + \delta(h + M)) = L - (L - M) - M \qquad (4.129)$$

very similar to (4.120).

4.6.3 Excitations of striped geometries

In general, we expect that we could start with one of these translationally invariant striped geometries and deform each edge independently, As shown schematically below.

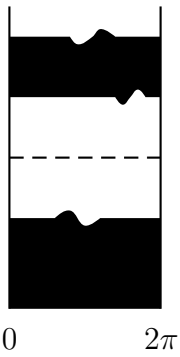

Figure 4.5: A schematic depicting possible independent deformations of each edge of an LM state.

Recall that the energy is given by

$$E[\phi] = \frac{1}{2\pi} \iint \tilde{\rho}(\theta, h)\, h\, dh\, d\theta \qquad (4.130)$$

Further, let us recall that $\phi \simeq h$ on the edge, while $\tilde{\rho} = 1, 0, -1$. We want to consider small deformations of each height, keeping the local density at nominal values, and the area of each region fixed. This is formalizing the idea that the field ϕ becomes multivalued, with $\phi(\theta)$ the height at each (anti) edge. The total field sums over these contributions

$\phi(\theta) = \phi^1(\theta) + \phi^2(\theta) - \tilde{\phi}^1(\theta)$. Here, we indicate the fields in order from the top down, with $\tilde{\phi}$ representing the anti-edge fields. To keep the area of each region fixed, we require that for each field $\int d\theta\, \delta\phi^i = \int d\theta\, \delta\tilde{\phi}^i = 0$, and we can substitute in the energy as an area integral to find that

$$E[\phi] = \frac{1}{2\pi}\sum_{i,j}\int d\theta \frac{(\phi^i + \tilde{\phi}^j)}{2}(\phi^i - \tilde{\phi}^j) = \frac{1}{2\pi}\sum_{i,j}\int d\theta \frac{1}{2}((\delta\phi^i)^2 - (\delta\tilde{\phi}^j)^2) + E_{LM} \quad (4.131)$$

We find that the energy splits into a (local) sum over fluctuations of each edge independently, but the ones associated with $\tilde{\phi}$ have a negative sign. This is an indication that the reference state $|\square_{L,M}\rangle$ is not the ground state. The fields $\tilde{\phi}$ can be thought of as ghosts (in the sense of negative energy states, not negative norm states). In the paper [82], such states are called *counter-gravitons*. The fields $\phi^{(i)}$ and $\tilde{\phi}^{(i)}$ will be the collective excitations of the configuration.

What we have done is formalize the suggestion of [82] that makes ϕ decompose linearly into pieces that work on each (anti-)edge independently. Now, we can take the Fourier transform to obtain the mode decomposition, as in [40].

We find that

$$a_s^\dagger = b_s^{(1)\dagger} + b_s^{(2)\dagger} - c_s^{(1)} \quad (4.132)$$

where the $b^{(i)}$ are excitations of the edges, and the $c^{(i)}$ modes are excitations of the anti-edges. We need to explain this equation. The mode $a_s^\dagger$ increases the energy by s units. This is the equation of motion of the mode $a_s^\dagger$. The modes $b_s^{(1)\dagger}, b_s^{(2)\dagger}$ also increase the energy by the same amount (which is equal to the momentum of the mode). The lowering mode for excitations of the anti edge destroys $(-s)$ units of energy, so it acts in the same way to increase the energy. This is the only way to make the equations consistent with energy conservation and with a linear expression for the modes $a_s^\dagger$ in

terms of the collective excitations of the state $|\Box_{LM}\rangle$. As long as we can show that the b, c have the correct commutation relations, we find that the equation (4.132) indicates that the UV fields (those that are canonical modes of the chiral free field) are related by a Bogolubov transformation to the collective fields (which we are calling the IR theory). It is not a complete Bogolubov transformation, because such transformations preserve the number of oscillators. The linear transformation can be completed to a full Bogolubov transformation if we add additional orthogonal fields to the a_s that are made of linear combinations of the b, c modes (we will expand on this idea in the next section).

The important point is that equation (4.132) is an approximation to the fluctuations about the state. It is clear that if the fields $\phi^{(i)}$ get too large that the edges will collide changing the topology. Our purpose right now is to actually derive this transformation from first principles by analyzing the physics of the state $|\Box_{LM}\rangle$ independent of the geometric intuition. We want to show that the decomposition can actually be derived from the combinatorial structure of the full Hilbert space of states.

The reference vacuum state $|\Box_{LM}\rangle$ is defined by $b\,|\Box_{LM}\rangle = c\,|\Box_{LM}\rangle = 0$. We will call an excitation a *classical configuration* if it is a coherent state excitation of the low lying modes of $b^{(i)}$ and $c^{(i)}$, assuming that they have canonical commutation relations. This can be derived semiclassically by following [80], but again, it does not explain what to do when the ϕ get large, so the commutation relations are approximately true on a sector of low amplitude.

Our goal now is to construct the operators b, c explicitly in the quantum theory and show that they have the correct (canonical) commutation relations when acting on a particular subspace of the Hilbert space of states, so that the equation (4.132) is indeed a Bogolubov transformation. To do this, the results of section 4.5 and appendix B are essential. This is the point where we are able to improve the discussion in [82] substan-

tially because we will have no guesswork. Moreover, we will be able to understand the cutoffs in field space implicitly and to study the cutoff dependence of various quantities.

The idea is to consider nearby excited states relative to $|\Box_{L,M}\rangle$, where, by nearby, we mean young tableaux states that differ from $|\Box_{L,M}\rangle$ by a few boxes. This is depicted in equation (4.133).

$|R\rangle =$ 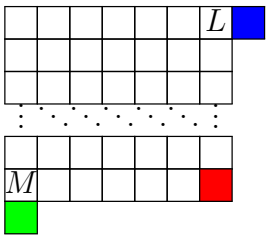

(4.133)

The states $|R\rangle$ are those that differ from the reference state $|\Box_{L,M}\rangle$ by adding (few) boxes in the corners marked by blue and green, and removing (few) boxes in the corner marked by red. Each of these can be done independently at large L, M. What this means is that the Hilbert space of nearby states factorizes into

$$\mathcal{H}_{\text{nearby}} \simeq \mathcal{H}_{\text{blue}} \otimes \mathcal{H}_{\text{green}} \otimes \mathcal{H}_{\text{red}} \tag{4.134}$$

Now, each of $\mathcal{H}_{\text{blue}}, \mathcal{H}_{\text{green}}, \mathcal{H}_{\text{red}}$ can be written as a small Young diagram. For $\mathcal{H}_{\text{blue}}$ and $\mathcal{H}_{\text{green}}$ this is pretty obvious. For $\mathcal{H}_{\text{red}}$ all we need to do is rotate the empty corners marked in red by $(180)^o$ and we get a proper Young diagram.

Relative to the reference state, the Young diagrams with blue and green boxes will have norm one, and so will the diagram with antiboxes. This is special to the original theory being described with Young diagrams states that all have the same norm [2]. Now, we can do the Fourier transform from Young diagrams to a Fock space description with

[2]This is easy to modify for theories of generalized free fermions as in [99] because the norms will factorize for each different color of Young diagram. See also [111] and references therein for how to compute energies of excitations in the special case of $\mathcal{N} = 4$ SYM. This is not essential for this paper.

canonical raising and lowering operators. This is essentially due to the uniqueness of the relations discussed in section 4.3. For each of these, we can apply the results of the previous section and the appendix B. We find that

$$\langle R|\, a_s^\dagger \,|\tilde{R}\rangle = (-1)^{f_{\rm hook}} \tag{4.135}$$

as long as the skew hook is an allowed transition from $\tilde{R}$ to R with s boxes. We have a similar expression for the other colored operators. The one difference for the red boxes is that as the red diagram is growing, the original Tableaux is being chipped away, but this is done by a skew hook that is at the interface of the red tableaux and the reference state: it is also an allowed skew hook of length s for the complement of the red tableaux. These are the operators that we have identified as $b_s^{(i)\dagger}$ and $b_s^{(i)}$, and for the antiboxes these are the $c^{(i)\dagger}, c^{(i)}$ operators. Because the Hilbert spaces factorize we obtain the following exact commutation relations

$$[b_s^{(i)}, b_t^{(j)\dagger}] = \delta^{ij} s \delta_{st} \tag{4.136}$$

$$[c_s^{(i)}, c_t^{(j)\dagger}] = \delta^{ij} s \delta_{st} \tag{4.137}$$

and all other commutators vanish. These commutation relations are true only when evaluated in states that are sufficiently close to the reference state, so that the boxes and anti-boxes do not interfere with each other. This is implicit in the full discussion, but it is worth emphasizing that these equations are not true for arbitrary excitations of the original system, only so in the effective field theory of nearby configurations. The extreme value where they could be right would be halfway along the reference state sides, so it is only for labels that are less than $L/2, M/2$, and total differences of energies that are much

less than LM. Beyond this scale we would claim that the modes become related to each other and there are fewer independent states. These give relations between the operators at high order. We call such transitions, where the number of states is reduced relative to the very naive counting of independent free fields, the stringy exclusion principle for the collective dynamics in the same sense as [86, 71].

We will label the nearby states as follows

$$|\Box_{LM} + R_1 - R_{\tilde{1}} + R_2\rangle \simeq |R_1\rangle \otimes |R_2\rangle \otimes |R_{\tilde{1}}\rangle \tag{4.138}$$

in a way that makes it clear that we are adding and substracting Young diagrams from each corner as is appropriate to the nature of the corner.

From here, one can easily check that the following is true

$$a_s\,|\Box_{LM} + R_1 - R_{\tilde{1}} + R_2\rangle = \sum_{\text{hooks}} (-1)^{f_{\text{hook}}}\,|\tilde{R}\rangle \tag{4.139}$$

where $\tilde{R}$ differs from the original state by removing a skew hook of length s. These can only be removed from either of the R_i, or added to the $R_{\tilde{i}}$. These are the only places where small hooks can be subtracted (or added). This means that

$$\begin{aligned} a_s \quad & |\Box_{LM} + R_1 - R_{\tilde{1}} + R_2\rangle = \sum (-1)^{f_{\text{hook}}}\,|\tilde{R}_1\rangle \otimes |R_2\rangle \otimes |R\rangle_{\tilde{1}} \\ + \quad & \sum |R_1\rangle \otimes (-1)^{f_{\text{hook}}}\,|\tilde{R}_2\rangle \otimes |R\rangle_{\tilde{1}} + \sum |R_1\rangle \otimes |R_2\rangle \otimes (-1)^{f_{\text{hook}}}|\tilde{R}_{\tilde{1}}\rangle \end{aligned} \tag{4.140}$$

This translates to

$$a_s = b_s^{(1)} + b_s^{(2)} + c_s^{\dagger(1)} \tag{4.141}$$

so we get what we want in equation (4.132) up to a sign for $c_s^\dagger$. Following the discussion

in section 4.4 this sign can be changed by a particle-hole transformation, which is a symmetry of the algebra of the raising and lowering operators that we have constructed. The choice we make is a convention that needs to be established, and this is used to match better our geometric intuition. There is no deeper meaning to it.

We have proven what we set out to: the UV modes can be written as a linear superposition of the collective modes of the configuration (the infrared modes) when acting on nearby states. Moreover, the collective modes ave canonical commutation relations. It is the presence of these collective modes that lets us know for sure that we have changed the topology. Their number dictates the number of edges (anti-edges).

4.7 Topology from uncertainty measurements

Now, we can further evaluate how non-classical these states are from the point of view of the original $a_s^\dagger, a_s$ oscillators, by computing quantities that appear in (4.126). That is, we want to compute

$$\langle a_s a_s^\dagger \rangle_{LM} = \langle a_s^\dagger a_s + s \rangle_{LM} \tag{4.142}$$

Using the MN rule, the $\langle a_s^\dagger a_s \rangle$ are evaluated by counting all the skew hooks of length s (this is the same as the number of hooks of length s, see appendix B). One can easily see that each hook has its corner on a diagonal band, as in equation (4.143).

$$|\square_{LM}\rangle \simeq$$ 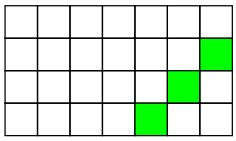 (4.143)

so we get that for low s (that is, $s \leq \min(L, M)$)

$$\langle a_s a_s^\dagger \rangle_{LM} = 2s \tag{4.144}$$

For simplicity we will assume that $L \geq M$, so that the first place where things change is at $s = M+1$. At this point the diagonal bands are of constant length M. Things change again when we want very large hooks at $s = L$, where the available diagonal bands start shrinking. We get the answer

$$\langle a_s a_s^\dagger \rangle_{LM} = \begin{cases} 2s & \text{if } s \leq M \\ M+s & \text{if } L \geq s \geq M \\ M+L & \text{if } L+M \geq s \geq L \\ s & \text{Otherwise} \end{cases} \tag{4.145}$$

We can also write this equation equivalently in terms of the average occupation per mode $N_s = \frac{a_s^\dagger a_s}{s}$. It is convenient to do this in two different (equivalent) ways so that

$$\tilde{N}_s = \langle N_s + 1 \rangle_{LM} = \begin{cases} 2 & \text{if } s \leq M \\ M/s+1 & \text{if } L \geq s \geq M \\ (M+L)/s & \text{if } L+M \geq s \geq L \\ 1 & \text{Otherwise} \end{cases} \tag{4.146}$$

and

$$\langle N_s \rangle_{LM} = \begin{cases} 1 & \text{if } s \leq M \\ M/s & \text{if } L \geq s \geq M \\ (M+L)/s-1 & \text{if } L+M \geq s \geq L \\ 0 & \text{Otherwise} \end{cases} \tag{4.147}$$

the number $\tilde{N}_s$ can be computed for more general multi-strip geometries for low s using

the Bogoliubov transformation. It is given by

$$\tilde{N}_s = \langle a_s a_s^\dagger \rangle_{\text{multi-stripe}}/s \simeq \frac{1}{s}\sum_i \langle b_s^{(i)} b_s^{(i)\dagger}\rangle_{\text{multi-stripe}} = n_{\text{edges}} \tag{4.148}$$

while

$$N_s = \langle a_s^\dagger a_s \rangle_{\text{multi-stripe}}/s \simeq \frac{1}{s}\sum_i \langle c_s^{(i)} c_s^{(i)\dagger}\rangle_{\text{multi-stripe}} = n_{\text{anti-edges}} \tag{4.149}$$

We can draw a few consequences from these equations.

First, since the numbers N_s are generally of order one, the states that we have considered so far have very low uncertainty in the fluctuations, comparable in size to the usual quantum uncertainty of the ground state. That uncertainty is multiplied by an integer for low s. In this sense, they should be regarded as being classical, because uncertainties are of typical quantum size. This integer that we get is exactly the number of edges. In this sense, the number of edges is measurable in the size of the quantum fluctuations of the UV modes of the theory (those that are given a priori without any reference to the particular state). It is important that there are a large number of modes for which this number is the same. This means that with a simultaneous measurement of various quantities that commute with each other we can do enough statistics to compute the topology (without destroying the full information of the state, but already knowing that the state is a rectangular tableau). We measure the topology by census-taking and finding consensus.

This is where the size of L, M actually start mattering. At roughly the same place where the stringy exclusion principe becomes important (at modes of order L, M) the numbers that effectively measure the topology of the state start changing.

In the large L, M limit, the number N_s becomes a continuous function of the rescaled

parameters $x = s/M$ (or s/L) and interpolates smoothly between n_{edges} for $x << 1$ and 1 for large x. This can be interpreted as the effective number of edges at the scale associated with x. In this sense, the measurement of topology is energy dependent. Since the energy goes like $E \simeq L^2$ at least for the square tableau, the stringy exclusion energy scales as $L \simeq \sqrt{E}_{LM}$ and can be effectively very high.

4.7.1 Coherent states of edge oscillators

We can now consider general classical coherent states of the b, c oscillators and as we have said above, we will think of these as new classical configurations. The coherent state is defined by the equations

$$(b_s - \langle b_s \rangle) \left| \text{Coh}_{\text{LM}} \right\rangle = 0 \tag{4.150}$$

and similar for the c. These belong the small Hilbert space for sufficiently small shifts (the tails at high occupation number will have negligible probability). The subscript LM is to indicate that this is a coherent state relative to the b, c oscillators of the LM state.

When we set out to compute the numbers N_s as above, they will depend greatly on the properties of the state we pick. The occupation number itself is *not robust* against taking general coherent states. What we mean by this is that we can change it by a large fraction (even in a lot of modes). However, consider the following operators that are shifted by a c-number

$$a_s - \langle a_s \rangle = \sum_i b_s^{(i)} - \langle b_s^{(i)} \rangle - \sum_j (c_s^{(j)\dagger} - \langle c_s^{(j)\dagger} \rangle) \tag{4.151}$$

Because the b, c operators shifted by a c-number still satisfy the canonical commutation

relations (the shift is an automorphism of the algebra of b, c operators), then we can repeat the calculations we did before including these shifts.

We find that for these states the same computation that we did before holds with the shifted oscillators. That is, we find that

$$\frac{1}{s}\langle|a_s - \langle a_s\rangle|^2\rangle_{\mathrm{Coh_{LM}}} = n_{\mathrm{edges}} \tag{4.152}$$

We can measure the number of edges if we measure the uncertainty, not the number operator itself. The expectation value of the number operator is the same as the uncertainty if the shift vanishes, but the uncertainty is not in general the number operator.

This means that to measure n_{edges}, we end up evaluating a non-linear function of the wave function. This is because the shift $\langle a_s\rangle$ depends on the state! In a certain sense this should not be a surprise. We already argued that the topology cannot be measured by an operator, because all coherent states relative to the trivial vacuum ($AdS_5 \times S^5$) of the chiral boson are of the same topology. But a non-linear function of the wave function is not an operator measurement. It is something that can be computed in quantum mechanics, and that moreover can be recovered with a set of observations on the system with different variables that do not commute with each other: a polynomial function involving the number operator and the expectation values of the raising and lowering operators. Once we measure the expectation values of the field $\langle\phi(\theta)\rangle$ we can recover the shifts we need. Given these shifts, we can evaluate an effective number operator for the shifted variable. This is a protocol for measuring the topology. It just cannot be done with one single observation.

Notice also that at least in this example, even though we can measure the topology with a few observations for low energy modes (from the UV point of view), measuring the

values of L, M themselves requires getting to the scale of the stringy exclusion principle (although the product LM is readily measured by the energy). This is not expected to persist in more general circularly symmetric LLM geometries, because the corresponding generalized effective Bogolubov transformation has coefficients that depend on L, M, N [82] (the details of this operation are beyond the scope of the present paper). This issue of indistinguishability of states based on simple measurements of the energy has also been alluded to in [66, 67], but it is also important to understand that the problem persists if we only have the expectation value of the UV fields and the energy. To reconstruct the classical geometry we need the expectation values of all of the b, c modes, not just the a modes. The a modes are the naive classical data needed on the boundary of AdS to specify the classical fields associated to ϕ in the bulk. The collection of a modes is the list of 'single particle' supergravity modes that can be excited. This description does not take into account that the field ϕ is effectively multi-valued. This has been discussed recently in the work by the authors of the present paper in [37], where it is argued that it gives an example where bulk reconstruction from classical boundary data fails (in the sense of [61, 62]). It is not clear at this stage if this is special to LLM states, or applicable in more general settings (formally, it works in all cases where the states are the large N limit of the extremal chiral ring [99]). This needs to be investigated further.

Indeed, following [67] we can consider more general operators of the low momentum modes (of the UV theory) and we find

$$\langle a_s^\dagger a_{s_1} \dots a_{s_m} \rangle_{LM} = 0 \tag{4.153}$$

with $m > 1$. This result is easily obtained by using the Bogolubov transformation and Wicks theorem with respect to the vacuum of the b, c oscillators and it's true as long as

$s < M$. What this means is that there are no obvious correlations between the low lying modes, nor any quantum correlation that can be used to measure L, M directly without going to high energy.

Another question that can be asked is how close this $|\square_{LM}\rangle$ state is to a regular coherent state of the free chiral boson. A rough estimate of a similar overlap to (4.124) suggests that

$$|\langle \square_{LM}\rangle \vec{\Lambda}|^2 \simeq \frac{1}{L^M} \simeq \exp(-M \log L) \tag{4.154}$$

which is exponentially suppressed at large M, L. This means that the new classical state is very far from any one *traditional classical state*. Alternatively, we can say that the state $|\square_{LM}\rangle$ can only be approximated well by an exponentially large superposition of classical states.

On taking double scaling limits in L, M, the new classical reference state is essentially orthogonal to all other standard classical states of the chiral boson theory and should not be thought of any longer as a Schrödinger cat state, but a classical state in its own right. This classical state has different topology than the standard classical states and this automatically implies that it has a different geometry. This is the sense in which these new states represent different classical limits of the chiral free boson theory. In particular, the existence of fluctuation fields $\delta\phi^{(i)}, \delta\tilde{\phi}^{(i)}$ with a well defined action on the small Hilbert space of the corners defines a semi-classical quantization on top of the classical state and can be used to argue that one can do effective and unitary quantum field theory in the background of the state $|\square_{LM}\rangle$.

4.7.2 Beyond classical states

If we consider a semiclassical state (the classical coherent of the b, c oscillators state with a few excitations of the b, c quanta), our consensus measurement can still be used to get to the topology. The point is that the few extra quanta can only affect a few of the modes for these measurements. The majority will have the same value of the uncertainty as before, and the majority vote will win.

Consider now a very different type of state: the thermal state at temperature $T >> 1$. This is a stand-in for the typical state of high energy. A lot of the physics associated with this state in the LLM setup has been addressed in [91]. For us, the energy per mode is equal to T for low enough modes, up to the cutoff scale (of order T), but the state also satisfies $\langle a_s \rangle = 0$. This means that the occupation number per mode is $N_s \simeq T/s$ and is a rapidly varying function with s. For us this means that the effective topology that counts the number of edges in the geometry is varying rapidly with scale: the state should not be thought of as a classical geometric state with a fixed topology (the topology can not be measured and have a meaningful answer in the consensus part of the test).

We can also consider the triangular diagram of equation 131 in [91], given by tableaux of the typical form

$|R_{2\text{step}}\rangle =$ 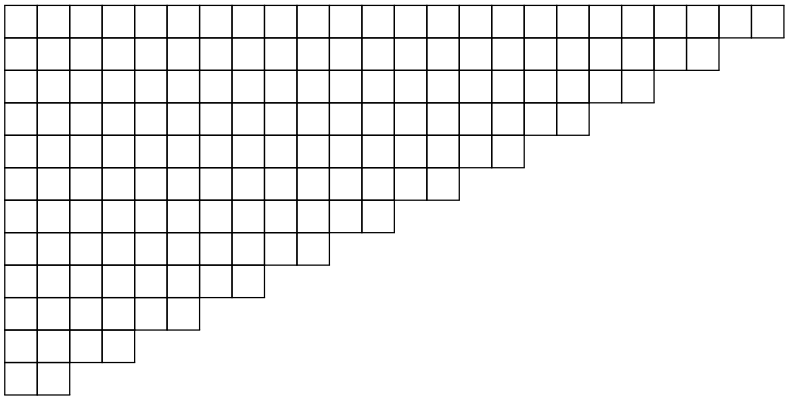 (4.155)

with L rows. It is easy to check that there are no hooks with a length that is a multiple 3. That is, there are no hooks of length $3k$ for every k. So, we find that $\tilde{N}_{3k} = 0$ for all k. This would suggest that the topology is that of the vacuum. However, when we consider other modes we find that

$$\langle a_s^\dagger a_s \rangle \simeq \langle a_1^\dagger a_1 \rangle = L \tag{4.156}$$

where L is the number of hooks of length 1, so again the energy per mode that is not a multiple of three is roughly fixed, but the effective number of edges varies wildly and we fail to find consensus. Now the number of edges is not even a smooth function for the rescaling parameter $x \simeq s/L$. It is only states that have few corners that are deemed sufficiently geometrical, to the extent that one can fix their topology by checking that N_s is independent of s for all s that are small (below a suitable stringy exclusion principle energy).

These states fail to be classical also in that any attempt to produce oscillators like the b, c oscillators fails because the naive stringy exclusion principle is very small: the equivalent of the red corners can at most remove one or two boxes before interfering with the addition of boxes in the anti-corners. In a sense, this is seen in that the edge of the tableaux is rough (very jagged) rather than a straight line.

These other examples show that the geometric states $|\Box_{LM}\rangle$ are essentially characterized by having low, but on average essentially constant, occupation number per low momentum (energy) mode of the UV theory. Also, the different modes must be very correlated to each other in order to be able to find fluctuation fields like the b, c systems above that implement the required partial Bogolubov transformation from the collective dynamics to the UV modes.

4.7.3 Geometries with folds

Thus far, we have primarily considered only a couple classes of states: coherent states and striped (i.e. LM) states. These are nice because we know how to write them down in terms of oscillators and/or young tableaux, which we know how to deal with. Of course, there are many other possible geometries in the full set of LLM states. There is a general class that is particularly tricky, so we will touch on this class here. These are the states that wrap in such a way that their number of edges that is a function of θ. For instance, the state drawn in figure 4.7.3.

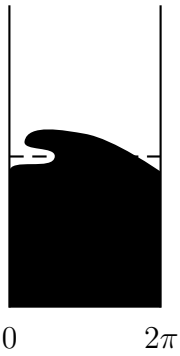

Figure 4.6: An example of a state with a number of edges that is dependent on θ.

If one were to do a local measurement of one of these states, then one would expect to find that the number of edges that varies with location. Here, we would like to determine if there is a way to compute $n_{\text{edges}}(\theta)$ from uncertainty computations. Notice that here we do not have an obvious candidate for the state in terms of Young tableaux. Instead we expect the state to be complicated in that basis. The reason to say so is that such geometries also arise in the study of the $c = 1$ matrix model [112] and in that case they result from Hamiltonian evolution of more standard coherent states. But already coherent states superpose a lot of Young tableaux, and such evolution would scramble a lot of the phases between the different basis elements. The fact that such states exist

point to the non-triviality of the classical limit in the $c = 1$ matrix model.

The local commutation relation of our field operator can be computed using $\left[a_k, a_j^\dagger\right] = k\delta_{k,j}$. We find

$$\left[\hat{\phi}(\theta), \hat{\phi}(\theta')\right] = \frac{i(2\pi)}{2}\left[\partial_\theta \delta(\theta' - \theta) - \partial_{\theta'}\delta(\theta' - \theta)\right] \tag{4.157}$$

As before with striped states, we will want to decompose our operators into pieces that act on each edge or anti-edge. Here, we will do this as follows

$$\hat{\phi}(\theta) = \sum_{I=0}^{n_{\text{edges}}(\theta)} \phi^I(\theta) - \sum_{J=0}^{n_{\text{anti-edges}}(\theta)} \tilde{\phi}^J(\theta) \tag{4.158}$$

where, as before, the tilde refers to operators that act on an anti-edge. Also note the operator-denoting hats are dropped on the edge fields for notational convenience. We see that unlike before, this decomposition is θ-dependent. That is, the range the indices run over depends on theta, just as the number of edges does.

It is easy to see that these subfields should obey the same local commutation relations as the field $\hat{\phi}(\theta)$ with signs that depend on if the field is at a regular edge or an anti-edge

$$\left[\phi^I(\theta), \phi^J(\theta')\right] = \frac{i(2\pi)}{2}\left[\partial_\theta \delta(\theta' - \theta) - \partial_{\theta'}\delta(\theta' - \theta)\right]\delta^{IJ} \tag{4.159}$$

and

$$\left[\tilde{\phi}^I(\theta), \tilde{\phi}^J(\theta')\right] = -\frac{i(2\pi)}{2}\left[\partial_\theta \delta(\theta' - \theta) - \partial_{\theta'}\delta(\theta' - \theta)\right]\delta^{IJ} \tag{4.160}$$

These signs ensure that the commutation relations of the field $\hat{\phi}(\theta)$ are preserved. One way to understand this is that the coefficient of the commutation relation of the ϕ field can be understood as the anomaly coefficient of the chiral boson. If we normalize this coefficient to one for ϕ, then we find that the ϕ^I have anomaly equal to one, and the

$\tilde{\phi}^J$ have anomaly minus one. The fact that there is one more ϕ^I than $\tilde{\phi}^J$ locally is the statement that the combined effective field theory of the $\phi^I, \tilde{\phi}^J$ has the same anomaly as the UV theory of ϕ. In this sense, the effective field theory near our reference states has anomaly matching between the UV representation and the collective degrees of freedom.

Now, we will call $\delta\phi$ the quantum field relative to the background field. That is, we call

$$\delta\phi^I = \phi^I - \langle\hat{\phi}^I\rangle \tag{4.161}$$

and similar for $\tilde{\phi}^J$ and $\hat{\phi}$.

To proceed further, we can consider breaking our field into raising and lowering operator pieces for each of the indices $\delta\hat{\phi} = \delta\phi^+ + \delta\phi^-$ as was done in the multi-edge regular geometry by Fourier transforms. Our problem in this case is that we do not know the vacuum state. In the standard multi-strip geometries this is achieved by requiring that in the translationally invariant multi-strip geometry, the Fourier modes of the operators for the edge modes are raising/lowering operators depending on if the mode adds or subtracts energy relative to the reference state, with a provision that changes the assignment for anti-edges relative to edges. This is demonstrated for the strip geometries with the explicit construction based on the Young diagram representation of states. Here we have to choose a vacuum, because the multi-fold geometries are not translation invariant. We would still want the raising/lowering operators of the field ϕ to be locally in the same decomposition as for multi-edge states and the lowering operators of the $\hat{\phi}^I, \hat{\phi}^J$ to act trivially on the reference states.

Combing this with our edge/anti-edge decomposition, we make the approximation that

$$\delta\phi^+(\theta) \simeq \sum_{I=0}^{n_{\text{edges}}(\theta)} \delta\phi^{I+}(\theta) - \sum_{J=0}^{n_{\text{anti-edges}}(\theta)} \delta\tilde{\phi}^{J-}(\theta) \tag{4.162}$$

where we know that the lowering operator on anti-edges adds energy, so should be grouped with the raising operator piece. We will call this the Local Multi-Edge approximation (LME approximation). Notice that this is a statement about raising and lowering operators relative to the state, so we have subtracted the classical value of the fields and only included the fluctuation piece. This is important because we want to compute the uncertainty in the measurement relative to the classical state (we did a similar step on the multi-edge geometries when we argued that the shift by the field vevs is an automorphism of the Weyl algebra).

Notice that the splitting into raising and lowering operators is not really local. However, it can be approximately local under some circumstances: as long as the region over which the splitting is done is much larger than the typical wavelength of the fields considered, the approximation makes sense. This means that the vacuum is very similar to the multi-edge setups locally on length scales that are small relative to where the folds begin and end. The finite size corrections should depend on the separation between the folds.

To proceed further, we start by convoluting the field operator $\hat{\phi}$ with a test function $f(\theta)$ to build a new operator

$$\hat{\phi}_f = \frac{1}{2\pi}\int_0^{2\pi} f\left(\theta\right)\hat{\phi}\left(\theta\right)d\theta \tag{4.163}$$

Our goal is to use these operators to estimate uncertainties and correlators with particular choices of f. The role that f plays is to select the correct wavelengths of the modes. If we are worried about the details where the folds are located, we can take f to be nearly vanishing near these regions, but we will not do so here.

It will turn out that the operators given by $\hat{\phi}_f, \hat{\phi}_g$ with $f = e^{im\theta}$ and $g = e^{-ik\gamma}$ is just

what we need. Notice that, in a more familiar form, this is simply

$$\hat{\phi}_{e^{im\theta}}\hat{\phi}_{e^{-ik\gamma}} = a_m a_k^\dagger \tag{4.164}$$

Now, let's try to compute the expectation value of this for a folded state, which we will call $|\text{fold}\rangle$.

$$\langle\text{fold}|\,\hat{\phi}_{e^{im\theta}}\hat{\phi}_{e^{-ik\gamma}}\,|\text{fold}\rangle = \frac{1}{(2\pi)^2}\int d\theta\, d\gamma\, e^{im\theta}e^{-ik\gamma}\,\langle\text{fold}|\,\hat{\phi}(\theta)\hat{\phi}(\gamma)\,|\text{fold}\rangle \tag{4.165}$$

We can break this up into its raising and lowering pieces

$$= \frac{1}{(2\pi)^2}\int d\theta\, d\gamma\, e^{im\theta}e^{-ik\gamma}\,\langle\text{fold}|\,\left(\phi^+(\theta)+\phi^-(\theta)\right)\left(\phi^+(\gamma)+\phi^-(\gamma)\right)|\text{fold}\rangle \tag{4.166}$$

Because of our choice of sign for the exponentials of f and g, if we actually write out the raising and lowering pieces, we find that upon integration, $\phi^+(\theta)$ and $\phi^-(\gamma)$ will vanish, leaving

$$= \frac{1}{(2\pi)^2}\int d\theta\, d\gamma\, e^{im\theta}e^{-ik\gamma}\,\langle\text{fold}|\,\phi^-(\theta)\phi^+(\gamma)\,|\text{fold}\rangle \tag{4.167}$$

We can now expand this in terms of pieces that act on each edge and anti-edge

$$\begin{aligned} = \frac{1}{(2\pi)^2}\int d\theta\, d\gamma\, e^{im\theta}e^{-ik\gamma}\,\langle\text{fold}|\,&\left(\sum_{I=0}^{n_{\text{edges}}(\theta)}\phi^{I-}(\theta) - \sum_{J=0}^{n_{\text{anti-edges}}(\theta)}\tilde{\phi}^{J+}(\theta)\right) \\ &\times\left(\sum_{I=0}^{n_{\text{edges}}(\theta)}\phi^{I+}(\gamma) - \sum_{J=0}^{n_{\text{anti-edges}}(\theta)}\tilde{\phi}^{J-}(\gamma)\right)|\text{fold}\rangle \end{aligned} \tag{4.168}$$

Here, if we zoom in on any small region in θ, we imagine that the folded state will look like a striped state. So, locally, we expect that these operators will act on the folded

state, just as they would on a young tableaux state, giving

$$\simeq \frac{1}{(2\pi)^2}\int d\theta\, d\gamma\, e^{im\theta}e^{-ik\gamma}\,\langle \text{fold}|\sum_{I=0}^{n_{\text{edges}}(\theta)}\left(\phi^{I-}(\theta)\phi^{I+}(\gamma)\right)|\text{fold}\rangle \tag{4.169}$$

We notice now that we can write this as

$$= \frac{1}{(2\pi)^2}\int d\theta\, d\gamma\, e^{im\theta}e^{-ik\gamma}\,\langle \text{fold}|\sum_{I=0}^{n_{\text{edges}}(\theta)}\left[\phi^{I}(\theta),\phi^{I}(\gamma)\right]|\text{fold}\rangle \tag{4.170}$$

This, again, only works in this way because of the sign of the exponentials in f and g, causing some of the terms to vanish upon integration. Others vanish because as you zoom in the state will look like a vacuum young tableaux state. Finally, we can use the known commutation relation, giving

$$= \frac{1}{(2\pi)^2}\int d\theta\, d\gamma\, e^{im\theta}e^{-ik\gamma}\,\langle \text{fold}|\sum_{I=0}^{n_{\text{edges}}(\theta)}\frac{i\,(2\pi)}{2}\left[\partial_\theta\delta\left(\gamma-\theta\right)-\partial_\gamma\delta\left(\gamma-\theta\right)\right]\delta^{II}|\text{fold}\rangle \tag{4.171}$$

Again, remember the decomposition is location dependent, with the index I running over each edge at each location. We see then that summing over δ^{II} simply gives the number of edges at each location.

$$= \frac{1}{(2\pi)^2}\int d\theta\, d\gamma\, e^{im\theta}e^{-ik\gamma}\,\langle \text{fold}|\frac{i\,(2\pi)}{2}\left[n_{\text{edges}}(\gamma)\partial_\theta\delta\left(\gamma-\theta\right)-n_{\text{edges}}(\theta)\partial_\gamma\delta\left(\gamma-\theta\right)\right]|\text{fold}\rangle \tag{4.172}$$

Integrating by parts off the delta functions onto the exponentials gives

$$= \frac{(m+k)}{2(2\pi)}\int d\theta\, e^{i(m-k)\theta}n_{\text{edges}}(\theta) \tag{4.173}$$

Recalling that the original operator was equivalent to $a_m a_k^\dagger$, we find

$$\langle \text{fold}| \, a_m a_k^\dagger \, |\text{fold}\rangle \simeq \frac{(m+k)}{2(2\pi)} \int_0^{2\pi} d\theta \, e^{i(m-k)\theta} n_{\text{edges}}(\theta) \tag{4.174}$$

So, we see that these matrix elements give the Fourier transform of the number of edges. Notice that if we had done the same computation starting with $f = e^{-im\theta}$ and $g = ik\gamma$, everything would have followed similarly, leading to

$$\langle \text{fold}| \, a_m^\dagger a_k \, |\text{fold}\rangle = \frac{(m+k)}{2(2\pi)} \int_0^{2\pi} d\theta \, e^{i(m-k)\theta} n_{\text{anti-edges}}(\theta) \tag{4.175}$$

The LME approximation also produces the following two results:

$$\langle a_k^\dagger a_m^\dagger \rangle_{fold} = \langle a_k a_m \rangle_{fold} = 0 \tag{4.176}$$

which result from no mixing between raising and lowering operators of the same collective fields.

As a consistency check, we get that

$$\langle \text{fold}| \, a_m^\dagger a_k \, |\text{fold}\rangle = (\langle \text{fold}| \, a_m a_k^\dagger \, |\text{fold}\rangle)^* \tag{4.177}$$

and that

$$\langle \text{fold}| \, a_m^\dagger a_k \, |\text{fold}\rangle = \langle \text{fold}| \, a_k a_m^\dagger \, |\text{fold}\rangle \tag{4.178}$$

for $m \neq k$, which follows because $n_{anti-edges} = n_{edges} - 1$, so they have the same Fourier coefficients for the non-constant mode.

As a check of this proposal, we can evaluate it in the case of the multi-strip geometries. We would then expect this to agree with our previous result for young tableaux states.

Here, we would find a constant number of edges, giving

$$\langle \mathrm{YT}| \, a_m a_k^\dagger \, |\mathrm{YT}\rangle = \frac{(m+k)}{2(2\pi)} \int_0^{2\pi} d\theta \, e^{i(m-k)\theta} n_{\mathrm{edges}} = m\delta_{m,k} n_{\mathrm{edges}} \tag{4.179}$$

as computed previously. And similarly for the anti-edge calculation.

The upshot of the computation is that we can argue that $n(\theta)$ is encoded in the expectation values of $\langle \mathrm{fold}| \, (a_m - \langle a_m \rangle)(a_k^\dagger - \langle a_k^\dagger \rangle) \, |\mathrm{fold}\rangle$. These are non-trivial correlations between the modes of the field, valid for modes m that are larger than the inverse of the separation between the folds (measured with respect to 2π). A pre-requisite for a state to have a non-trivial topology is that $n(\theta) \neq 1$ someplace. This means that at least one of these correlators (generalized uncertainties) is different than the ones in the vacuum. If $n(\theta)$ is non-constant, then some correlators with $m \neq k$ must be non-vanishing.

A test to determine if a state could in principle be geometric is that since the Fourier coefficients only depend on $m - k$, there has to be a large degree of consistency between the correlations of the different modes. That is, even for semiclassical states with multi-edges, one can build a consensus measurement of $n(\theta)$: most of the modes that should be identical (with the proper normalization dependent on m, k) and determine the consensus measurement of the Fourier transform of $n(\theta)$, but again, it is not a single operator measurement on the Hilbert space of states that produces the result.

At this stage we do not have a clear understanding on how to incorporate the finite size corrections. They should be small for short wavelengths. We should also expect that there are additional small corrections to the LME approximation related to how the transitions from one value of n to another are handled. At this stage the LME approximation is not systematic and is used instead to set a benchmark for how such correlations should behave. This issue needs to be studied further and is beyond the

scope of the present paper.

Notice that eventually we also run into trouble at high frequencies, because we expect there to be a local bound on the momentum. In the Young tableaux case this occurs when the hooks at different corners start interfering with each other. A similar phenomenon should appear locally at each location of θ and should indicate a local stringy exclusion principle.

4.8 Entanglement measurements of topology

The particular model we have studied, as a quantum mechanical theory is a free field theory. The Hilbert space is a Fock space with a natural set of raising and lowering operators (a set of commuting algebras), and we can think of this Fock space as having a canonical product structure

$$\mathcal{H}_{\text{tot}} \simeq \mathcal{H}_1 \otimes \mathcal{H}_2 \otimes \cdots \otimes \mathcal{H}_\infty \tag{4.180}$$

where the Hilbert space basis is defined by kets that have have all but finitely many oscillators in the ground state. The Hilbert space itself is the L^2 completion of states made from this basis. We use the monicker $\mathcal{H}_\infty$ to indicate the infinite product for all sufficiently large $\mathcal{H}_n$. Because we have this canonical factorization structure, it is possible to take a pure state in $\mathcal{H}$ and find a reduced density matrix for each of the modes, $\hat{\rho}_1$, $\hat{\rho}_2$ etc, or for more modes grouped together $\hat{\rho}_{ij}, \hat{\rho}_{ijk}$ etc. It is the structure under this class of factorizations that we will try to understand for the states studied in the previous

section. The total Hamiltonian is

$$\hat{H} = \sum_s a_s^\dagger a_s = \sum_s s\hat{N}_s \tag{4.181}$$

We will aim to measure the entanglement entropies for each of these density matrices to characterize the state. The idea is to understand the entanglement structure of the state and to try to use that structure to measure the topology of the geometry etc. In a sense, this is putting to flesh the idea that entanglement can be the source of geometry a la Van Raamsdonk [72]. It is unclear how to implement this calculation as a calculation of entanglement entropy in gravity by a minimal surface [79]. This is mainly studying the momentum space entanglement in the quantum field theory (in [113] this information is related to the Wilsonian effective action).

Consider a state that is an energy eigenstate of the full Hamiltonian (e.g. $|\square\rangle_{LM}$, which has energy $E = ML$). We can decompose any such state, singling out the j^{th} oscillator, to find the reduced density matrix. If we do this, we can write the state as follows

$$|\psi\rangle = \sum_n \xi_n |n\rangle_j \otimes |w_n\rangle \tag{4.182}$$

where $|w_n\rangle$ includes occupation information about all the other oscillators. We can now use

$$\hat{H}|\psi\rangle = \sum_n \xi_n \hat{H}|n\rangle_k \otimes |w_n\rangle = \sum_n \xi_n (n + \sum_{k\neq j} k\hat{N}_k)|n\rangle_j \otimes |w_n\rangle = E_\psi |\psi\rangle \tag{4.183}$$

We see the unevaluated part of the Hamiltonian $\sum_{k\neq j} k\hat{N}_k$ acts only on $|w\rangle_n$. When we dot this with ${}_j\langle\tilde{n}|$, we find that the states $|w_n\rangle$ are different eigenstates of a Hermitian

operator.

$$\sum_{k\neq j} k\hat{N}_k \left|w_{\tilde{n}}\right\rangle = (E_\psi - \tilde{n}) \left|w_{\tilde{n}}\right\rangle \tag{4.184}$$

As such, they are orthogonal and can be made orthonormal. The reduced density matrix for ρ_j can be obtained from tracing with any orthonormal basis and we choose the $\left|w\right\rangle_n$ themselves. We find then that the reduced density matrix is diagonal in the energy basis

$$\hat{\rho}_j = \sum_n \left|\xi_n\right|^2 \left|n\right\rangle_{j\ j} \left\langle n\right| = \sum_n p_n \left|n\right\rangle_{j\ j} \left\langle n\right| \tag{4.185}$$

where the p_n are the probabilities to find the state $|\psi\rangle$ has the j^{th} oscillator with occupation n upon a measurement of $\hat{N}_j$. Our goal is to compute the coefficients $1 \geq p_n \geq 0$, and therefore the entropy

$$s_j = -\sum_n p_n \log p_n \tag{4.186}$$

for each mode j.

We will start by considering the state $\left|\triangle\right\rangle_n$, for simplicity. The idea is that we can compute quantities like

$${}_n\langle\Delta|a_1^{\dagger k} a_1^k|\Delta\rangle_n = 1 \tag{4.187}$$

if $k \leq n$. Otherwise it vanishes. This also can equivalently be written as $a_1^{n+1}\left|\triangle\right\rangle_n = 0$ because there are no states with negative energy. This in particular implies that $p_k = 0$ for $k > n$ so we only have to determine finitely many of the p_k. This results trivially from applying the Murnaghan-Nakayama rule in operator form repeatedly.

Because this number is only made of expectation values of operators that act on $\mathcal{H}_1$, the complete information is encoded in the density matrix $\hat{\rho}_1$. This equation can be written as

$$\mathrm{tr}(\hat{\rho}_1 a_1^{\dagger k} a_1^k) = 1 \tag{4.188}$$

One can easily evaluate the matrix elements of the operator in the number basis

$$a_1^{\dagger k} a_1^k \left|j\right\rangle = \frac{j!}{(j-k)!} \left|j\right\rangle \tag{4.189}$$

The equation (4.188) reads

$$\sum_{j=0}^{n} p_j \frac{j!}{(j-k)!} = 1 \tag{4.190}$$

for all $0 \leq k \leq n$ and together with $p_j = 0$ for $j > n$ is a complete linear system so all of the p_j can be determined. The first of these equations is $\mathrm{tr}(\hat{\rho}_1) = 1$. The second one is $\langle \hat{N}_1 \rangle = 1$. We can preform the same computation for the other modes, say the j^{th}. Computing $\hat{\rho}_j$ leads to

$$\sum_{l=0}^{[n/k]} p_l^{(j)} \frac{l!}{(l-k)!} = 1/j^k \tag{4.191}$$

which can be solved to give us the probabilities, $p_l^{(j)}$ (the probability for the j^{th} oscillator to have occupation l).

Now, let us consider $|\square_{LM}\rangle$ states. Again, the simplest way to understand reduced density matrices starts by understanding that the density matrices $\hat{\rho}_j$ are diagonal in the occupation number basis. So, our job is to compute

$$\langle a_j^{\dagger k} a_j^k \rangle_{LM} = \mathrm{tr}(\hat{\rho}_j a_j^{\dagger k} a_j^k) \tag{4.192}$$

and to use these equations to compute the elements of $\hat{\rho}_j$. It will prove helpful to use our partial Bogoliubov transformation (4.132). From

$$a_j = b_j^{(1)} + b_j^{(2)} - c_j^{(1)\dagger} \tag{4.193}$$

where, recall that each piece now acts on a particular edge or anti-edge. The computations

can be performed for small enough k (below the stringy exclusion principle) by using Wick contractions of the c oscillators only

$$\langle a_j^{\dagger k} a_j^k \rangle_{LM} \simeq {}_{b,c}\langle 0| \left(c_j^{(1)}\right)^k \left(c_j^{(1)\dagger}\right)^k |0\rangle_{b,c} \tag{4.194}$$

where we explicitly write the LM state as the vacuum state for the $b_j^{(I)}$ and $c_j^{(J)}$ oscillators. This can be computed and gives

$${}_{b,c}\langle 0| \left(c_j^{(1)}\right)^k \left(c_j^{(1)\dagger}\right)^k |0\rangle_{b,c} = k! j^k \tag{4.195}$$

for small enough k. At larger k eventually we find that acting with too many a_j kills the state, and that generically the equation (4.195) is an upper bound for the quantities we want. For the case of more edges, we get a similar answer

$${}_c\langle 0| \left(\sum_{I=0}^{n_{\rm edges}} c_j^{(I)}\right)^k \left(\sum_{J=0}^{n_{\rm anti-edges}} c_j^{(J)\dagger}\right)^k |0\rangle_c = k! j^k n_{\rm anti-edges}^k \tag{4.196}$$

This is because now there are $n_{\rm anti-edges}$ c fields. We write this set of equations as

$$\sum_{J=0}^{n_{\rm anti-edges}} p_j \frac{j!}{(j-k)!} = k! n_{\rm anti-edges}^k \tag{4.197}$$

Notice, we have the same equation for each oscillator. This can be seen easily from writing it in terms of canonical normalization oscillators, rather than oscillators with the field theory normalization that was computed in equation (4.36), and this is exact below the stringy exclusion principle. After the stringy exclusion principle is crossed we do not understand sufficiently well how the values on the right hand side taper off and eventually vanish.

This suggests that a good approximation to the entropies can be had if we don't impose the stringy exclusion principle at all, assuming that for sufficiently high values of k the elements of the density matrix are already sufficiently suppressed that their contribution to the entanglement entropy is negligible when we make them slightly smaller.

To solve (4.197) when we don't have bounds, we consider a (thermal) partition function given by

$$Z[x] = \sum_{j=0}^{\infty} x^j \tag{4.198}$$

where we are saying $p_j \propto x^j$. Consider acting with $x^k \partial_x^k$ on $Z[x]$. We get

$$x^j \partial_x^k Z[x] = \sum_{j=0}^{\infty} x^k j(j-1)\dots(j-k+1)x^{j-k} = \sum_{j=0}^{\infty} \frac{j!}{(j-k)!} x^j \tag{4.199}$$

which is of the form we want. To normalize the answer, we should divide by the sum of the non-normalized p and we get that the following should be true

$$\mathcal{N} \sum_{j=0} p_j \frac{j!}{(j-k)!} = Z[x]^{-1} x^k \partial_x^k Z[x] = k! n_{\text{anti-edges}}^k \tag{4.200}$$

with $\mathcal{N}$ the normalization. Now, the sums are straightforward to compute, and give

$$Z[x]^{-1} x^k \partial_x^k Z[x] = (1-x)x^k k! \frac{1}{(1-x)^{k+1}} = k! \left(\frac{x}{1-x}\right)^k \tag{4.201}$$

so that the equations are solved if

$$n_{\text{anti-edges}} = \frac{x}{1-x} \tag{4.202}$$

or equivalently

$$x = \frac{n_{\text{anti-edges}}}{1 + n_{\text{anti-edges}}} \tag{4.203}$$

We should take this to mean that the moments of the density matrix $\hat{\rho}_j$ are identical to those of a thermal density matrix for all low enough moments. This means that the two density matrices should be very similar. In the thermal density matrix the large p_k are exponentially suppressed. Indeed, the thermal density matrix is the one that maximizes the entropy if we fix the number operator $\langle \hat{N} \rangle$, so at worst we get an upper bound for the entanglement entropy mode per mode.

Let us try to explain this. At first sight, this seems strange. The reason why having an approximately thermal density matrix is strange is that the state we started with $|\Box_{LM}\rangle$ has a supergravity dual that is free from horizons. However, notice that the method of computing the moments based on (4.132) starts from a partial Bogolubov transformation where three modes $b^{(1,2)}$ and c^1 are mixed. We can find the other two linear combination of modes that gives rise to a full Bogolubov transformation. Use for example

$$d_s^\dagger = \frac{1}{\sqrt{2}}(b_s^{(1)\dagger} - b_s^{(2)\dagger}), \quad e_s^\dagger = \sqrt{2} c_s^\dagger - \left(\frac{b_s^{(1)} + b_s^{(2)}}{\sqrt{2}} \right) \tag{4.204}$$

We can compute the moments of the distribution in two different ways. In one, we use the oscillator basis b, c and the vacuum $|0\rangle_{bc}$ to get the answer. In the other way, we integrate out the fields e, f in the vacuum $|0\rangle_{bc}$ and compute a density matrix for the a modes directly. This Bogolubov transformation generically produces a squeezed state, and integrating the d, e modes gives rise to a Gaussian density matrix [3]. This Gaussian density matrix is not pure, but thermal, as is typical in gravitational computations [60].

[3]This is explained for example in [114] and references therein, where this statement follows from a simple generalization of eq. 40, and see also appendix B

Notice that this density matrix is not computed directly in the full Hilbert space $\mathcal{H}$, but is rather computed in the small (nearby) Hilbert space from equation (4.134)

$$\mathcal{H}_{\text{nearby}} \simeq \mathcal{H}_{\text{blue}} \otimes \mathcal{H}_{\text{green}} \otimes \mathcal{H}_{\text{red}} \tag{4.205}$$

which is readily generalized to the other more general multi-edge solutions.

What is interesting is that the factorization of the full Hilbert space induces a factorization in the nearby Hilbert space. This is because the algebra of observables $a^\dagger, a$ acts simply on H_{nearby}. That is, the operators do not take the states out of H_{nearby} when we use simple observables made of few such a below the stringy exclusion principle.

Indeed, this factorization structure and the corresponding quasi-thermal structure of the state persists even when we consider coherent states of the b, c modes. These can be obtained by a shift in the algebra of the b, c fields. This is an automorphism of the algebra. Similarly, the answer is simple in terms of the shifted modes $a_s - \langle a_s \rangle = \sum b_s^{(i)} - \langle b_s^{(i)} \rangle - (c_s^{(i)\dagger} - \langle c_s^{(i)\dagger} \rangle)$ that appeared in equation (4.151) and similar for the d, e modes. Integrating out the d, e modes or the shifted d, e modes gives the same result. The density matrix for the shifted a modes will still be Gaussian, and the entanglement entropy of $\hat{\rho}_1$ does not change: it is independent of the choice of basis in which we perform the computations. This entropy will only depend on the expectation value of the (shifted) occupation number. Since this will be roughly the same for all modes below the stringy exclusion principle, we find that after a straightforward computation

$$s_i = (n_{\text{edges}} \log(n_{\text{edges}})) - n_{\text{anti-edges}} \log(n_{\text{anti-edges}}) \tag{4.206}$$

and we can measure n_{edges} by consensus of the entanglement entropies of the different modes. This is not too different from the analysis in the previous section.

An additional interesting fact we observe is that in the small Hilbert space, the different a modes arise from integrating out different d, e modes. The density matrices $\hat{\rho}_{ij}$, $\hat{\rho}_{ijk}$ etc. are factorized! This means that there is no mutual information between the different modes a_s for sufficiently small s. One expresses this by saying that there is no entanglement between the modes a_s. The entanglement occurs between these low-momentum modes and very high momentum modes (at or beyond the stringy exclusion principle). We can say that these geometries arise from a special kind of UV-IR entanglement, but that there is no IR-IR entanglement contributing to the geometry.

Indeed, to the naive classical holographic observer that can only measure simple combinations of the low a modes, the information of the d, e modes is almost completely hidden (except for the total energy and that they act to purify the state). This suggests that for these backgrounds the reconstruction procedure [61, 62] will fail to construct excitations of the d, e modes, which are clearly contributing to bulk fields of supergravity modes. The precise way in which this could happen in these geometries is very interesting but is also beyond the scope of the present paper. A partial answer has been discussed in [37].

Another interesting calculation to do is to understand how big an overlap between a state like $|\Box_{LM}\rangle$ and a general coherent state of the free field theory can be. The best way to estimate this is to realize that the mode per mode entropy bounds how much overlap there is mode per mode. As coherent states are factorized between the modes, we get rather easily that

$$|\langle \Box_{LM}\rangle \, \mathrm{Coh}|^2 << \exp(-\sum_{i=1}^{L} s_i) \sim \exp(-L s_1) \tag{4.207}$$

which is exponentially suppressed in the dynamically generated cutoff. This means that

when we think of the states $|\square_{LM}\rangle$ and other multi-edge geometries they are always an exponentially large superposition of coherent states around the trivial geometry. This is important in other setups with black holes [110].

4.8.1 Entanglement measurements of Geometries with folds

We can do a similar analysis of the entanglement entropy, mode per mode, for the geometries with folds. On a first pass, because of the LME approximation, for a single mode we find that the uncertainty of each mode is given by

$$\langle (a_k - \langle a_k \rangle)(a_k^\dagger - \langle a_k^\dagger \rangle) \rangle = \frac{k}{2\pi} \int_0^{2\pi} n(\theta) d\theta = k n_{av} \tag{4.208}$$

with the average number of edges denoted by n_{av}. Moreover we have that $\langle (a_k^\dagger - \langle a_k^\dagger \rangle)^2 \rangle = 0$.

The state for mode k results from a Bogolubov transformation of the collective modes with a shift. Integrating out the 'orthogonal' modes, the result is a regular thermal state for the shifted mode k. Such a thermal state is completely determined by the n_{av}. The entanglement entropy of such a mode is

$$s_k = (n_{av}) \log(n_{av}) - (n_{av} - 1) \log(n_{av} - 1) \tag{4.209}$$

so again, mode per mode, the entanglement entropy of a single mode is constant and measures the average number of edges over θ. This again makes it possible to measure n_{av} by a consensus measurement on semiclassical states (those that differ from a folded geometry by a finite number of collective excitations).

Now, we also find that the LME approximation implies that there are non-trivial

correlations between the different modes. Therefore the density matrix does not factorize anymore. This implies that there is mutual information between the different collections of modes that one can produce. This is determined uniquely by the Fourier transform of $n(\theta)$. Studying the detailed structure information of all of these correlations is beyond the scope of the present paper.

We should note that as is usual with entanglement entropy (mode per mode) and mutual information between modes, one can do unitary transformations on each of the subfactors without changing the answer. A particularly interesting unitary is $\exp(i\alpha_s a_s^\dagger a_s/s)$, which rotates the (shifted) s oscillator by a phase α_s. These unitaries preserve the entanglement entropy mode per mode, but they modify the correlators as follows

$$\langle a_m a_k^\dagger \rangle \to \langle a_m a_k^\dagger \rangle \exp(i(\alpha_k - \alpha_m)) \tag{4.210}$$

etc. Now the phase of the correlation $\langle a_m a_k^\dagger \rangle$ should match the phase of $\langle a_{m+w} a_{k+w}^\dagger \rangle$, but generically these unitaries do not do that, however, the mutual information of the factorization is not changed. This means that a simple unitary operator destroys the 'uncertainty measurement' of geometry without changing the entanglement entropy measurement. This indicates that the entanglement entropy measurement of topology is much weaker than the uncertainty measurement of topology: states that are (clearly) non geometric would pass the entanglement entropy consensus measurement of topology, but not the uncertainty measurement tests.

Notice also that if $n_{av} = 0$, then the state is a coherent state: a minimum uncertainty packet in each of the Hilbert spaces and the entropy for each sub-Hilbert space for a mode k or any collection of them is zero. In general this implies that the other correlators should vanish. This means that there are inequalities between the generalized correlators that

need to be satisfied. Violations of these inequalities should in general lead to 'negative probabilities': violations of unitarity. Some examples of such violations can be understood in generalized half-BPS solutions of type IIB supergravity that have closed time-like curves [115, 116]. Studying these inequalities would also be very interesting, but again, this is beyond the scope of the present article.

4.9 Discussion

We have discussed topology changes in the set of LLM geometries and their dual realization. We focused on a particular simple limit where the full mini-superspace of half BPS geometries is quantum mechanically given by a free theory: the free chiral boson.

We found that since the coherent states of the free chiral boson are overcomplete, any state in the quantum theory can be written as a superposition of this class of states. These coherent states all have the same 'trivial topology' as the vacuum. It is curious that one can construct states with different topology (also known as bubbling solutions) just by superposing states with a trivial topology, and the new topologically distinct states are macroscopically very different from any of the states that we are superposing. The overlaps between the new state and the elements of the overcomplete basis of coherent states are all exponentially suppressed. We state this by saying that topology changes can be triggered by superposition. This is a superposition of an exponentially large number of states, not a naive Schödinger cat state that superposes just two distinct geometries.

A simple, yet deep, consequence of this fact is that topology can not be measured by a single operator measurement. That is, the Hilbert space of states does not admit an orthogonal decomposition into different topological types. So if topology cannot be

measured by an operator, it seems reasonable that finer geometric information might suffer the same fate. This puts into question how (a seemingly unitary) effective field theory of gravity can be compatible with this non-operator property.

To understand the physics of our example, it became important to understand the physical states in more than one basis of vectors for the Hilbert space of states. The set of wave functions can be written either in an oscillator basis for the chiral modes, or in terms of a Young Tableaux basis (the free fermion realization of matrix models). We carefully developed the dictionary between them, which is a generalized Fourier transform. An important result is that the set of raising and lowering operators of the free chiral boson act simply on the Young tableaux basis. We were able to show that this action encodes the Murnaghan-Nakayama rule for evaluating characters of the symmetric group, and the sign that is needed for this rule is supplied by Fermi statistics.

Armed with these tools we were able to show that topology changes are characterized by two important properties. First, a local field in the free field chiral boson becomes effectively multivalued so that in the simplest case

$$\phi(\theta) = \phi^1(\theta) + \phi^2(\theta) - \tilde{\phi}^1(\theta) \tag{4.211}$$

The total field, which in our case can be identified with the charge current density, can be written effectively as contributions from edges of the droplet distribution. This decomposition is valid only for nearby states to a reference state with a different topology from the vacuum. The important result for us is that the fields $\phi^{1,2}$ and $\tilde{\phi}^1$ on the subspace of nearby states states are each given by a chiral free boson, and they all commute with each other. The $\tilde{\phi}$ field has negative energy states rather than positive energy. When we mode expand, this decomposition is a partial Bogolubov transformation. This result

puts into firmer footing observations that have been made in [82], where we can also extend the ideas straightforwardly to fairly general coherent states.

On the face of it, this dynamical generation of new degrees of freedom is a violation of the Zamolodchikov c-theorem. A theory with central charge $c = 1$ in the UV flows to a theory which is seemingly of central charge $c = 3$ in the IR. It is better to write this central charge as follows $c_{IR} = (2, 1)$, where we are indicating by the decomposition the fact that the first two act to increase the energy, and the other set of oscillators acts to decrease the energy. This is the signature of the energy as a quadratic form, similarly as is done with spacetime dimensions. It is the fact that we can lower the energy around the new vacuum that allows the violation of the c-theorem: the vacuum of the new state is not stable. This property essentially arises from trying to do effective field theory in a very special non-vacuum state. Notice that $c_{UV} = 2 - 1$, so something similar to an index is preserved in the flow, indeed we found that this is the chiral anomaly of the system. The positive energy bosons carry anomaly one, and the negative energy bosons carry anomaly (-1).

The second property of the solutions with new topology is that they are characterized by having low uncertainty mode per mode in the mode expansion of the field ϕ. In this sense, the states can be said to be classical. We found that this uncertainty can be used as an order parameter to measure the topology. One can also similarly use the entanglement entropy of these modes to characterize the topology. The type of measurement that gets the topology is either an uncertainty measurement or an entropy measurement. Numerically, this results from measuring several quantum observables that don't commute with each other. We use this information to form an algebraic combination of the measurements that can be used to measure the topology. This ends up being a non-linear measurement on the wave functions. To offset the possibility

that one or a few of the new modes is excited in a non-classical state, the non-linear measurement needs to be performed on a large number of modes. The majority rule decides the topology by what we have termed a consensus measurement.

It is clear that this can be generalized beyond the simple stripe geometries we consider for more intricate bubbles. The multi-valuedness should then be thought of on a local basis in the coordinate θ, and the partial Bogolubov transformation should also be thought of in terms of a local expansion. We did a partial analysis of this setup with an approximation that describes the state as a locally multi-edge geometry. we observed that within this approximation one could find that generalized correlators encoded the fourier transform of the number of edges.

Also, the partial Bogolubov transformation makes it clear that the set of nearby states is somewhat compatible with effective field theory. The effective quantum fields are the new collective modes $\phi^I, \tilde{\phi}^J$. They exist on a neighborhood of the reference state. These collective fields do not stretch all the way to the UV. They have an effective cutoff given by the stringy exclusion principle, which depends on the details of the reference state. Because these modes only exist relative to some reference background they should be thought of as being background dependent. This seems to get around the problem of geometry being quantized by operators in a semiclassical approximation: the operators that are needed to do so are state dependent in a way that depends weakly on the state, which is not too different from the background field method.

To bubble or not to bubble

Given that we can trigger changes in topology by superposition and that we can get all possible topologies this way, we can argue that thinking of a quantum gravity theory as a sum (or path integral) over all topologies is at best ambiguous.

There are cases where this sum over topologies is absolutely correct. For example, in the topological string one can sum over topologies associated with crystal melting [117]. In that case, each shape of the melted crystal is a different topology. The limit shape of the crystal is the geometry of the string at large distances. The partition function depends on a probe brane and there is a parameter a that describes how far the probe brane is from the crystal. At large a, the molten crystal can be ignored. For $a \simeq 1$ one gets the quantum corrected stringy geometry, and for $a \simeq g_s$ one is in the quantum foam regime.

We can form an analogy with this setup. The basis of Young tableaux states is a complete basis of states. Each of these is topologically distinct in the naive classical supergravity approximation. The reason for this is that even though one might have the same spacetime topology for two configurations (same number of disks), one should also count the quantized flux through each cycle as topological data (this can not be deformed by small amounts, but only by integers, due to the Dirac quantization condition). In this basis, *any state is in principle a superposition of an infinite number of distinct topologies that can be measured*. This is not a complete set of all the possible topologies, only those that can be realized by rotationally invariant configurations. One can expect that for sufficiently classical states, like those that are close to our reference states, one can define an average (coarse-grained) topology that only counts the big corners, but not the small indentations of corners (these are small semiclassical excitations around the reference state). The distinction between geometry and excitations about a geometry depends on energy (this replaces the parameter a of the topological string). Our consensus measurement of topology necessitates a discussion of where we set the stringy exclusion principle. Unless we already know the state, this is not known a priori. Indeed, in our discussion in this paper, this is usually state dependent. When we try to go to lower

energies for the probes, the geometry appears to bubble more, while when we go to much higher energies than the stringy exclusion principle dictates, the topology looks trivial. In our case, this is tied to how entangled the different long wavelength modes of the oscillators are to the UV degrees of freedom in the free chiral boson. We can not discuss this entanglement without first defining what we mean by long wavelength versus short wavelength.

On the other hand, we can also define the theory entirely in terms of classical coherent states of the trivial topology as we argued in this paper. This is a different partition of unity (a different choice of basis states for the Hilbert space). In this case, the definition of topology depends on the precise superposition of states that we take. More precisely, it is contingent on our ability to find a reasonable nearby space of excitations to a given reference state that can be associated to small deformations of a classical geometry. This is a background dependent formulation of the dynamics, similar to how one treats the background field method. What is curious is that the existence of the new topologies implies that there is more than one classical limit of the free chiral boson field theory. This is to be understood in a double scaling limit.

In a certain sense, what we should be doing instead is to argue that the topology is not meaningful on its own: all versions of topology that we have discussed so far should be allowed at the same time, but most of them will not be useful descriptions of the system. This is very familiar when we think about dualities in field theory and string theory. Different duality frames are more or less useful depending on the size of particular cycles, or in the strength of certain coupling constants. The prescription that is more classical and permits us to get results with the least effort should be the preferred duality frame. In this sense, we should argue that at least some aspects of topology in the study of bubbling solutions correspond to a choice of duality frame. The frame that

most easily describes a configuration should be preferred. When we move away from simple configurations maybe none of the descriptions is useful on their own, but there we have a picture of a duality web where as we move between configurations, we get natural transitions in the topology of spacetime without any apparent singularity.

What is obvious is that if we want to have it both ways, we are double counting. This has implications for the fuzzball proposal [118] (see also [119]) and the counting of states in those geometries. It might be the case that in these other setups all different geometries and topologies are superpositions of more basic coherent states with a fixed topology. Understanding this intriguing possibility is beyond the scope of the present work.

Decoding the hologram

A natural question to ask is to what extent, given a state with a different topology than the vacuum of $AdS_5 \times S^5$, is one able to recover the geometry from naive holographic data on the boundary. The techniques that usually permit one to do so are elaborations on the Fefferaman-Graham expansion of the metric, extended to other fields [4]. A hologram would give us the solutions for the vacuum expectation values of single trace operators in the boundary, and that data should be useable to decipher the geometry of the solution.

As noticed in [67], this data seems to be insufficient to understand the geometry of circularly symmetric solutions of supergravity, as there is some ambiguity in how to do that. For us, this data is given by the expectation values of the modes of the chiral boson. For standard coherent states around the vacuum topology, this data is sufficient to reconstruct the coherent state.

For solutions around a geometric circularly symmetric solution with non-trivial topol-

ogy, it was first noticed in [82] that the excitations of the mode expansion of the "trace" modes on the UV theory (the free chiral boson) decompose into linear combinations of modes at each edge. In this paper, we have proven this result and argued that the partial Boguliubov transformation can be completed to a full Boguliubov transformation. We have also seen that the long wavelength modes of the mode expansion of the chiral boson of the UV theory act simply on these geometric states, and only a subset of the nearby Hilbert space is accessible by these actions. This is a general property of having a partial Boguliubov transformation. If we restore factors of N, and we have a solution with many annuli and energy of order N^2, the wavelength of the modes of the chiral boson become dependent at energies of order N (this is the stringy exclusion principle scale). More precisely, they fail to be planar at energies of order $\sqrt{N}$ (see for example [120]), which are still larger than the naive Planck scale $N^{1/4}$.

A naive low energy observer would probe wavelengths up to the order of the Planck scale. When extended to the boundary, the modes would all have long wavelengths with respect to the stringy exclusion principle. The other modes of the Boguliubov transformation become invisible and have to be treated as being traced over. We cannot decode the hologram with the naive boundary data. This is true even if we have measured the approximate radii of the circular droplets. In essence, we only measure a linear combination of the geometric modes, and the other linear combinations are not accessible to the holographic observer at infinity. The modes that are visible are effectively in a generalized thermal state mode per mode and they are very entangled with the UV modes.

This suggests that the reconstruction of local fields in the bulk from the boundary, a la [61], is generically suspect in a low energy approximation for states with non-trivial topologies. This setup ignores the information of the transplanckian modes and the

underlying UV theory, which at this scale is not really geometric in the classical sense any longer. If one acts with these types of mode operators of very high energy, one disturbs the underlying geometry by either adding a D-brane or making excitations that make the droplets meet with each other. A fluctuation this large is non-local any longer.

Also, entanglement by itself is a very coarse description of the state and is not necessarily very useful. Although we have been able to realize horizon free geometries, where measuring the momentum space entanglement can be used as an order parameter to describe the topology, and we realize precisely some ideas in [72] in a different context, the precise set of states for which we get such a geometry are not uniquely determined by this information. It is the construction of the modes that describe the fluctuations to the nearby states to a reference state that actually represent the full details of the physics.

Final remarks

One of the main conclusions of this paper is that even though we have a complete Hilbert space of states in which quantum mechanics is valid, the measurement of topology is not the result of an operator measurement. If topology is measured classically by integrating out a density made of polynomials of the curvature of the metric over the manifold, as we expect for gauge invariant operators in gravity, the fact that the topology cannot be measured by an operator seems to indicate that the metric (even modulo gauge invariance issues) is also not described by an operator. In our construction, the metric fluctuations around a sufficiently classical state exist relative to that state, but the construction of such operators does not extend to the full phase space of the theory. The generic state is non-geometric, but the semiclassical analysis is valid where it should be. This seems to be one of the properties that we need in order to claim that spacetime is emergent and not fundamental.

The holographic modes at infinity always exists. In our case, they are the mode expansion of the free chiral boson. These (boundary) modes give an approximation to something that looks geometric in a Fefferman-Graham expansion. However, the modes in the interior do not necessarily exist as operators. They might only be constructible around particular classical configurations. The proposal we have for this phenomenon is inherently non-linear: the modes that may exists in a superposition of states, do not exist in any one of the states that we are superposing. This emergence of modes depends on the entanglement of the soft modes with the UV and with each other. A non-linear proposal for quantum mechanics defining the physics inside of the horizon has been put forward by Papadodimas and Raju [121]. This proposal depends crucially on this entanglement, and essentially only on this entanglement (the state is pure but typical, so the details of the state are fairly random). For us, the entanglement of the modes is clearly not enough. The modes that we build are all outside the horizon and their existence depends on the state being just right.

Chapter 5

Code Subspaces for LLM Geometries

5.1 Introduction

The existence of gauge/gravity dualities [3, 4, 5] is remarkable and with each passing day we discover a new piece to their puzzle. Part of why these theories are so mysterious is because they often have non-intuitive and surprising properties that seem to lead to paradoxes. One of these was recently resolved by Almheiri, Dong, and Harlow [122]. The puzzle they addressed was that a local field at a point in the bulk should have vanishing commutators with fields that are spatially separated from them, including the boundary. A point in the center of global AdS would be spatially separated from the boundary at $t = 0$ (they belong to the same Cauchy slice) and would therefore have to commute with all local operator insertions on the boundary. Such a field should act trivially on the Hilbert space of states, and yet, be encoded as a non-trivial operator on the boundary. That is, bulk information seemed to be non-localized in the boundary

theory in an unexpected way. Their resolution was that though this might seem strange, it is not an entirely new phenomenon and in fact has a very nice interpretation in terms of quantum information theory. The idea is that the holographic correspondence acts as a quantum error correcting code. The commutation properties that are required are true in a subspace of the Hilbert space called the code subspace. It is this restriction to the code subspace that makes it possible to have the vanishing commutators in an effective sense, rather than as a statement on the full Hilbert space of states, where such properties are forbidden by quantum field theory theorems. Since their original work, there has been much progress in reinterpreting gauge/gravity dualities as holographic codes (for instance [123, 124, 125]). In this paper, we will push the idea further. We find that the language of code subspaces is a natural home for effective field theory and further, this can be seen explicitly within the framework of the LLM geometries [63].

In standard quantum information theory, if one wants to encode a message, one utilizes a Hilbert space of states larger than is necessary. One then constrains allowed messages to a particular subspace, the code subspace. For instance, one might use a few qubits to send a one qubit message, this provides a larger Hilbert space to work with and allows the messenger to choose whatever subspace they like to work within. In [122], the authors defined a set of code subspaces in AdS/CFT to be those formed as the linear span of

$$|\Omega\rangle\,,\ \phi_i(x)\,|\Omega\rangle\,,\ \phi_i(x_i)\phi_j(x_2)\,|\Omega\rangle\,,\ldots \tag{5.1}$$

where the $\phi_i(x)$ make up some finite set of local bulk operators, which can be realized in the CFT with the Hamilton-Kabat-Lifschitz-Lowe reconstruction of bulk operators [61]. Almheiry et al. take $|\Omega\rangle$ to be the ground state of the system (though they say one

could also consider other semiclassical background states, as we will do explicitly). The quantum error correcting properties of the gauge/gravity duality code make it possible to have a realization of the fields ϕ in the code subspace that commute with operators on the boundary, as long as one restricts the evaluation to states that belong to the code subspace.

In this work, we start by discussing effective field theory around a given classical background. We consider the Hilbert space accessible to an experimenter, which can be built by acting on the background state with some set of effective fields, in a way similar to equation (5.1). That is, we want to construct a space similar to the code subspace of vacuum AdS, within the confines of effective field theory and show that this has a lot of desirable properties for addressing more general questions of quantum gravity. Because an experimenter will not have access to infinite energy, they cannot act with all fields in the theory, but rather they are constrained by some cutoff (both in momentum and occupation number). It will turn out that the details of what cutoff is appropriate for each background will depend on the particular background under consideration. That is, the formulation of effective field theory is state dependent in relation to the reference state that we choose to expand from. We observe that the space built in this way exactly matches the structure of the code subspace defined in [122] and we expand on this fact. This is also very similar to how the Hilbert space of nearby states is built around black hole states in the work of Papadodimas and Raju [121, 126], by starting with a reference state. We discuss this philosophy in section 5.2.

In the rest of the paper, we deal specifically with the example of the LLM Geometries, which are dual to the half-BPS states of $\mathcal{N} = 4$ SYM. This is a very useful setup to work with as it is a place where we understand both the geometric description [63] and the field theory Hilbert space well [64, 65]. In fact, most of the exact computations turn

out to be combinatorial in nature [38] (see also [127]). In section 5.3, we build some necessary technology to do computations. We show that there are two convenient bases for describing the set of half-BPS states: one that can be classified by Young diagrams and one built by taking traces of powers of a matrix Z. In this section, we provide the details of these two bases, describing how to go between them and computing their inner products. These will be the tools we need both for the remainder of this work, and to help generalize some constructions that were carried out in our previous work [38] for finite N.

The states are dual to the set of half-BPS states in type IIB supergravity: the LLM geometries. Each geometry in this set can be classified by a black and white coloring of the plane. We consider the set of concentric ring configurations, because they are dual to states that are simple to describe in terms of Young diagrams [63, 90]. Although in principle other such geometries could be analyzed, the control of the states in the field theory dual is poor and relies on approximations. With the concentric configurations, we can make exact statements in the Hilbert space of states. These states dual to concentric rings will be the background states upon which we build our code subspaces. The nearby states that make up the subspace are built by acting with effective gravity field perturbations on each edge of the rings, which causes them to deform. With a bit of work, we are able to write down these fields explicitly so that we can build the states as in (5.1) in a way that is suitable for our purposes. This is the content of section 5.4.

By only considering the geometric description, the aforementioned cutoffs are not immediately clear and although in principle one should be able to derive them, it takes a considerable amount of effort. So, instead, in section 5.5, we go back to the representation of the states in terms of Young diagrams, where things become clearer. The well behaved concentric ring configurations correspond to diagrams with few corners. The effective

fields are build out of modes that act only in a particular corner of the diagram and one can reproduce directly the supergravity analysis entirely with combinatorial techniques. These techniques have been developed in various papers for different settings (see [120, 82, 106, 38, 127] and references therein).

In section 5.6, we undertake the problem of understanding the cutoff. The cutoff is provided by constraining the excitations so that they do not simultaneously affect multiple corners of the diagram and by requiring that they are sufficiently *planar*. This corresponds to each field only acting on a single edge of the concentric rings and having small energy, although the energy of an individual quantum can be much larger than the Planck scale[1]. We can write these excitations in terms of modes that act in a particular corner of the Young diagram and from these build a Fock space representation.

In section 5.7 we expand on some of our previous work [38, 40], where we compute the topology of the states within a given code subspace. Previously, we were in the strict $N \to \infty$ limit, but here we go beyond that, taking N to be large, but finite. As before, we find that we can extract the topological information from entanglement and uncertainty calculations, though it requires more work: a number can not be guessed any longer from a single mode, but it requires many modes instead. Here we also find a close connection with the recent work of Balasubramanian, et. al. [128], who showed the existence of entanglement shadows in the LLM geometries. We find that similarly, the extrapolate dictionary seems to stop at the outermost anti-edge of the concentric ring diagrams. This is the second edge starting from the outside going inward in the radial direction of the LLM plane and it is the same place where the entanglement shadow begins.

Finally, in section 5.8 we consider the overlap that can occur between different code subspaces. We look specifically at an example where you start with two different back-

[1]The energy of an individual quantum can scale like $N^{1/2}$, rather than $N^{1/4}$

ground states and add particular excitations to each, which results in having prepared two identical states from the viewpoint of Young diagrams, but whose construction indicates that they should be assigned different metric operators. We discuss the ambiguities that arise because of this fact, which in particular obscures one's ability to write down a globally well defined metric operator.

5.2 Code subspaces and effective field theory

In this section, we will discuss doing effective field theory around some classical background. We will consider the constraints put on an experimenter in this set-up and will show how what we end up with matches previous definitions of code subspaces.

Let us start by assuming we are given a quantum state $|B\rangle$ that is dual to a classical background for a field or gravitational theory. Eventually we will analyze a field theory with a gravitational dual, using the gauge/gravity duality. Here, the state $|B\rangle$ will correspond to a classical background in the bulk, rather than the boundary theory. Though $|B\rangle$ is a classical background, we need to be careful, because in the quantum theory the quantum fluctuations can never be zero. Instead, we should think of $|B\rangle$ as a coherent state, where (effective) quantum fields have minimal uncertainty relative to the background. We also want to be careful because we will often have a cutoff to account for. For instance, if $|B\rangle$ is a ground state for a gapped system, $|0\rangle$, the cutoff might be in the energy available to us. This will restrict us in two different ways. First, it will require that the only modes that can be excited are long wavelength fluctuations (of small enough energy) and further, we will be restricted in the occupation number of any one such mode, so that the energy cutoff also imposes an amplitude cutoff for any one mode. Generally, this could be configuration dependent if for example, the gap for

some additional excitation depends on a vacuum expectation value. This is common in supersymmetric field theories when we have a moduli space of vacua.

In analyzing this system, we might want to understand what a Hilbert space of *nearby* states to the background $|B\rangle$ would look like. The state $|B\rangle$ belongs to a Hilbert space of states $\mathcal{H}$ that defines the full quantum theory. It is tempting to consider the set of states $|\psi\rangle \in \mathcal{H}$ such that they differ from $|B\rangle$ by a small amount, ϵ inside the Hilbert space $| \, |\psi\rangle - |B\rangle \, | < \epsilon$. There are many problems with this prescription, and we will enumerate a few of them in what follows. First, the set of states $|\psi\rangle$ is not a linear subspace of $\mathcal{H}$: we cannot do quantum mechanics restricted to the nearby states. Secondly, the set of such states $|\psi\rangle$ makes no mention of the cutoff nor to the effective fields.

We want to define the set of *nearby* states to be those that can be generated from $|B\rangle$ by the action of the effective fields, and so that it is also a linear space. That is, we want the set of nearby states to be a Hilbert space in its own right: a Hilbert space where an experimenter can act and make observations, and in principle make predictions for those observations as well, within the constraints that would be imposed by the apparatus and how it acts in effective field theory. Such sub-Hilbert spaces can be thought of as code subspaces: the set of observables of the experimenter is constrained to lie in the code subspace. At the technical level, the idea will be to first decompose the fields $\phi_i(x) = \langle \phi_i(x) \rangle_B + \sum_\lambda f_{i,\lambda}(x) a^\dagger_{i,\lambda} + \sum_\lambda f^*_{i,\lambda}(x) b_{\lambda,i}$ into raising/lowering operators of approximate wavelength λ. We need to include the b modes to allow for the possibility that the field ϕ_i is complex, otherwise we have $b \simeq a^\dagger$. For brevity, we will take the field to be real. We also need to require that the $a, a^\dagger$ approximately satisfy the Weyl commutation relations. To impose a cutoff, we state that the set of λ is restricted. We also impose that $|B\rangle$ is annihilated by the lowering operators a. This second condition is what defines the state operationally to be effectively a coherent state.

We make use of the modes of the fields $\phi_i(x)$ acting on $|B\rangle$ to generate new states

$$|(i_1, \lambda_1), \dots (i_k, \lambda_k); B\rangle = \prod_j a^\dagger_{i_j,\lambda_j} |B\rangle \tag{5.2}$$

for some such collection of pairs (i_j, λ_j). We can think of this state as the background state $|B\rangle$ with some finite number of cutoff respecting excitations turned on. We will call our cutoff Λ. Usually, we interpret Λ as a UV cutoff in effective field theory around a ground state, so that energies (frequencies) ω of individual excitations are bounded above by $\omega \leq \Lambda$. Here, we are constrained so that our set of excitations collectively stay below Λ. The cutoff Λ should not be in general thought of as simply a fixed shortest wavelength, nor as just an upper bound on the energy. It can also be dependent on position and on the differing modes. In the work [122], the cutoff is implicit in the sense that we do not form a black hole. In the work of Papadodimas and Raju, the cutoff is described by not having too many actions on the reference state [126]. This is again an implicit cutoff.

We will call the Hilbert space

$$\mathcal{H}_{B,\Lambda} = Span(|(i_1, \lambda_1), ...(i_k, \lambda_k); B\rangle \ \ |\{(i_1, \lambda_1), ...(i_k, \lambda_k)\} \leq \Lambda) \tag{5.3}$$

the code subspace associated with the background $|B\rangle$ and the cutoff Λ. This will be sometimes abbreviated to $\mathcal{H}_{\text{code}}$. This is in accordance with the definition of code subspace found in the work of Almheiry, Dong, Harlow [122] on quantum error correction and it also matches the effective description of states generated from a reference black hole state in the work of Papadodimas and Raju [126, 108]. This also matches the definition of the nearby Hilbert space of states in our previous work [38]. The advantage of

using the language of code subspaces is that it makes three items automatic. First, it is a Hilbert space, so that we can do quantum mechanics inside $\mathcal{H}_{\text{code}}$. Secondly, effective fields act simply on it. Finally, there is an explicit cutoff Λ, so this does not need to be repeated again and again: it is part of the definition of the code subspace itself.

If the state $|B\rangle$ is an excited state (not a ground state), one can in principle find many states that have a similar energy to $|B\rangle$ but that are not generated in this way. One should think of the code subspace $\mathcal{H}_{B,\Lambda}$ as the set of states that is accessible to an experimenter who can control the excitations of the fields ϕ_i below the cutoff. In this sense, this is the natural home for effective field theory. As an experimenter builds a better experiment, the cutoff might change and more states can become available. However, the effective field theory description might break down. This is not a failure of quantum mechanics, but of the simplified description of the Hilbert space of available states that the experimenter can access.

With this definition, the fields ϕ_i have been given to us, at the very least in an implicit form, as well as the mode expansion. In general, we could expect that there are non-linear field redefinitions to worry about, as they might generate states that do not belong to the code subspace. We also have to worry that under time evolution the states might exit the code subspace. As long as we can stay comfortably inside H_{code} for some fixed amount of time we will be content. To do so we will also include a temporal cutoff in the time during which experiments can be performed. The second problem is not obviously an immediate issue if $|B\rangle$ is an energy eigenstate, but the problem will kick in as soon as we act on the state. We do not address these issues directly for general setups, rather, we will leave these issues implicit in the definition of Λ itself, thinking of it as a set of all the necessary cutoff information.

One might think that this is overly pedantic. The purpose of this paper is to show that

this structure is the only sense in which one can do effective field theory in a particular subsector of a gravitational theory. It will turn out that different code subspaces will generically be incompatible. That is, assume that a state belongs to two such code subspaces $|\psi\rangle \in \mathcal{H}_{B,\Lambda}, \mathcal{H}_{B',\Lambda'}$. The topology of $|B\rangle$, $|B'\rangle$ and the number of (effective) fields might differ substantially to the point where even though the state $|\psi\rangle$ is well defined, we cannot say what topology it has (the one of $|B\rangle$ or $|B'\rangle$) nor the number of fields. More importantly, one code subspace might recycle a field of another code subspace nonlinearly into many fields. What this will mean is that the physical answer to many (interpretational) questions can only be answered inside the different code subspaces, but not in the full Hilbert space $\mathcal{H}$.

Our goal in the rest of the paper will be to explain how to construct a particular collection of code subspaces explicitly, including the effective fields and the cutoff and to show precisely how they are incompatible.

5.3 The action of traces on Young tableaux

We will now consider a particular set-up, where we can study effective field theory explicitly. The half-BPS states of $\mathcal{N} = 4$ SYM on the sphere are in one to one correspondence with the gauge invariant local operators that are build out of polynomials of a single scalar field $Z(x)$ (which we will take to be in the adjoint in the adjoint of $U(N)$). This space is converted into a Hilbert space via the operator state correspondence that is available in conformal field theories. We write the map as follows $\mathcal{O} \to |\mathcal{O}\rangle$. For us to understand the Hilbert space of states, we need to determine the norms of states. The norms of states that correspond to local operators come the Zamolodchikov norm of the

operator, obtained from the two point function as follows

$$\langle \mathcal{O}^\dagger(x)\mathcal{O}(0)\rangle = \frac{\langle \mathcal{O}\rangle \, \mathcal{O}}{|x|^{2\Delta_\mathcal{O}}} \tag{5.4}$$

What we need now is the complete list of operators in a basis that is suitable for computations. This problem was solved in [64], where it was noted that a Schur polynomial basis was orthogonal (this is based on the fact that characters of Z in irreducible representations of $U(N)$ are orthogonal) and where their norms were computed. However, there is another basis made of string states, which are traces, that is also useful and can be used to define the supergravity fields of $AdS_5 \times S^5$. It is the traces that are used to define the extrapolate dictionary of AdS/CFT [4]. Thus, it is necessary to study both basis to get to the complete physical description. For this section we follow mostly the results obtained in [64, 38] where the main results are proved in detail. The new result we find is to compute the actions for Young Tableaux states that are normalized according to the results of [64] rather than the $N \to \infty$ limit discussed in [38].

There are two natural ways to construct gauge invariant operators from a matrix Z. One of them is to take traces of powers of Z, $\mathrm{Tr}(Z^m)$ and to consider the set of linear combinations of multi-traces of Z. The other is to think of an $N \times N$ matrix Z as an element of $GL(N, \mathbb{C})$. Then we can take the character of Z in some representation of the group $GL(N, \mathbb{C})$, R, and denote the result as $\chi_R(Z)$. The latter are classified by Young diagrams.

These two bases of gauge invariant operators generate the same linear space and can be related to each other algebraically, the details can be found in [64]. For example, the fundamental representation, with Young Tableau $\square$, can be related to $\mathrm{Tr}(Z)$ via its

character as

$$\chi_{\square}(Z) = \mathrm{Tr}(Z). \tag{5.5}$$

To write the relationship for other states, we need a few more definitions. Let $[\sigma]$ be a conjugacy class of S_n. The conjugacy class of $[\sigma]$ is in one to one correspondence with group elements σ of the same cycle decomposition, where there are $n_j([\sigma])$ cycles of length j, so that $n = \sum_j j n_j([\sigma])$. See appendix E for details on how the cycle decomposition is obtained from a group element. To each such cycle, we associate the trace $\mathrm{Tr}(Z^j)$, so that to the element $[\sigma]$ we can associate the monomial in the traces

$$[\sigma] \to \prod_j (\mathrm{Tr}(Z^j))^{n_j([\sigma])}. \tag{5.6}$$

If R is represented by a Young diagram with n boxes, which we indicate by R_n, then

$$\chi_{R_n}(Z) = \frac{1}{n!} \sum_{[\sigma] \in \mathrm{Conj[S_n]}} \chi_R([\sigma]) d_\sigma \prod_i (\mathrm{Tr}(Z^i))^{n_i([\sigma])} \tag{5.7}$$

where d_σ is the number of elements of the conjugacy class, $\chi_R([\sigma])$ is the character of σ in the representation of the group S_n with the same Young diagram as R_n (these are in one to one correspondence via Schur-Weyl duality). This explains how to write the basis $\chi_R(Z)$ in terms of traces. The map is invertible (the fact that the relationship between conjugacy classes and representations is invertible is true for any finite group, see [129]). The result of this inversion is

$$(\mathrm{Tr}(Z^i))^{n_i([\sigma])} = \sum_{[R] \in \mathrm{Reps[S_n]}} \chi_R([\sigma^{-1}]) \chi_R(Z) \tag{5.8}$$

which was shown in [38].

In what follows, we will define the variables $t_\ell = \mathrm{Tr}(Z^\ell)$, and we will label the representations of R directly in terms of Young diagrams. The length of the cycle ℓ will be called the degree of t_ℓ, and the number of boxes of a Young diagram n will be the degree of the Young diagram. With this convention we have that $[\sigma] \to \prod_i t_i^{n_i([\sigma])}$. The sum $\sum_\ell n_\ell \ell = n$, so we have that the degree of each of the monomials is equal to the degree of the Young diagram, and acting with an extra trace $\mathrm{Tr}(Z^\ell)$ will be multiplication by t_ℓ. Acting with t_ℓ on $\chi_R(Z)$ (by multiplication), will have degree $\deg(R) + \ell$ and can be expressed in terms of the basis of the $\chi_{\tilde{R}}$, with $\deg(\tilde{R}) = \deg(R) + \ell$.

For example, we can take the state

$$(6,4,2,1) = \tag{5.9}$$

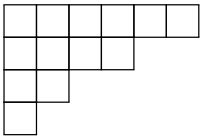

where we label $R = (6,4,2,1)$ by the length of the rows of the Young diagram and we think of the Young diagram as the gauge invariant operator $\chi_R(Z)$ itself. Now, we want to act with one of the t_ℓ, and see what linear combination of representation characters we get. The answer is actually simple.

We will do the particular example of $t_4(6,4,2,1)$. Acting with t_4 will give us the

following result

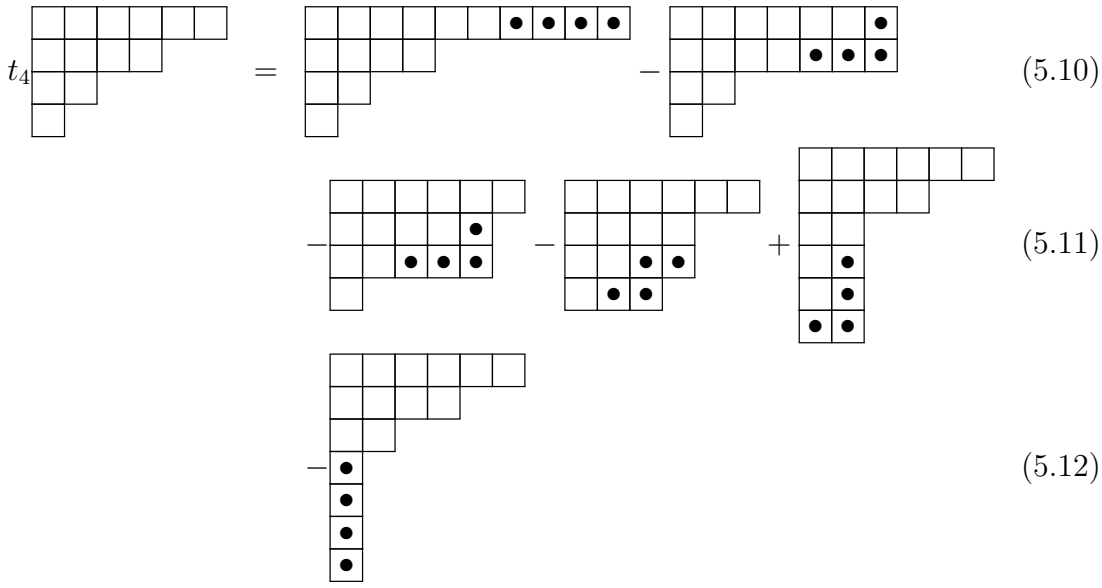

where we have indicated with circles the extra boxes that are attached to the original Young diagram R. The action on any given Young diagram is given by applying the following rules [38]:

1. The original Young diagram sits inside the added boxes.

2. The set of new extra boxes are arranged in a pattern where they all touch each other and give rise to a proper diagram when combined with the original.

3. The set of new boxes snake around the edge of the old diagram (this means that no square pattern set of 2×2 boxes can be found in the new boxes). Sets of boxes with this property are called skew-hooks.

4. The coefficients are all ± 1. The sign is determined by how many rows the new boxes cover: $+1$ if the new boxes sit in an odd number of rows, and (-1) if it is even.

5. The sum is over all possible ways of attaching a skew hook of the right length (in this case four, as we acted with t_4) to the original Young diagram.

We can write these conditions as follows

$$t_\ell \, \chi_Y(Z) = \sum_{h \in \text{Skew hooks of length } \ell} (-1)^{H(h)-1} \chi_{Y+h}(Z) \tag{5.13}$$

where the symbol $H(h)$ indicates the height of the hook (the number of rows it subtends). Also, the length of a skew hook, $|h|$, is the number of boxes it has.

As we have argued, the space of gauge invariant operators is endowed with a metric, the Zamolodchikov metric. This is a positive definite metric and is identified with the Hilbert space norm in the quantum theory on the cylinder. The norm for each Young diagram state $|Y\rangle$ can be evaluated as follows. We first label the boxes of the diagram, adding one as we go to the right and subtracting one as we go down

$$(6,4,2,1) = \begin{array}{|c|c|c|c|c|c|} \hline +0 & +1 & +2 & +3 & +4 & +5 \\ \hline -1 & 0 & +1 & +2 \\ \cline{1-4} -2 & -1 \\ \cline{1-2} -3 \\ \cline{1-1} \end{array} \tag{5.14}$$

That is, to each box in position (i,j) (the label i refers to the column, and the label j refers to the row of the box) we associate the number $i-j$. The norm is then computed as follows:

$$\langle Y \rangle \, Y = \alpha^{\#\text{boxes}} \prod_{(i,j) \in \text{boxes}} (N+i-j) \tag{5.15}$$

where α is a normalization constant for the matrix field Z. Also, different Young tableaux are orthogonal. This was deduced in [64]. To simplify matters, we choose $\alpha = N^{-1}$. Then

we have that

$$\langle Y\rangle\, Y = \prod_{(i,j)\in \text{boxes}} \left(1+\frac{i-j}{N}\right) \tag{5.16}$$

so that the large $N\to\infty$ limit is simple and all the norms for each Young tableaux state are equal to one. We are interested in a finite but large N.

Now, since the Young diagram states are orthogonal, we can consider a dual basis for the Young diagrams $|\check{Y}'\rangle$, so that we have the relation

$$\langle \check{Y}'\rangle\, Y = \delta_{Y,Y'} \tag{5.17}$$

and it is easy to see that

$$|\check{Y}\rangle = |Y\rangle \,/\, \langle Y\rangle\, Y \tag{5.18}$$

Using this dual basis, we can write the action (5.13) as follows

$$\langle \check{Y}+h|\, t_n\, |Y\rangle = (-1)^{H(h)}\delta_{|h|,n} \tag{5.19}$$

where again, $|h|$ is the number of boxes in the skew hook h and $|Y+h\rangle$ refers to a state $|Y\rangle$ with an added hook h. If we choose the basis to be orthonormal, we find that

$$\langle \check{Y}+h|\, t_n\, |Y\rangle = \frac{\sqrt{\langle Y\rangle\, Y}}{\sqrt{\langle Y+h\rangle\, Y+h}}\, \langle \hat{Y}+h|\, t_n\, |\hat{Y}\rangle \tag{5.20}$$

where we are using $|\hat{Y}\rangle$ to represent an orthonormal state (as opposed to the state in the dual basis, which has a down check instead of a hat). So the action in the orthonormal

basis is represented by

$$\langle \hat{Y} + h| \, t_n \, |\hat{Y}\rangle = (-1)^{H(h)} \delta_{|h|,n} \frac{\sqrt{\langle Y+h\rangle \, Y+h}}{\sqrt{\langle Y\rangle \, Y}} = (-1)^{H(h)} \delta_{|h|,n} \prod_{(i,j)\in \text{boxes of h}} \sqrt{\left(1+\frac{i-j}{N}\right)} \tag{5.21}$$

And the adjoint action is

$$\langle \hat{Y} - h| \, t_n^\dagger \, |\hat{Y}\rangle = (-1)^{H(h)} \delta_{|h|,n} \frac{\sqrt{\langle Y\rangle \, Y}}{\sqrt{\langle Y-h\rangle \, Y-h}} = (-1)^{H(h)} \delta_{|h|,n} \prod_{(i,j)\in \text{boxes of h}} \sqrt{\left(1+\frac{i-j}{N}\right)} \tag{5.22}$$

With this formula, we now have the main computational tool we need for the rest of the paper. It should be noted that if we take the limit where i, j are finite and $N \to \infty$, the set of Young tableaux states all have trivial norm and the coefficients for the action of the traces are all ± 1. In this case, the half BPS states are described exactly by a $c = 1$ left-moving chiral boson in $1 + 1$ dimensions.

5.4 Defining the code subspaces for concentric configurations.

Let us consider a particular case of an LLM geometry that is time independent and that is therefore an eigenstate of the Hamiltonian of the $\mathcal{N} = 4$ SYM theory on the $S^3 \times \mathbb{R}$ boundary. The LLM geometries are described by droplet configurations on the plane, and as they are time evolved they rotate uniformly about an origin in the LLM plane. The ground state is described by a disk, and the rotation center is located exactly at the center of the disk. For another configuration to be similarly time independent, the droplet configuration must be invariant under rotations around such an origin. This results in a droplet configuration that is described by a set of concentric rings. Because

the configurations are time independent, they have an extra isometry symmetry in the supergravity description. This extra symmetry is exactly the rotation of the configuration around the origin. This is a diffeomorphism that does not vanish at infinity and is realized as a proper symmetry of the configuration. This is the symmetry associated with either time translation or to being an eigenstate of the R-charge.

A particular example of a geometry is visualized in figure 5.1. The radii of the boundaries are labeled as follows $r_1 > \tilde{r}_1 > r_2 > \tilde{r}_2 > \ldots$, from the outermost boundary inwards. We will call these edges and anti-edges, depending on if they are labeled with an r_i or a $\tilde{r}_i$, that is, if they go from black to white (edges) or if they go from white to black (anti-edges) when tracing a straight line from the origin. This is in accordance with the convention established in [38]. The important geometric parameters are the

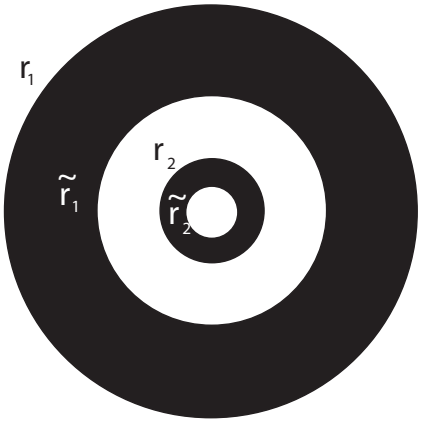

Figure 5.1: A circularly invariant LLM geometry. The radii are labeled by $r, \tilde{r}$, depending on if they go from black region to white region, or viceversa, starting from the outside and going inwards.

radii $r_1, \tilde{r}_1, \ldots$ which are necessary to uniquely identify the geometry. We will assume that we are working at fixed large N, and that the disk representing the ground state has been normalized to have radius equal to one. We will also assume that the $r_i, \tilde{r}_i$ are

of order one. The area of the black region is given by

$$A = \pi \sum_i (r_i^2 - \tilde{r}_i^2) = \pi \tag{5.23}$$

which is the same as the area of the unit disk. This gives us one relation between the radii.

The energy of the state (geometry) is given by

$$E \propto N^2 \left(\sum_i r_i^4 - \tilde{r}_i^4 \right) - N^2 \tag{5.24}$$

As long as the radii are moderately spaced, the solution is weakly curved and effective field theory is valid. Small deformations of the geometry that preserve the supersymmetry can be characterized by having the $r_i, \tilde{r}_i$ vary with the angle around the origin as follows $r_i(\theta) = r_i + \delta r_i(\theta)$, $\tilde{r}_i(\theta) = \tilde{r}_i + \delta\tilde{r}_i(\theta)$ with $\delta r, \delta\tilde{r} << 1$ and more precisely, we require that the configuration is fairly smooth so that the wiggles are not too pronounced. This is what we mean by long wavelength fluctuations. This is depicted in figure 5.2. Larger deformations will have either short wavelength (rougher edges), or larger amplitude resulting in more pronounced creases.

From the point of view of supergravity, it is obvious that to each of the radii $r_i, \tilde{r}_i$ we can associate a function of one variable θ that preserves the supersymmetry of the configuration and that therefore the effective field theory – restricted to the half-BPS states– is now described by many functions of θ. Since each $r_i, \tilde{r}_i$ can be in principle deformed independently of the others, we have to associate an effective field with each such (anti-) edge. Each such field should result in a left chiral field $\phi_i(\theta), \tilde{\phi}_i(\theta)$, just like the single edge of the ground state results in such a field.

In the limit where the $\delta r_i, \tilde{\delta} r_i << 1$, we can expand the area of the regions to linear

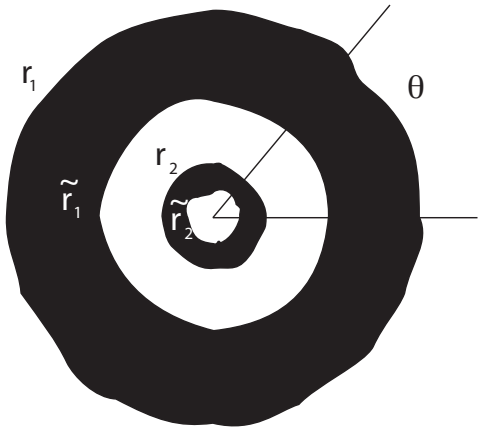

Figure 5.2: A slightly deformed circularly invariant LLM geometry. The radii are now given by $r_i(\theta), \tilde{r}_i(\theta)$

order in these deformations. We get that the areas of the regions are given by one of the two expressions (the left for black regions and the right for white)

$$A_i = \frac{1}{2}\int d\theta(r_i^2(\theta) - \tilde{r}_i^2(\theta)), \tilde{A}_i = \frac{1}{2}\int d\theta(\tilde{r}_i(\theta)^2 - r_{i+1}(\theta)^2) \tag{5.25}$$

and to leading order in fluctuations we get that the variations in the area are given by

$$\delta A_i = \int d\theta(r_i \delta r_i(\theta) - \tilde{r}_i \delta\tilde{r}_i(\theta)), \delta\tilde{A}_i = \int d\theta(\tilde{r}_i \delta\tilde{r}_i(\theta) - r_{i+1}\delta r_{i+1}(\theta)) \tag{5.26}$$

Because the areas are quantized in natural units due to Dirac quantization condition, we need to require that the $\delta A_i = \delta\tilde{A}_i = 0$, and this implies that

$$\int d\theta \delta r_i(\theta) = \int d\theta \delta\tilde{r}_i(\theta) = 0 \tag{5.27}$$

We infer that the fluctuations have a Fourier expansion with the zero mode missing for each fluctuation.

For quantization, we also need the Poisson bracket between the $\delta r_i(\theta)$. This was calculated in [130]. One can derive it from the Hamiltonian and locality in θ. Basically, we need that

$$\{H, \delta r_i(\theta)\} = \dot{r}_i(\theta) = -\partial_\theta r_i(\theta) \tag{5.28}$$

and similarly for $\delta\tilde{r}_i$. Since the energy function is the Hamiltonian, the Poisson bracket is as follows

$$\{\delta r_i(\theta), \delta r_j(\phi)\} = \frac{\delta_{ij}}{N^2 r_j(\theta)^2}\partial_\phi \delta(\theta - \phi) \tag{5.29}$$

whereas for the other variables we find a sign change

$$\{\delta\tilde{r}_i(\theta), \delta\tilde{r}_j(\phi)\} = -\frac{\delta_{ij}}{N^2 \tilde{r}_j(\theta)^2}\partial_\phi \delta(\theta - \phi) \tag{5.30}$$

that follows because the Hamiltonian for the $\delta\tilde{r}$ is actually negative definite. The cross term vanishes.

We interpret the prefactor in front of the derivative of the delta function as an effective notion of the Planck constant $\hbar$ for the corresponding background field determined by the geometric data. As is usual in the AdS/CFT correspondence, $\hbar$ scales as $1/N^2$, and this is the normalized Newton constant [2].

With these conventions, the canonically normalized fluctuating fields ϕ^C, and $\tilde{\phi}^C$ depend on the values of the geometric parameters $r_i, \tilde{r}_i$, as follows

$$\phi_i^C(\theta) = N r_i \delta r_i(\theta) = \frac{N}{2}\delta(r_i^2(\theta)) \tag{5.31}$$

and similarly for $\tilde{\phi}^C$. The Fourier modes of the $\phi^C, \tilde{\phi}^C$ will have canonical commutation

[2]Notice that if we scale $r, \delta r$ by the same scale factor to remove the $1/N^2$ pieces, we find that the normalized value of the radius R then scales as $R \simeq \sqrt{N}$, and the area of the disk is proportional to N.

relations, such that

$$\phi_i^C(\theta) = \sum_n \phi_{i,n}^C \exp(in\theta) \tag{5.32}$$

and

$$\{\phi_{i,n}^C, \phi_{j,m}^C\} = n\delta_{ij}\delta_{n,m} \tag{5.33}$$

whereas for the $\tilde{\phi}$ we get a sign change

$$\{\tilde{\phi}_{i,n}^C, \tilde{\phi}_{j,m}^C\} = -n\delta_{ij}\delta_{n,m} \tag{5.34}$$

One can then show that the $\phi_n^C, \tilde{\phi}_n^C$ are either raising or lowering operators with energy $n, -n$ respectively (the $\tilde{C}$ fluctuations reduce the energy).

Now that we have our canonical mode fields, we can define the code subspaces as in section 5.2. We just take the concentric ring background configuration and act with the raising operators $\phi_{-n}^C, \tilde{\phi}_m^C$ a finite number of times, with a cutoff on n, m and the number of raising operators acting on the reference state, which is specified by the radii, and the quantization condition that all the lowering modes of the effective edge fields are in their ground state. The precise details of the cutoff are yet to be specified, and the result should be understood to be a leading order approximation in a large N expansion, so there might be $1/N$ corrections that need to be studied more carefully.

Notice that the definition of the code subspace is fairly straightforward, but the determination of the effective modes took some work. It also assumes a particular action of the modes of the fields on the reference state and by relying heavily on the classical analysis in gravity, we do not have a direct access to how the cutoff should be correctly implemented.

A second issue that needs attention is to make sure that the code subspace that

we have defined this way is compatible with the holographic boundary operator actions. That is, we want to show that acting with the operators that preserve the supersymmetry and that are realized in the boundary does not take us out of the code subspace. To do this, we need to notice that the boundary operators measure the multipole moments of the droplet distribution. These can be written as follows

$$\phi_n \simeq \int \rho(r,\theta)\left[r\exp(-i\theta)\right]^n r dr d\theta \tag{5.35}$$

where ρ is the region of the plane that is filled. After some manipulations where we do the radial integral first [37], these modes are written as follows

$$\phi_n = \frac{1}{n+2}\int \sum_i \left[r_i(\theta)\exp(-i\theta)\right]^n r_i^2(\theta) - \left[\tilde{r}_i(\theta)\exp(-i\theta)\right]^n \tilde{r}_i^2(\theta) d\theta \tag{5.36}$$

To linearized order we have that $r_i(\theta) = r_i + \delta r_i(\theta)$, so we find that

$$\phi_n = \int \sum_i \left[r_i^{n+1}\delta r_i(\theta)\exp(-in\theta) - \tilde{r}_i^{n+1}\delta r_i(\theta)\exp(-in\theta)\right] d\theta \tag{5.37}$$

which in terms of the canonical fields becomes

$$\phi_n = N^{-1}\sum_i \left[r_i^n \phi_{i,n}^C - \tilde{r}_i^n \tilde{\phi}_{i,n}^C\right] \tag{5.38}$$

The factor of $1/N$ in the prefactor is to be thought of as $\sqrt{\hbar}$, which is the standard size for quantum fluctuations. In this sense, we should remove it and the normalized operator for boundary insertions should be given by

$$\hat{\phi}_n = \sum_i \left[r_i^n \phi_{i,n}^C - \tilde{r}_i^n \tilde{\phi}_{i,n}^C\right] \tag{5.39}$$

With these conventions we have that for the ground state where $r_1 = 1$ and all other $r_i, \tilde{r}_i$ vanish, we have that

$$\hat{\phi}_n = \phi^C_{1,n} \tag{5.40}$$

Since the field $\hat{\phi}$ is in general clearly a linear combination of operators in the code subspace, it belongs to the code subspace. To go beyond linearized order, we need to normal order the expressions. The non-linear terms that are generated will be polynomials in $\phi^C_{i,n}$ and $\tilde{\phi}^C_{i,n}$ suppressed by additional powers $1/N$.

What we want to do now is reproduce these same results without relying on the semi-classical description, but directly in terms of the matrix variables. What is important for us is that the concentric circle configurations have a simple description in terms of Young tableaux [63]. Therefore it is possible to analyze the physics of the cutoff in terms of the trace variables as in section 5.3. This will permit us to describe the cutoffs better and to verify directly the expression (5.39). This can be understood as a test of the LLM geometry map. We will tackle this problem in the next section.

5.5 Code subspaces in the Young tableaux formalism

As is by now well understood, concentric ring classical configurations in the LLM plane correspond to Young tableaux with only a few corners (see [90] for more details).

A typical such Young tableaux looks as portrayed in the diagram (5.41)

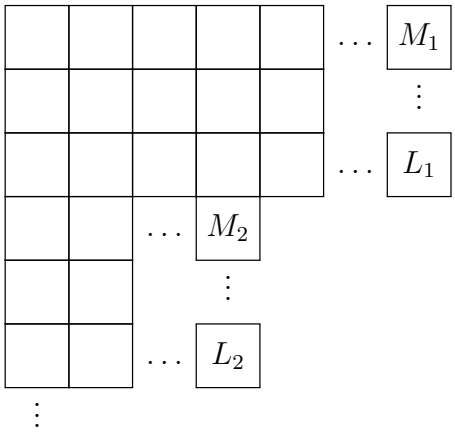

(5.41)

where the length of the long rows are of size $M_1, M_2, \ldots$, and the depth of the columns is $L_1, L_2, \ldots$. With these conventions, the empty corners to the right of the M_i (concave corners) have coordinates given by

$$(i, j) \in \{(M_1 + 1, 1), (M_2 + 1, L_1 + 1), \ldots (M_k + 1, L_{k-1} + 1)\} \tag{5.42}$$

Similarly, the convex corners of the edge of the tableaux are given by the coordinates

$$(i, j) \in \{(M_1, L_1) \ldots (M_k, L_k)\} \tag{5.43}$$

We will call this state the reference state $|\Omega\rangle$. It is around this state that we want to build an effective field theory of the LLM states that mirrors the gravity construction. To such a tableaux with widely spread out corners we can associate a Hilbert space of small fluctuations. These are additional small tableaux that can be attached to each corner. In the young diagram depicted in (5.44), we see an example of adding a small tableaux to the concave corner depicted with the symbol + and also a tableaux that

is substracted from the convex corner and depicted with the symbol $-$. This idea was originally sketched in [82], but was not fully realized at the time. It was implemented in the strict $N \to \infty$ limit in [38] and better estimates for various quantities were obtained in [127].

Here we have a full implementation of the details at finite N.

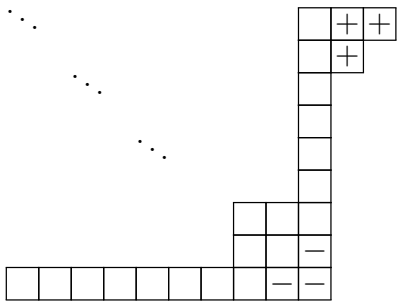

(5.44)

It is easy to see that we can define a small Hilbert space for each corner. This Hilbert space is the set of small Young tableaux (whose sides are much smaller than the sides of the big tableaux with few corners). There will generically be two types of corners: the ones that have + boxes, and the ones that have $-$ boxes. These correspond to the two types of corners of the reference tableaux. For convenience, we will label them with the (i, j) values of the first corner that we can add or substract, and each of these corner Hilbert spaces will be called $\mathcal{H}_{(i.j)}$. By construction, we find the small Hilbert space of states relative to the reference state $|\Omega\rangle$, which we will call the code subspace, can be decomposed as follows

$$\mathcal{H}_{\text{code}|\Omega\rangle} = \prod_k \mathcal{H}_{(M_k+1, L_{k-1}+1)} \otimes \prod_k \mathcal{H}_{(M_k, L_k)} \tag{5.45}$$

As of yet, we have not specified the size of the factors of code subspace. We will proceed to do this later. What we need to do right now is to understand in a little more detail

the $\mathcal{H}_{(i.j)}$ factors. The idea is that each of these is characterized by a Young diagram. There are two cases to consider: the + subspaces and the − subspaces.

Let us begin with the + subspaces. These are labeled by $\mathcal{H}_{(M_k+1,L_{k-1}+1)}$. What we are interested in to begin with are the factors associated with adding and substracting boxes, as in equation (5.22). We will use new sets of relative labels to the reference corner $(\Delta_i, \Delta_j) = (i - M_k, j - L_{k-1})$. In this way the square root factors from before read

$$\left(1 + \frac{i-j}{N}\right)^{1/2} \to \left(1 + \frac{M_k - L_{k-1}}{N} + \frac{\Delta_i - \Delta_j}{N}\right)^{1/2} \simeq \left(1 + \frac{M_k - L_{k-1}}{N}\right)^{1/2} \tag{5.46}$$

in the limit where N is large and the Δ_i, Δ_j are of order one.

When we add a skew hook with s boxes to a Young diagram that belongs $\mathcal{H}_{(M_k+1,L_{k-1}+1)}$, we would associate the factor

$$\left(1 + \frac{M_k - L_{k-1}}{N}\right)^{s/2} \tag{5.47}$$

and we need to identify this with an action as we would have in equation (5.39). The correct identification to have a match is that

$$r_k = \left(1 + \frac{M_k - L_{k-1}}{N}\right)^{1/2} \tag{5.48}$$

With this, we find that

$$r_k^2 = 1 + \frac{M_k - L_{k-1}}{N} \tag{5.49}$$

so that the M_k, L_{k-1} are clearly geometric. To have r_k of order one, we need M_k, L_{k-1} to be of order N. For convenience, we add $L_0 = 0$ so that the uppermost corner can be treated uniformly with the others. This is very similar to equations obtained in

[111] (which generalize previous results in [131]), where it was argued that one needs to replace N by an effective N to account for anomalous dimension computations for giant magnon states. The techniques used in those papers use the technology of restricted Schur polynomials, rather than the skew hook representation of the actions of traces.

The idea now is that to each such corner we will assign a set of variables $t_{k,\ell} := t_{M_k,L_{k-1},\ell}$ labeled by an integer ℓ, such that they act as traces in the small Young tableaux alone. That is, we write is as follows

$$\langle \hat{Y}_k + h| \, t_{k,n} \, |\hat{Y}_k\rangle = (-1)^{H(h)}\delta_{|h|,n} \tag{5.50}$$

where Y_k is the small Young tableaux in the corner.

Now we need to do something similar with the convex corners. The beginning setup is the same, starting at the (M_k, L_k) corner but now we are substracting boxes. The relative coordinates will now be given by

$$(\Delta_i, \Delta_j) = (L_k - j, M_k - i) \tag{5.51}$$

so that they are both positive. Notice that we have switched the i, j labels in the definition of the left. With this convention we get that the corresponding square root factor is still of the form

$$\left(1 + \frac{i-j}{N}\right)^{1/2} = \left(1 + \frac{M_k - L_k}{N} + \frac{\Delta_i - \Delta_j}{N}\right)^{1/2} \underset{N\to\infty}{\longrightarrow} \left(1 + \frac{M_k - L_k}{N}\right)^{1/2} \tag{5.52}$$

where both Δ_i and Δ_j appear with the same sign as before. Notice that Δ_i increases as

we go up the diagram, and Δ_j increases as we go to the left. This way we find that

$$\tilde{r}_k^2 = 1 + \frac{M_k - L_k}{N} \tag{5.53}$$

What this means is that the vertical direction in the $-$ tableaux should be thought of in a similar way to the horizontal direction in a $+$ tableaux, and similarly the horizontal direction in the $-$ tableaux should be thought of as the vertical direction in a $+$ tableaux. That is, the conventions for the tableaux are reflected. We now want to introduce $\tilde{t}_{k,\ell}$ variables that act only in convex corners. To get an equation that works as (5.50), we need to modify it to look as follows

$$\langle \hat{Y}_{\tilde{k}} + h| \, \tilde{t}_{k,n} \, |\hat{Y}_{\tilde{k}}\rangle = (-1)^{W(h)} \delta_{|h|,n} \tag{5.54}$$

where instead of measuring the height of the skew hook, we measure the width of the skew hook in the $-$ boxes. For hooks with an odd number of boxes, the vertical and horizontal parity coincide. Whereas for skew hooks with an even number of boxes, they are opposite. This means that relative to the usual conventions, we have set up $\tilde{t}_\ell$ to act as $-t_\ell$ for ℓ even. It is more convenient to have $\tilde{t}_\ell$ to have a uniform negative sign in all actions. This is done by changing signs in the definition of $Y_{\tilde{k}} \to (-1)^{\#\text{boxes}} Y_{\tilde{k}}$. That way both even and odd $\tilde{t}_{k,\ell}$ act with a minus sign relative to the usual convention.

We can now ask how t_ℓ acts on a state in the code subspace. It is straightforward to show that in general we can write

$$t_\ell \simeq \sum_k \left(r_k^\ell \, t_{k,\ell} - \tilde{r}_k^\ell \, \tilde{t}_{k,\ell}^\dagger \right) \tag{5.55}$$

which is an equation that seems identical to equation (5.39). The minus sign for the $\tilde{t}$

variables is the minus sign that we just introduced. This is part of the definition of how the $\tilde{Y}$ diagrams should be understood.

Because the different $t_k, \tilde{t}_k$ act on different subfactors of $\mathcal{H}_{\text{code}}$, they automatically commute. Moreover, they also commute with each other's adjoints. The only non trivial commutation relations are between t_k and their own adjoint, or between $\tilde{t}_k$ and their adjoints. To get a good match we need to show that the $t_k, \tilde{t}_k$ variables should have canonical commutation relations. This was proven in our previous work [38] for tableaux without restrictions. Since the tableaux are restricted in size, this cannot be true for general states. After all, the representation of a harmonic oscillator algebra is always infinite. This is the first formal cutoff we encounter. The commutation relations that we need

$$[t^\dagger_{k,\ell}, t_{k,m}] = \ell\, \delta_{\ell,m} \tag{5.56}$$

should be valid inside the factor of the code subspace, but *only when sandwiched between states in the code subspace*. If the $t_{k,\ell}$ take us out of the code subspace, then we need to define their action. The bounds are implicit in that the small tableaux have small sizes, and the definition of their limits is still to be determined more carefully. Here we see that the language of the code subspace is helping us to understand that the commutation relations we need are valid in a restricted subspace of the Hilbert space, and they can be arbitrary outside. The language of these relations automatically assumes that we are inside the code subspace. This is also the way the code subspaces do their work in [122].

Now, by construction we have that multiplication by the $t_{k,\ell}, \tilde{t}_{k,\ell}$ act as raising operators in the small factors. Since t_ℓ adds boxes and $\tilde{t}_{k,\ell}$ substracts them, $\tilde{t}_\ell$ is more similar to $t^\dagger_\ell$. That is why we need to write the equation (5.55) with daggered operators for the $\tilde{t}$ variables.

For convenience, since multiplying by $t_{k,\ell}$ is like a raising operator and their adjoint is like a lowering operator, we will rewrite the equation in a more standard Fock space language. We do this by stating that

$$t_{k,\ell} \rightarrow b^\dagger_{k,\ell} \tag{5.57}$$

$$\tilde{t}_{k,\ell} \rightarrow c^\dagger_{k,\ell} \tag{5.58}$$

$$t^\dagger_{k,\ell} \rightarrow b_{k,\ell} \tag{5.59}$$

$$\tilde{t}^\dagger_{k,\ell} \rightarrow c_{k,\ell} \tag{5.60}$$

These identifications are valid inside the code subspace. The b, c oscillators have canonical commutation relations. The action of $t_{k,\ell}$ becomes

$$t_\ell = \sum_k \Big(r^\ell_k b^\dagger_{k,\ell} - \tilde{r}^\ell_k c_{k,\ell} + O(1/N) \Big) \tag{5.61}$$

and we ignore the $1/N$ corrections when we match to supergravity. Now it is clear that (5.61) is identical in form to (5.39). Where the field modes have canonical commutation relations, just like the supergravity modes do. This implements the requirements of equation (5.39) exactly. That is, the code subspace in the Young tableaux basis can be put into correspondence exactly with the code subspace in supergravity.

Moreover, we have seen that there is an implicit cutoff on the size of the small tableaux. This is not immediately apparent in the supergravity construction where one is formally taking the limit $N \rightarrow \infty$ first. To argue for the cutoffs, one needs to follow [71] and argue that a type of stringy exclusion principle (similar to [86]) is responsible for a cutoff on the number of modes and their amplitudes. To proceed further, we need to understand the implicit cutoffs explicitly and explore the physics that is *beyond classical*

supergravity.

5.6 Cutoff physics in the Young tableaux formalism

The first step in the process of understanding the cutoff is to describe when the linearization implied by equation (5.55) is correct. In essence, we want to understand how when multiplying by t_ℓ, the subleading terms in N in the expression (5.46) or (5.52) accumulate when we vary ℓ and take ℓ large. This limit will give us a UV cutoff on the effective modes beyond which non-linearities matter.

The idea is that the products on each skew hook will be of the form

$$|\langle \hat{Y}_k + h| \, t_\ell \, |\hat{Y}_k\rangle| = \prod_{k=\alpha+1}^{\alpha+\ell} \left(r_m^2 + k/N\right)^{1/2} = r_m^\ell \exp(\sum_k \log(1 + k/(N r_m^2))) \tag{5.62}$$

and we will look at cases where r_m is of order 1 and $k << N$. The term in the exponential can be further approximated by

$$\sum_k k/(N r_m^2)) = O(\ell^2/(N r_m^2)) \tag{5.63}$$

We want these corrections to be small for each skew hook, which means that we want in general $\ell^2/(N r_m^2) << 1$. That means that we should have the label ℓ scaling at most as $\ell < \epsilon N^{1/2}$ where ϵ is a small number (this is the same scaling that is observed in studies of the BMN string [120], that ends up being a special case of the LLM geometries: the vacuum geometry). For us it is a choice that tells us how big of an error we should allow. A similar (slightly weaker) limit is obtained from three point functions [132] (see also [133] and references therein for earlier work on the exact three point functions).

That is, the code subspaces associated with the corners have a bound on the size of

skew hooks. We also want the bound to apply to excited states, so all the Δ_i and Δ_j should also fit in this bound. In essence, the allowed Young tableaux on each corner is essentially a tableaux that fits in a square of order $\sqrt{N} \times \sqrt{N}$ around each corner. If the L_i, M_i are well separated from each other, the different tableaux on each corner cannot interfere with each other, because the horizontal or vertical difference between the corners is of order N. Since such a small tableaux has energy that is equal to the number of boxes in the tableaux, this means that the excitation energy above (below) the reference state is bounded and of order at most N. This is subleading in the supergravity description, because the energy of the supergravity solutions is of order N^2, but it is also a typical energy of a single giant graviton whose scale is of order the AdS radius. This limit where the linear structure starts breaking down is due to $1/N$ corrections given by interactions of the local string excitations (as perceived by the extrapolate dictionary).

Remember that the Planck scale quanta are associated to energies of order $N^{1/4}$. An energy of order $N^{1/2}$ is roughly the energy of a Planck sized object that has been boosted by an ultra-relativistic factor of $\gamma \simeq N^{1/4}$. This means that the physics of these modes does not break down at the Planck scale, but at much higher energies and the notion of (local) Lorentz invariance for single particle states should be well respected at energies of order the Planck scale itself. Since the total size of the circle associated with the edge of the droplet is of order $N^{1/4} l_P$, the Lorentz contraction obtained from a boost of $N^{1/4}$ gives an effective circle of size ℓ_P (similar boost arguments have been used to describe matrix black holes [134]). In essence, the physics is breaking down when for a boosted object at the Planck scale, the Lorentz contracted circle on which it is moving is of order the Planck length.

Our description of the cutoff is that the allowed Young tableaux need to fit inside a square of size $w_i \times w_i$ where each w_i scales as $N^{1/2}$. We can restrict the action of the

b, c modes so that if a skew hook falls outside these squares we get zero. This would modify the canonical commutation relations between these modes only for tableaux that are nearly filling the allowed squares. Also, the restriction in depth is similar to the restriction that representations for $SU(M)$ vanish if their associated Young tableaux have a column of length larger than or equal to M. This restriction makes traces of length larger than or equal to M dependent non-linearly on the smaller traces (these are the Mandelstam relations and they are closely related to the Cayley Hamilton relation, see for example [135]). The additional b, c modes become (non-linearly) redundant when we hit this bound. The maximal bound on ℓ for each of the b, c modes is fixed by the size of the square regions, and all small Young tableaux states can be generated from the action of b, c, modes with these cutoffs (as long as we act by zero when we get out of the confining boxes).

5.7 Uncertainty and entropy

In our previous work [38] we argued that in the strict $N \to \infty$ case one could calculate the topology of LLM geometries by measuring the uncertainty and the entropy of the mode expansion for the t_ℓ actions on the corresponding Young tableaux state. Our purpose now is to understand how the answer changes when we take N finite, or more precisely, when we take N to be very large and the L, M scale with N. In this way, we can take equation (5.39) or equivalently (5.61) and compute the uncertainties for the actions by traces. The result is very simple, by using Wick's theorem in the b, c oscillators (this is the original technique we used in [40], with the understanding that the tails of distributions contribute a very small amount). This is combinatorially equivalent to

computing directly with the Young tableaux [38, 127], and we get the following answers

$$\langle t_s^\dagger t_m \rangle_\Omega = s\delta_{sm} \sum_i r_i^{2m} \equiv s\delta_{sm} S_m \tag{5.64}$$

$$\langle t_m t_s^\dagger \rangle_\Omega = s\delta_{sm} \sum_i \tilde{r}_i^{2m} \equiv s\delta_{sm} \tilde{S}_m \tag{5.65}$$

for the reference state $|\Omega\rangle$, where we have defined the quantities $S_m, \tilde{S}_m$ on the right hand side as the result of the computations.

For the previous case studied by us, the answers are given by specializing to $r_i = \tilde{r}_i = 1$ for all i, in which case we would immediately get the number of edges and anti edges by computing these expectation values.

What we see in this case is that now the answer on the right hand side is geometric. We get an algebraic sum of the powers of the r_i, or the powers of the $\tilde{r}_i$. These are symmetric functions of the r_i or the $\tilde{r}_i$ respectively. If there is a finite number of these given by $N_{\text{edges}}, N_{\text{anti-edges}}$, we will find that there are algebraic relations between them. The first order for a non-trivial relation will be exactly when we have enough variables on the left hand side above to be able to compute the r_i by solving for the roots of a polynomial. To obtain the coefficients A_i of the polynomial equation from the S_m, one uses Newton's equations given as follows

$$A_1 + S_1 = 0 \tag{5.66}$$

$$2A_2 + S_1 A_1 + S_2 = 0 \tag{5.67}$$

$$\vdots \tag{5.68}$$

$$nA_n + S_1 A_{N-1} + \cdots + S_{N-1} A_1 + S_n = 0 \tag{5.69}$$

Once we pass the point where we have saturated the number of the different r_i, the

corresponding A_n will vanish: the rest of the putative $r_i, \tilde{r}_i$ would vanish [3].

In this sense, it is possible to get the topology for a concentric LLM geometry. One can follow a similar argument for coherent states of the b, c oscillators, only as long as the notion of coherent states fits nicely within the cutoffs of the code subspace that were discussed in the previous section. In this sense, the deformations away from circularity of the droplets are of subleading order in N. The easiest way to see this is that a classical shape deformation should typically cost an energy of order N^2, but the cutoff windows we have discussed only allows for changes in energy of order N.

Going a little bit further in comparison to our previous work, we notice that as long as we ignore the cutoffs, we can think of $t_\ell \propto a_\ell^\dagger$ and $t_\ell^\dagger \propto a$ as raising and lowering operators themselves. To go from the b, c oscillators to the a oscillators we are writing a partial Bogolubov transformation (we have less a's than b and c combined).

An important question is what is the normalization of the oscillators. This can be used to compute the expectation value of the number operators. This can be done by computing the commutator as follows

$$\langle [t_\ell^\dagger, t_\ell] \rangle_\Omega = \ell \sum_i r_i^{2\ell} - \ell \sum_i \tilde{r}_i^{2\ell} = \ell(S_\ell - \tilde{S}_\ell) = \hbar_{eff} \tag{5.70}$$

and on the right hand side we identify this with an effective $\hbar$ in the commutation relation. The expectation value of the number operator evaluated on the reference state $|\Omega\rangle$, which defines our vacuum, is then

$$n_\ell = \langle \hat{N}_\ell \rangle_\Omega = \frac{\langle t_\ell t_\ell^\dagger \rangle_\Omega}{\hbar_{eff}} = \frac{\langle a^\dagger a \rangle_\Omega}{[a, a^\dagger]} = \frac{\tilde{S}_\ell}{S_\ell - \tilde{S}_\ell} \tag{5.71}$$

[3]The S_i are also Schur polynomials related to the totally antisymmetric representation for a matrix with eigenvalues r_i or $\tilde{r}_i$.

Similarly we have that

$$n_\ell + 1 = \langle \hat{N}_\ell + 1 \rangle_\Omega = \frac{S_\ell}{S_\ell - \tilde{S}_\ell} \tag{5.72}$$

From these expectation values we can assign an entropy to the linear mode a_ℓ. This is the entanglement entropy of the mode a in the vacuum Ω, and since the vacuum is obtained by a partial Bogolubov transformation, we get that the reduced density matrix for the modes $a, a^\dagger$ look thermal (they are a Gaussian state). This entropy is given by

$$s_\ell = (n_\ell + 1)\log(n_\ell + 1) - n_\ell \log(n_\ell) \tag{5.73}$$

which is again dependent on the geometric radii $r_i, \tilde{r}_i$.

The meaning of this entropy is clear in the $N \to \infty$ limit where we are analyzing an effective field theory, but at finite N it is more problematic because of all the cutoffs. The main problem is that the Hilbert space itself does not factorize. We want to use this number as an entropy also at finite N, so we need a way to interpret it as an entropy.

One way to think about this entropy is that since the modes $a, a^\dagger$ act simply on the code subspace, they should induce an (approximate) factorization in the code subspace itself, but not the full Hilbert space. Indeed, these modes commute with the other modes so long as one is close to the reference state. What we can do now is to assign an entropy to an algebra $\mathcal{A}$ acting on the reference state Ω. The idea is that we need to produce a representation of the algebra by acting on Ω with the elements of the algebra, as follows $\mathcal{H}_\mathcal{A} \simeq Span\{\mathcal{O}\Omega\}$, where the $\mathcal{O} \in \mathcal{A}$. This is what gets around having a factorization of the full Hilbert space.

If we think of the state Ω as a general state for $\mathcal{A}$, we would get that $\Omega = \sum |n\rangle |\tilde{n}\rangle$ where the label n runs over all possible states in the representation of $\mathcal{A}$ and $\mathcal{A}$ does not act on $\tilde{n}$ (here neither n nor $\tilde{n}$ are normalized nor orthogonal). If we have a factorization

of the algebra in the algebraic sense, the $|\tilde{n}\rangle$ would be a representation of the commutant of $\mathcal{A}$ in the algebra of operators in the full Hilbert space.

This procedure induces a reduced density matrix for the $\mathcal{A}$ factor such that all the expectation values for $\mathcal{A}$ are reproduced

$$\mathrm{tr}(\rho_{\mathcal{A}}\mathcal{O}) = \langle\Omega|\,\mathcal{O}\,|\Omega\rangle \tag{5.74}$$

and we can associate the entropy s_ℓ with this density matrix. For example, if $\mathcal{A}$ is the algebra of a spin 1/2 representation at one site in a spin chain (the set of Pauli matrices) , this density matrix would coincide with the reduced density matrix for the set of states on that site.

If the algebra $\mathcal{A}$ acts in such a way that no element of the algebra annihilates the state, there is a second copy of $\mathcal{A}$, $\mathcal{A}^*$ that acts on $\mathcal{H}_{\mathcal{A}}$ and commutes with $\mathcal{A}$. This second copy can be thought of as the thermal double of $\mathcal{A}$ (this is the Tomita-Takesaki theory, as discussed in [126]). Roughly speaking, the state will look as follows

$$\sum_n \zeta_n\,|n\rangle\,|\tilde{n}\rangle \tag{5.75}$$

where the ζ_n are a collection of numbers and the $|n\rangle$ enumerate the possible states for the algebra $\mathcal{A}$ that diagonalize the density matrix, while the $|\tilde{n}\rangle$ would be the representation of the elements of the double copy. If we have an infinite algebra like the Weyl algebra of the harmonic opscillator and its unique infinite dimensional unitary representation, we might fall outside the code subspace where our analysis is valid. To avoid the infinite size representation and to fit the algebra inside the code subspace, we just need to truncate to states whose occupation number is bellow a cutoff induced by the code subspaces themselves. For us, the associated density matrix we need is diagonal in the oscillator

basis (this is because $\langle a^2 \rangle = \langle (a^\dagger)^2 \rangle = 0$ and of the fact that the state is Gaussian), so we truncate it

$$\rho \simeq \sum_{n<n_{max}} |\zeta_n|^2 |n\rangle \langle n| \tag{5.76}$$

If we had a more complicated state this might not be possible. To reiterate, we are trying to show how a notion of entropy fits the number in (5.73) at finite N and in the presence of cutoffs. For the states at hand, as long as the $\zeta_n \to 0$ sufficiently fast (which is usually true in an approximately thermal state), if the algebra is truncated or not becomes a moot point: the entropy is going to be dominated by the ζ_n where n is small anyhow.

In the case above, we think of the representation space of $\mathcal{A}^*$ as a purification of ρ, so the $\mathcal{A}^*$ should be associated to the purification inside Ω for the generators of the oscillator algebra $a, a^\dagger$. Because we have a partial Bogolubov transformation, we can compute this purification directly in terms of modes of the effective oscillators, rather than abstractly.

The idea is as follows. Consider the two effective oscillators given by

$$B_n^\dagger = \frac{1}{\sqrt{S_n}} \sum r_i^n b_n^{(i)\dagger} \tag{5.77}$$

$$C_n^\dagger = \frac{1}{\sqrt{\tilde{S}_n}} \sum \tilde{r}_i^n c_n^{(i)\dagger} \tag{5.78}$$

It is easy to check that these oscillators are normalized, and that the state $|\Omega\rangle$ is the ground state for the B, C oscillators. From these oscillators it follows that

$$t_n = \sqrt{S_n} B_n^\dagger - \sqrt{\tilde{S}_n} C_n \tag{5.79}$$

and now it looks like part of a Bogolubov transformation between only two modes.

Normalizing the mode of the left hand side, which we will call $a_n^\dagger$, we need to take

$$a_n^\dagger := \frac{t_n}{\sqrt{\hbar_{eff}}} = \frac{1}{\sqrt{S_n - \tilde{S}_n}}(\sqrt{S_n}B_n^\dagger - \sqrt{\tilde{S}_n}C_n) = \cosh(\gamma_n)B_n^\dagger - \sinh(\gamma_n)C_n \tag{5.80}$$

and similarly for its adjoint. The mode $a_n^\dagger$ is entangled with the mode

$$d_n^\dagger = \cosh(\gamma_n)C_n^\dagger - \sinh(\gamma_n)B_n \tag{5.81}$$

that acts as the purification of the a_n mode. Indeed, the B, C oscillators can be recovered from a, d, and the ground state is a pure state of the B, C modes. It is easy to check that the state $|\Omega\rangle$ in the a, d basis is a squeezed state between the the a, d modes. When tracing over d we get a thermal density matrix for a, whose entropy is determined by the expectation value of the number operator: it maximizes the entropy given the constraint.

What is important for us is that the modes B, C for moderately large n are concentrated on the outermost edge of the concentric circle configuration, and the outermost anti-edge. That is, most of the weight of the B, C oscillators is concentrated on the modes at r_1 and $\tilde{r}_1$ respectively $b^{(1)}, c^{(1)}$. The amplitudes for the other modes are exponentially suppressed in n. What this means is that for generic modes, the extrapolate dictionary can not penetrate beyond the geometric locus characterized by $\tilde{r}_1$. By the Tomita -Takesaki analysis of [126], we can generate the states $|n\rangle_a |m\rangle_d$ from the state $|\Omega\rangle$ by acting with a alone. In practice, this means we can recover the algebra of the d modes with an ensemble by having the reference ground state.

Notice that the extrapolate dictionary seems to stop exactly at the outermost anti-edge. This was also suggested by the work of [128], which argued that there was an entanglement shadow in these geometries (a region where extremal Ryu-Takayanagi surfaces [79] can not penetrate) and that the extremal surface that can enter the deepest

stops exactly at this place.

In practice what this means is that the information inside the region of the outermost anti-edge is inaccessible. One can equally say that it is protected from quantum errors generated by acting with the extrapolate dictionary. This information is encoded in the modes b, c that are orthogonal to B, C.

Overall, the finite N picture is similar to what we found before in [38, 40]. The topology can be deduced from the uncertainties, although the procedure is more complicated. Also the entropy of the extrapolate dictionary modes is maximal given those uncertainties. Similar arguments can be used when we shift the reference ground state to a coherent state of the b, c modes that fits comfortably inside the code subspace.

5.8 Obstructions to having a globally well defined quantum metric

So far, we have found ourselves with a cutoff that is of order $\sqrt{N}$ on the modes, and we have assumed that the spacing between the radii is of order one. From the point of view of Young tableaux, this is a situation where the lengths of the horizontal or vertical edges of the reference state are of order N. Our goal now is to push ourselves to a situation where we make some of these edges small enough so that the cutoff of $\sqrt{N}$ is already too large. That is, we want to take $M_i - M_{i+1}$ or $L_i - L_{i+1}$ to be of order $\sqrt{N}$ themselves. The idea now is to understand to what extent it is possible for us to define a metric operator in these setups. We only need to analyze the simplest case, with

$L_1 \simeq \sqrt{N}$, as in (5.87), and we will call this reference state $|\Omega_1\rangle$.

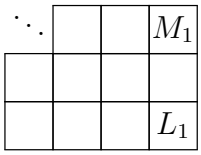

(5.82)

To analyze how one might get interference between the rows, we need to also analyze another reference state

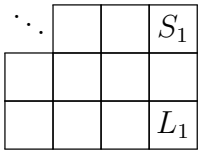

(5.83)

with $S_1 = M_1 + 1$. This reference state differs from the previous one by adding one column, and call this reference state $|\Omega_2\rangle$. The idea now is to look for a state that belongs to the code subspace generated from $|\Omega_1\rangle$ and $|\Omega_2\rangle$. The idea is to check if it is possible to find a globally defined metric that agrees between the two code subspaces as understood above in terms of building up perturbations relative to the reference state. The simplest such state is given by

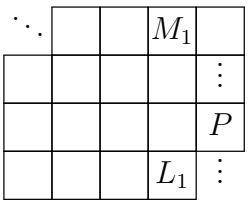

(5.84)

where we have a column of length P added to $|\Omega_1\rangle$ and that can be thought of as removing a column of length $L_1 - P$ to $|\Omega_2\rangle$.

The first state can be thought of as a superposition of states that have excitations around $|\Omega_1\rangle$ which are built from the $b^\dagger_{\Omega_1}$ modes. Such states are superpositions of excitations of the top edge $r_1|_{\Omega_1}$. Relative to the reference state $|\Omega_2\rangle$, they are instead built by superpositions of modes $c^\dagger_{\Omega_2}$, which originate in $\tilde{r}_1|_{\Omega_2}$. From the point of view

of the two different code subspaces, we attach the excitation to different edges. This assignment is not local: we cannot specify the edge uniquely in a way that is independent of the reference state. The answer depends on the choice of reference state. We can even do this with superpositions of states of this type that lead to coherent states (for example, in [38] it was understood that a particular generating series of these states is a coherent state). Such generating series are of the type

$$\sum_P \xi^P |P\rangle_{\Omega_1} \tag{5.85}$$

$$\sum_P \tilde{\xi}^{L_1-P} |L_1 - P\rangle_{\Omega_2} \tag{5.86}$$

where ξ is a complex number. In order to get the same state, we need that $\xi = 1/\tilde{\xi}$. In our previous work, the range for P was infinite, so convergence required that $|\xi| < 1$ and similarly for $\tilde{\xi}$, so naively only one such state can be a nice coherent state. In practice, because of the cutoffs, the superposed coherent state does not belong completely to either of the two code subspaces nor is it exactly a coherent state, but the state can have a large overlap with states that do belong to either code subspace. The condition for large overlap is that $|\xi| < 1$ or $|\tilde{\xi}| < 1$. However, the state at fixed P is a superposition of objects of either type. Indeed, these objects are D-branes (giant gravitons [71]) that can be thought of as having nucleated at one edge (and belonging to it) and being moved to the other edge. This is shown in figure 5.3. Indeed, one can define a third code subspace that is a strip geometry plus a D-brane. In one code subspace the state is an excitation of r_1, in a second code subspace, the state is an excitation of $\tilde{r}_1$ and in the third code subspace the state is a strip geometry plus a D-brane (this is interpreted as a state with a different topology than the other two).

Now, it is clear that there is no absolute boundary between these. The cutoffs are of

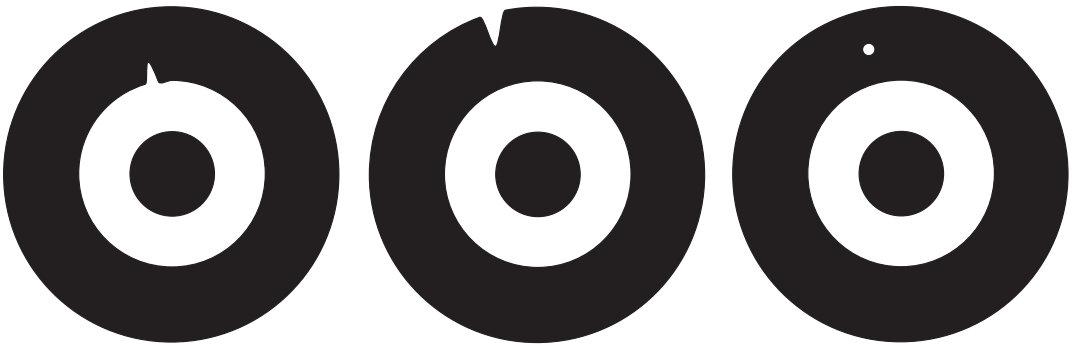

Figure 5.3: LLM diagrams of three (identical) states with D-brane excitations that can be thought of as having nucleated in different ways in different code subsapces, and this results on them being pictured differently.

order $\sqrt{N}$, but can be adjusted. What this means is that in practice $|\Omega_1\rangle$ and $|\Omega_2\rangle$ do not define a single code subspace. They define families of code subspaces that differ by the cutoffs. The state $|P\rangle_{\Omega_1}$ may or may not belong to either of these code subspaces.

Also notice that it gets more ambiguous when we try states of the form

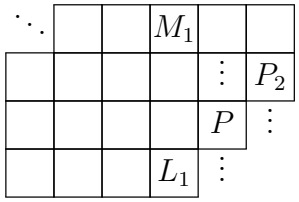

(5.87)

The first column is either an excitation of the b modes or the c modes depending on the code subspace, but the second column is an excitation of the b modes in both code subspaces. The only condition on the Young tableaux is that $P_2 \leq P$, but to belong to the different code subspaces, one needs to check that the cutoffs are not violated. We also find that there is a new code subspace $|\Omega_3\rangle$, with $S_2 = M_1 + 2$ where both of them would be assigned to excitations of $\tilde{r}_1|_{\Omega_3}$. We can keep on going this way so that the first w_1 columns are c excitations and the next one is a b excitation, versus all of them being b excitations. one also gets code subspaces with one, two, up to w_1 D-branes if one wants

to. This ambiguity makes it impossible to answer a question as to what is the metric as an operator that is independent of the choice of code subspace. Each code subspace has a different answer, and they are not compatible with each other.

In this case we can even say that the code subspaces with D-branes have different topology than the two original reference states. They also have a different spectrum of excitations: apart for the b, c modes they also have the moduli of the D-branes themselves (these can be thought of as the additional coordinates $\xi = \tilde{\xi}^{-1}$ when we separate the D-branes from the code subspaces).

If one states that the metric information is encoded in the state as a message, what we are seeing is that different code subspaces that share the same state decode different messages. It is intriguing to speculate that different messages (different notions of the metric) are all allowed in the same sense that stringy dualities allow for more than one interpretation of the geometry, but only one of them will be sufficiently classical. From what we have determined so far it is not yet clear that this is what is going on. So far we have done calculations in the absence of a concrete value for the string scale, relative to the Planck scale. To study the physics of the string scale would require studying modes that do not preserve as much supersymmetry. Such a problem is beyond the scope of the present paper.

One should be able to argue similarly for folded geometries. These geometries with folds are defined by stating that the number of $r, \tilde{r}$ variables is a function of the angle. The local supergravity analysis of the Poisson structure around each edge is the same [130], but one would have to define the mode expansions of the effective fields carefully. Different choices should be generically related by a linear transformation of the mode functions on each edge to a new set of functions. Such differences are accounted for by a Bogolubov transformation of the modes. There is no obvious preferred basis distinguished

by the energy of the modes, because the reference state is no longer an eigenstate of the Hamiltonian. Unfortunately the dual field theory analysis is much more complicated because the construction of the corresponding dual states is not combinatorial. Our previous work [40, 38] dealt with these geometries in a particular approximation, but this approximation was not deduced from first principles. Studying this problem is very interesting as it should provide further details. Such analysis is beyond the scope of the present paper.

5.9 Conclusion

In this paper, we draw parallels between effective field theory, especially within the framework of the LLM geometries, and the notion of holographic code subspaces. We found that the nearby Hilbert space of states around some classical background, which is built by acting on the reference state with some number of effective fields results in a space defined in the same way as the code subspace developed in [122]. It further matches the little Hilbert space of [108]. We give explicit examples of code subspaces in the case of the LLM geometries, where we use concentric ring configurations as our reference state. To analyze this, we go beyond the infinite N limit of our previous work. We show that the allowed effective fields are comprised of state dependent operators, insofar as analyzing the metric of a state depends on a choice of a code subspace in which to analyze it. Further, we find that there is not a clear line between different code subspaces, and, in fact, there are states that clearly belong to multiple such subspaces. This makes it ambiguous to write down a globally well defined metric operator, as the interpretation of how to obtain a metric depends on the reference state that one builds the code space from. We have argued that this obstruction is essentially what forces us

to state that it is only possible to interpret physics in an effective field theory of gravity within the framework of code subspaces. If one thinks of the geometry of a quantum state as a quantum message, different code subspaces decode different messages from the same state.

A note of caution should be in order. Our results do not preclude having a globally well defined quantum metric, as long as one is willing to abandon the setup we have devised: the collection of reference states with perturbative semiclassical excitations on them. These are constructed in a way that guarantees that effective field theory works, as long as one is restricted to the code subspaces. Such a different setup could be in conflict with effective field theory instead.

In this paper we dealt essentially exclusively with concentric ring LLM geometries. This is because the dual field theory states are well understood as combinatorial objects. In principle, a similar answer can be obtained for more general geometries, which can include folds (these are dealt in an approximate way in [38]). These geometries with folds are characterized by the fact that the number of $r, \tilde{r}$ variables is a function of the angle. The supergravity analysis is more complicated because the modes necessarily mix in the extrapolate dictionary, and the cutoffs might depend non-trivially in the angle. These are interesting avenues of future research that can not be treated with the Young diagram technique. To address these, one should understand the cutoffs directly in the supergravity description.

Another setup that is interesting is to deal with the superstar ensemble (as in [91]), which has properties more similar to a black hole. A big question here is to what extent we can use information the uncertainty and entropy in the extrapolate dictionary to make statements about geometry. This is currently under research [136].

So far, all this work has been done for half BPS geometries. It would be very in-

teresting to extend these ideas further to geometries that have less supersymmetry, or to excitations around such half BPS configurations that have less supersymmetry. Such excitations could give additional insight into the more general structure of code subspaces and the corresponding cutoffs. Some of these can even be stringy states.

Chapter 6

Conclusions and Future Directions

In a full theory of quantum gravity, what are the *good* observables? For instance, can one represent the metric by a quantum operator? If not, should we think of it as a *good* observable? What other objects might we consider instead? These are the types of questions that have driven my research, with my primary goal being to help contribute to the search for a complete theory of quantum gravity. My favorite tool comes from the AdS/CFT correspondence [3]. As I would like to learn about quantum gravity, my work has primarily been to perform calculations on the field theory side and see what lessons we can learn about quantum gravity. I am also interested in helping to further develop the duality itself, as we are still far from understanding the full dictionary. Therefore, I enjoy analyzing questions about, for instance, which CFTs have a gravity dual and vice versa or how much information is necessary from the boundary theory to determine the bulk geometry, at least to a good approximation. To address these questions, the work contained in this thesis was dealing with two different systems: Perturbed Conformal Theories and LLM Geometries. In the future, I intend to both continue working in these directions, as well as analyzing new avenues for advancing our knowledge. I have broken

my concluding remarks into two sections, one for each part of the thesis. In each section, I briefly review some of our findings, as well as touch on ideas for future work.

6.1 Conformal Perturbation Theory

Part I of this thesis contained my work on conformal perturbation theory (CPT), starting with an unspecified conformal theory in an arbitrary number of spacetime dimensions and perturbing it by a scalar operator with arbitrary scaling dimension. There, we were able to compute universal results, such as in chapter 2 [35], where we computed the first order correction to the one point function. This quantity initially had both UV and IR divergences. We were able to provide an IR regulator by putting the CFT on a cylinder and saw that the remaining UV divergences were logarithmic and had the same form as the standard ones seen in dimensional regularization. We further showed that this matched the dual calculation on the AdS side, providing a piece of support to the conjecture. We also considered a time dependent set-up, where we quenched from the perturbed to the unperturbed theory and calculated the energy after the quench, which ultimately depended on the correction to the one point function, showing that it is also universal. This supported and further explained the work [43, 50].

In chapter 3 [36], we pushed this work further. Corrections to correlation functions in CPT all have a form similar to the standard Feynman integrals found in QFT. By including various functions in the integrals, can make them more convergent and make progress. Different functions will, of course, have different physical interpretations. One, as seen in the earlier work, comes from transforming the two point function to its form on a cylinder. In this work, we consider the Fourier transform of the two point function and the correction to the two point function where the perturbation has a $1/|x^\alpha|$ scaling

profile. We also look at the first order correction to the three point function, which takes a similar form to the second order correction to the two point function. Again, all of these results were universal. Finally, we found that for time dependent perturbations on the cylinder, there are resonances matching those that would be expected in time dependent perturbation theory.

We are currently pushing this work in a couple different directions. On one path, we are attempting to compute and interpret scattering states in AdS in terms of their field theory dual, using CPT. We are looking at, for instance, the amplitudes for such a process to occur. I am also analyzing how working in Mellin space might help with our computations. Beyond these specific calculations, I am interested in seeing more generally what progress can be made in discovering new quantum field theories by perturbing away from a conformal theory. This has the potential to carving out new regions in the space of all possible QFTs. One might, for instance, wonder if there are more non-Lagrangian QFTs out there (like the (2,0) superconformal theory in six dimensions, which currently has no know Lagrangian description).

6.2 Half BPS States

Examples of gauge/gravity dualities where we currently understand both sides well are few. One of these comes from considering the set of half BPS states of $\mathcal{N} = 4$ SYM. These are useful because the extra symmetry allows us to perform highly controlled computations on both sides. Lin, Lunin, and Maldacena classified the set of non-singular supergravity duals to these, the LLM geometries [63]. In chapters 6 and 7 [38, 40], D. Berenstein and I worked in the infinite N limit of this system, where the field theory can be described by a free chiral boson in 1+1 dimensions, which can simply represented

by an infinite set of harmonic oscillators. We built extensive technology to analyze this system, which we then used to ask questions about quantum gravity. One of our most interesting findings was that there cannot exist a topology measuring operator for these states, which leads one to doubt the existence of one in quantum gravity more generally. Fortunately, we were able to show that one can extract the topology for a certain class of states via entanglement and uncertainty computations. This advances the idea that there is an intimate relationship between geometry and entanglement [79, 137, 72, 78]. As previously stated, this was all in the infinite N limit, where there exists a canonical factorization, which made computing the entropies straightforward.

In chapter 8 [39], we made some progress beyond the infinite N case, showing that one can still extract topological information from uncertainty and entanglement computations. There, we also clarified some peculiarities of this system in terms of the language of quantum information. Using effective field theory methods, we considered classes of states formed by acting on topologically distinct reference states with small energy excitations. This way of building states looks precisely the same as the code subspaces built by Almheiri, Dong, and Harlow in [122]. There, they considered building a code subspace by acting low energy fields on the ground state, whereas we considered many code subspaces, each formed by acting on a reference state with low energy fields. We found that many physical questions (for instance, about the topology) could only be asked within a particular subspace, as one might find differing answers in the full Hilbert space. In this way, one needs to consider the code subspaces in order for the dictionary to work unambiguously. This state dependence is reminiscent of that found by Papadodimas and Raju [126, 108]. Currently, I am working to make further progress beyond leading order, looking at, for instance, the first non-zero contribution to the three point functions to see what we can learn.

In chapter 5 [37], we asked questions about the duality itself. We analyzed whether one can reconstruct the bulk using only classical boundary data (specifically, only expectation values), again for LLM geometries. We found that this is ambiguous, as one set of classical boundary data corresponds to many bulk geometries and one can only distinguish between these with access to more information. This went against what was previously thought about bulk reconstruction.

Finally, I have more recently been thinking about a different class of half BPS states. The LLM geometries that we have been considering thus far are non-singular, but there also exist half BPS states of $\mathcal{N} = 4$ SYM that are dual to singular geometries. These can further by separated into those with and without closed timelike curves. Happily, the former were found to be dual to non-unitary states in the CFT [116]. It would be interesting to further explore, within these dualities, physically bad states are always dual to other physically bad states or not. And, further, if this is something we want or need out of our duality.

A subset of the singular geometries without closed timelike curves form the superstar geometries [138, 91]. These have naked singularities, but are near horizon forming. While there has previously been some work on these states, there is still a lot we have to learn. For instance, to what extent can we think of these as black hole solutions? And, how deep into the bulk can we probe them with currently understood methods?

Appendix A

Integral with three centers

We compute the integral given by

$$I[\overrightarrow{\omega}, \alpha_1, \alpha_2, \alpha_3, d] = \int d^d x \frac{1}{|x-\omega_1|^{2\alpha_1}|x-\omega_2|^{2\alpha_2}|x-\omega_3|^{2\alpha_3}} \tag{A.1}$$

This integral was originally studied in [139], where the answer is given in terms of an Appell Function, see also [55]. We follow instead the treatment of [56], which expresses the final answer in terms of an integral of modified Bessel functions.

We will introduce a Schwinger parameter for each term in the denominator. This gives

$$= \int d^d x \int_0^\infty \frac{ds_1\, ds_2\, ds_3\, s_1^{\alpha_1-1}\, s_2^{\alpha_2-1}\, s_3^{\alpha_3-1}}{\Gamma[\alpha_1]\,\Gamma[\alpha_2]\,\Gamma[\alpha_3]} \exp\left(-s_1|x-\omega_1|^2 - s_2|x-\omega_2|^2 - s_3|x-\omega_3|^2\right) \tag{A.2}$$

Completing the square in the exponential gives

$$= \int d^d x' \int_0^\infty \frac{ds_1\, ds_2\, ds_3\, s_1^{\alpha_1-1}\, s_2^{\alpha_2-1}\, s_3^{\alpha_3-1}}{\Gamma[\alpha_1]\,\Gamma[\alpha_2]\,\Gamma[\alpha_3]} \times \exp\left(-s_t\left[(x')^2 - \frac{(s_1\omega_1 + s_2\omega_2 + s_3\omega_3)^2}{s_t^2} + \frac{(s_1\omega_1^2 + s_2\omega_2^2 + s_3\omega_3^2)}{s_t}\right]\right) \quad \text{(A.3)}$$

where $x' = x - \frac{(s_1\omega_1+s_2\omega_2+s_3\omega_3)}{s_t}$ and $s_t = s_1 + s_2 + s_3$. We can now easily perform the integral over x' because it is gaussian. This all gives

$$I = \pi^{d/2} \int_0^\infty \frac{ds_1\, ds_2\, ds_3\, s_1^{\alpha_1-1}\, s_2^{\alpha_2-1}\, s_3^{\alpha_3-1}}{\Gamma[\alpha_1]\,\Gamma[\alpha_2]\,\Gamma[\alpha_3]\, s_t^{d/2}} \exp\left[\frac{(s_1\omega_1 + s_2\omega_2 + s_3\omega_3)^2}{s_t} - \left(s_1\omega_1^2 + s_2\omega_2^2 + s_3\omega_3^2\right)\right] \quad \text{(A.4)}$$

We can simplify the exponential, leaving

$$I = \pi^{d/2} \int_0^\infty \frac{ds_1\, ds_2\, ds_3\, s_1^{\alpha_1-1}\, s_2^{\alpha_2-1}\, s_3^{\alpha_3-1}}{\Gamma[\alpha_1]\,\Gamma[\alpha_2]\,\Gamma[\alpha_3]\, s_t^{d/2}} \exp\left[-\frac{s_1 s_2 \omega_{12}^2 + s_2 s_3 \omega_{23}^2 + s_3 s_1 \omega_{31}^2}{s_t}\right] \quad \text{(A.5)}$$

Now introduce a change of variables

$$s_j = \frac{V}{2v_j} = \frac{v_1 v_2 + v_2 v_3 + v_3 v_2}{2v_j} \quad \text{(A.6)}$$

These result from finding a change of variables such that $s_1 s_2 s_3/(s_t s_i) \propto v_i$, and the factor of two is the same convention as in the appendix in [56].

The measure will change as $ds_1 ds_2 ds_3 = \frac{V^3}{8v_1^2 v_2^2 v_3^2} dv_1 dv_2 dv_3$. Our integral now takes the form

$$= \pi^{d/2} \int_0^\infty \frac{V^3}{8\Gamma^3 v_1^2 v_2^2 v_3^2} \frac{dv_1 dv_2 dv_3}{\left[\frac{V}{2}(v_1^{-1}+v_2^{-1}+v_3^{-1})\right]^{d/2}} \prod_{j=1}^{3} \left(\frac{V}{2v_j}\right)^{\alpha_j - 1} \exp\left[-\frac{1}{2} v_j \Omega_j^2\right] \quad \text{(A.7)}$$

$$= \frac{\pi^{d/2}}{(2)^{\alpha_t - d/2}} \int_0^\infty \frac{1}{\Gamma^3} \frac{1}{\left(v_1^{-1}+v_2^{-1}+v_3^{-1}\right)^{d-\alpha_t}} \prod_{j=1}^{3} dv_j v_j^{\alpha_t - d/2 - \alpha_j - 1} \exp\left[-\frac{1}{2} v_j \Omega_j^2\right] \quad \text{(A.8)}$$

where $\Omega_1^2 = (\omega_2 - \omega_3)^2$, $\Omega_2^2 = (\omega_1 - \omega_3)^2$, and $\Omega_3^2 = (\omega_2 - \omega_1)^2$, and where we have used

$$V^{\alpha_t - d/2} = \frac{(v_1 v_2 v_3)^{\alpha_t - d/2}}{\left(v_1^{-1}+v_2^{-1}+v_3^{-1}\right)^{d/2-\alpha_t}} \quad \text{(A.9)}$$

we also have used the shorthand $\Gamma^3 = \Gamma[\alpha_1]\Gamma[\alpha_2]\Gamma[\alpha_3]$.

We now introduce a fourth Schwinger parameter for the sum $\sum v_i^{-1}$, which gives

$$= \frac{\pi^{d/2}}{(2)^{\alpha_t - d/2}} \int_0^\infty \frac{dt t^{d-\alpha_t - 1}}{\Gamma\left[\alpha_1\right]\Gamma\left[\alpha_2\right]\Gamma\left[\alpha_3\right]\Gamma\left[d-\alpha_t\right]} \prod_{j=1}^{3} dv_j v_j^{\alpha_t - d/2 - \alpha_j - 1} \exp\left[-\frac{1}{2} v_j \Omega_j^2 - \frac{t}{v_j}\right] \quad \text{(A.10)}$$

Notice that if $d = 2\alpha_t$ this is not necessary and the integral is elementary (this is a special case of the magic identities [140]). Continuing on, we would like to write this in terms of the modified Bessel function

$$K_\nu(z) = \frac{1}{2}\left(\frac{z}{2}\right)^\nu \int_0^\infty e^{-u - \frac{z^2}{4u}} u^{-\nu-1} du \quad \text{(A.11)}$$

To do this, we simply change variables to $\frac{1}{2} v_j \omega_{kl}^2 = u_j$, $du_j = \frac{1}{2} dv_j \omega_{kl}^2$, $v_j = \frac{2u_j}{\omega_{kl}^2}$.

Our integral becomes

$$= \frac{\pi^{d/2}}{(2)^{\alpha_t - d/2}} \int_0^\infty \frac{dt t^{d-\alpha_t-1}}{\Gamma[\alpha_1]\Gamma[\alpha_2]\Gamma[\alpha_3]\Gamma[d-\alpha_t]} \prod_{j=1}^{3} du_j \left(\frac{2}{\Omega_j^2}\right)^{\alpha_t - d/2 - \alpha_j} u_j^{\alpha_t - d/2 - \alpha_j - 1} \exp\left[-u_j - \frac{t\Omega_j^2}{2u_j}\right] \tag{A.12}$$

$$= \pi^{d/2} (2)^{\alpha_t - d} \int_0^\infty \frac{dt \left(\sqrt{t}\right)^{d/2-2}}{\Gamma[\alpha_1]\Gamma[\alpha_2]\Gamma[\alpha_3]\Gamma[d-\alpha_t]} \prod_{j=1}^{3} \Omega_j^{-\alpha_t + d/2 + \alpha_j} K_{d/2+\alpha_j-\alpha_t}\left(\sqrt{2t}\Omega_j\right) \tag{A.13}$$

It turns out that this expression is sufficient to extract the divergence structure that we are interested in. To see the relation to secular resonances, we need only the parts that include the frequency.

Appendix B

The Murnaghan-Nakayama rule

A standard problem in the group theory of the symmetric group S_n is the computation of the characters of conjugacy classes $[\sigma]$ in a given representation R. That is, we want to compute

$$\chi_R([\sigma]) \tag{B.1}$$

and as is explicitly presented in section 4.3, we need these characters to implement the Fourier transform relating the "string basis" and the "D-brane basis" of our Hilbert space.

The representations R of S_n will be labeled by Young diagrams with n boxes, while the conjugacy classes will be presented in a cycle form $[\sigma] = t_1^{w_1} \dots t_k^{w_k}$ with $\sum k w_k = n$. The Murnaghan-Nakayama rule gives a recursive way to evaluate $\chi_R([\sigma])$ in terms of $\chi_{\tilde{R}}([\tilde{\sigma}])$, where we have that $[\sigma] = [\tilde{\sigma}]t_s$ for some t_s, and the $\tilde{R}$ is a set of representations of S_{n-s} related to R and s in a particular way.

The rule is easiest to explain with an example first.

Consider for example the tableaux with 10 boxes given by

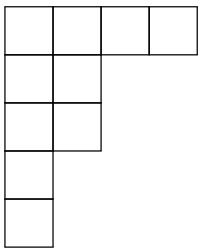

(B.2)

which is a partition of 10. Assume that we want to compute the characters for splitting into two traces (only group elements with two different cycles) of the diagram. There are 5 such possibilities: $5+5, 6+4, 7+3, 8+2, 9+1$. Let us compute the splitting into $5+5$. The first step is to find the hooks of the diagram, and to decorate the diagram with the hook lengths, in the standard way

8	5	2	1
5	2		
4	1		
2			
1			

(B.3)

This will be useful, as hooks are in one to one correspondence with skew hooks, which are of interest to us, and the corresponding pairs have the same length. We see that there are two (skew) hooks of length 5. We first remove one of the two length 5 skew hooks, as shown in the figure

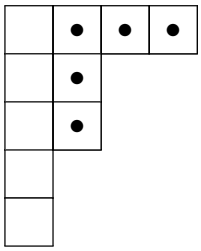

(B.4)

the other option is

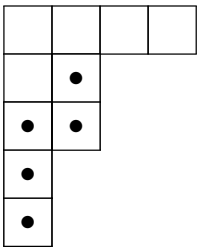

(B.5)

As you can see, a skew-hook is a regular hook that has been moved to the edge of the tableaux. Like standard hooks, they do not contain a 2×2 squares. As previously stated, the set of skew-hooks and regular hooks are in one to one correspondence, so one reads of the allowed skew-hook lengths by reading the lengths of the ordinary hooks.

A sign is assigned to each such skew hook. The sign is (-1) if the number of rows covered by the skew hook is even, or $(+1)$ if this is odd. After removing the skew-hook we are left with a proper partition, and we are also left with a cycle decomposition of the remnant of the group element (or conjugacy class). The Murnaghan-Nakayama rule states that to obtain the character of a diagram, sum over the characters of the remnant of the group element on the remnant tableaux with the sign of the skew-hook accounted for. Let us do so for the example above.

To simplify, we will notate a young diagram by the length of its rows. Thus, the full diagram is $(4, 2, 2, 1, 1)$, and we will notate the conjugacy class by the lengths of the cycles. That is, $[5, 5]$.

For the example above, one skew hook has an odd number of rows and the other has an even number of rows, so the sign is $(+1)$ and (-1) respectively. The rule then gives

$$\chi_{4,2,2,1,1}([5,5]) = \chi_{1,1,1,1,1}([5]) - \chi_{4,1}([5]) = 1 + 1 = 2 \tag{B.6}$$

where the character of the remnant character is also ± 1 and is determined by the number

of rows it contains. Since there are no hooks of length $6, 7, 9$ (as made explicit by our diagram with the hook lengths notated), we also find immediately that

$$\chi_{4,2,2,1,1}([6,4]) = \chi_{4,2,2,1,1}([7,3]) = \chi_{4,2,2,1,1}([9,1]) = 0 \tag{B.7}$$

while for the last one, we find

$$\chi_{4,2,2,1,1}([8,2]) = \chi_{1,1}([2]) = -1 \tag{B.8}$$

A convenient way to think about the Murnaghan-Nakayama rule is that it gives the action of the lowering operators $s\partial_{t_s}$ on the Young diagram basis, and so it does not just compute the characters, but the action of the lowering operator on the Hilbert space of states. Let us discuss this with a few examples. Consider first the state

$|t_1 t_2^2\rangle =$ 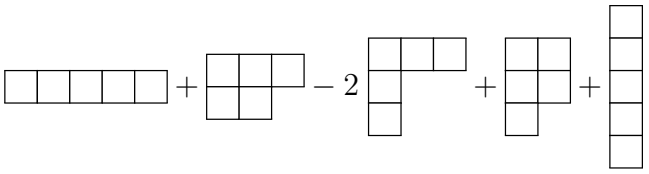 (B.9)

We could act on this state with the lowering operator a_1. The conjugacy class states are just Fock space states, so we know

$$a_1 |t_1 t_2^2\rangle = |t_2^2\rangle \tag{B.10}$$

We could further compute the necessary characters using the MN rule and expand the new state as

$|t_2^2\rangle =$ 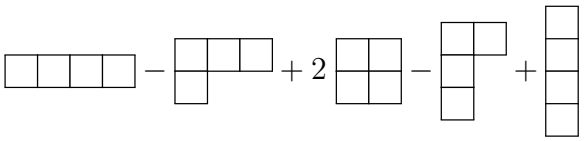 (B.11)

Alternatively, we could have considered applying the lowering operator directly to the diagrams. Our lowering operator is a_1, so it removes skew hooks of length 1 as shown

a_1 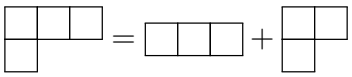 (B.12)

There were two possible ways to remove skew hooks of length 1, so we end with a sum of the two possibilities. On the other hand, if we apply this to the trivial representation, there is only one way to remove a hook, so we have

a_1 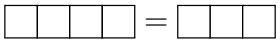 (B.13)

Applying the lowering operator to the full state, we find

$a_1|t_1t_2^2\rangle = a_1$ 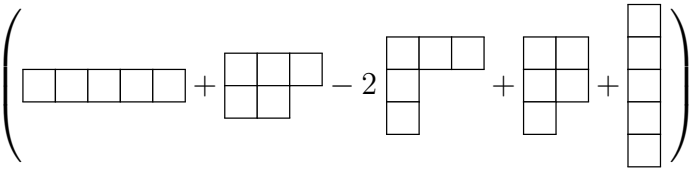 (B.14)

$=$ 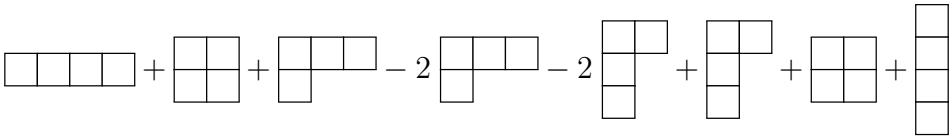 (B.15)

We see that if we simplify this, we get the same expression for the state $|t_2^2\rangle$ shown above.

We would expect that if we apply any a_j to our original state $|t_1t_2^2\rangle$ with $j > 2$ that this should kill the state. Let's see how this works diagrammatically. Of course, there are no skew hooks of length greater than 5, as each diagram has only five boxes, so any a_j with $j > 5$ will kill the state. As a less trivial example, let's consider acting with a_3.

This gives

$$a_3|t_1t_2^2\rangle = a_3$$ 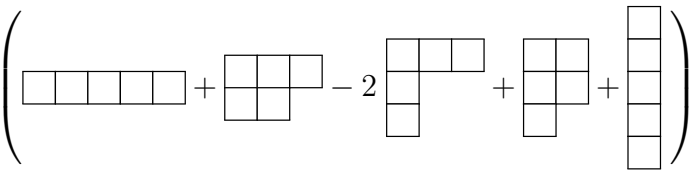 (B.16)

$$=$$ 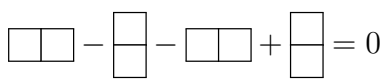 $$= 0$$ (B.17)

where we remember that if the height of the hook is even, then the diagram changes sign. Notice also that there were no allowed hooks of length 3 in the third diagram, so that piece vanishes.

Finally, we would expect that if we apply any a_j on the state $|t_j\rangle$, then we should get $a_j|t_j\rangle = j|0\rangle$, where the factor of j comes from the commutation rules for our raising and lowering operators: $[a_i, a_j^\dagger] = \delta_{ij}j$. We will represent the vacuum diagrammatically as $\bullet$. As an example of this, we have

$$a_4|t_4\rangle = a_4$$ 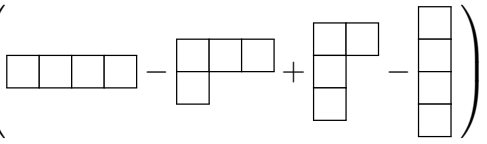 (B.18)

$$= \bullet + \bullet + \bullet + \bullet = 4\,\bullet = 4\,|0\rangle$$ (B.19)

where each piece was exactly a skew hook of length 4 and so became the vacuum state when hit with a_4. Also, note the sign changes come from the height of the hooks.

One can see that this is indicative of the general case. This is handled by using the fact that

$$|R\rangle = \sum \frac{\chi_R[\sigma]}{\prod k_k^w w_k!} \prod t_k^{w_k} \tag{B.20}$$

Now, let us try to remove one t_s from the above equation, by acting with $s\partial_{t_s}$ on a

monomial $\prod t_k^{w_k}$. We get $sw_s t_s^{w_s-1}$. The extra factor of s and w_s cancel terms in the denominator, so that we get regular denominators as would correspond to $[\sigma]/t_s = [\tilde{\sigma}]$ for any sigma that has a t_s in it.

Now we use that $\chi_R[\sigma] = \sum(-1)^* \chi_{\tilde{R}}([\tilde{\sigma}])$ where $(-1)^*$ is the sign assigned by the Murnaghan-Nakayama rule. That is, we find that

$$s\partial_{t_s} |R\rangle = \sum \frac{(-1)^* \chi_{\tilde{R}}[\tilde{\sigma}]}{\prod k_k^w w_k!} (sw_s)[\sigma]/t_s = \sum_{\text{hooks of length } s} (-1)^* |\tilde{R}\rangle \tag{B.21}$$

and because we recognize that the sum is over $[\tilde{\sigma}]$ unrestricted, we find that on the right hand side we sum over the states $\tilde{R}$ with the Murnaghan-Nakayama rule sign and nothing else.

Appendix C

Assigning Young Tableaux to Fermions states

The ground state of the multiple particle system $\bullet$ is defined by the Slater determinant

$$\bullet \simeq \lim_{N\to\infty} |-1/2\rangle\,|-3/2\rangle\ldots|-N/2\rangle_{antisymmetrized} \tag{C.1}$$

where, as in the text, we shift our allowed energies so that particles sit at half integer levels. And, as usual, the ground state has the full infinite tower of negative states occupied. This can be represented pictorially as follows, as in figure C.1, where dots represent filled states and circles represent holes.

A complete basis of states is given by

$$|\{n\}\rangle \simeq \lim_{N\to\infty} |n_1\rangle\,|n_2\rangle\ldots|n_N\rangle_{\text{antisymm}} \tag{C.2}$$

with $n_1 > n_2 > n_3 > \cdots > n_N$, half integers, and for all sufficiently large j we require that $n_j = -\frac{2j-1}{2}$. This state is represented by filling in each n_j energy level with a dot.

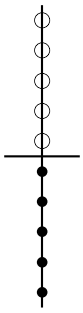

Figure C.1: Vacuum State of Fermi Sea

If a particular value of j is missing, it is left empty (circles in the drawings).

To each state, we will assign a Young diagram whose j-th row has $r_j = n_j - (\frac{1}{2} - j)$ boxes (and if $r_j = 0$ we leave those rows empty and without boxes). By inverting this expression, we can go the other way, assigning a state of the Fermions to a Young diagram. We then relate these diagrams to representations of the symmetric group.

A trivial representation (totally symmetric if considered as a representation of $U(N)$ instead of S_n) corresponds to an excitation out of the sea, with an energy equal to the number of boxes. That is, the state given by

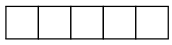 (C.3)

corresponds to the figure C.2

Further, the totally anti-symmetric state corresponds to a hole, where an n-box representation corresponds to a hole n spaces below zero. That is,

 (C.4)

corresponds to the figure C.3.

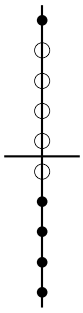

Figure C.2: Excitation with 5 units of energy on the highest Fermion

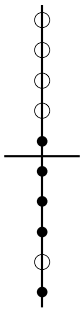

Figure C.3: Excitation with 1 unit of energy on the highest five fermions, or equivalent, a hole with 5 units of energy has been excited

Basically, a tableaux is assigned by taking the highest fermion energy available and subtracting the energy of the highest occupied fermion in the ground state and assigning that many boxes to the first row of the tableaux. We then do the same with the second highest energy fermion, and so on until all the subsequent fermions in the excited state have the same energy as the corresponding fermions in the vacuum, where we stop assigning boxes.

Appendix D

Can Topology and Geometry be Measured by an Operator Measurement in Quantum Gravity?

One of the main claims of the AdS/CFT correspondence [3] is that it provides a definition of quantum gravity for spacetimes that are asymptotically of the form $AdS \times X$. It is natural to ask: what does this holographic description tell us about the nature of observables in the quantum theory of gravity?

By an observable, we mean a Hermitian (linear) operator on the Hilbert space of states as is usual in quantum mechanics. In this context, is the metric a quantum mechanical observable? Is topology measurable by an observable? And if the answer is no, then when are they sufficiently well approximated by observables?

We define $\hat{T}$ to be a topology measuring operator if different eigenvalues correspond to different topologies of the dual gravity theory and the zero eigenvalue is reserved for the trivial topology alone. Here trivial means the same topology as the ground state.

Our main conclusion is that such topology measuring operators do not always exist. We support this by providing an example where one can prove that there is no such operator.

The example arises from studying the states that preserve half of the supersymmetries of $\mathcal{N} = 4$ Super -Yang-Mills theory (SYM) and their dual geometries.

The set of states we are interested in forms a Hilbert space in its own right. Quantum mechanics is therefore valid and quantum mechanical questions can be answered unambiguously. The relevant Hilbert space of states near the free field theory limit $g_{YM} \to 0$ has been analyzed in [64]. An orthogonal basis of states of energy $E = n$ can be represented by partitions of n, which can be written in terms of Schur polynomials and are classified by Young tableaux for $U(N)$. These states can also be represented in terms of free fermion dynamics for N fermions in the lowest Landau level on a plane [65]. This description gives rise to a geometric interpretation of states as incompressible droplets in two dimensions. These free fermions can also be described by the incompressible droplets of the integer quantum Hall effect [141].

The geometric droplet shape is exactly the geometric data that is required to build a horizon-free solution of type IIB supergravity that respects the same amount of supersymmetry and that also asymptotes to $AdS_5 \times S^5$, as constructed by Lin, Lunin, and Maldacena [63]. We will call these the LLM geometries. In these geometries, different droplet topologies correspond to different spacetime topologies.

There exists a limit of the LLM geometries where a complete minisuperspace theory characterizing all the states with the requisite amount of supersymmetry, as a quantum theory, is identical to the Hilbert space of a free chiral boson on a circle in 1+1 dimensions. This limit is the strict $N \to \infty$ limit of the theory, with the energy above the ground state kept finite. The mode expansion of the chiral boson can be related to traces of the $\mathcal{N} = 4$ SYM fields Z by $a_n^\dagger \simeq \mathrm{tr}(Z^n)$ via the usual operator-state correspondence and

the understanding that single traces go to single particle modes [4]. In this limit, the oscillators give a rise to a free Fock space, with a free mode for every n. We will take the existence of this limit as a statement of fact and it is in this limit that our statements can be made rigorously. Many of the technical details that are required to prove some claims in this paper will appear in a forthcoming paper by the authors [38].

This paper makes the claim that topology cannot be measured by operators. To make the claim, we need the following assumptions about the particular setup we have:

1. All coherent states of the chiral boson theory with finite energy have trivial topology (the same as the vacuum) and are to be thought of as smooth classical geometries.

2. The set of these coherent states is over-complete, so every other state in the Hilbert space can be obtained by superposition of this family of states.

3. There are states in the Hilbert space that have a different topology than the vacuum and can also be thought of as classical states of the gravitational theory.

From these assumptions, it follows that there is no operator $\hat{T}$ in the Hilbert space that measures the topology. We now prove this statement by contradiction, assuming the existence of $\hat{T}$.

From assumption one above, all coherent states have trivial topology, so $\hat{T}\,|\mathrm{Coh}\rangle = 0$. Any other state $|\psi\rangle$ that is a superposition of coherent states will satisfy

$$\hat{T}\,|\psi\rangle = \hat{T}\int_{\mathrm{Coh}} A_{\mathrm{Coh}}\,|\mathrm{Coh}\rangle = \int_{\mathrm{Coh}} A_{\mathrm{Coh}}\hat{T}\,|\mathrm{Coh}\rangle = 0 \tag{D.1}$$

so the ket $|\psi\rangle$ is an eigenstate of the topology operator with eigenvalue zero: it has trivial topology. By condition two above, this includes all possible states. Therefore, if such an operator exists, all states have trivial topology. This contradicts the third assumption

A related argument where overcompleteness is used to indicate problems with defining either topology operators or geometric operators is found in [109, 108]. These arguments are made in the $ER = EPR$ context [78] for setups with entangled black holes, and the topology change is hidden behind a horizon in an Einstein-Rosen bridge.

We will now elaborate on the basis for assumptions one and three. Assumption two is a well known fact for studying states of a finite number of harmonic oscillators. It can be extended to the case of an infinite number of oscillators by carefully taking the appropriate limits.

A geometric picture of the states can be obtained as follows: in the LLM geometries, all states can be drawn as a two color picture in two dimensions. The individual droplet areas of both colors are quantized. As we are focusing on $N \to \infty$, keeping the energy finite, all relevant states are close to the circular droplet that makes the vacuum. We want to focus on the edge of the droplet, by using an area preserving map

$$dx\, dy \simeq r\, dr\, d\theta = dh\, d\theta \tag{D.2}$$

where the variable h will be measured relative to the circular droplet. In this setup, the $N \to \infty$ limit is taken by sending $r \to \infty$, keeping h finite. In this limit, $|h|$ can be as large as we need it to be. The topology of the (h, θ) space is a cylinder. The vacuum has the area below $h = 0$ completely filled, and above $h = 0$ completely empty. We can excite fermions from the filled region to the empty region and will characterize this shift by a density function $\Delta\rho$, which takes on a value $+1$ for regions above $h = 0$ and -1 below. Conservation of the fermion number is implemented by $\int dh\, d\theta\, \Delta\rho = 0$. The

energy relative to the vacuum is measured by

$$E \simeq \int d\theta\, dh\, h(\theta)\, \Delta\rho(h,\theta) \tag{D.3}$$

This follows easily from the computations in [63], being careful about subtracting the energy of the vacuum.

A typical geometric fluctuation is depicted in figure D.1. The fluctuation is described

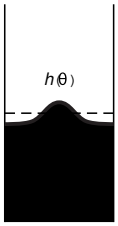

Figure D.1: A geometric fluctuation of the vacuum, characterized by $h(\theta)$.

by a single height function $h(\theta)$ that represents the edge of the droplet.

The function $h(\theta)$ is the excess density of fermions at the angle θ. It gets matched to the charged current of the chiral boson as $h(\theta) \propto \partial_\theta X(\theta)$. Conservation of fermion number is described by $\int d\theta\, \partial_\theta X(\theta) = 0$. That is, the field $\partial_\theta X$ has no zero mode. This is exactly as is expected from studies of the quantum Hall effect (see for example [142, 83]). It follows from integrating $\Delta\rho$ over a column in equation (D.3) that the energy goes to $E \simeq \frac{1}{2\pi} \int d\theta : \partial_\theta X(\theta)^2 :$, where the normal ordering ensures that the vacuum has zero energy. This is the standard expression for the energy in the chiral boson theory. The factor of 2π is a choice of convention for normalization of the field Fourier modes.

A coherent state of the free chiral boson will result in a unique (sufficiently smooth) single valued $h(\theta) \propto \langle \partial X(\theta) \rangle$ such that the classical energy of the state as computed in (D.3) is equal to the expectation value of the energy of the corresponding quantum

state. All of these solutions have a classical LLM geometry that can be reconstructed uniquely from $h(\theta)$. The topology of the geometry is encoded in the topology of the fermion droplet. All of these states have trivial topology in the LLM setting: one edge with circle topology winding once around the circle direction θ. This justifies assertion one.

Now we need to justify assertion three. This can be done with figure (D.2). The

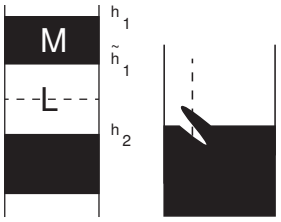

Figure D.2: Examples of two colorings with non-trivial geometry. On the left, the areas L, M have quantized area L, M respectively. On the right, we depict a more general folded configuration.

idea is that we can also do a two coloring of the cylinder that preserves the net area and is such that the topology is now characterized by a strip-geometry. In this case, there are three edges winding around the circle, two of them go from black to white (at heights h_1, h_2) and the other one goes from white to black (at height $\tilde{h}_1$). Edges with the opposite coloring will be called anti-edges. We call this state the reference state $|\square_{LM}\rangle$. This state is easily constructible in terms of Young diagrams [63]. One can also consider folded configurations (which are not translation invariant) as in the drawing on the right of figure (D.2).

Small fluctuations of the state $|\square_{LM}\rangle$ will be characterized by three functions $h_1(\theta) = h_1^{(0)} + \delta h_1(\theta)$, $h_2(\theta) = h_2^{(0)} + \delta h_2(\theta)$, and $\tilde{h}_1(\theta) = \tilde{h}_1^{(0)} + \delta \tilde{h}_1(\theta)$. Quantization of the area is implemented by requiring that none of the δh have a zero mode in the Fourier coefficients. This can easily be generalized to more stripes. A straightforward computation of the

energy of such a geometry shows that the energy, relative to the reference state, is given by

$$E \simeq E_{LM} + \int d\theta \sum_i \left(\delta h_i(\theta)^2 - \delta \tilde{h}_i(\theta)^2 \right) \tag{D.4}$$

with the edge modes having positive excess energy and the anti-edge modes having negative excess energy. The net fermion over density at position θ is $\partial X(\theta) \simeq h_1(\theta) + h_2(\theta) - \tilde{h}_1(\theta)$. The absence of the zero mode for $\partial X(\theta)$ results in $h_1^{(0)} + h_2^{(0)} - \tilde{h}_1^{(0)} = 0$. This determines the location of the reference height, which tells us that the reference state depends only on L, M, with no extra parameters.

We now claim that the new topology is generated by making the height function in $|\Box_{LM}\rangle$, $h(\theta)$ multivalued. The function $h(\theta)$ is related linearly to $\partial X(\theta)$ in the classical coherent state setup. The net $\partial X(\theta)$ that reflects a proper observable in the quantum system is obtained by a signed sum over these multi-values. Indeed, because all the edges are similar, one can imagine that to each of the edges one could associate a chiral boson field theory so that $\partial X(\theta) = \partial X_1(\theta) + \partial X_2(\theta) - \partial X_{\tilde{1}}(\theta)$. Because in equation (D.4) the tilded modes have the wrong sign, the notion of raising and lowering operators is reversed. We can rewrite this equation in a mode expansion

$$a_n^\dagger = b_n^{(1)\dagger} + b_n^{(2)\dagger} - c_n^{(\tilde{1})} \tag{D.5}$$

where the b modes refer to regular edges, and the c modes to the anti-edges. Notice, without the lowering operator pieces in equation (D.5), the necessary commutation relations of the a_n modes could not be satisfied. This also gives the correct equations of motion for ∂X, with each of the modes satisfying them on their own. The negative energy associated with the modes c is crucial, so that the notion of positive and negative frequency can reverse the assignment of raising and lowering operators. This equation

can be thought of as a partial Bogolubov transformation mode by mode. The reference state is characterized by $b_n^{(i)} |\square_{LM}\rangle = c_n^{(\tilde{i})} |\square_{LM}\rangle = 0$ for all n. A similar analysis for a folded configuration would require decomposing in modes that also have position resolution (a wavelet transform) and the multivaluedness would have to be assessed locally in θ with some resolution. Folded configurations cannot evolve from unfolded configurations in this setup, but they can in the $c = 1$ matrix model [112]. A proper analysis of folded configurations and how to extract their topology is beyond the scope of the present paper.

The linearity of the mode decomposition for strip geometries has already been suggested in [82] (see also the more recent [111]). The construction of such modes is purely combinatorial and depends on knowing how to manipulate the states labeled by Young tableaux carefully. The commutation relations of the b, c modes are canonical for *states near the reference state*. This can be deduced from [80]. We take these to be

$$[b_n^{(i)}, b_n^{(j)\dagger}] = n\delta^{i,j} \tag{D.6}$$

and similar for c, with all other commutators vanishing. These assertions are proven in the companion work to this paper [38], where the details on the cutoff and the applicability of these commutation relations are deduced from first principles. The nearby states form a small Hilbert space in their own right. The commutation relations are valid when inside the small Hilbert space, but they get corrected as we try to include more states.

These new modes only extend to values of order $n << M, L$. Beyond that they do not exist as independent operators [38]. This is a type of stringy exclusion principle of the same type as the one implemented in [71]. It is dynamically generated and depends on the reference state (depends on L, M). The modes b, c do not exist for any of the coherent states $|\text{Coh}\rangle$ that we have discussed previously. For those states, the height function is

single-valued. We should not be able to extend the definition of these modes to those states. We claim we are prevented from doing so by the stringy exclusion principle. The existence of these strip-geometry states justifies our third assumption, and therefore completes our argument that one cannot have a topology measuring operator.

Does this lack of a topology measuring operator mean we simply cannot determine the topology of the spacetime? In the remainder of the paper, we will give two resolutions: one that involves measuring classicality of the state and one that involves its entanglement. Both of these rely on computing quantities that are non-linear in the wavefunction, rather than performing a single operator measurement.

Consider forming coherent states of the b, c oscillators, which can be interpreted as new classical solutions relative to the state $|\Box_{LM}\rangle$, with $\delta h^i(\theta) \propto \langle \partial X^i(\theta) \rangle$ and similar for the anti-edges. These are allowed as long as the tails in the coherent state can be truncated without appreciable loss of information.

The existence (construction) of the b, c modes means we can do (unitary) effective field theory in the nearby Hilbert space with them. We just need to restrict ourselves to being well below the stringy exclusion principle. The small Hilbert space is constructed by acting with finitely many raising operators $b^\dagger, c^\dagger$, keeping the total energy in the b modes less than $\min(\mathrm{L}/2, \mathrm{M}/2)$, and the total negative energy in the c modes less than $\min(\mathrm{L}/2, \mathrm{M}/2)$. In that regard, the operators $a_n^\dagger, a_n$ well below the (dynamical) stringy exclusion principle act inside the small Hilbert space, leaving the new state inside it. Any quantum mechanical question about them can be answered in principle in the small Hilbert space: they belong to the effective field theory. This explains why effective field theory is still valid in the gravity theory.

Consider taking the expectation value of the number operator $\hat{N}_n$ for mode a_n in the

reference state (this is easy to do for multi-edge geometries). We find that

$$\langle n^{-1}a_n^\dagger a_n\rangle_{LM} = N_{\text{anti-edges}} \quad \langle n^{-1}a_n a_n^\dagger\rangle_{LM} = N_{\text{edges}} \tag{D.7}$$

so the expectation value of the number operator (on reference states) can be used to measure the topology, mode per mode. The number operator can change a lot when we consider coherent states of the b, c modes. Let us call one such state $|\psi\rangle$. Consider instead of the number operator, the uncertainty. A straightforward manipulation shows that

$$\langle n^{-1}(a_n^\dagger - \langle a_n^\dagger\rangle_\psi)(a_n - \langle a_n\rangle_\psi)\rangle_\psi = N_{\text{anti-edges}} \tag{D.8}$$

We see that the topology of the coherent state of the b, c oscillators, the new classical states, can be measured by computing the net fluctuations of the modes $a_n^\dagger$. These are still of quantum size (order one), so the state can be said to be approximately classical for each of the modes a_n. In taking a double scaling limit $\hbar \to 0$, implemented by taking $L, M \to \infty$ and rescaling the fields by appropriate powers of L, M, the rescaled uncertainty vanishes. In this sense, these topologically different drawings provide new classical limits of the free chiral boson. Similar limits for folded setups have been considered in the $c = 1$ matrix model [112], where it is found that in general $\langle h(\theta)^2 - \langle h(\theta)\rangle^2\rangle$ is large, but does not measure the number of edges directly.

The topology for the state $|\square_{LM}\rangle$ is measurable by the uncertainty. This is a non-linear operation in the Hilbert space: it is not a single operator measurement, but a test of classicality. If we want to extend the measurement of topology to the semiclassical limit, where we allow a few quanta of the b, c modes to be in a state that is not a coherent state, we find that to measure the topology, we have to ask each mode a_n what value of uncertainty they measure. The few modes that are outliers can be discarded and the

majority rule will be used. We call this a census measurement. The best answer for the topology will be given by the consensus of the majority. This depends highly on what scale we use to cut off the census. This should be determined by the stringy exclusion principle, which is related to the value of L, M. But, we do not know these a priori: the state is given to us as a black box. If the cutoff is set at a scale much larger than L, M, most of the a_n modes will be in the vacuum and we would find that state has a trivial topology. If the cutoff is set well below L, M, the consensus might give a different topology than if we measure near L, M. This is because the b, c, modes may be forming thinner striped states on their own.

We will next use the idea that spacetime geometry and entanglement seem to be intimately related. We compute the entanglement entropy using the Bogoliubov transformation. Starting with a coherent state of the b, c modes, we find

$$S_n = N_{\text{edges}} \ln N_{\text{edges}} - N_{\text{anti-edges}} \ln N_{\text{anti-edges}} \tag{D.9}$$

where everything but the a_n modes have been traced out. As with the previous method, we need to perform this computation for many modes and find consensus to determine the topology of nearby semi-classical states. We can only be sure of the accuracy of this calculation for modes below the stringy exclusion principle. The connection we find between topology and entanglement supports the ideas of Van Raamsdonk [72]. Related ideas about connectedness being related to entanglement are currently being developed by Almheiri et al. [110].

It is important to note that we have been working in the strict $N \to \infty$ limit. At finite N, there is no longer a canonical factorization of the Hilbert space, so computing the entanglement entropy becomes ambiguous. This suggests that the uncertainty

measurement definition of topology might be preferable in general.

Further, at finite N, the Planck scale scales as $\ell_p^{-1} \simeq N^{1/4}$. If $L, M >> N^{1/4}$, there are many more modes with energy below ℓ_p^{-1} in the geometry with the striped topology than when computed in the ground state of the system. These all commute with each other. To describe these multi-droplet geometries, one needs to borrow supersymmetric modes from the UV [37]. To end up with the extra finite energy modes, whose energies are of order one, one needs the UV modes to be excited. That way, the UV modes don't annihilate the reference state and one can form a bound state of a mode that raises the energy with another mode that lowers it. These UV states that lower the energy count as large negative energy excitations relative to the reference state. Bound states at threshold between the large positive energy excitations and the large negative energy excitations provide a consistent solution to the presence of the extra modes, including an explanation for the modes c with negative energy.

To summarize, we have shown that states with non-trivial topology can be formed by superposing topologically trivial states. We have shown that in our examples, the topology for multi-strip geometries can be accessed either by computing the uncertainty or the entanglement entropy of the different modes. Neither of these two methods of measurement correspond to a single operator measurement in the Hilbert space of states.

Appendix E

Conjugacy classes of S_n

Consider the group of permutations S_n. The list of irreps of S_n is in one to one correspondence with Young diagrams with n boxes. The cardinality of this set is also equal to the cardinality of the set of conjugacy classes of the group S_n, which we label by a group element representative $[\sigma]$. The element σ acts on the set of n elements as a one to one function $\sigma : \{1, \dots n\} \to \{1, \dots, n\}$, sending $i \to \sigma(i)$. We can also represent this as a cycle decomposition

$$\sigma = (n_1^{(1)} n_2^{(1)} \dots n_{k_1}^{(1)})(n_1^{(2)} \dots n_{k_2}^{(2)}) \dots \tag{E.1}$$

where the set of elements $\{n_\ell^{(j)}\}$ is the set $\{1, \dots n\}$. It follows that $n = \sum k_i$ Each $m \in \{1, \dots, n\}$ only appears once, and the elements on each parenthesis are called a cycle. We can recover the action on the set by the convention that $\sigma(n_m^{(j)}) = n_{m+1}^{(j)}$, with $n_{k_j+1}^{(j)} \equiv n_1^{(j)}$. Basically, the cycles represent the iterated action of σ on individual elements of the set $\{1, \dots n\}$. An individual cycle $(n_1^{(1)} n_2^{(1)} \dots n_{k_1}^{(1)})$ is said to have length k_1. We can choose the k_i to be non-decreasing by permuting the order in which the

individual cycles are presented. This does not change the assignment of σ.

Bibliography

[1] A. Einstein, H. Lorentz, H. Minkowski, and H. Weyl, *On the electrodynamics of moving bodies*, *The principle of relativity* (1952) 37–65.

[2] A. Einstein, *Die grundlage der allgemeinen relativitätstheorie*, *Annalen der Physik* **354** (1916), no. 7 769–822.

[3] J. M. Maldacena, *The Large N limit of superconformal field theories and supergravity*, *Int. J. Theor. Phys.* **38** (1999) 1113–1133, [hep-th/9711200]. [Adv. Theor. Math. Phys.2,231(1998)].

[4] E. Witten, *Anti-de Sitter space and holography*, *Adv. Theor. Math. Phys.* **2** (1998) 253–291, [hep-th/9802150].

[5] S. S. Gubser, I. R. Klebanov, and A. M. Polyakov, *Gauge theory correlators from noncritical string theory*, *Phys. Lett.* **B428** (1998) 105–114, [hep-th/9802109].

[6] G. 't Hooft, *Dimensional reduction in quantum gravity*, *Conf. Proc.* **C930308** (1993) 284–296, [gr-qc/9310026].

[7] L. Susskind, *The World as a hologram*, *J. Math. Phys.* **36** (1995) 6377–6396, [hep-th/9409089].

[8] R. Bousso, *The Holographic principle*, *Rev. Mod. Phys.* **74** (2002) 825–874, [hep-th/0203101].

[9] B. Sundborg, *Stringy gravity, interacting tensionless strings and massless higher spins*, *Nucl. Phys. Proc. Suppl.* **102** (2001) 113–119, [hep-th/0103247]. [,113(2000)].

[10] M. A. Vasiliev, *Conformal higher spin symmetries of 4-d massless supermultiplets and osp(L,2M) invariant equations in generalized (super)space*, *Phys. Rev.* **D66** (2002) 066006, [hep-th/0106149].

[11] A. Mikhailov, *Notes on higher spin symmetries*, hep-th/0201019.

[12] E. Sezgin and P. Sundell, *Massless higher spins and holography*, *Nucl. Phys.* **B644** (2002) 303–370, [hep-th/0205131]. [Erratum: Nucl. Phys.B660,403(2003)].

[13] A. Strominger, *The dS / CFT correspondence*, *JHEP* **10** (2001) 034, [hep-th/0106113].

[14] C. M. Hull, *Timelike T duality, de Sitter space, large N gauge theories and topological field theory*, *JHEP* **07** (1998) 021, [hep-th/9806146].

[15] E. Witten, *Quantum gravity in de Sitter space*, in *Strings 2001: International Conference Mumbai, India, January 5-10, 2001*, 2001. hep-th/0106109.

[16] A. Strominger, *Inflation and the dS / CFT correspondence*, *JHEP* **11** (2001) 049, [hep-th/0110087].

[17] V. Balasubramanian, J. de Boer, and D. Minic, *Notes on de Sitter space and holography*, *Class. Quant. Grav.* **19** (2002) 5655–5700, [hep-th/0207245]. [Annals Phys.303,59(2003)].

[18] J. M. Maldacena, *Non-Gaussian features of primordial fluctuations in single field inflationary models*, *JHEP* **05** (2003) 013, [astro-ph/0210603].

[19] A. Bagchi, *Correspondence between Asymptotically Flat Spacetimes and Nonrelativistic Conformal Field Theories*, *Phys. Rev. Lett.* **105** (2010) 171601, [arXiv:1006.3354].

[20] A. Bagchi and R. Fareghbal, *BMS/GCA Redux: Towards Flatspace Holography from Non-Relativistic Symmetries*, *JHEP* **10** (2012) 092, [arXiv:1203.5795].

[21] O. Aharony, S. S. Gubser, J. M. Maldacena, H. Ooguri, and Y. Oz, *Large N field theories, string theory and gravity*, *Phys. Rept.* **323** (2000) 183–386, [hep-th/9905111].

[22] E. D'Hoker and D. Z. Freedman, *Supersymmetric gauge theories and the AdS / CFT correspondence*, in *Strings, Branes and Extra Dimensions: TASI 2001: Proceedings*, pp. 3–158, 2002. hep-th/0201253.

[23] J. Polchinski, *Introduction to gauge/gravity duality*, in *String Theory And Its Applications: TASI 2010 From meV to the Planck Scale*, pp. 3–45. World Scientific, 2012.

[24] G. T. Horowitz and J. Polchinski, *Gauge/gravity duality*, gr-qc/0602037.

[25] J. Penedones, *TASI lectures on AdS/CFT*, in *Proceedings, Theoretical Advanced Study Institute in Elementary Particle Physics: New Frontiers in Fields and Strings (TASI 2015): Boulder, CO, USA, June 1-26, 2015*, pp. 75–136, 2017. arXiv:1608.0494.

[26] R. M. Wald, *General relativity*. University of Chicago press, 2010.

[27] S. M. Carroll and J. Traschen, *Spacetime and geometry: An introduction to general relativity*, *Physics Today* **58** (2005), no. 1 52.

[28] K. S. Thorne, C. W. Misner, and J. A. Wheeler, *Gravitation*. Freeman, 2000.

[29] J. B. Hartle, *Gravity: An introduction to einstein?s general relativity*, 2003.

[30] J. Polchinski, *String theory. Vol. 1: An introduction to the bosonic string*. Cambridge University Press, 2007.

[31] J. Polchinski, *String theory. Vol. 2: Superstring theory and beyond*. Cambridge University Press, 2007.

[32] D. Tong, *String Theory*, arXiv:0908.0333.

[33] M. Green, J. Schwarz, and E. Witten, *Superstring theory, vols. i and ii*, 1987.

[34] B. Zwiebach, *A first course in string theory*. Cambridge university press, 2004.

[35] D. Berenstein and A. Miller, *Conformal perturbation theory, dimensional regularization, and AdS/CFT correspondence*, *Phys. Rev.* **D90** (2014), no. 8 086011, [arXiv:1406.4142].

[36] D. Berenstein and A. Miller, *Logarithmic enhancements in conformal perturbation theory and their real time interpretation*, arXiv:1607.0192.

[37] D. Berenstein and A. Miller, *Reconstructing spacetime from the hologram, even in the classical limit, requires physics beyond the Planck scale*, *Int. J. Mod. Phys.* **D25** (2016), no. 12 1644012, [arXiv:1605.0528].

[38] D. Berenstein and A. Miller, *Superposition induced topology changes in quantum gravity*, arXiv:1702.0301.

[39] D. Berenstein and A. Miller, *Code subspaces for LLM geometries*, *Class. Quant. Grav.* **35** (2018), no. 6 065003, [arXiv:1708.0003].

[40] D. Berenstein and A. Miller, *Can Topology and Geometry be Measured by an Operator Measurement in Quantum Gravity?*, *Phys. Rev. Lett.* **118** (2017), no. 26 261601, [arXiv:1605.0616].

[41] A. Buchel, L. Lehner, and R. C. Myers, *Thermal quenches in N=2* plasmas*, *JHEP* **08** (2012) 049, [arXiv:1206.6785].

[42] A. Buchel, L. Lehner, R. C. Myers, and A. van Niekerk, *Quantum quenches of holographic plasmas*, *JHEP* **05** (2013) 067, [arXiv:1302.2924].

[43] A. Buchel, R. C. Myers, and A. van Niekerk, *Universality of Abrupt Holographic Quenches*, *Phys. Rev. Lett.* **111** (2013) 201602, [arXiv:1307.4740].

[44] S. R. Das, D. A. Galante, and R. C. Myers, *Universal scaling in fast quantum quenches in conformal field theories*, *Phys. Rev. Lett.* **112** (2014) 171601, [arXiv:1401.0560].

[45] D. E. Berenstein, R. Corrado, W. Fischler, and J. M. Maldacena, *The Operator product expansion for Wilson loops and surfaces in the large N limit*, *Phys. Rev.* **D59** (1999) 105023, [hep-th/9809188].

[46] D. Marolf, *States and boundary terms: Subtleties of Lorentzian AdS / CFT*, *JHEP* **05** (2005) 042, [hep-th/0412032].

[47] D. Z. Freedman, S. D. Mathur, A. Matusis, and L. Rastelli, *Correlation functions in the CFT(d) / AdS(d+1) correspondence*, *Nucl. Phys.* **B546** (1999) 96–118, [hep-th/9804058].

[48] I. R. Klebanov and E. Witten, *AdS / CFT correspondence and symmetry breaking*, *Nucl. Phys.* **B556** (1999) 89–114, [hep-th/9905104].

[49] M. Bianchi, D. Z. Freedman, and K. Skenderis, *Holographic renormalization*, *Nucl. Phys.* **B631** (2002) 159–194, [hep-th/0112119].

[50] S. R. Das, D. A. Galante, and R. C. Myers, *Universality in fast quantum quenches*, *JHEP* **02** (2015) 167, [arXiv:1411.7710].

[51] V. A. Smirnov, *Evaluating Feynman integrals*, *Springer Tracts Mod. Phys.* **211** (2004) 1–244.

[52] S. A. Hartnoll and C. P. Herzog, *Impure AdS/CFT correspondence*, *Phys. Rev.* **D77** (2008) 106009, [arXiv:0801.1693].

[53] G. T. Horowitz, J. E. Santos, and D. Tong, *Optical Conductivity with Holographic Lattices*, *JHEP* **07** (2012) 168, [arXiv:1204.0519].

[54] G. T. Horowitz, J. E. Santos, and D. Tong, *Further Evidence for Lattice-Induced Scaling*, *JHEP* **11** (2012) 102, [arXiv:1209.1098].

[55] C. Coriano, L. Delle Rose, E. Mottola, and M. Serino, *Solving the Conformal Constraints for Scalar Operators in Momentum Space and the Evaluation of Feynman's Master Integrals*, *JHEP* **07** (2013) 011, [arXiv:1304.6944].

[56] A. Bzowski, P. McFadden, and K. Skenderis, *Implications of conformal invariance in momentum space*, *JHEP* **03** (2014) 111, [arXiv:1304.7760].

[57] L. P. Kadanoff, *Multicritical behavior at the kosterlitz-thouless critical point*, *Annals of physics* **120** (1979), no. 1 39–71.

[58] B. A. Burrington, A. W. Peet, and I. G. Zadeh, *Operator mixing for string states in the D1-D5 CFT near the orbifold point*, *Phys. Rev.* **D87** (2013), no. 10 106001, [arXiv:1211.6699].

[59] A. Bzowski, P. McFadden, and K. Skenderis, *Evaluation of conformal integrals*, *JHEP* **02** (2016) 068, [arXiv:1511.0235].

[60] S. W. Hawking, *Particle Creation by Black Holes*, *Commun. Math. Phys.* **43** (1975) 199–220. [,167(1975)].

[61] A. Hamilton, D. N. Kabat, G. Lifschytz, and D. A. Lowe, *Local bulk operators in AdS/CFT: A Boundary view of horizons and locality*, *Phys. Rev.* **D73** (2006) 086003, [hep-th/0506118].

[62] D. Kabat, G. Lifschytz, and D. A. Lowe, *Constructing local bulk observables in interacting AdS/CFT*, *Phys. Rev.* **D83** (2011) 106009, [arXiv:1102.2910].

[63] H. Lin, O. Lunin, and J. M. Maldacena, *Bubbling AdS space and 1/2 BPS geometries*, *JHEP* **10** (2004) 025, [hep-th/0409174].

[64] S. Corley, A. Jevicki, and S. Ramgoolam, *Exact correlators of giant gravitons from dual N=4 SYM theory*, *Adv. Theor. Math. Phys.* **5** (2002) 809–839, [hep-th/0111222].

[65] D. Berenstein, *A Toy model for the AdS / CFT correspondence*, *JHEP* **07** (2004) 018, [hep-th/0403110].

[66] V. Balasubramanian, B. Czech, K. Larjo, and J. Simon, *Integrability versus information loss: A Simple example*, *JHEP* **11** (2006) 001, [hep-th/0602263].

[67] K. Skenderis and M. Taylor, *Anatomy of bubbling solutions*, *JHEP* **09** (2007) 019, [arXiv:0706.0216].

[68] V. Balasubramanian, B. Czech, K. Larjo, D. Marolf, and J. Simon, *Quantum geometry and gravitational entropy*, *JHEP* **12** (2007) 067, [arXiv:0705.4431].

[69] M. Gunaydin and N. Marcus, *The Spectrum of the s**5 Compactification of the Chiral N=2, D=10 Supergravity and the Unitary Supermultiplets of U(2, 2/4)*, *Class. Quant. Grav.* **2** (1985) L11.

[70] H. J. Kim, L. J. Romans, and P. van Nieuwenhuizen, *The Mass Spectrum of Chiral N=2 D=10 Supergravity on S**5*, *Phys. Rev.* **D32** (1985) 389.

[71] J. McGreevy, L. Susskind, and N. Toumbas, *Invasion of the giant gravitons from Anti-de Sitter space*, *JHEP* **06** (2000) 008, [hep-th/0003075].

[72] M. Van Raamsdonk, *Building up spacetime with quantum entanglement*, *Gen. Rel. Grav.* **42** (2010) 2323–2329, [arXiv:1005.3035]. [Int. J. Mod. Phys.D19,2429(2010)].

[73] A. Almheiri, D. Marolf, J. Polchinski, and J. Sully, *Black Holes: Complementarity or Firewalls?*, *JHEP* **02** (2013) 062, [arXiv:1207.3123].

[74] S. W. Hawking, *Space-Time Foam*, *Nucl. Phys.* **B144** (1978) 349–362.

[75] S. W. Hawking and D. N. Page, *Thermodynamics of Black Holes in anti-De Sitter Space*, *Commun. Math. Phys.* **87** (1983) 577.

[76] E. Witten, *Anti-de Sitter space, thermal phase transition, and confinement in gauge theories*, *Adv. Theor. Math. Phys.* **2** (1998) 505–532, [hep-th/9803131].

[77] J. M. Maldacena, *Eternal black holes in anti-de Sitter*, *JHEP* **04** (2003) 021, [hep-th/0106112].

[78] J. Maldacena and L. Susskind, *Cool horizons for entangled black holes*, *Fortsch. Phys.* **61** (2013) 781–811, [arXiv:1306.0533].

[79] S. Ryu and T. Takayanagi, *Holographic derivation of entanglement entropy from AdS/CFT*, *Phys. Rev. Lett.* **96** (2006) 181602, [hep-th/0603001].

[80] L. Grant, L. Maoz, J. Marsano, K. Papadodimas, and V. S. Rychkov, *Minisuperspace quantization of 'Bubbling AdS' and free fermion droplets*, *JHEP* **08** (2005) 025, [hep-th/0505079].

[81] D. J. Gross and W. Taylor, *Two-dimensional QCD is a string theory*, *Nucl. Phys.* **B400** (1993) 181–208, [hep-th/9301068].

[82] R. de Mello Koch, *Geometries from Young Diagrams*, *JHEP* **11** (2008) 061, [arXiv:0806.0685].

[83] M. Stone, *Schur Functions, Chiral Bosons and the Quantum Hall Effect Edge States*, *Phys. Rev.* **B42** (1990) 8399–8404.

[84] G. Mandal, *Fermions from half-BPS supergravity*, *JHEP* **08** (2005) 052, [hep-th/0502104].

[85] N. V. Suryanarayana, *Half-BPS giants, free fermions and microstates of superstars*, *JHEP* **01** (2006) 082, [hep-th/0411145].

[86] J. M. Maldacena and A. Strominger, *AdS(3) black holes and a stringy exclusion principle*, *JHEP* **12** (1998) 005, [hep-th/9804085].

[87] M. T. Grisaru, R. C. Myers, and O. Tafjord, *SUSY and goliath*, *JHEP* **08** (2000) 040, [hep-th/0008015].

[88] A. Hashimoto, S. Hirano, and N. Itzhaki, *Large branes in AdS and their field theory dual*, *JHEP* **08** (2000) 051, [hep-th/0008016].

[89] V. Balasubramanian, M. Berkooz, A. Naqvi, and M. J. Strassler, *Giant gravitons in conformal field theory*, *JHEP* **04** (2002) 034, [hep-th/0107119].

[90] A. E. Mosaffa and M. M. Sheikh-Jabbari, *On classification of the bubbling geometries*, *JHEP* **04** (2006) 045, [hep-th/0602270].

[91] V. Balasubramanian, J. de Boer, V. Jejjala, and J. Simon, *The Library of Babel: On the origin of gravitational thermodynamics*, *JHEP* **12** (2005) 006, [hep-th/0508023].

[92] V. Balasubramanian, J. de Boer, S. El-Showk, and I. Messamah, *Black Holes as Effective Geometries*, *Class. Quant. Grav.* **25** (2008) 214004, [arXiv:0811.0263].

[93] L. J. Dixon, J. A. Harvey, C. Vafa, and E. Witten, *Strings on Orbifolds*, *Nucl. Phys.* **B261** (1985) 678–686.

[94] L. J. Dixon, J. A. Harvey, C. Vafa, and E. Witten, *Strings on Orbifolds. 2.*, *Nucl. Phys.* **B274** (1986) 285–314.

[95] M. R. Douglas and G. W. Moore, *D-branes, quivers, and ALE instantons*, hep-th/9603167.

[96] W. Fulton and J. Harris, *Representation Theory: A First Course*. Graduate Texts in Mathematics. Springer New York, 1991.

[97] R. Dijkgraaf, G. W. Moore, E. P. Verlinde, and H. L. Verlinde, *Elliptic genera of symmetric products and second quantized strings*, *Commun. Math. Phys.* **185** (1997) 197–209, [hep-th/9608096].

[98] R. Dijkgraaf, E. P. Verlinde, and H. L. Verlinde, *Matrix string theory*, *Nucl. Phys.* **B500** (1997) 43–61, [hep-th/9703030].

[99] D. Berenstein, *Extremal chiral ring states in the AdS/CFT correspondence are described by free fermions for a generalized oscillator algebra*, *Phys. Rev.* **D92** (2015), no. 4 046006, [arXiv:1504.0538].

[100] D. Berenstein, D. H. Correa, and S. E. Vazquez, *Quantizing open spin chains with variable length: An Example from giant gravitons*, *Phys. Rev. Lett.* **95** (2005) 191601, [hep-th/0502172].

[101] D. Berenstein and E. Dzienkowski, *Open spin chains for giant gravitons and relativity*, *JHEP* **08** (2013) 047, [arXiv:1305.2394].

[102] D. Berenstein and E. Dzienkowski, *Giant gravitons and the emergence of geometric limits in beta-deformations of $\mathcal{N} = 4$ SYM*, *JHEP* **01** (2015) 126, [arXiv:1408.3620].

[103] H. L. Verlinde, *Bits, matrices and 1/N*, *JHEP* **12** (2003) 052, [hep-th/0206059].

[104] J. Polchinski, *Dirichlet Branes and Ramond-Ramond charges*, *Phys. Rev. Lett.* **75** (1995) 4724–4727, [hep-th/9510017].

[105] A. Sen, *Tachyon matter*, *JHEP* **07** (2002) 065, [hep-th/0203265].

[106] D. Berenstein, *Giant gravitons: a collective coordinate approach*, *Phys. Rev.* **D87** (2013), no. 12 126009, [arXiv:1301.3519].

[107] D. Berenstein, *A Matrix model for a quantum Hall droplet with manifest particle-hole symmetry*, *Phys. Rev.* **D71** (2005) 085001, [hep-th/0409115].

[108] K. Papadodimas and S. Raju, *Remarks on the necessity and implications of state-dependence in the black hole interior*, *Phys. Rev.* **D93** (2016), no. 8 084049, [arXiv:1503.0882].

[109] L. Motl, "Finding and abandoning incorrect general relativity lore." http://motls.blogspot.com/2013/06/finding-and-abandoning-incorrect.html, 2013.

[110] A. Almheiri, X. Dong, and B. Swingle, *Linearity of Holographic Entanglement Entropy*, *JHEP* **02** (2017) 074, [arXiv:1606.0453].

[111] R. de Mello Koch, C. Mathwin, and H. J. R. van Zyl, *LLM Magnons*, *JHEP* **03** (2016) 110, [arXiv:1601.0691].

[112] S. R. Das and S. D. Mathur, *Folds, bosonization and non-triviality of the classical limit of 2d string theory*, *Physics Letters B* **365** (1996), no. 1-4 79–86.

[113] V. Balasubramanian, M. B. McDermott, and M. Van Raamsdonk, *Momentum-space entanglement and renormalization in quantum field theory*, *Phys. Rev.* **D86** (2012) 045014, [arXiv:1108.3568].

[114] C. T. Asplund and D. Berenstein, *Entanglement entropy converges to classical entropy around periodic orbits*, *Annals Phys.* **366** (2016) 113–132, [arXiv:1503.0485].

[115] M. M. Caldarelli, D. Klemm, and P. J. Silva, *Chronology protection in anti-de Sitter*, *Class. Quant. Grav.* **22** (2005) 3461–3466, [hep-th/0411203].

[116] G. Milanesi and M. O'Loughlin, *Singularities and closed time-like curves in type IIB 1/2 BPS geometries*, *JHEP* **09** (2005) 008, [hep-th/0507056].

[117] A. Iqbal, N. Nekrasov, A. Okounkov, and C. Vafa, *Quantum foam and topological strings*, *JHEP* **04** (2008) 011, [hep-th/0312022].

[118] S. D. Mathur, *Black Holes and Beyond*, *Annals Phys.* **327** (2012) 2760–2793, [arXiv:1205.0776].

[119] I. Bena and N. P. Warner, *Resolving the Structure of Black Holes: Philosophizing with a Hammer*, arXiv:1311.4538.

[120] C. Kristjansen, J. Plefka, G. W. Semenoff, and M. Staudacher, *A New double scaling limit of N=4 superYang-Mills theory and PP wave strings*, *Nucl. Phys.* **B643** (2002) 3–30, [hep-th/0205033].

[121] K. Papadodimas and S. Raju, *An Infalling Observer in AdS/CFT*, *JHEP* **10** (2013) 212, [arXiv:1211.6767].

[122] A. Almheiri, X. Dong, and D. Harlow, *Bulk Locality and Quantum Error Correction in AdS/CFT*, *JHEP* **04** (2015) 163, [arXiv:1411.7041].

[123] E. Mintun, J. Polchinski, and V. Rosenhaus, *Bulk-Boundary Duality, Gauge Invariance, and Quantum Error Corrections*, *Phys. Rev. Lett.* **115** (2015), no. 15 151601, [arXiv:1501.0657].

[124] F. Pastawski, B. Yoshida, D. Harlow, and J. Preskill, *Holographic quantum error-correcting codes: Toy models for the bulk/boundary correspondence*, *JHEP* **06** (2015) 149, [arXiv:1503.0623].

[125] B. Freivogel, R. A. Jefferson, and L. Kabir, *Precursors, Gauge Invariance, and Quantum Error Correction in AdS/CFT*, *JHEP* **04** (2016) 119, [arXiv:1602.0481].

[126] K. Papadodimas and S. Raju, *State-Dependent Bulk-Boundary Maps and Black Hole Complementarity*, *Phys. Rev.* **D89** (2014), no. 8 086010, [arXiv:1310.6335].

[127] H. Lin and K. Zeng, *Detecting topology change via correlations and entanglement from gauge/gravity correspondence*, arXiv:1705.1077.

[128] V. Balasubramanian, A. Lawrence, A. Rolph, and S. Ross, *Entanglement shadows in LLM geometries*, arXiv:1704.0344.

[129] W. Fulton and J. Harris, *Representation theory: a first course*, vol. 129. Springer Science & Business Media, 2013.

[130] L. Maoz and V. S. Rychkov, *Geometry quantization from supergravity: The Case of 'Bubbling AdS'*, *JHEP* **08** (2005) 096, [hep-th/0508059].

[131] R. de Mello Koch, N. Ives, and M. Stephanou, *Correlators in Nontrivial Backgrounds*, *Phys. Rev.* **D79** (2009) 026004, [arXiv:0810.4041].

[132] D. Garner, S. Ramgoolam, and C. Wen, *Thresholds of large N factorization in CFT_4: exploring bulk spacetime in AdS_5*, *JHEP* **11** (2014) 076, [arXiv:1403.5281].

[133] A. Dhar, G. Mandal, and M. Smedback, *From gravitons to giants*, *JHEP* **03** (2006) 031, [hep-th/0512312].

[134] T. Banks, W. Fischler, I. R. Klebanov, and L. Susskind, *Schwarzschild black holes from matrix theory*, *Phys. Rev. Lett.* **80** (1998) 226–229, [hep-th/9709091].

[135] D. E. Berenstein and L. F. Urrutia, *The Relation between the Mandelstam and the Cayley-Hamilton identities*, *J. Math. Phys.* **35** (1994) 1922–1930, [hep-th/9305156].

[136] V. Balasubramanian, D. Berenstein, A. Lewkowycz, A. Miller, O. Parrikar, and C. Rabideau, "Work in progress."

[137] V. E. Hubeny, M. Rangamani, and T. Takayanagi, *A Covariant holographic entanglement entropy proposal*, *JHEP* **07** (2007) 062, [arXiv:0705.0016].

[138] R. C. Myers and O. Tafjord, *Superstars and giant gravitons*, *JHEP* **11** (2001) 009, [hep-th/0109127].

[139] E. E. Boos and A. I. Davydychev, *A Method of the Evaluation of the Vertex Type Feynman Integrals*, *Moscow Univ. Phys. Bull.* **42N3** (1987) 6–10. [Vestn. Mosk. Univ. Fiz. Astron.28N3,8(1987)].

[140] J. M. Drummond, J. Henn, V. A. Smirnov, and E. Sokatchev, *Magic identities for conformal four-point integrals*, *JHEP* **01** (2007) 064, [hep-th/0607160].

[141] M. E. Cage, K. Klitzing, A. Chang, F. Duncan, M. Haldane, R. Laughlin, A. Pruisken, and D. Thouless, *The quantum Hall effect*. Springer Science & Business Media, 2012.

[142] M. Stone, *Edge waves in the quantum hall effect*, *Annals of Physics* **207** (1991), no. 1 38–52.